
بسم الله الرحمن الرحيم

In the name of Allah, the Beneficent, the Merciful

CHAPTER ONE

Equation (5.6) may then be re-written :-

$$0 = \sqrt{\frac{2e}{m}}\, N \left[\frac{2m}{M}\, Q_m\, \epsilon^2\, F_o(\epsilon) + \int_{\epsilon}^{\epsilon + \epsilon_{ex}} \epsilon' Q_{ex}(\epsilon')\, F_o(\epsilon')\, d\epsilon' \right.$$

$$\left. + \left(\int_{\epsilon}^{\frac{\epsilon}{1-A} + \epsilon_i} + \int_{0}^{\frac{\epsilon}{A} + \epsilon_i} \right) \epsilon' Q_i(\epsilon')\, F_o(\epsilon')\, d\epsilon' \right]$$

$$+ E \sqrt{\frac{2e}{m}}\, \frac{1}{3NQ_m} \left\{ \epsilon E \frac{\partial F_o(\epsilon)}{\partial \epsilon} + \alpha \epsilon F_o(\epsilon) \right\}$$

$$+ \sqrt{\frac{2e}{m}}\, \frac{\partial}{\partial x} \int_{0}^{\epsilon} \frac{1}{3NQ_m} \left\{ \epsilon' E \frac{\partial F_o(\epsilon')}{\partial \epsilon'} + \alpha \epsilon' F_o(\epsilon') \right\} d\epsilon' \quad . \quad (5.9)$$

The distribution function and hence R_i, v and D are now independent of x and equation (5.7) becomes :-

$$R_i - \alpha v + \alpha^2 D = 0 \quad (5.10)$$

$$\alpha = \frac{v - \sqrt{v^2 - 4 R_i D}}{2D} \quad (5.11)$$

$$R_i = \sqrt{\frac{2e}{m}}\, N \int_{0}^{\infty} \epsilon' Q_i\, f(\epsilon')\, d\epsilon' \quad (5.12)$$

The coefficient α is the value of the primary ionization coefficient, also the energy distribution function is normalised so that :-

$$\int_{0}^{\infty} \epsilon^{\frac{1}{2}} F_o(\epsilon)\, d\epsilon = 1 \quad . \quad (5.13)$$

The appropriate transport equation obtained from equation (5.7) is :-

$$\frac{\partial n}{\partial t} = D_o \left(\frac{\partial^2 n}{\partial x^2} + \frac{\partial^2 n}{\partial y^2} \right) - v_o \frac{\partial n}{\partial z} \quad , \quad (5.14)$$

where the drift velocity, v_o, is given by :-

$$v_o = - \frac{E}{3} \sqrt{\frac{2e}{m}} \int_0^\infty \frac{\varepsilon}{NQ_m} \frac{\partial F_o(\varepsilon)}{\partial \varepsilon} \, d\varepsilon \quad , \tag{5.15}$$

and the diffusion coefficient, D_o, is given by :-

$$D_o = \frac{1}{3} \sqrt{\frac{2e}{m}} \int_0^\infty \frac{\varepsilon}{NQ_m} F_o(\varepsilon) \, d\varepsilon \quad . \tag{5.16}$$

The value of D_o is the value of D_r (the radial diffusion coefficient) since the earlier solution did not differentiate between D_r and D_L .

The electron mean energy is given by :-

$$\bar{\varepsilon} = \int_0^\infty \varepsilon^{\frac{3}{2}} F_o(\varepsilon) \, d\varepsilon \quad . \tag{5.17}$$

CHAPTER SIX

CHAPTER SIX

RESULTS FOR ELECTRON SWARMS IN A MIXTURE OF ARGON GAS AND METAL VAPOURS

6.1 THEORETICAL CONSIDERATION

The theoretical results have been computed for the electron swarm parameters by using the Boltzmann's equation in a mixture of argon gas and metal vapours, namely (Ar+ K, Ar+ Na and Ar+ Cs) for E/N regions between 2.83 and 283 Td and for a range of metal vapour percentages of 0.001% to 20%, (see Appendix A).

The sets of metal vapour/gas cross-sections have been obtained from the results of previous workers. For different percentages of metal vapour and argon gas, calculations have been made for the ionization coefficient, α_T/N, the drift velocity, v_d, the ratio of rates of excitation and ionization, the ratio of radial diffusion coefficient to mobility D_r/μ, and the mean electron energy, $\bar{\epsilon}$, as functions of E/N.

6.2 CROSS-SECTION IN A MIXTURE OF ARGON GAS AND POTASSIUM VAPOUR

Three types of cross-sections in argon gas are used for the analysis and these represent excitation, ionization collision and momentum transfer cross-section. Details are given in Table 6.1 and the variation of cross-section with electron energy is shown in Fig. 6.1. The momentum transfer cross-section, NQ_m, used in the present calculations were published by Frost and Phelps (1964) for energies up to 500 eV. All the excitation processes are represented by a single excitation cross-section, NQ_{EX}, which is 1.3 times the semi-empirical values of de Heer and Jansen (1975),

and has an onset energy of 11.6 eV. Ionization processes are represented by cross-sections published by Rapp and Englander -Golden (1965) who gave ionization cross-section, $NQ_{Ion.}$, having onset energy of 15.8 eV.

For potassium vapour, three types of cross-sections are also used. These are the momentum transfer cross section, $NQ_{m.}$, the excitation cross-section, $NQ_{Ex.}$, and ionization cross-section, $NQ_{Ion.}$, respectively. The momentum transfer cross-section has a high peak of $NQ_{m.} = 2.5 \times 10^{6}\ m^{-1}$, occurring at an energy of 0.16 eV. There is then a rapid fall of the cross-section to a value of $NQ_{m.} = 1.7 \times 10^{4}\ m^{-1}$, occurring at an energy of 0.7 eV. That is followed by an almost horizontal section up to the high energies. This type of momentum curve is found to be necessary in order to fit the experimental measured values of the drift velocity (Lucas, 1981). Fig. 6.2 shows the good degree of fit and is within 15% of the measured values over a wide range of E/N. Because of the rapid rate of change of the momentum cross-section for the electron energies in the region of 0.2 - 0.6 eV, it is not possible to get an exact fit. There are two excitation cross-sections. The first is published by Chen and Gallagher (1978) having an onset energy of 1.61 eV and the second by Walters (1976) having an onset energy of 2.60 eV. The ionization cross-section, with the onset energy of 4.34 eV is by Zapesochnyi and Aleksakin (1969). The relevant references for the momentum transfer cross-section, the excitation cross-section and ionization cross-section are given in Table 6.2 for potassium vapour. The actual cross-section values for both argon gas and potassium vapour cross-section are shown in Fig. 6.1, and tabulated in Appendix B.

6.3 RESULTS AND DISCUSSION

Once a set of cross-sections has been compiled, and used in a simulated electron swarm motion in metal vapour, e.g. potassium, it is then possible to determine theoretically the swarm parameters in a mixture of gases and metal vapours. Theoretical results for the swarm parameters have been obtained by using Boltzmann's equation over the range 2.83 to 283 Td and are tabulated in Appendix A.

The graph of the ionization coefficient (α_T/N) against E/N is shown in Fig. 6.3. This graph illustrates the values of ionization coefficient in pure potassium vapour varying from 1.4×10^{-25} to 1.1×10^{-20} cm^2 which is lower than the values of pure argon gas varying from 2.06×10^{-25} to 7.37×10^{-17} cm^2. Between these two graphs, there are three further graphs for percentages of potassium vapour from 5 % to 20 % K and these show that the higher percentage of potassium vapour used the lower is the ionization coefficient obtained. Fig. 6.4 shows clearly that the lowest percentages of potassium ions (0.01 % K^+), the values of ionization coefficient are small, while at highest percentages of potassium ions (1 % K^+), the values of ionization coefficients are large and bigger than the values of the ionization coefficients in pure argon gas (see Fig. 6.3).

Fig. 6.5 shows that for low E/N $\leq$ 20 Td, there is an enhanced coefficient caused by the production of potassium ions, K^+, by direct ionization. Fig. 6.5 also illustrates that the ionization coefficient in a mixture of argon gas and potassium vapour is very large compared with the ionization coefficient in argon gas, as illustrated by the peak in the curve as a function of percentage (and fraction) of potassium vapour.

The drift velocity, v_d, in a mixture of argon gas and potassium vapour, is shown in Fig. 6.6, which shows that the values in pure argon gas varying from 0.04 to 2.06 x 10^7 cm/sec, are higher than the values in pure potassium vapour. As the percentage of potassium vapour is increased, there is an overall increase in drift velocities, especially at 20% K, the drift velocity varies from 0.8 x 10^5 to 4.14 x 10^7 cm/sec.

Fig. 6.7 illustrates the variation of the ratio of radial diffusion coefficient to mobility, D_r/μ with E/N. The value of D_r/μ in pure potassium vapour varies from 0.14 to 0.57 V, which is lower than the value in pure argon gas which varies from 7.03 to 9.85 V. There are four other curves confined between these two curves, which show that a higher percentage of potassium vapour produces a lower mean energy. Over the same range of E/N, (14.1 to 283 Td), the ratio of radial diffusion coefficient to mobility in potassium vapour is greater than the mean energy throughout the entire range. This confirms that the electron energy distribution is non-Maxwellian because, otherwise, a relationship of ($\frac{D_r}{\mu} = \frac{2}{3}\bar{\epsilon}$) would be expected. This non-Maxwellian energy distribution occurs because of the large excitation cross-sections with the onset energies of 1.61 eV and 2.60 eV.

Mean electron energy $\bar{\epsilon}$ is plotted as a function of E/N in Fig. 6.8. This figure shows that the values in pure potassium vapour range from 0.01 to 0.52 eV, and in pure argon gas from 5.09 to 8.85 eV. Between these two curves there are four further curves for a percentage mixture of potassium vapour from 1% to 20% K. Lower values of electron energies are obtained from a higher percentage of potassium vapour because of the higher momentum cross-section of potassium vapour. There exists a fast-rising excitation

TABLE 6.1: SOURCES OF ARGON COLLISION CROSS-SECTIONS

CROSS-SECTION	ONSET-ENERGY eV	SOURCE
* MOMENTUM TRANSFER	$\frac{2m}{M} = 2.69 \times 10^{-5}$	FROST AND PHELPS (1964)
EXCITATION	11.6	de HEER AND JANSEN (1975)
IONIZATION	15.8	RAPP AND ENGLANDER-GOLDEN (1965)

* Modified

TABLE 6.2 : SOURCES OF POTASSIUM VAPOUR COLLISION CROSS-SECTIONS

CROSS-SECTION	ONSET-ENERGY eV	SOURCE
MOMENTUM TRANSFER	$\frac{2m}{M} = 27.8 \times 10^{-6}$	LUCAS (1981)
RESONANCE EXCITATION 4^2P 3D	 1.61 2.60	CHEN AND GALLAGHER (1978) WALTERS (1976)
IONIZATION	4.34	ZAPESOCHNYI AND ALEKSAKIN (1969) McFARLAND (1965)

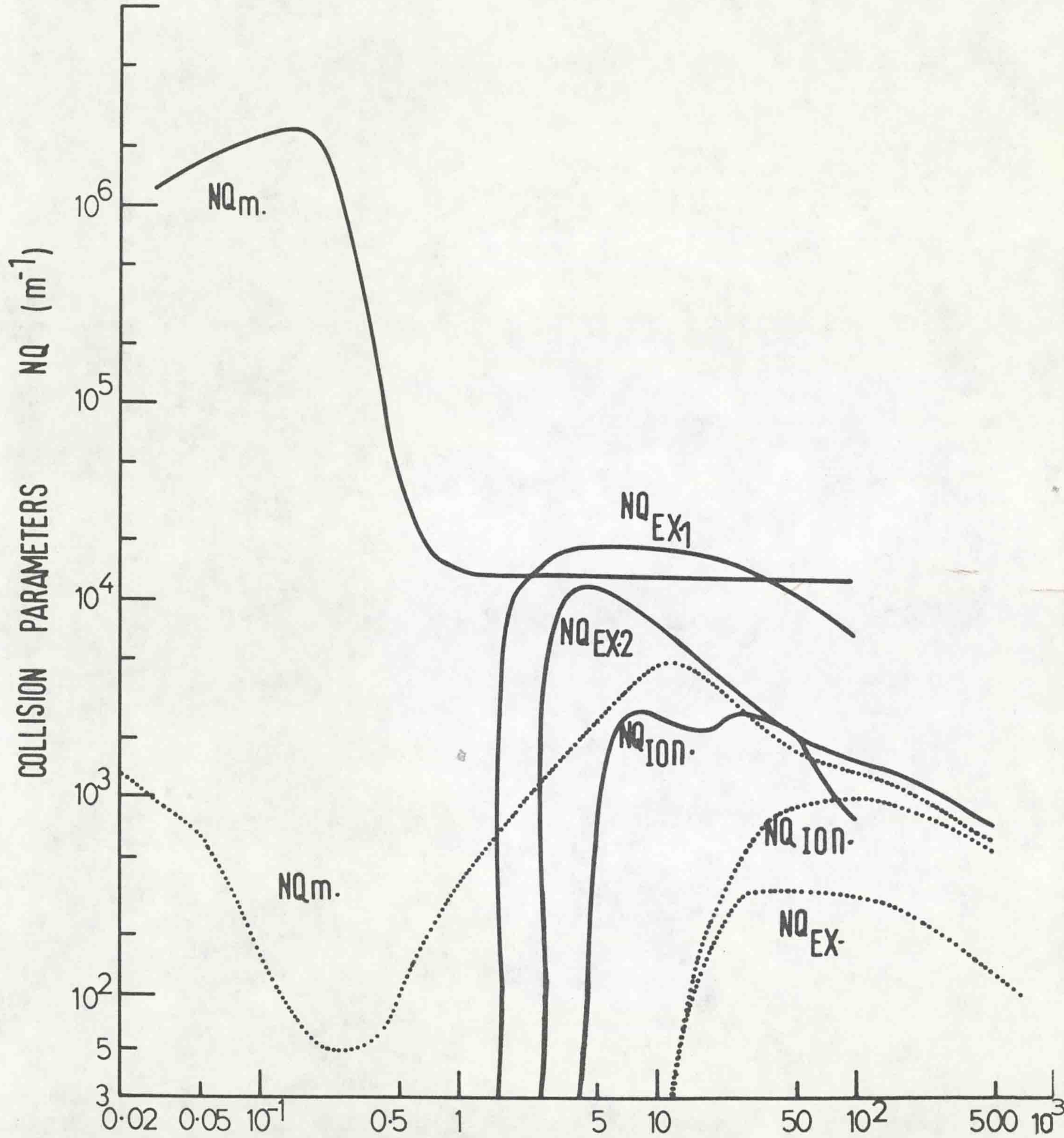

Fig(6·1) COLLISION IN ARGON GAS AND POTASSIUM VAPOUR

(——— K, ·····Ar)

CHAPTER ONE

INTRODUCTION

For many years ionized gases have been subject to extensive studies and investigations. Research in this direction has had a decisive influence on various technological developments and theoretical approaches, and has found many applications. In the past, gaseous electronics has been used successfully to explain the operation of such devices as the thyratron, Geiger counter, mercury arc rectifier, high voltage gas switches, gas insulators and in recent years, an active interest has developed in the explanation of the physical processes involved in gas lasers, which in themselves have found wide applications (see review articles by Levine and De Maria, 1971, and Arecehi and Schulz-Dubois, 1972).

For design purposes an accurate knowledge of the electrical properties of gases is essential. To be able to understand the behaviour of ionized gases under certain conditions, one must have detailed information about electron mean energies, diffusion coefficients and attachment and detachment coefficients. It is also necessary to understand the chemistry of the processes by studying the ion reactions which take place and also radiation studies help to clarify the situation as far as lasers are concerned.

There is an active group at Liverpool engaged upon research into gaseous electronics and within this group Dr. J. Lucas specialises in the study of electron swarm motion in gases. In particular, four of the swarm parameters which describe the motion of the electrons are studied, namely the ionization coefficient, α_T, the radial diffusion coefficient, D_r, the electron

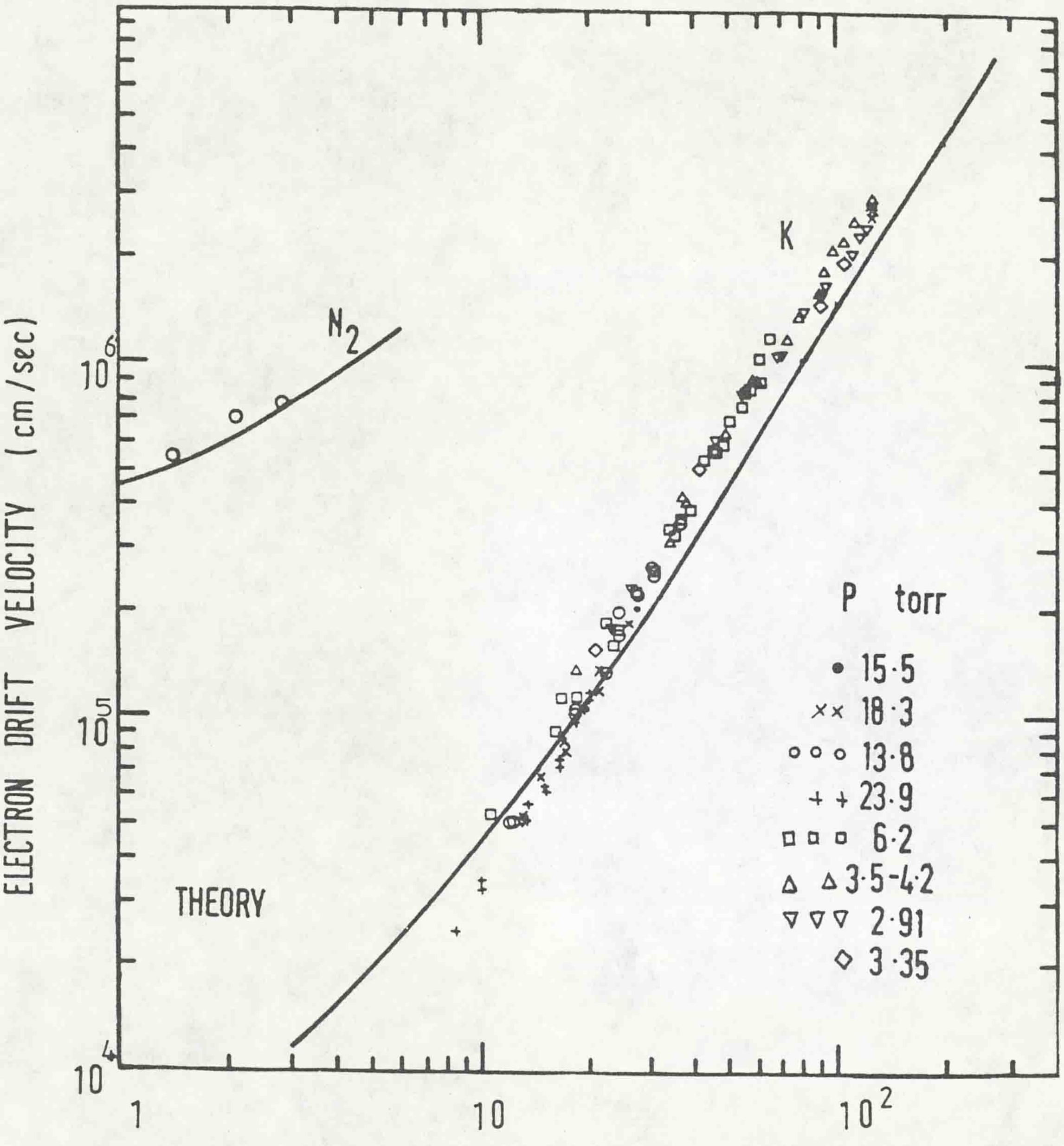

Fig (6.2) DRIFT VELOCITY IN POTASSIUM VAPOUR

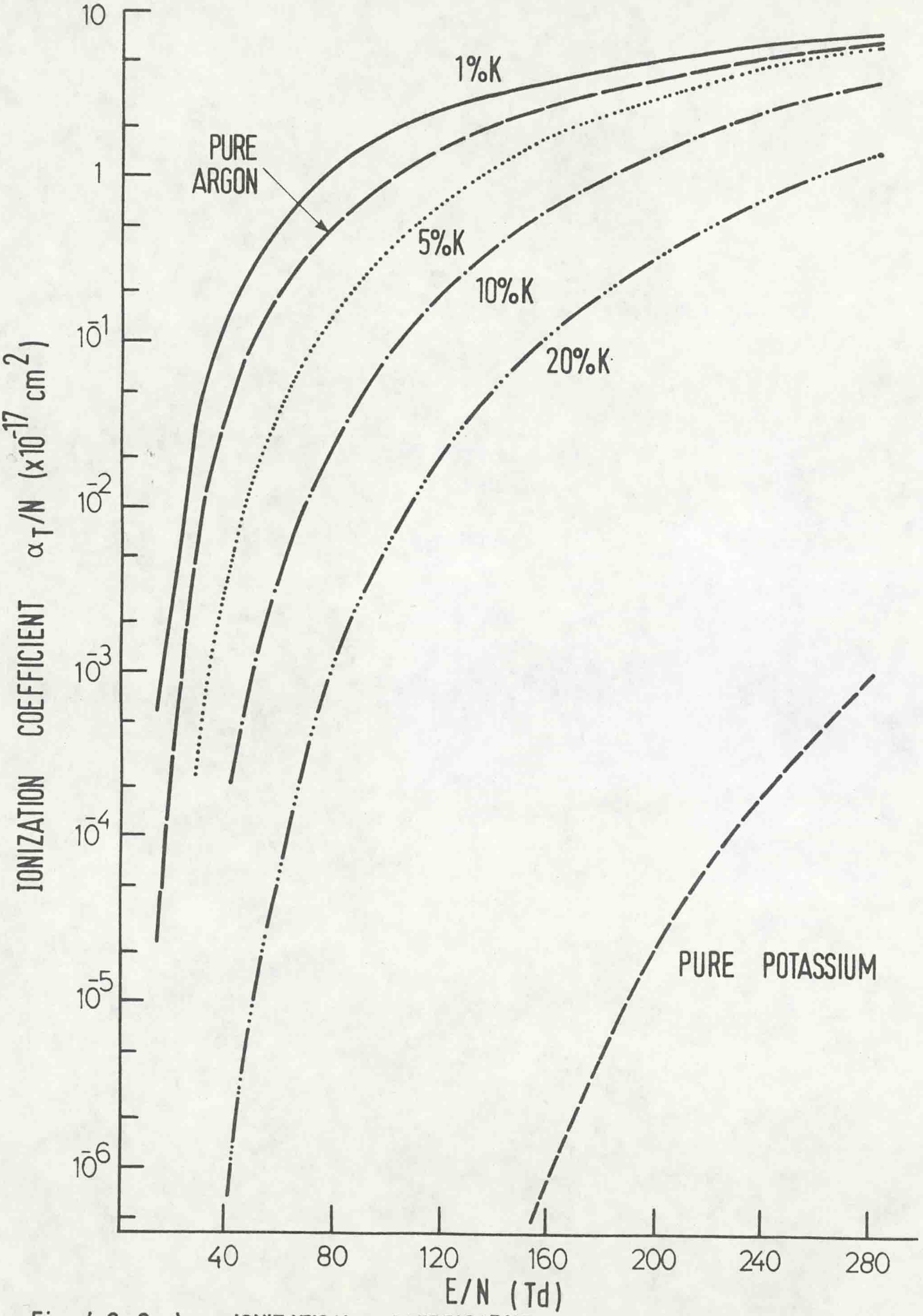

Fig (6.3) IONIZATION COEFFICIENT IN MIXTURES OF POTASSIUM AND ARGON

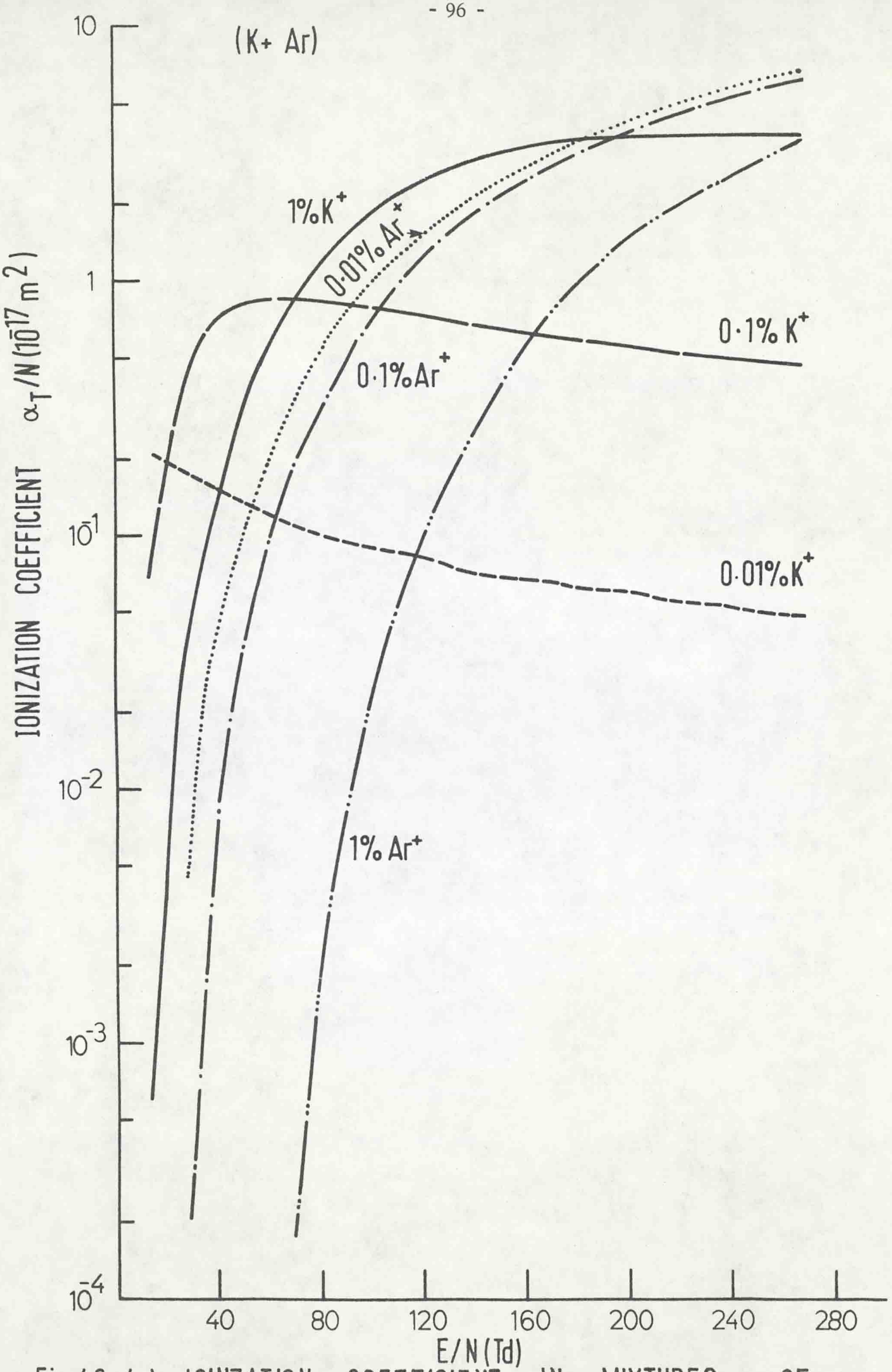

Fig (6·4) IOINZATION COEFFICIENT IN MIXTURES OF POTASSIUM AND ARGON

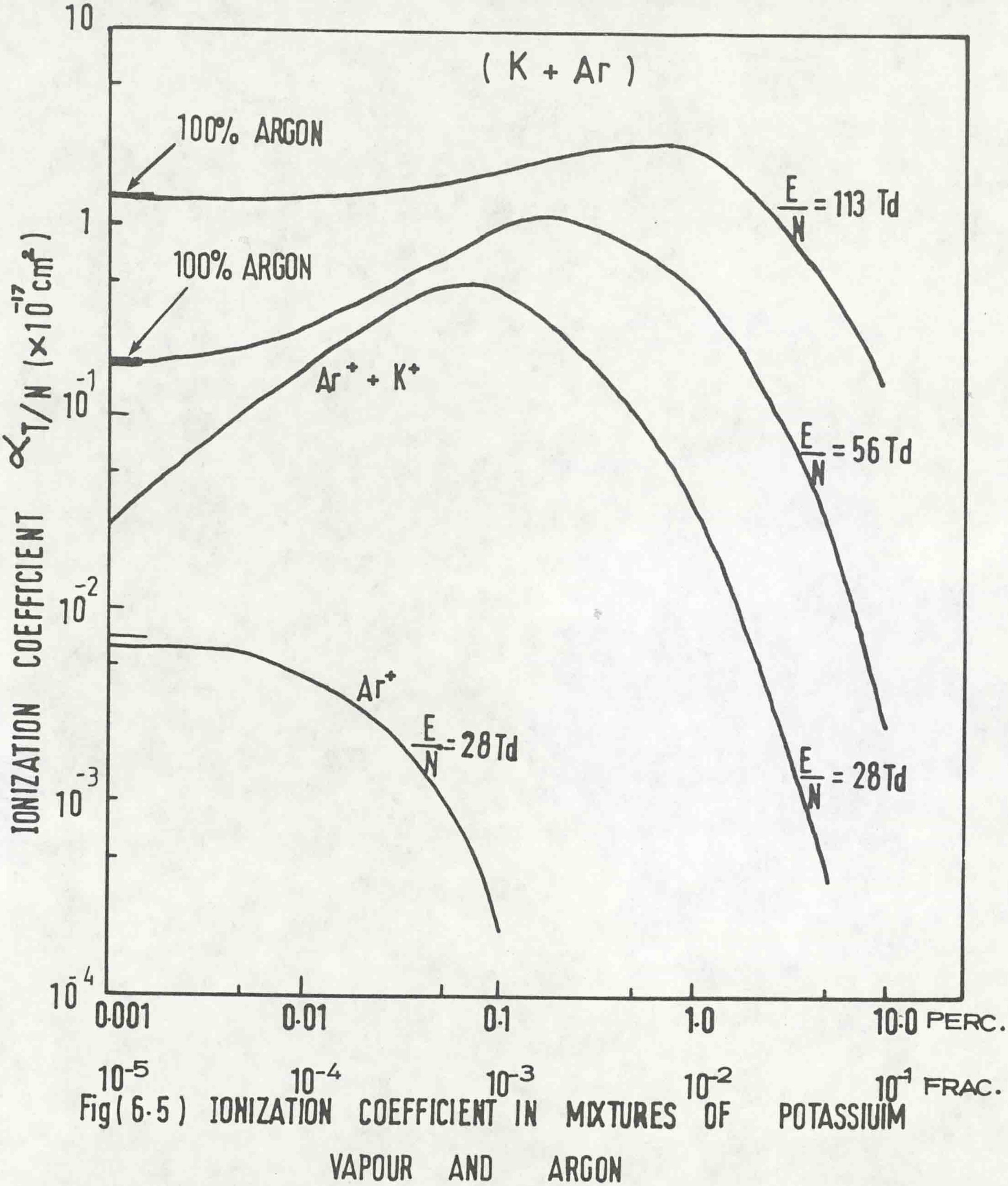

Fig (6·5) IONIZATION COEFFICIENT IN MIXTURES OF POTASSIUM VAPOUR AND ARGON

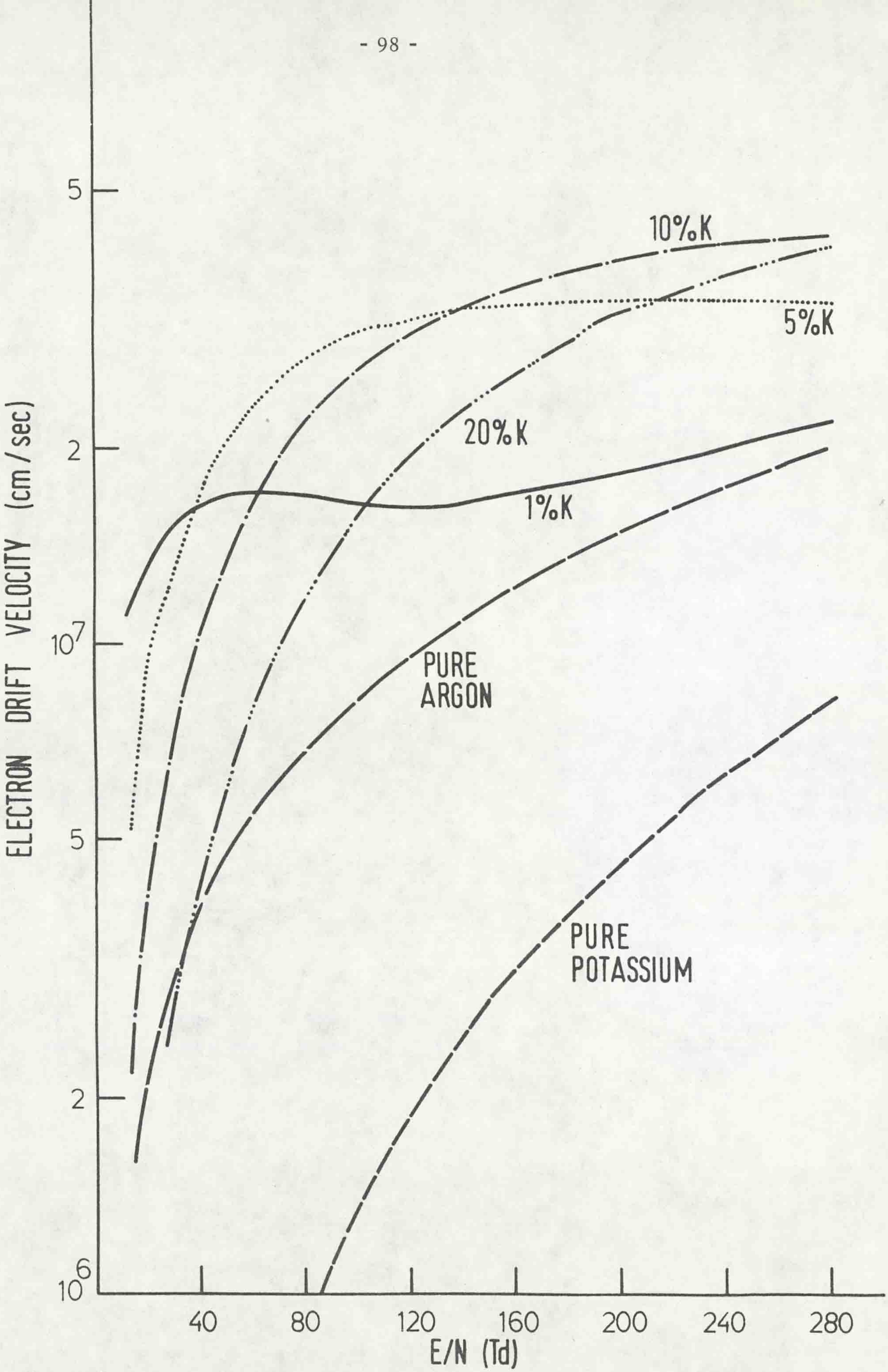

Fig (6·6) DRIFT VELOCITY IN MIXTURES OF POTASSIUM AND ARGON

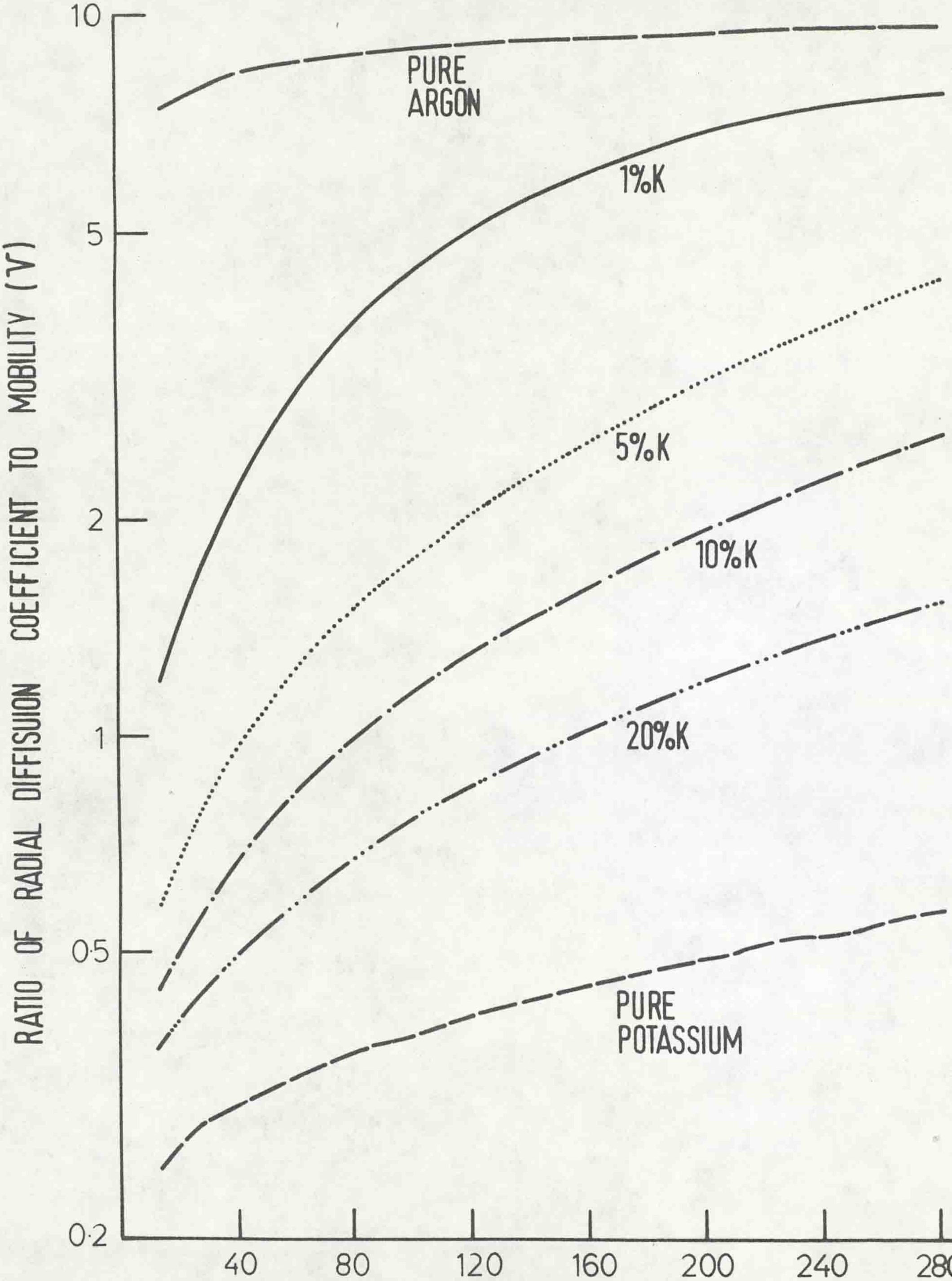

Fig (6·7) RATIO OF RADIAL DIFFUSION COEFFICIENT TO MOBILITY IN MIXTURES OF POTASSIUM AND ARGON

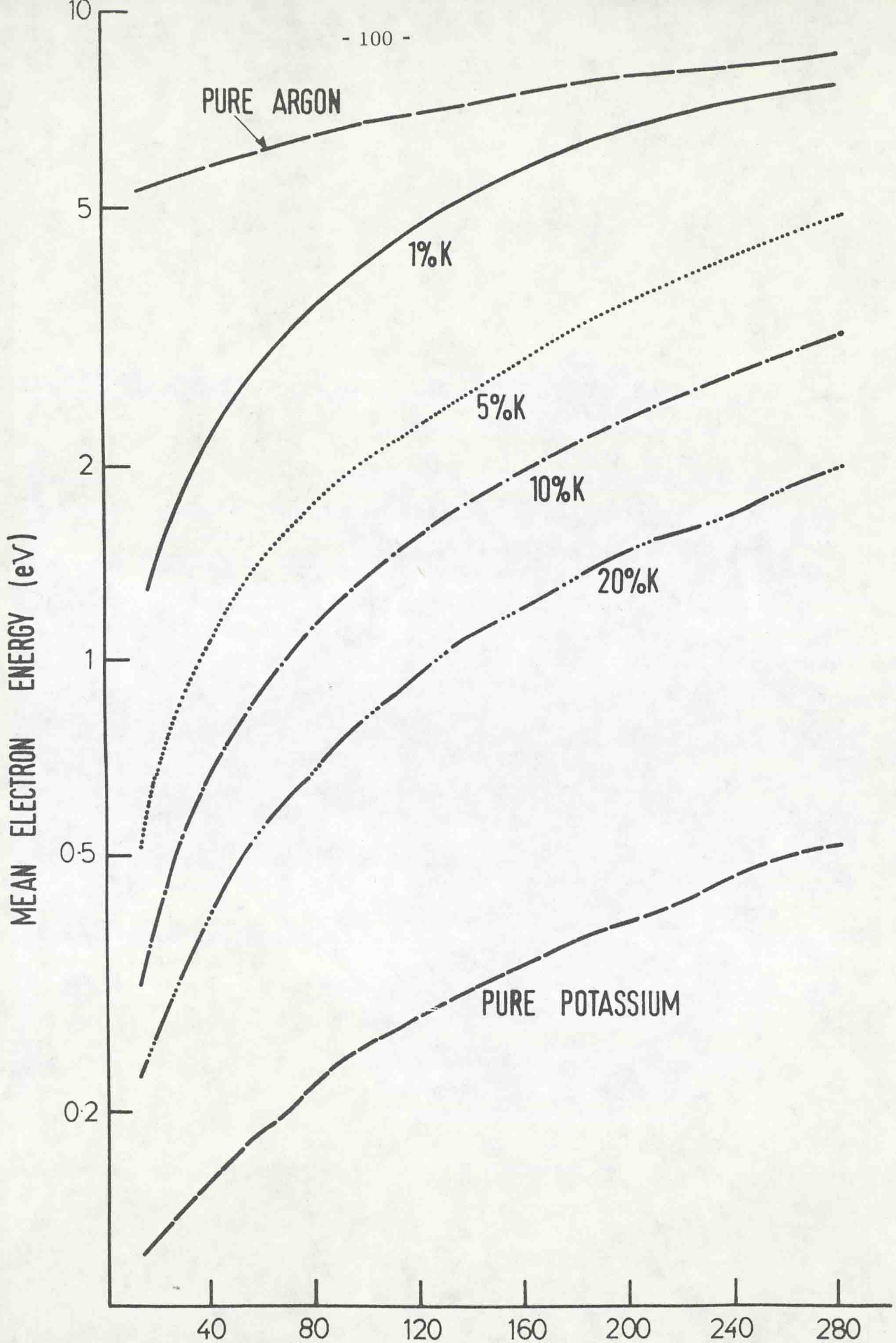

Fig (6·8) MEAN ELECTRON ENERGY IN MIXTURES OF POTASSIUM AND ARGON

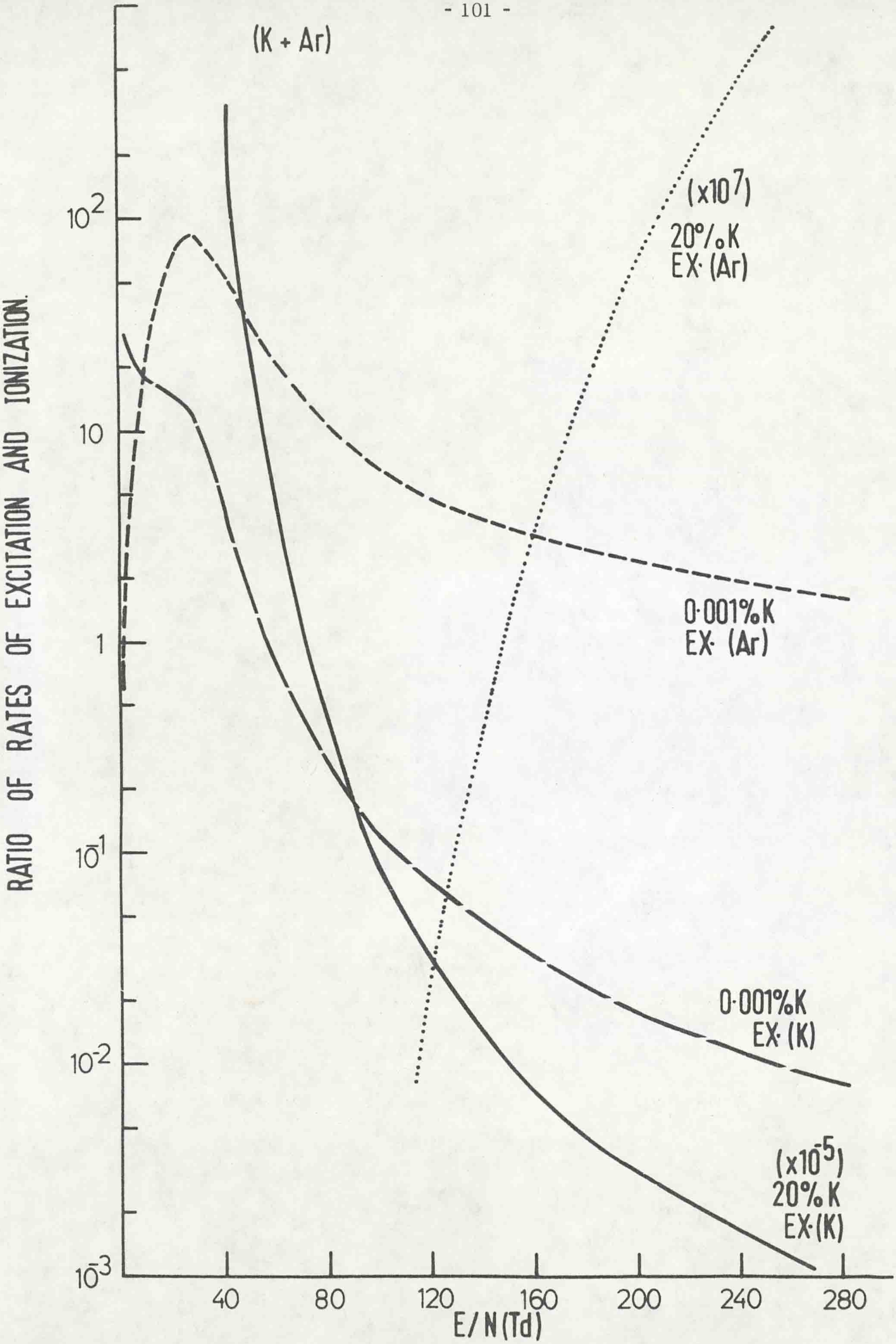

Fig (6 · 9) RATIO OF RATES OF EXCITATION AND IONIZATION IN MIXTURES OF POTASSIUM AND ARGON

coefficient at low E/N, as shown in Fig. 6.9. For small percentages of potassium vapour, the coefficient due to the second excitation cross-section is very small and may be neglected.

6.4 CROSS-SECTION IN A MIXTURE OF ARGON GAS AND SODIUM VAPOUR

The cross-section in sodium vapour together with the cross-sections in argon gas are shown in Fig. 6.10, and tabulated in Appendix B. Three types of cross-sections in sodium vapour are used and these are the momentum transfer cross-section, the excitation cross-section and the ionization cross-section. The momentum transfer cross-section has a maximum peak of $NQ_{m.} = 2.7 \times 10^{5}\ m^{-1}$ located at an energy of 0.15 eV followed by a rapid fall of the cross-section to a value of $NQ_{m.} = 2.7 \times 10^{3}\ m^{-1}$, given at an energy of 4 eV. This kind of momentum curve in sodium vapour is adopted such as to agree with the measured drift velocity by Nakamura and Lucas (1978). Three excitation cross-sections, $NQ_{Ex.}$, have been measured by Zapesochnyi (1967). The excitation onset energies are taken as 2.10, 3.62 and 4.12 eV respectively. The ionization cross-section, $NQ_{Ion.}$, is given by Zapesochnyi and Aleksakin (1969) having an onset energy of 5.14 eV. Table 6.3 shows the sources of cross-sections in sodium vapour. (For argon gas, cross-sections have been discussed in Section 6.2).

6.5 RESULTS AND DISCUSSION

Using Boltzmann's equation the theoretical results of ionization coefficient, α_T/N, drift velocity, v_d, ratio of radial diffusion coefficient to mobility, D_r/μ, mean electron energy, $\bar{\epsilon}$, and the ratio of rates of excitation and ionization have been obtained over the range of 2.83 to 283 Td

in a mixture of argon gas and sodium vapour and are summarised in tables (see Appendix A). Fig. 6.11 illustrates the variation of ionization coefficient (α_T/N) with E/N. This figure shows that the values of ionization coefficient in pure argon gas vary from 2.06×10^{-25} to 7.37×10^{-17} cm^2 and are higher than the values of ionization coefficient in pure sodium vapour which vary from 9.7×10^{-34} to 5.9×10^{-18} cm^2. There are three further curves, between the pure argon gas curve and pure sodium curve, containing percentages of mixtures of sodium vapour increased from 7 % to 20 % Na and this shows clearly that the lower the percentage of sodium vapour used, the higher the value of the ionization coefficient. At 1 % Na, the values of ionization coefficient are higher than the values of pure argon gas, but Fig. 6.12 shows that at the smallest percentages of sodium ions (0.01 % Na^+), the ionization coefficient is very small, from 0.17 to 0.04×10^{-17} cm^2, while at increasing the percentages of sodium ions (1 % Na^+), the values of ionization coefficient are increased. At the same time, at lowest percentages of argon ions (0.01 % Ar^+) a higher ionization coefficient is obtained. The ionization coefficient is plotted again against the percentage (and fraction) of sodium vapour in Fig. 6.13, which indicates that the production of sodium ions, Na^+, by direct ionization causes an enhanced coefficient. The ionization coefficient of argon is much lower than the ionization coefficient of the argon-sodium vapour mixture, as may be seen from examining the peak in the curves.

The values of drift velocity have been evaluated theoretically and are shown in Fig. 6.14, as a function of E/N, which shows that the values of drift velocity in pure sodium vapour ranges from 0.4×10^5 to 1.23×10^7 cm/sec, and are smaller than the values of drift velocity in pure argon gas

drift velocity, v_d, and the longitudinal diffusion coefficient, D_L. These parameters are determined theoretically by consideration of the energy balance and continuity equations (see Fig. 1.1). Initial experimental work involved the measurement of the ionization coefficient and radial diffusion coefficient by a steady-state technique for inert and molecular gases, using a method based on the work by Townsend (1947). More recently a new technique, the time of flight technique, was developed by Snelson (1974) which could obtain valuable information about the electron drift velocity and longitudinal diffusion coefficient. Directly influencing the swarm parameters is the electron energy distribution, calculations of which have been made using the Boltzmann equation and the Monte Carlo simulation technique (Saelee, 1976). Table 1.1 shows the existing state of research work done by various workers in the gaseous electronics group at Liverpool. Work by workers outside this group has been tabulated and presented in many texts, works by Dutton (1975) and Laborie et al (1968, 1971) being particularly relevant to the present work.

The research work detailed in this thesis has continued in the tradition of the Liverpool group, original measurements of swarm parameters have been made in several gases and mixtures of gases with metal vapours.

Time of flight measurements of the electron drift velocity and longitudinal diffusion coefficient have been made in oxygen and methane for E/N in the range up to 848 Td (1 Td = 10^{-17} V cm^2). The time of flight technique has also been applied to measure the radial diffusion coefficient in oxygen, methane and sulphur hexafluoride at high E/N between 13 and 5650 Td. A Monte Carlo technique has been used to simulate the electron swarm motion in oxygen and methane (see Table 1.2). A set of elastic

which vary from 0.04 to 2.06 x 10^7 cm/sec. Above these two curves there are four curves with the percentage of sodium vapour increased between 1% to 20% Na which illustrates that the value of drift velocity in the mixture is increased with the increasing sodium vapour percentages, especially at 20% Na. The drift velocity varies from 0.03 to 4.38 x 10^7 cm/sec.

The graph of the ratio of radial diffusion coefficient to mobility against E/N is shown in Fig. 6.15. The values for the ratio of radial diffusion coefficient to mobility in pure argon gas increase with E/N up to 283 Td at which it reaches a maximum value of 9.85 V, while the values for the ratio of radial diffusion coefficient in pure sodium vapour vary from 0.11 to 0.64 V. The area between these two curves is occupied by four further curves with percentages ranging from 1% to 20% Na, which show that at the lowest percentage of sodium vapour a higher mean energy is obtained. The values of ratio of radial diffusion coefficient to mobility in sodium vapour are smaller than the mean electron energy throughout the range of E/N, which shows that the electron energy distribution is of the Maxwellian type for which $D_r/\mu = \frac{2}{3}\,\bar{\epsilon}$.

The values of mean electron energy as a function of E/N are illustrated in Fig. 6.16, which shows that the values in pure argon gas change from 5.09 to 8.85 eV, while the values in pure sodium vapour change from 0.11 to 0.97 eV. Four curves are drawn between these two curves with percentage mixture of sodium vapour increased from 1% to 20% Na. Because of higher values in momentum transfer cross-section of sodium vapour, a higher energy is gained from the lower percentage of sodium vapour.

The ratio of rates of excitation and ionization is plotted against E/N as

TABLE 6.3 : SOURCES OF SODIUM VAPOUR COLLISION CROSS-SECTIONS

CROSS-SECTION	ONSET-ENERGY eV	SOURCE
* MOMENTUM TRANSFER	$\frac{2m}{M} = 4.74 \times 10^{-5}$	NAKAMURA AND LUCAS (1979)
* EXCITATION		ZAPESOCHNYI (1967)
3S - 3P	2.10,	
3P - 3D	3.62,	
Combined (3P-4D, 5S, 5D, 6S, 6D)	4.12	
IONIZATION	5.14	ZAPESOCHNYI AND ALEKSAKIN (1969) McFARLAND (1965)

* Modified

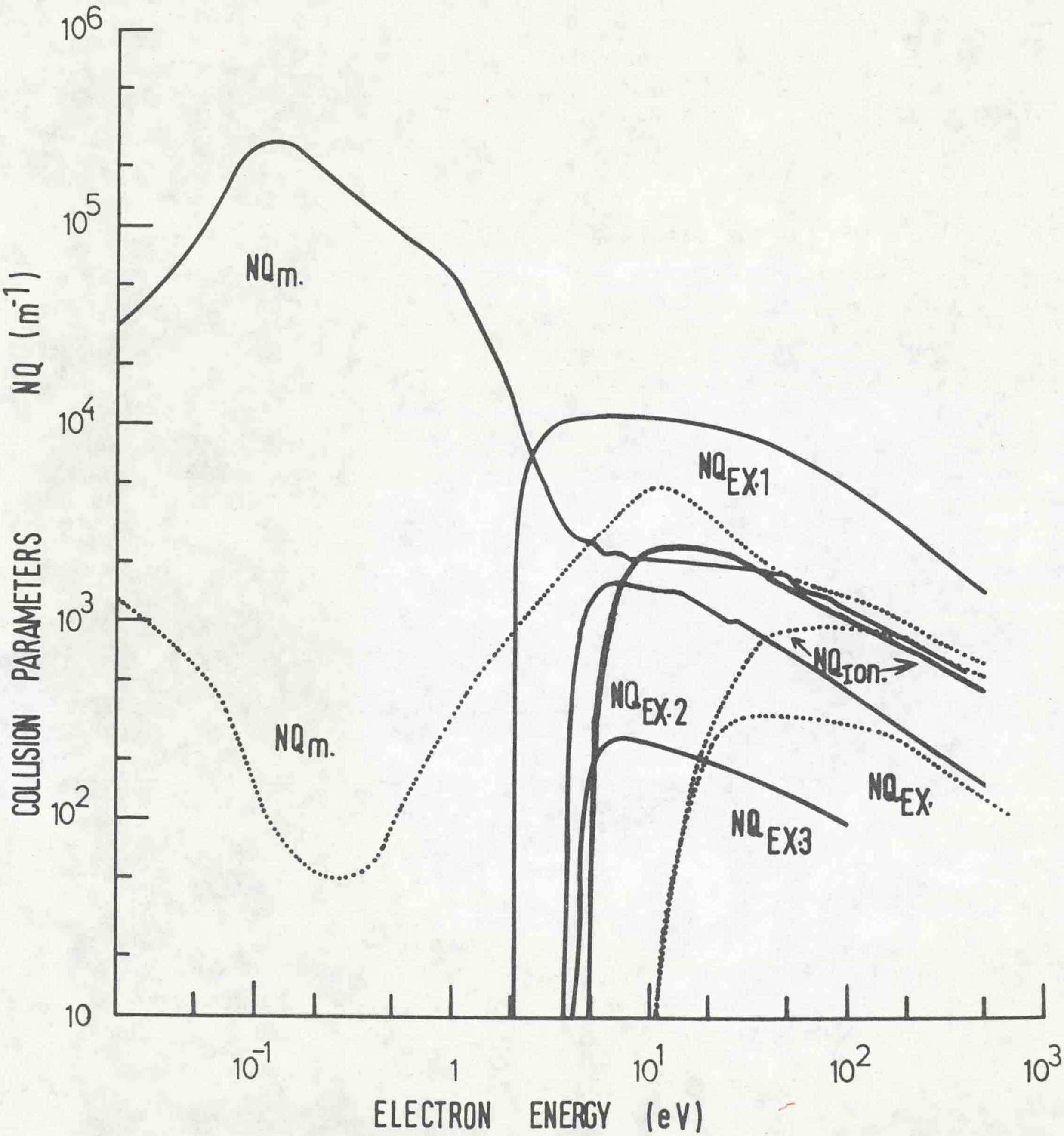

Fig.(6·10) COLLISIONS IN ARGON GAS AND SODIUM VAPOUR
(——Na,------ Ar)

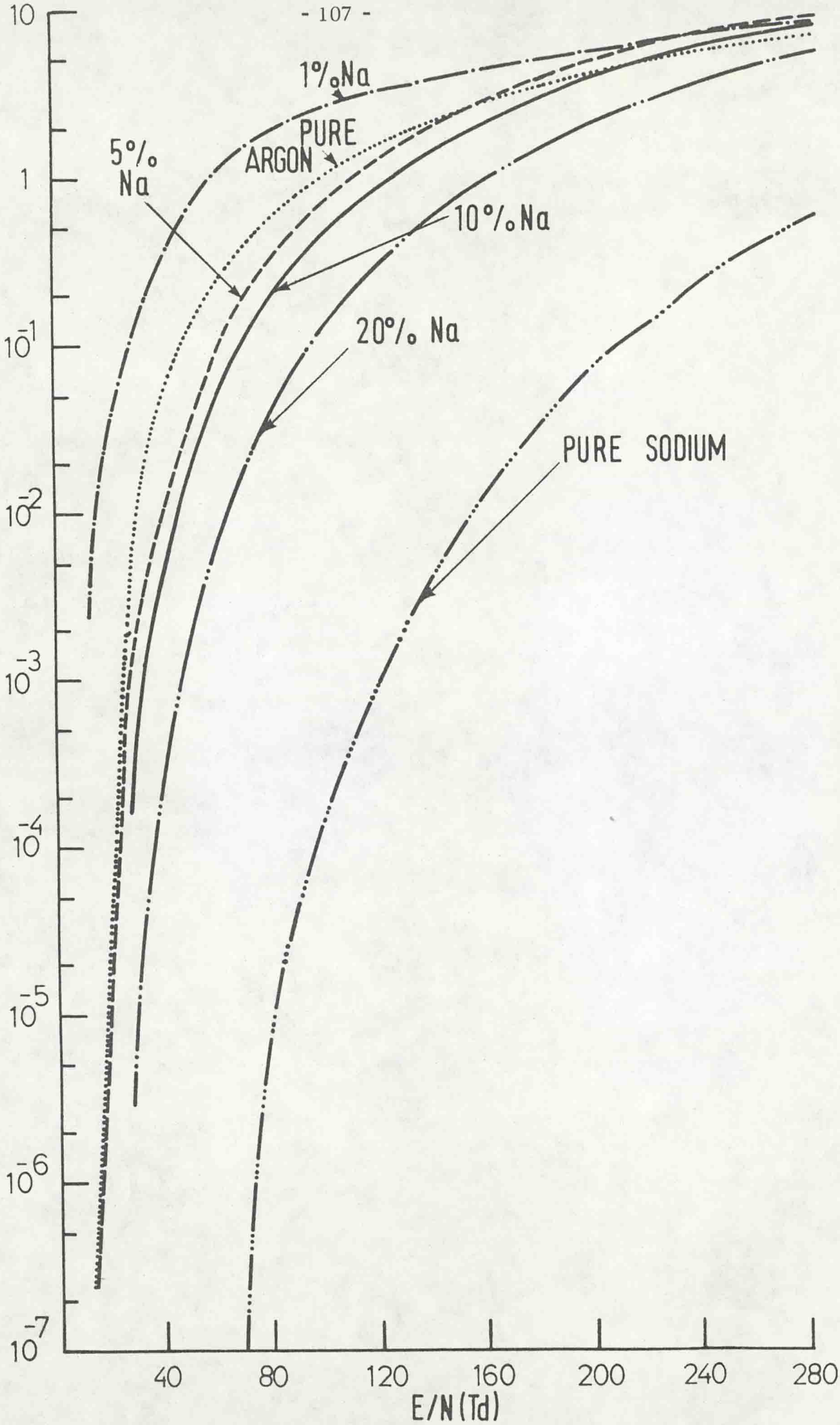

Fig.(6·11) IONIZATION COEFFICIENT IN MIXURES OF SODIUM AND ARGON

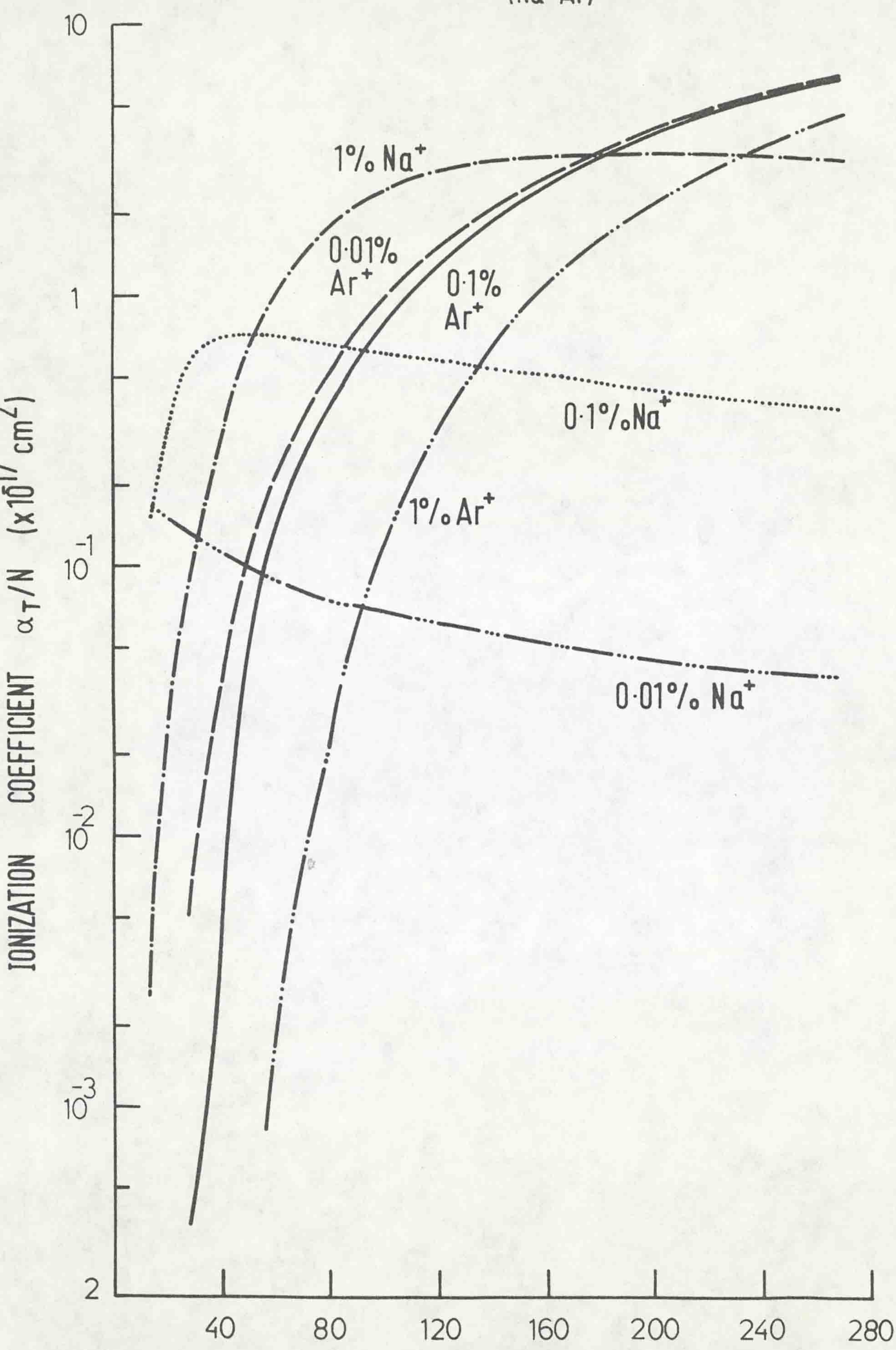

Fig. (6·12) IONIZATION COEFFICIENT IN MIXTURES OF SODIUM AND ARGON

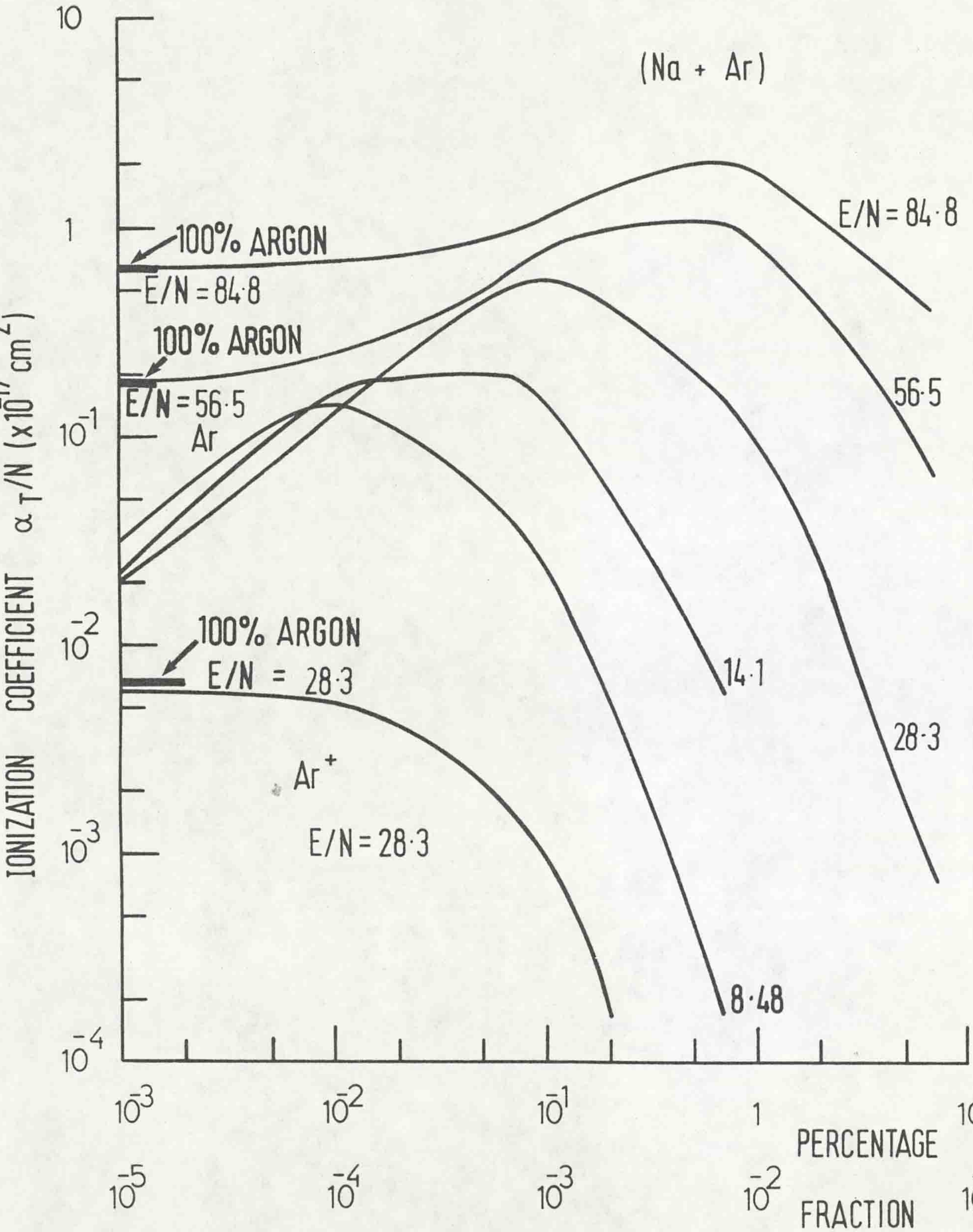

Fig.(6·13) IONIZATION COEFFICIENT IN MIXTURES OF SODIUM AND ARGON

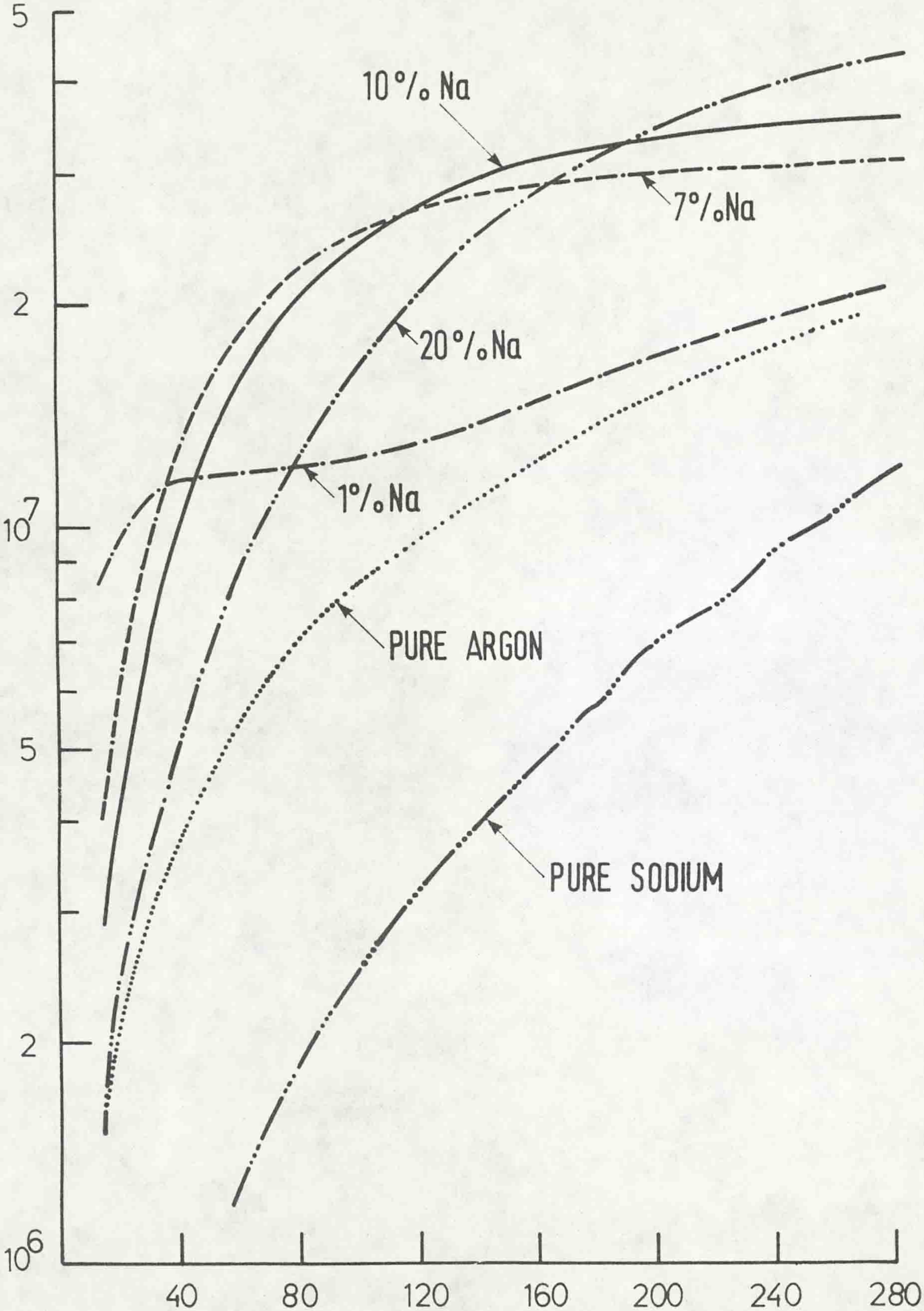

Fig.(6·14) DRIFT VELOCITY IN MIXURES OF SODIUM AND ARGON

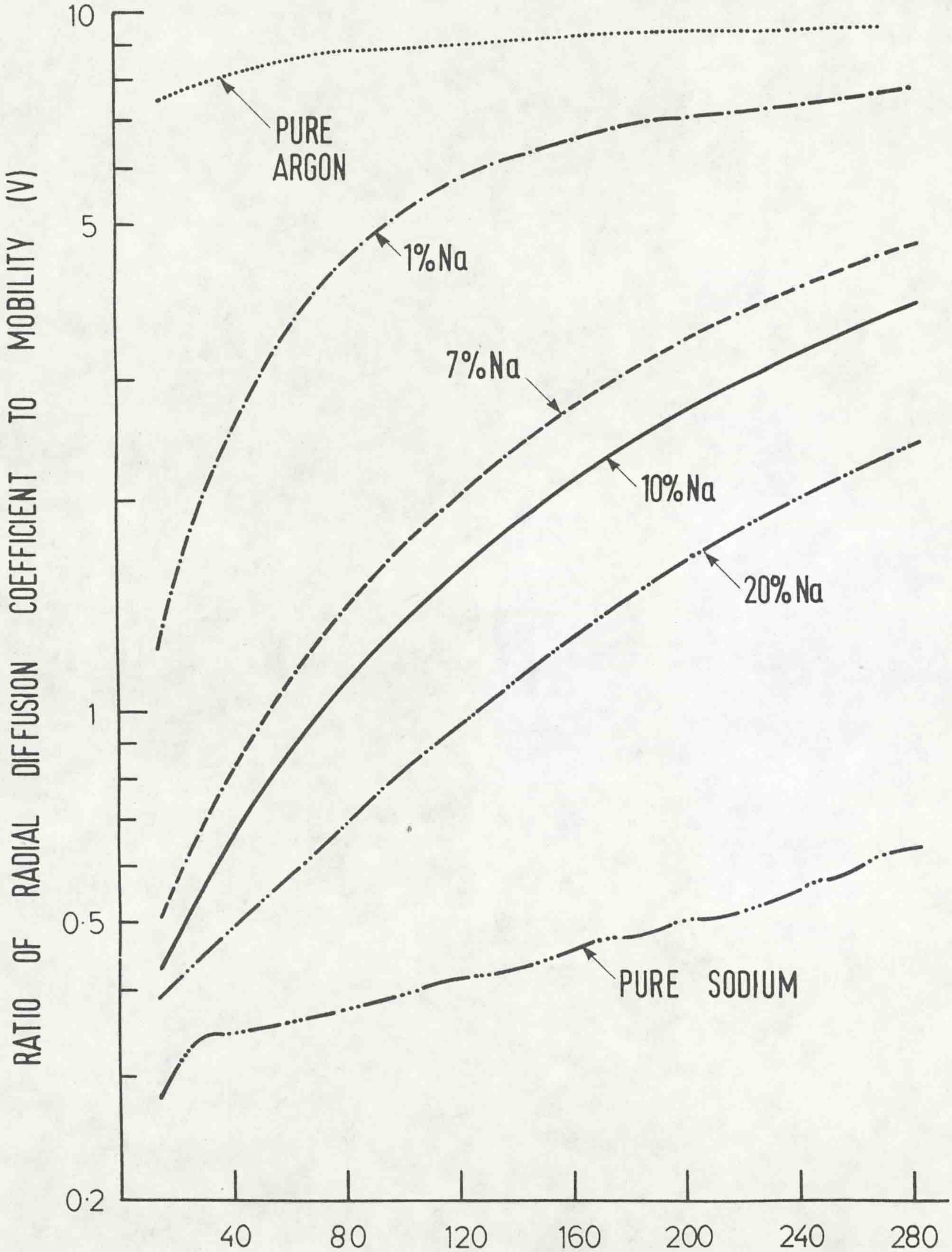

Fig.(6·15) RATIO OF RADIAL DIFFUSION COEFFICIENT TO MOBILITY IN MIXTURES OF SODIUM AND ARGON

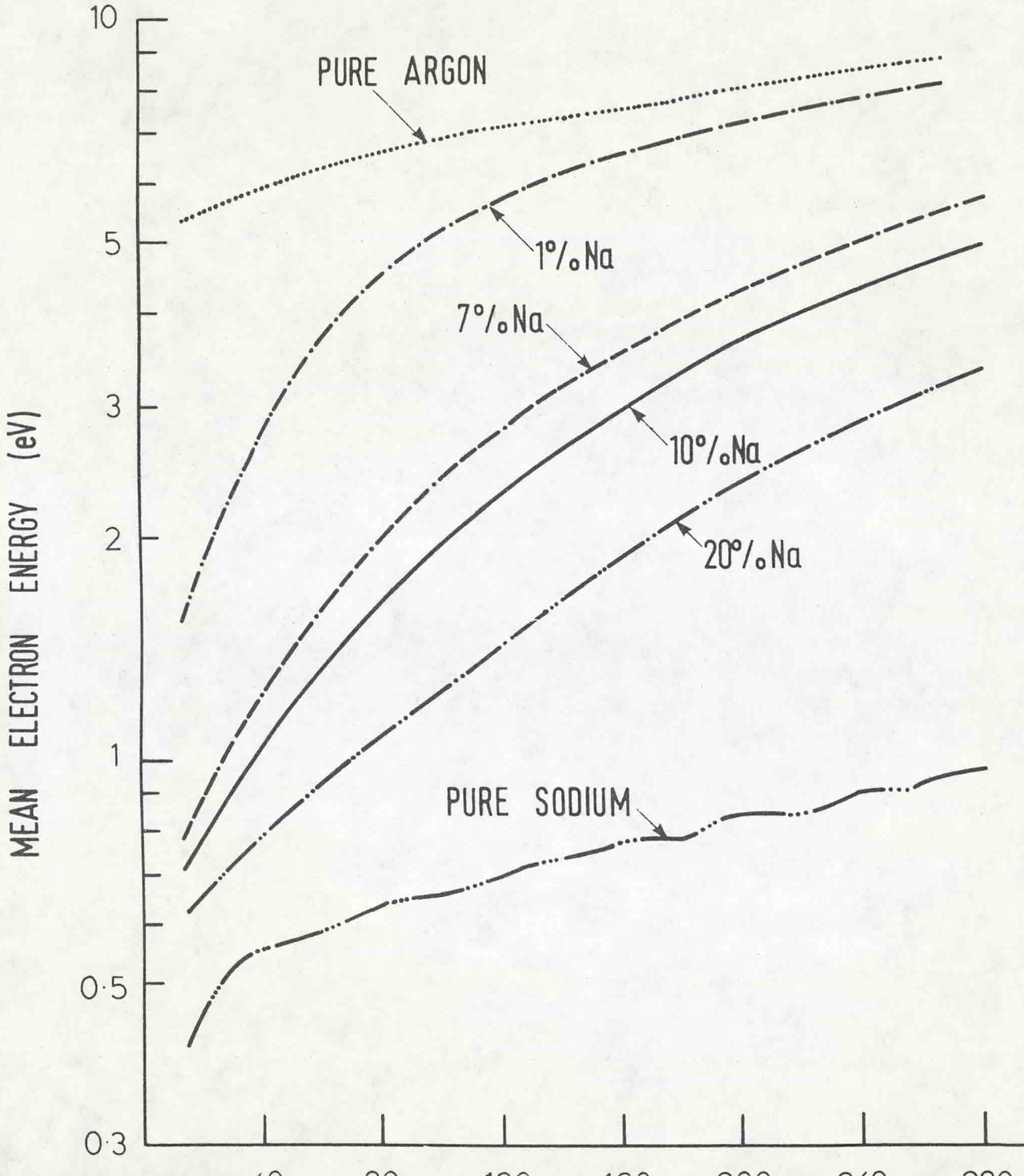

Fig. (6·16) MEAN ELECTRON ENERGY IN MIXTURES OF SODIUM AND ARGON

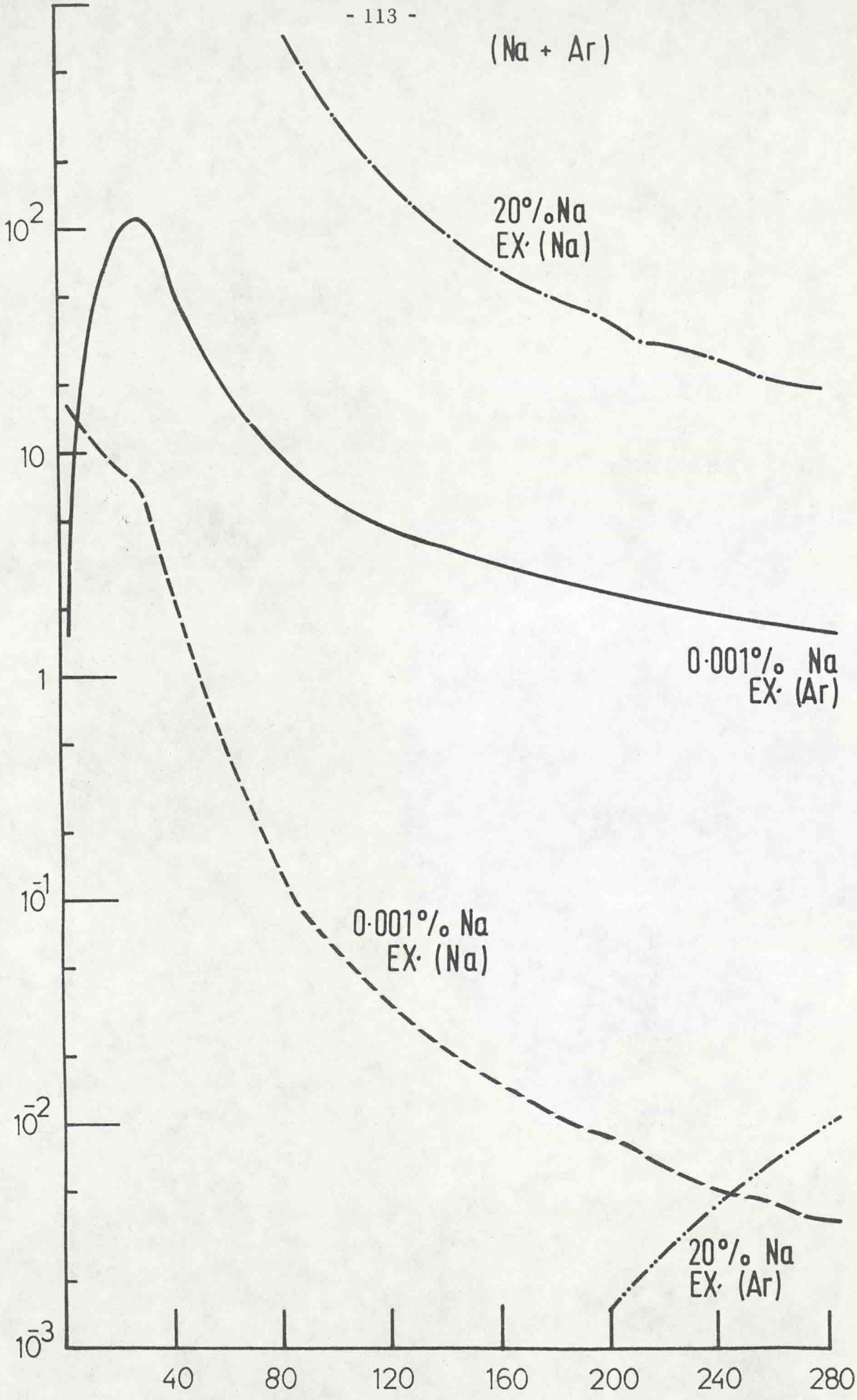

Fig. (6·17) RATIO OF RATES OF EXCITATION AND IONIZATION IN MIXTURES OF SODIUM AND ARGON

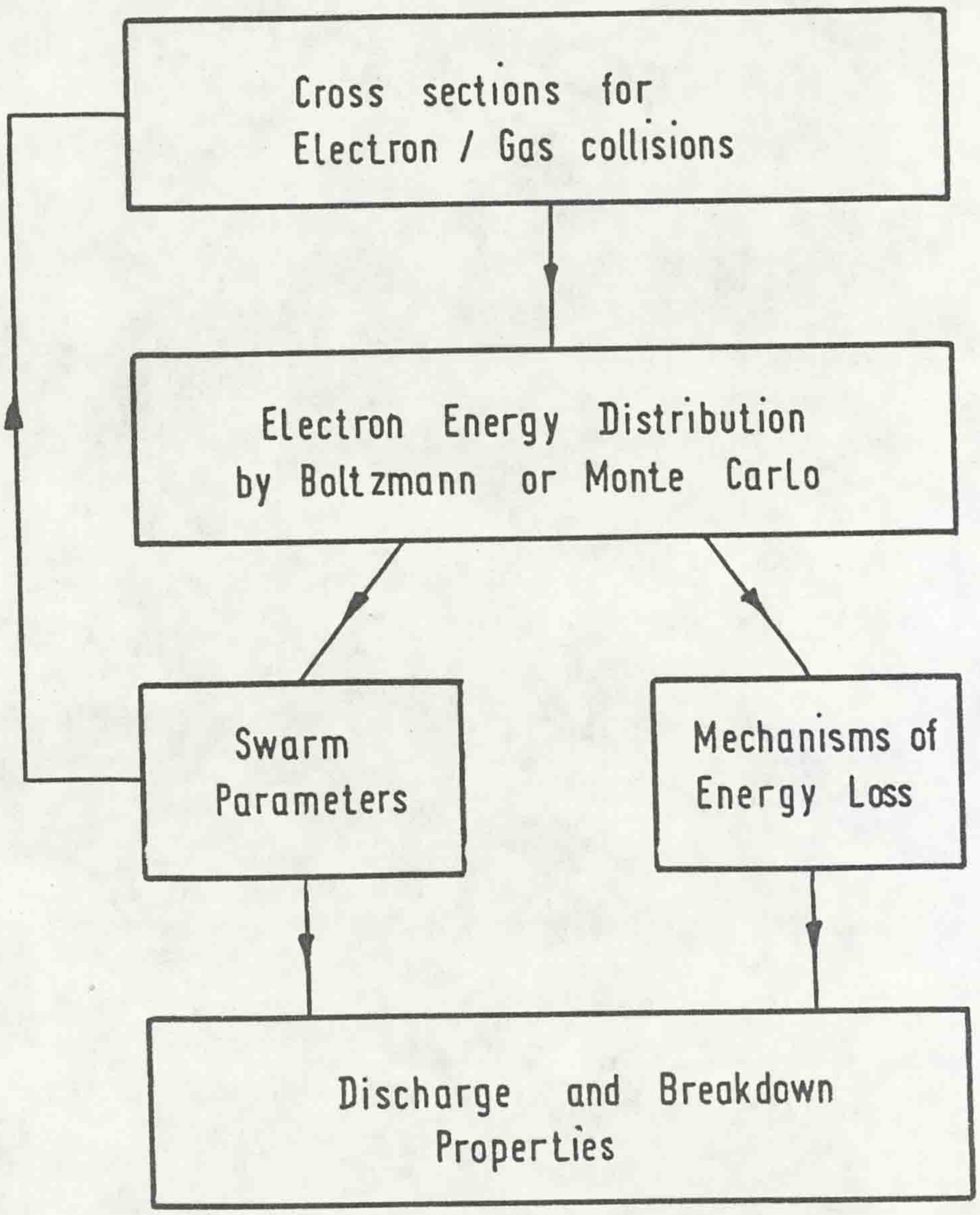

Fig.(1.1) THE INTERRELATIONSHIP BETWEEN SWARM PARAMETERS

shown in Fig. 6.17, which shows that at low E/N there is a rapid increase of excitation coefficient which is due to the large excitation cross-sections having an onset energy of 2.10, 3.62, and 4.12 eV respectively.

6.6 CROSS-SECTION IN A MIXTURE OF ARGON GAS AND CAESIUM VAPOUR

The electron-caesium metal collisions are grouped into three types i.e. momentum transfer, excitation and ionization. The shape of the momentum transfer cross-section, NQ_{m}, was found by Saelee and Lucas (1979). The momentum increases sharply from 0.03 eV to give a peak value of $NQ_{m} = 2.45 \times 10^{6}\ m^{-1}$ at about 0.16 eV. As the electron energy increases up to a higher energy the momentum cross-section takes a form of almost horizontal section. This sort of momentum curve in caesium vapour is used in order to satisfy the measured drift velocity by Saelee and Lucas (1979). Two excitation cross-sections, NQ_{Ex}, have been used and these from the ground state to the 6^2P 1/2 and 6^2P 3/2 levels which have been measured by Zapesochnyi (1967) who gave the onset energies as 1.39 and 1.45 eV, respectively. The cross-sections for ionization, NQ_{Ion}, by collision with electrons have been measured by Nygaard (1968). The onset energy of ionization is given as 3.89 eV. The references for caesium vapour cross-sections are given in Table 6.4. The set of cross-sections for caesium vapour, together with argon gas cross-sections, are shown in Fig. 6.18 and tabulated in Appendix B.

6.7 RESULTS AND DISCUSSION

A computation method has been developed to calculate electron swarm parameters by using Boltzmann's equation. Over the range 2.83

to 283 Td, a result for ionization coefficient, α_T/N, drift velocity, v_d, ratio of radial diffusion coefficient to mobility, D_r/μ, mean electron energy, $\bar{\epsilon}$, and the ratio of rates of excitation and ionization have been obtained in caesium vapour and argon gas mixture. These results are tabulated in Appendix A. The ionization coefficient is shown with E/N in Fig. 6.19, which shows that the values of ionization coefficient in pure argon gas change from 2.06×10^{-25} to 7.37×10^{-17} cm^2, and are higher than the values of ionization coefficients of pure caesium vapour, which changes from 1.2×10^{-24} to 1.2×10^{-22} cm^2. A percentage mixture of caesium vapour used is from 5 % to 20 % Cs, and as a result, there are three further curves occurring between the pure argon gas curve and pure caesium vapour curve, which illustrates that the lower the percentage of caesium vapour introduced, the higher the ionization coefficient produced. The values of ionization coefficient at 1 % Cs range between 1.86×10^{-31} to 8.62×10^{-17} cm^2, and they are higher than those of pure argon gas. At the highest percentage of caesium (1 %) the production of Ar^+ is always lower (denoted by 1 % Ar^+) than the production of Cs^+ (denoted by 1 % Cs^+), as shown in Fig. 6.20. For lower percentages of caesium the production of Cs^+ is higher than the production of Ar^+ only at low E/N.

Fig. 6.21 shows the ionization coefficient varies with the percentage (and fraction) of caesium vapour. Comparing the values of ionization coefficient in the mixture of argon gas and caesium vapour with the values of ionization coefficient in argon gas a maximum value occurs in the curves as E/N increases. Also this figure indicates that the large amount of caesium ions, Cs^+, was produced by direct ionization to get an enhanced coefficient.

The values of drift velocity in caesium vapour and argon gas mixture

have been obtained and are shown in Fig. 6.22 as a function of E/N. The maximum value of drift velocity in pure argon gas was 2.06×10^7 cm/sec which is much larger than the maximum value of drift velocity in pure caesium vapour measured as 3.94×10^6 cm/sec. Also this figure illustrates that as the percentage of caesium vapour is decreased, there is a rapid decrease in the values of drift velocity, especially at 1 % Cs where the drift velocity varies from 0.22 to 2.10×10^7 cm/sec, while at 10 % Cs the drift velocity varies from 0.17 to 2.98×10^7 cm/sec.

The variation of ratio of radial diffusion coefficient to mobility with E/N is presented in Fig. 6.23. The values of ratio of radial diffusion coefficient in pure caesium vapour are varying between 0.23 to 0.42 V which is smaller than the values in pure argon gas ranging from 7.03 to 9.85 V. Four further curves with percentages of caesium vapour between 1 % to 20 % Cs are located between the two curves of pure argon gas and pure caesium vapour, which indicates that the highest percentage of caesium vapour produces the lowest mean energy. The values of radial diffusion coefficient are higher than the values of mean electron energy until it reaches E/N = 141 Td.

The values of mean electron energy are higher than the values of radial diffusion coefficient for the range of $155 \leq E/N \leq 283$ Td as compared with Fig. 6.24 which shows also that the values of pure argon gas are higher than the values of pure caesium vapour. As the percentage of caesium vapour increases between 1 % to 20 % Cs the values of mean electron energy decrease.

The graph of ratio of rates of excitation and ionization as a function of E/N is shown in Fig. 6.25. This figure shows that at small percentages of caesium vapour (0.001 % Cs) a sharp increase is caused in excitation coefficient at

E/N $\simeq$ 40 Td, as shown by the peak in the curve, this is due to the large excitation cross-sections in caesium vapour.

TABLE 6.4 : SOURCES OF CAESIUM VAPOUR COLLISION CROSS-SECTIONS

CROSS-SECTION	ONSET-ENERGY eV	SOURCE
MOMENTUM TRANSFER	$\frac{2m}{M} = 82.6 \times 10^{-7}$	SAELEE AND LUCAS (1979)
EXCITATION $6^2P_{\frac{1}{2}}$ $6^2P\ 3/2$	1.39, 1.45	ZAPESOCHNYI (1967)
IONIZATION	3.89	NYGAARD (1968)

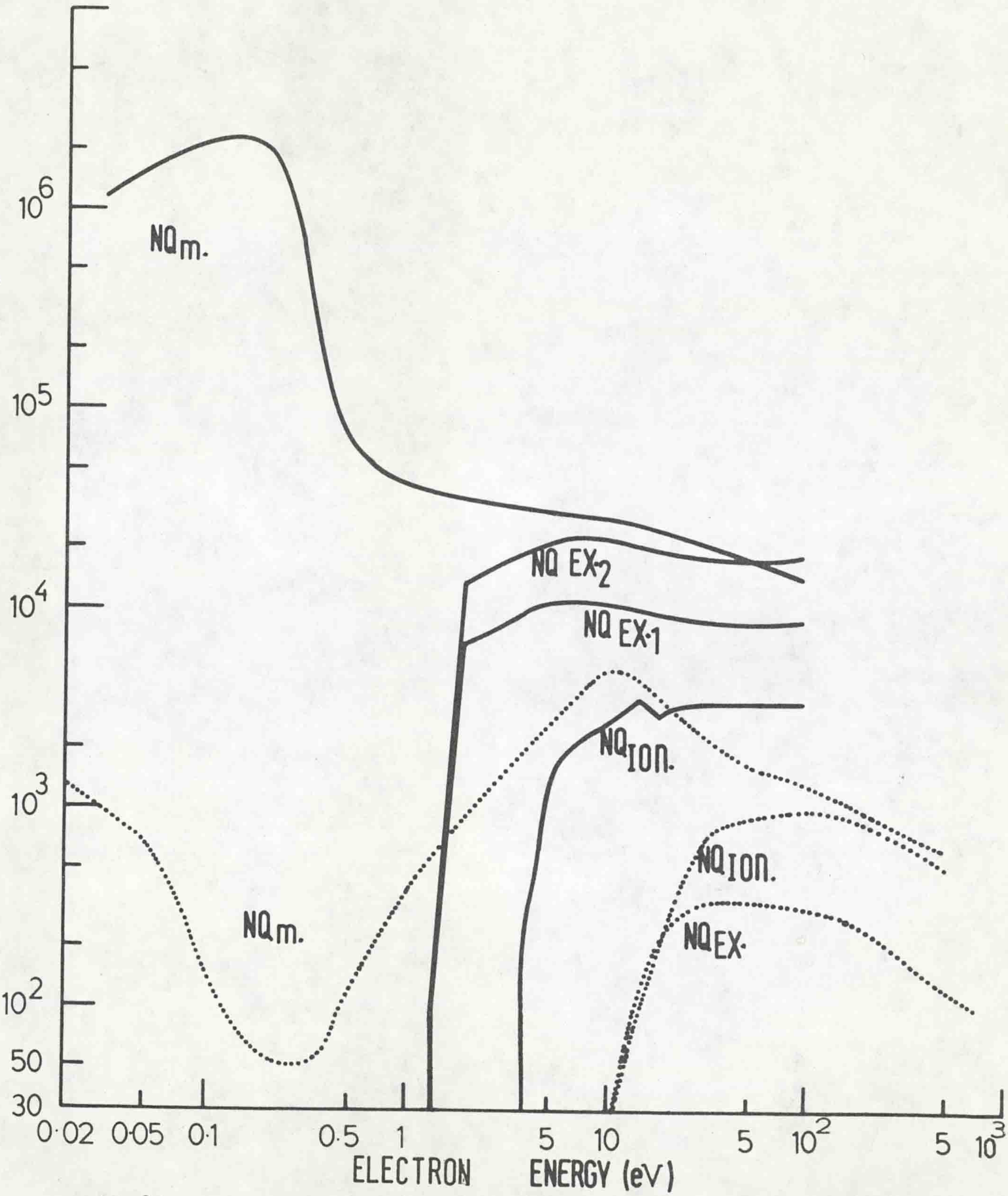

Fig.(6.18) COLLISION IN ARGON GAS AND CAESIUM VAPOUR
(——Cs, ...Ar)

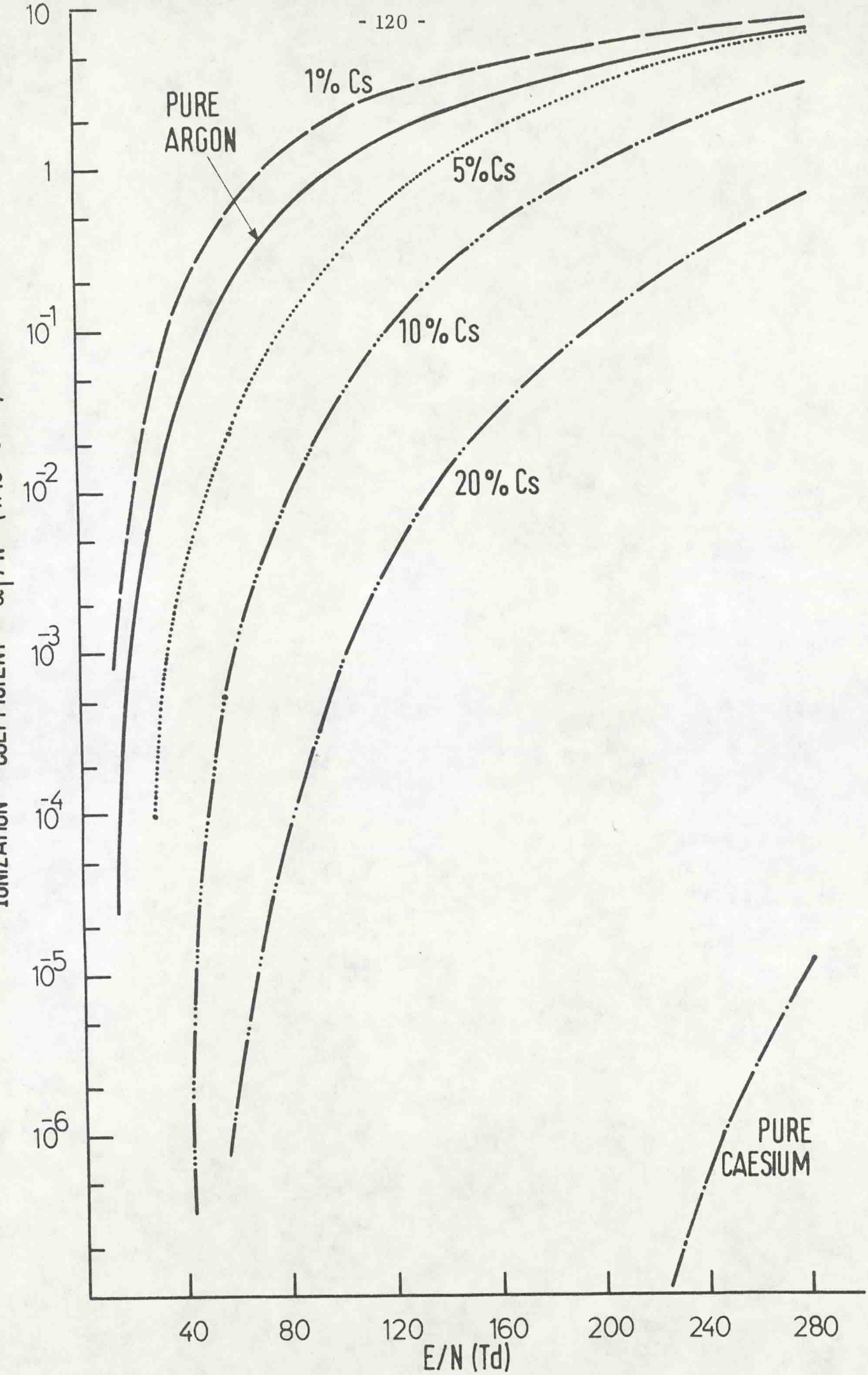

Fig. (6·19) IONIZATION COEFFICIENT IN MIXTURES OF CAESIUM AND ARGON

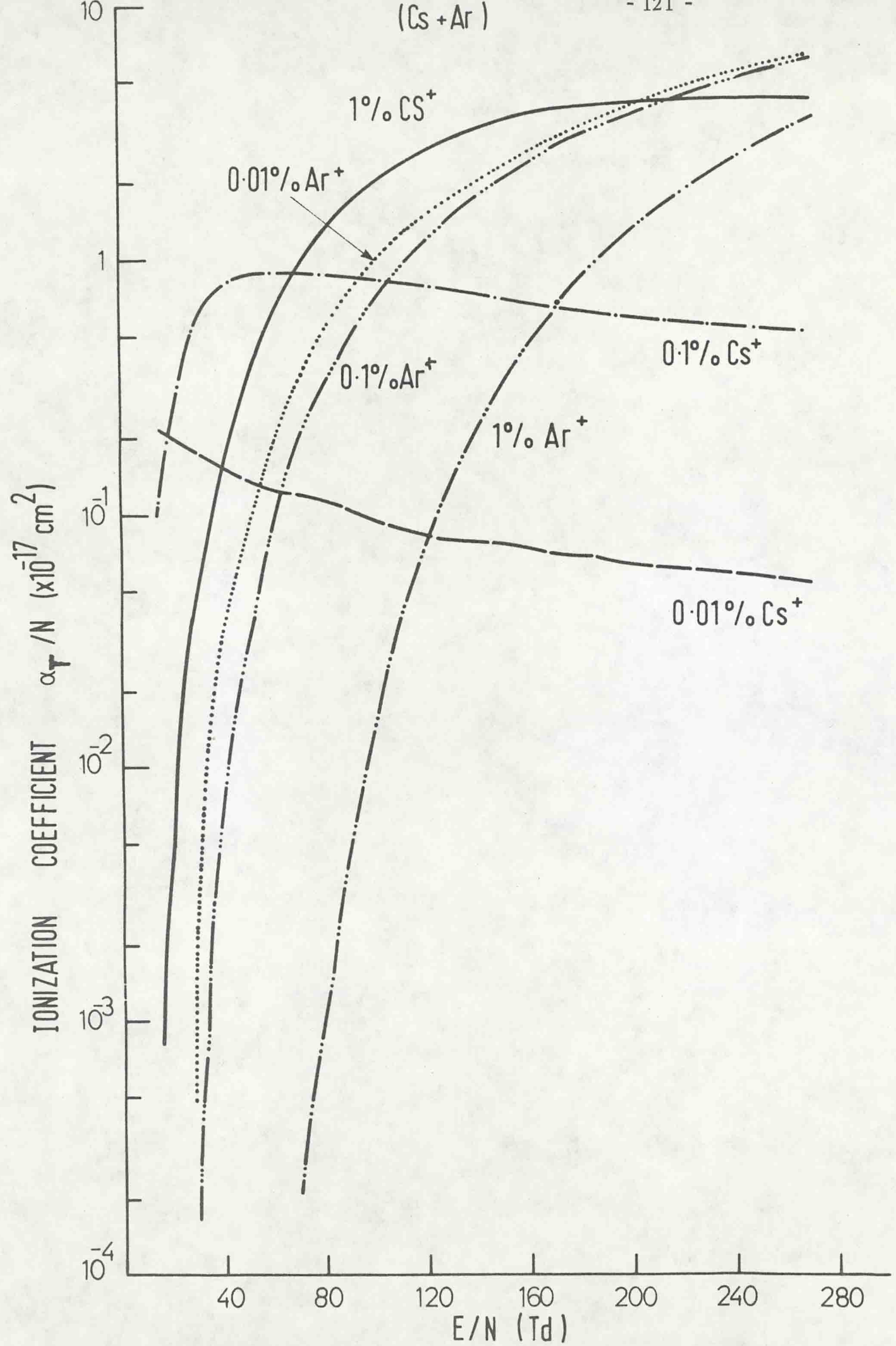

Fig. (6·20) IONIZATION COEFFICIENT IN MIXTURES OF CAESIUM AND ARGON

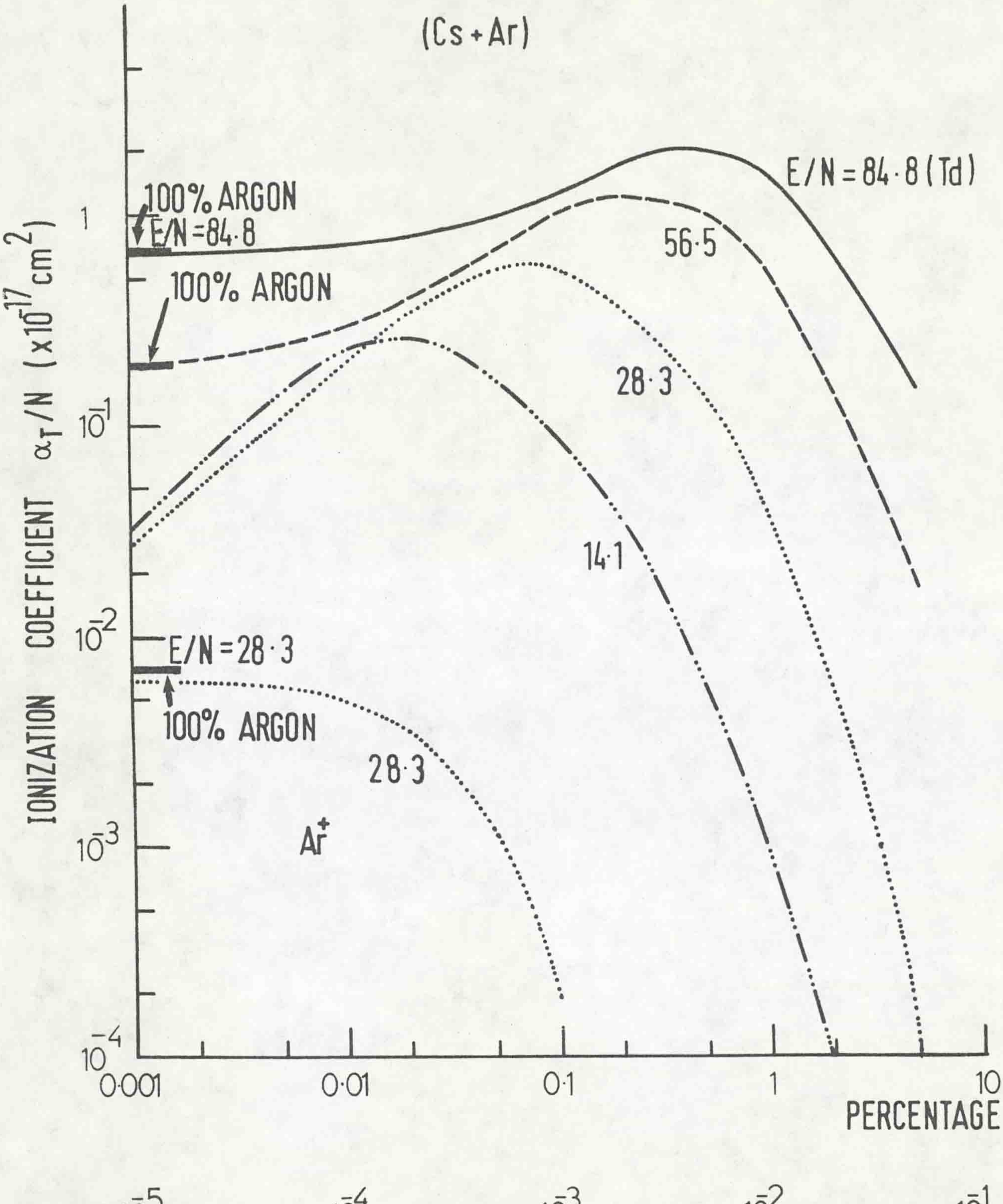

Fig. (6·21) IONIZATION COEFFICIENT IN MIXTURES OF CAESIUM AND ARGON

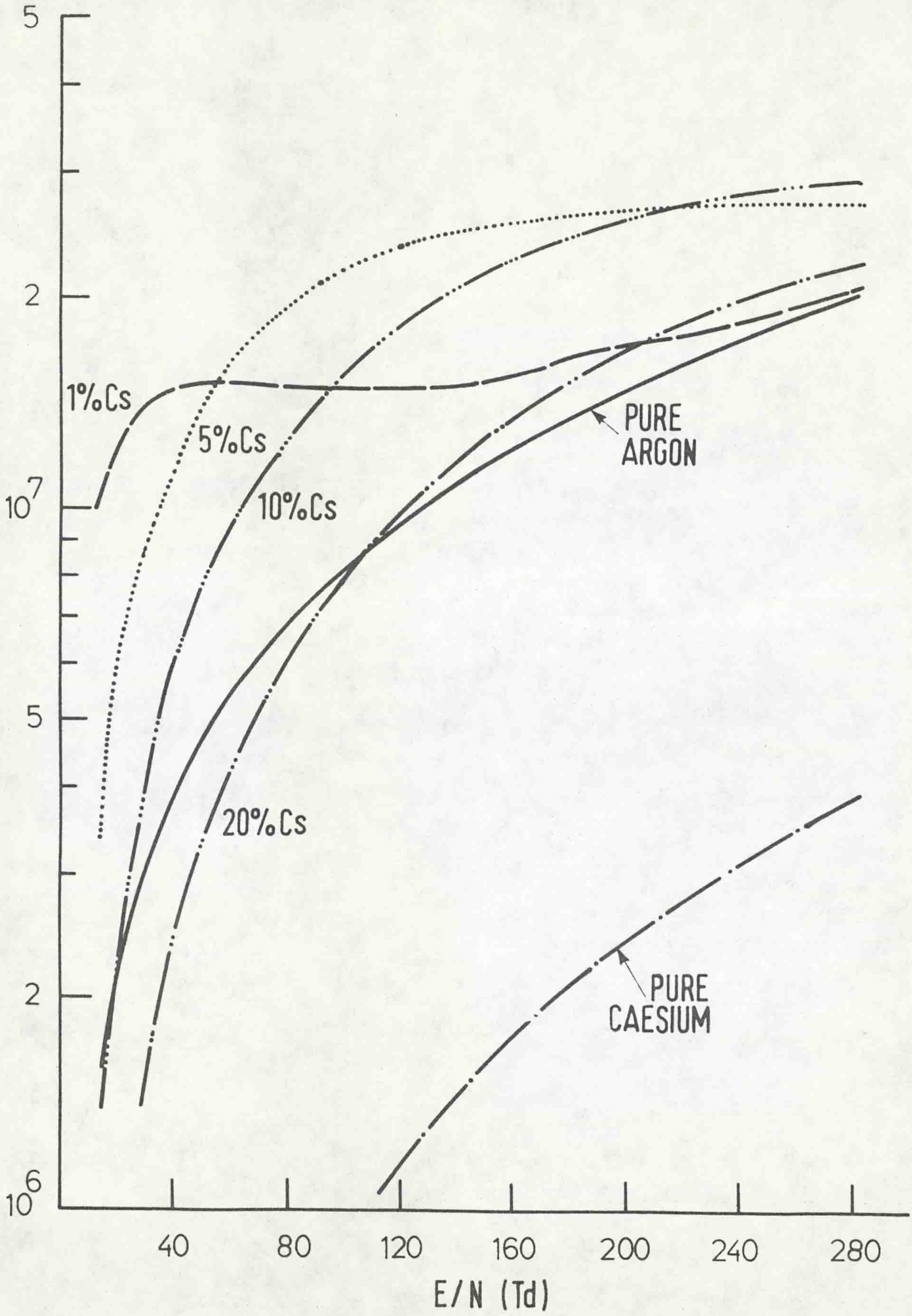

Fig. (6·22) DRIFT VELOCITY IN MIXTURES OF CAESIUM AND ARGON

TABLE 1.1 : SOURCE OF PREVIOUS WORK DONE IN GASES AND METAL VAPOURS

Gas or Metal	EXPERIMENTAL			THEORETICAL
	α_T	v_d, $(\frac{D_L}{\mu})_d$	$(\frac{D_r}{\mu})_d$	α_T, v_d, $(\frac{D_L}{\mu})_d$, $(\frac{D_r}{\mu})_d$, ϵ
H_2	Kontoleon et al (1971) and (1973)	Snelson and Lucas (1975) and Saelee et al (1977)	Kucukarpaci (1978) M.Eng.	Saelee and Lucas (1977) Kucukarpaci and Lucas (1979) Al-Amin (1980), M.Eng.
N_2				
CO	Lakshminaras-imha et al (1974)			
CO_2				
Ar	Lakshminaras-imha and Lucas (1977)	Kucukarpaci and Lucas (1981)	Al-Amin (1980) M.Eng.	Kucukarpaci and Lucas (1981)
He				
Kr				
Ne				
Hg		Nakamura and Lucas (1978) (v_d only)		Nakamura and Lucas (1978) (v_d, D_r/μ and ϵ only)
Tl				
Na				
Cs		Saelee and Lucas (1979) (v_d only)		Saelee and Lucas (1979) (v_d, D_r/μ and ϵ only) and This Thesis
K		Lucas (1981) (v_d only)		Lucas (1981) (except D_L/μ) and This Thesis

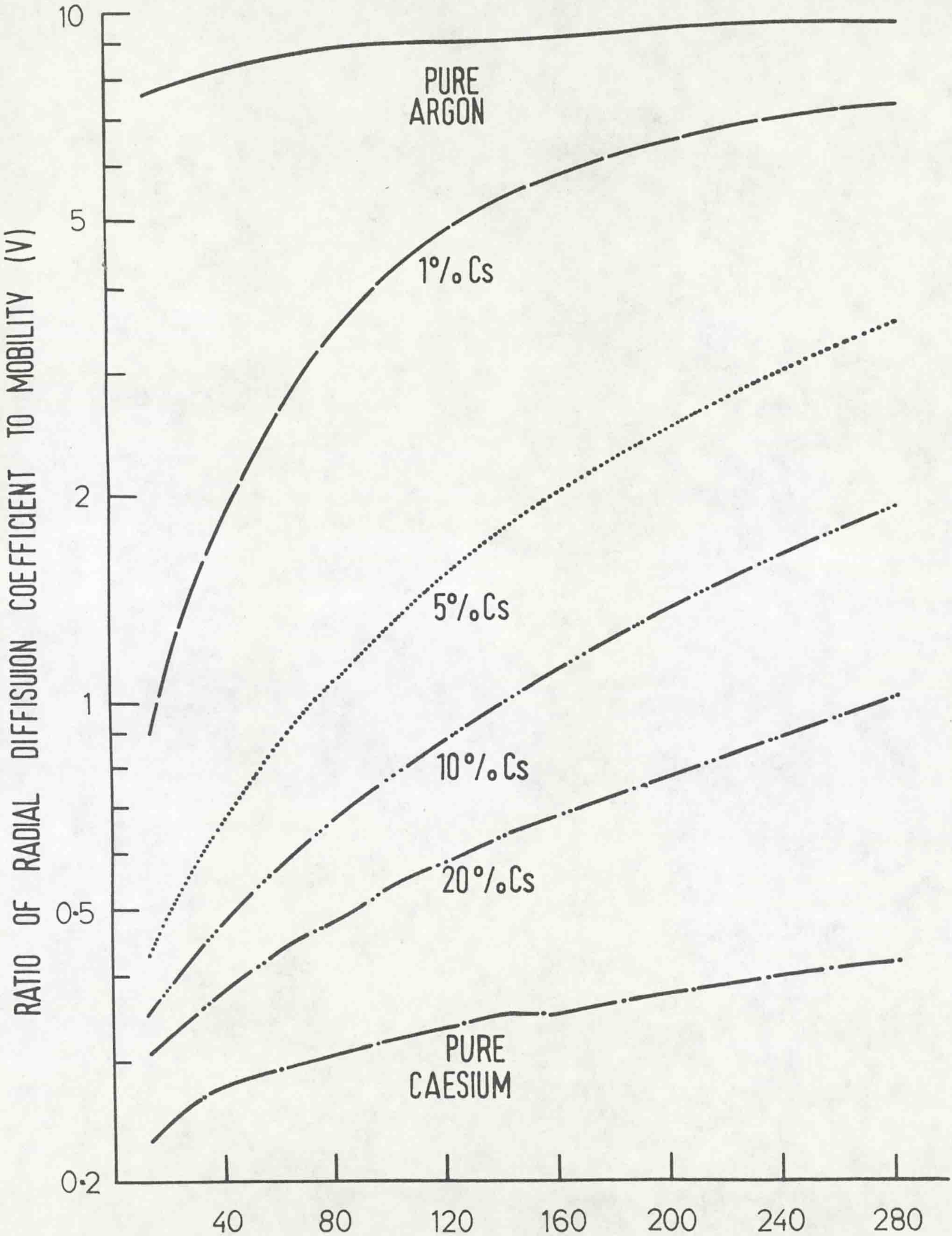

Fig. (6·23) RATIO OF RADIAL DIFFUSION COEFFICIENT TO MOBILITY IN MIXTURES OF CAESIUM AND ARGON

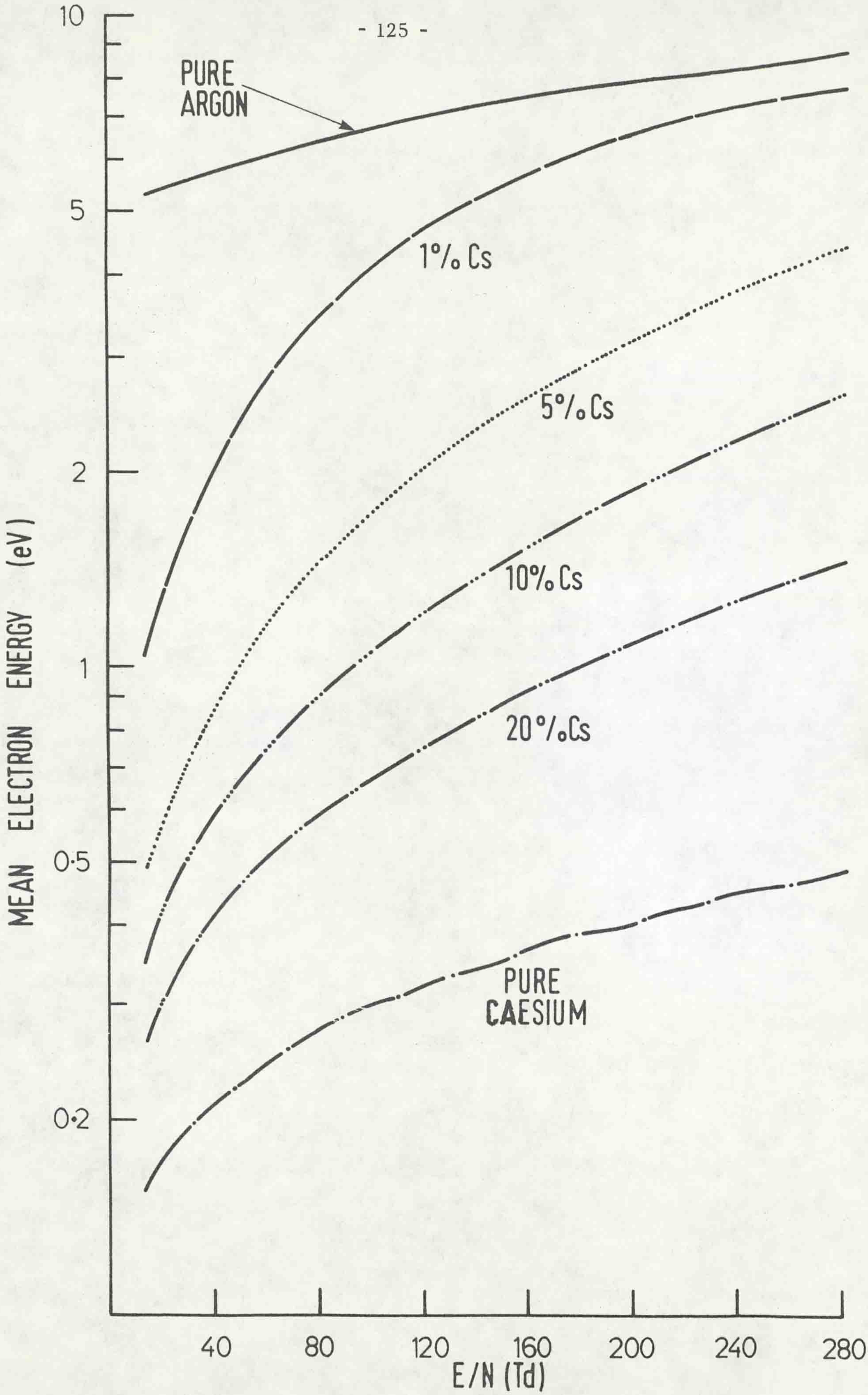

Fig. (6·24) MEAN ELECTRON ENERGY IN MIXTURES OF CAESIUM AND ARGON

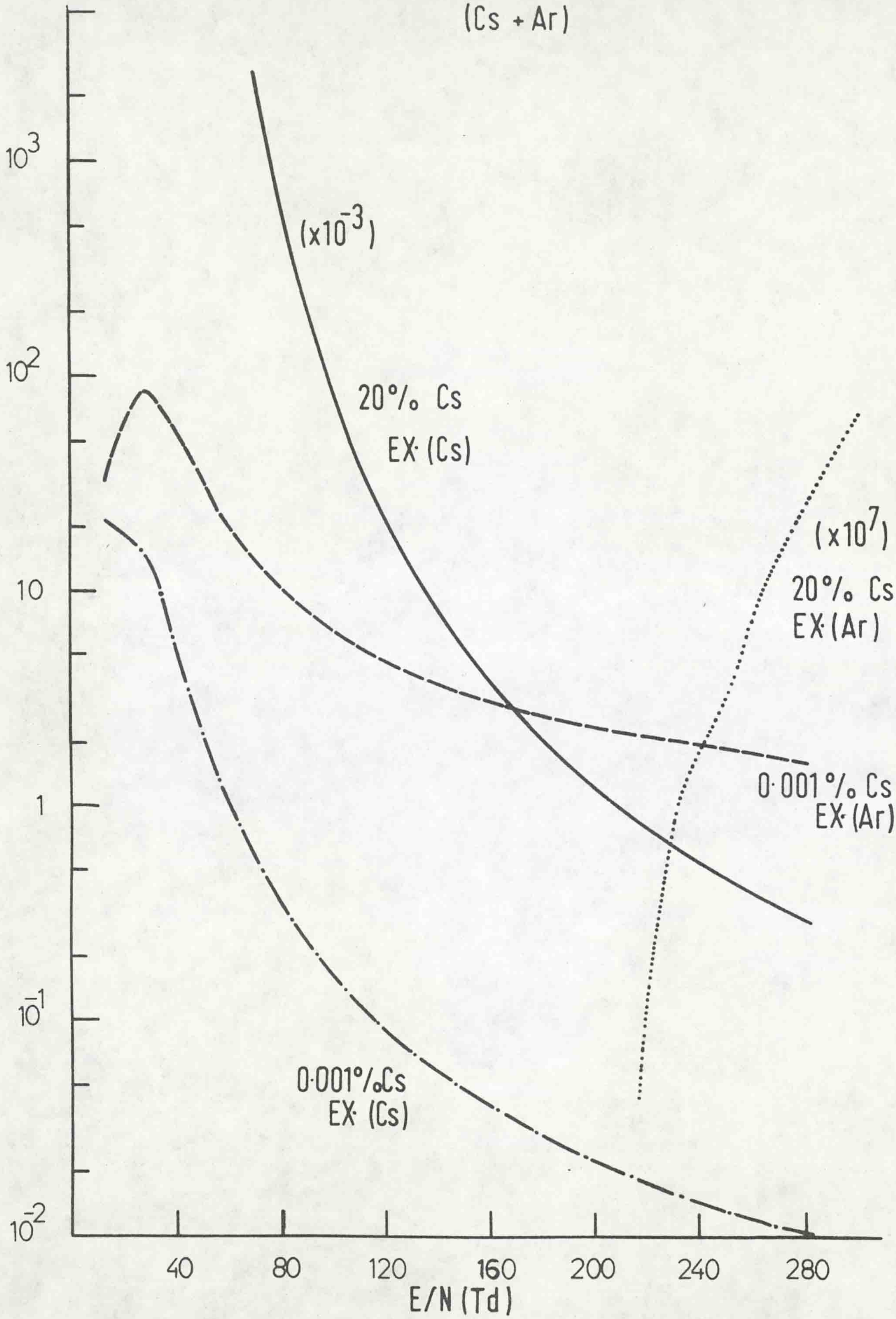

Fig. (6·25) RATIO OF RATES OF EXCITATION AND IONIZATION IN MIXTURES OF CAESIUM AND ARGON

CHAPTER SEVEN

CHAPTER SEVEN

FUTURE WORK

The measurement of electron swarm parameters by the time of flight technique has so far been restricted to measurement of the electron drift velocity and both longitudinal and radial diffusion coefficient. The technique may be extended to allow measurement of the ionization coefficient to be obtained in this way and hence the effects due to the presence of secondary electrons can be avoided.

Preliminary work on the measurement of electron swarm parameters in high temperature metal vapours has also been done. Nakamura and Lucas (1978) and Saelee and Lucas (1979) have measured electron drift velocities in mercury, thallium, sodium vapours, and caesium vapours, but there are many difficulties, the main one being the confinement of the vapour at high temperatures. This has been achieved by using a heat-pipe in which metal vaporised in the evaporation zone travels to the condensation zone which is force cooled. Upon condensing, the liquid metal travels back to the evaporation zone by using surface tension effects to draw it back along a porous, stainless steel wick. Metal vapours are interesting in that they are a possible media for the high power lasers operating in the visible region, thus avoiding the expensive germanium optics of infra-red lasers. The design of a new heat-pipe apparatus which will be capable of measuring drift velocities and ionization coefficient in high temperature vapours should be undertaken. A pulse of U.V. radiation incident on the cathode will generate the initial electrons. Due to the simplicity of the system any difficulties with condensation of the vapour on the electrodes should be greatly reduced, and it is intended that this design will allow

measurements to be made in the higher temperature vapours.

The experimental measurements taken for this thesis have involved the measurement of electron currents both by steady state and time of flight (TOF) conditions. One interesting development which should be pursued is the examination of the property of the electron swarms by looking at the emitted radiation. Such a technique has been introduced by Blevin et al (1976), and has the advantage of giving measurement which has reduced electrical noise. It is also a method by which a coefficient (α_R) can be measured for radiation as is available from Monte Carlo and Boltzmann calculations. Each gas produces many channels for loss of energy by radiation and each of these channels may be investigated by defining an effective radiation coefficient (α_R). Such a measurement would allow the collision cross-section to be more clearly identified and defined.

REFERENCES

REFERENCES

1. Al-Amin, S.A.J., "Electron Diffusion in Gases", 1980, M.Eng. Thesis, The University of Liverpool.

2. Arecehi, F.T. and Schulz-Dubois, E.O., "Laser Hand Book", 1972, Vol. 1 and 2, North Holland Publishing Company.

3. Arnot, F.L., "The Diffraction of Electrons in Gases", 1931, Proc.Roy. Soc., A133, 615-36.

4. Bhalla, M.S. and Craggs, J.D., "Measurement of Ionization and Attachment Coefficients in Carbon Monoxide in Uniform Fields", 1961, Proc. Phys. Soc., 78, 438-47.

5. Bhalla, M.S. and Craggs, J.D., "Measurement of Ionization and Attachment Coefficients in Carbon Dioxide in Uniform Fields", 1960, Proc. Phys. Soc., 76, 369-77.

6. Blevin, H.A., Fletcher, J. and Marzec, L.M., "The Motion of Electron Swarms in Uniform Electric Fields", 1976, J.Phys.D.Appl.Phys., 9, 465-79.

7. Bowman, C.R. and Miller, W.D., "Excitation of Methane, Ethane, Ethylene, Propylene, Acetylene, Propyne, and 1-Butyne by Low-Energy Electron Beams", 1965, J.Chem.Phys., 42, No.2, 6681-86.

8. Bowman, C.R. and Gordon, D.E., "Drift Velocity of Slow Electrons in Methane, Ethane, Ethylene, Propylene, Acetylene and 1-Butene", 1967, J.Chem.Phys., 46, 1878-83.

9. Bradbury, N.E. and Nielsen, R.A., "Absolute Values of the Electron Mobility in Hydrogen", 1936, Phys.Rev., 49, 388-93.

10. Brose, H.L., "The Motions of Electrons in Oxygen", 1925, Phil.Mag., 50, 536-46.

11. Brose, H.L. and Keyston, J.E., "Collisions of Slow Electrons with Methane Molecules", 1935, Phil.Mag., 20, 902-13.

12. Bruche, E., "Wirkungsquerschnitt und Molekulbau", 1927, Ann.Physik., 83, 1065- 128.

13. Bruche, E., "Wirkungsquerschnitt und Molekulbau in der Kohlenasserstoffreihe: CH_4-C_2H_6-C_3H_8-C_4H_{10}", 1930, Ann.Physik, 4, 387-408.

14. Bullard, E.C. and Massey, H.S.W., "The Elastic Scattering of Slow Electrons in Gases-II", 1932, Proc. Roy.Soc., A133, 637-51.

15. Chanin, L.M. and Rork, G.D., "Measurements of the First Townsend Ionization Coefficient in Neon and Hydrogen", 1963, Phys.Rev., 132, 2547-53.

16. Chen, S.T. and Gallagher, A.C., "Electron Excitation of the Resonance Lines Of the Alkali-Metal Atoms", 1978, Phys.Rev. A.,17, 551-60.

17. Cheo, P.K., "CO_2 Lasers", in Levine, A.K. and Demaria, A.J. (Eds.): "Advances in Lasers", Vol. 3, (Marcell Dekker, 1971), Chap. 2.

18. Cochran, L.W., Forester, D.W., "Diffusion of Slow Electrons in Gases", 1962, Phys. Rev., 126, 1785-88.

19. Cookson, A.H. "Positive-Ion and Electron Drift Velocities in Compressed Nitrogen and Methane", 1966, Brit. J. Appl. Phys., 17, 1069-74.

20. Cookson, A.H., Ward, B.W. and Lewis, T.J., "Townsend's First Ionization Coefficient for Methane and Nitrogen", 1966, Brit. J.Appl. Phys., 17, 891-903.

21. Corrigan, S.J.B., "Dissociation of Molecular Hydrogen by Electron Impact", 1965, J.Chem.Phys., 43, 4381-86.

22. Davies, D.K. and Jones, E., "Note on Ionization Coefficients in Methane", 1963, Proc. Phys.Soc., London, 82, 537-42.

23. DeHeer, F.J. and Jansen, R.H.J., "Total Cross-Section for Electron Scattering by Ne, Ar, Kr and Xe", 1979, J.Phys.B. Atom-Molec. Phys., 12, 979-1002.

24. Doehring, A., "Messung Anlagerungswahrscheinlichkeit von Elektronen an Sauerstoff Mittels-einer Laufzeitmethode", 1952, Z-Naturforsch., 7A, 253-70.

25. Duncan, C.W. and Walker, I.C., "Collision Cross-Section for Low Energy Electrons in Methane", 1972, J.Chem.Soc. Faraday Trans. II (2), 68, 1514-21.

26. Ehrhardt, H., Langhans, L., Linder, F., and Taylor, H.S. "Resonance

Scattering of Slow Electrons from H_2 and CO Angular Distributions", 1968, Phys.Rev., 173, 222-30.

27. Ellis, J.M., "Electron Diffusion in Gases", 1965, Ph.D. Thesis, The University of Liverpool.

28. Fink, X., and Huber, P., "Wanderungsgeschwindigkeit und Diffusionskonstante von Elektronen in Methan", 1965, Helv. Phys. Acta., 38, 717-35.

29. Fleming, I., Gray, D.R., and Rees, J.A., "The Drift and Diffusion of Electrons in Oxygen Containing Traces of Hydrogen", 1972, J.Phys.D., Appl.Phys., 5, 291-96.

30. Franke, W., "Uber den Zeitlichen Verlauf der Lichtemission Einer Gasentladung", 1960, Z.Phys., 158, 96-110.

31. Frommhold, L., "Eine Untersuchung der Elektronen Komponente von Elektronenlawinen", 1959, Z.Phys., 156, 144-58.

32. Frommhold, L., "A Study of the Electron Component of Electron Avalanches", (In) Proceedings of the Fourth International Conference on Ionization Phenomena in Gases (Uppsala, Sweden 17-21 August, 1959), N.Robert Nilsson, Editor, North-Holland Publishing Company, Amsterdam, 1, 115-17, 1960.

33. Frommhold, L., "Eine Untersuchung der Elektronen Komponent von Elektronenlawich im Homogenen Feld II", 1960, Z-Physik, 160, 554-67.

34. Frommhold, L., "Uber Verzogerte Elektronen in Elektronenlawinen, Insbesondere in Sauerstoff und Luft, Durch Bildung und Zerfall Negativer Ionen $\bar{O}$", 1964, Fortschr, Physik, 12, 597.

35. Frost, L.S. and Phelps, A.V., "Momentum-Transfer Cross-Section for Slow Electrons in He, Ar, Kr and Xe from Transport Coefficient", 1964, Phys.Rev., 136, A, 1538-45.

36. Hake, R.D. and Phelps, A.V., "Momentum-Transfer and Inelastic-Collision Cross-Sections for Electrons in O_2, CO and CO_2", 1967, Phys. Rev., 158, 70-84.

TABLE 1.2 : SUMMARY OF WORK DONE IN GASES AND MIXTURES AND REPORTED IN THIS THESIS

GAS OR MIXTURE	THEORETICAL RESULTS (Monte Carlo)	EXPERIMENTAL RESULTS (Time of Flight)	
	α_T, v_d, $(D_L/\mu)_d$, $(D_r/\mu)_d$, ϵ	$(D_r/\mu)_d$	v_d, $(D_L/\mu)_d$
O_2	THIS THESIS	THIS THESIS	
SF_6		THIS THESIS	
CH_4	THIS THESIS	THIS THESIS	
K + Ar	THIS THESIS		
Na+ Ar	THIS THESIS		
Cs + Ar	THIS THESIS		

37. Harrison, J.A., "A Computer Study of Uniform-Field Electrodes", 1967, Brit.J.Appl.Phys., 18, 1617-27.

38. Harrison, M.A. and Geballe, R., "Simultaneous measurements of Ionization and Attachment Coefficients", 1953, Phys. Rev., 91, 1-7.

39. Healey, R.H. and Kirkpatrick, C.B., 1939 (see Healey and Read, "Behaviour of Slow Electrons in Gases", 1941, Page 94, Amal. Wireless Ltd., Sydney).

40. Herreng, P., "Mesure de la-Mobilite des Electrons dans l'Oxygene et de leur Probabilite de Fixation sur les Molecules de Ce Gaz ", 1952, Cahiers Phys., 38, 1-16.

41. Heylen, A.E.D., "Townsend's First Ionization Coefficient in Pure Nitrogen", 1959, Nature, 183, 1545-6.

42. Heylen, A.E.D., "Influence of Molecular Bonding on the Townsend Ionization Coefficient of Hydrocarbon Gases", 1963, J.Chem.Phys., 38, 765-71.

43. Huxley, L.G.H. and Crompton, R.W., "A Note on the Diffusion in a Gas of Electrons from a Small Source", 1955, Proc.Roy.Soc., B68, 381-3.

44. Huxley, L.G.H., "The Structure of a Stream of Electrons and Ions Drifting and Diffusion in a Gas when Ionization by Collision and Molecular Attachment are Present", 1959, Aust.J.Phys.,12, 171-83.

45. Huxley, L.G.H., Crompton, R.W. and Bagot, C.H., "A New Method for Measuring the Attachment of Slow Electrons in Gases", 1959, Aust.J.Phys., 12, 303-08.

46. Huxley, L.G.H. and Crompton, R.W., "The Diffusion and Drift of Electrons in Gases", 1974, Wiley, New York.

47. Itoh, T. and Musha, T., "Monte Carlo Calculations of Motion of Electrons in Helium", 1960, J.Phys.Soc. Japan, 15, 1675-80.

48. Jones, E. and Llewellyn Jones, F., "The Experimental Determination of The Primary Ionization Coefficients at Low Gas Pressures",

1958, Proc.Phys.Soc., 72, 363-8.

49. Kontoleon, N., "Electron Diffusion in Gases", 1971, Ph.D. Thesis, The University of Liverpool.

50. Kontoleon, N., Lucas, J. and Virr, L.E., "Measurement of Discharge Parameters for Electron Swarms in Hydrogen", 1971, Proc. 10th Int. Conf. on Phenomenon in Ionized Gases, Oxford, 54.

51. Kontoleon, N., Lucas, J. and Virr, L.E., "The Measurement of the Ratio of Radial Diffusion Coefficient to Mobility and the Amplification Coefficient for Electrons at High E/p", 1972, J.Phys.D: Appl.Phys., 5, 956-65.

52. Kontoleon, N., Lucas, J., and Virr, L.E., "Electron Swarm Parameters in Nitrogen", 1973, J.Phys.D : Appl.Phys., 6, 1237-46.

53. Kruithoff, A.A. and Penning, F.M., "Determination of the Townsend Ionization Coefficient for Pure Argon", 1936, Physica, 3, 515-33.

54. Kucukarpaci, H.N., "Electron Swarm Motion in Molecular Gases", 1978, M.Eng. Thesis, The University of Liverpool and Ph.D. Thesis(to be produced).

55. Kucukarpaci, H.N. and Lucas, J., "Simulation of Electron Swarm Parameters in Carbon Dioxide and Nitrogen for High E/N", 1979, J.Phys.D : Appl. Phys., 12, 2123-38.

56. Kucukarpaci, H.N. and Lucas, J., "Electron Swarm Parameters in Argon and Krypton", 1981, J.Phys.D: Appl.Phys., 14, 2001-14.

57. Kucukarpaci, H.N., Saelee, H.T. and Lucas, J., "Electron Swarm Parameters in Helium and Neon", 1981, J.Phys.D : Appl.Phys., 14, 9-25.

58. Laborie, P., Rocard, J.M. and Rees, J.A., "Electronic Cross-Sections Macroscopic Coefficients", Vol. 1 and 2, 1968 and 1971, Dunod, Paris.

59. Lakshminarasimha, C.S., "Electron Swarm Parameters in Gases", 1974, Ph.D. Thesis, The University of Liverpool.

60. Lakshminarasimha, C.S., Lucas, J. and Kontoleon, N., "Diffusion and Ionization Studies for Electron Swarms in Carbon Monoxide and Carbon Dioxide", 1974, J.Phys.D : Appl. Phys., 7, 2545-53.

61. Lakshminarasimha, C.S., Lucas, J., and Snelson, R.A., "Time-of-Flight Electron-Swarm Studies of Ionization and Attachment in Gases", 1975, Proc. IEE., 122, 1162-65.

62. Lakshminarasimha, C.S. and Lucas, J., "The Ratio of Radial Diffusion Coefficient to Mobility for Electrons in Helium, Argon, Air, Methane and Nitric Oxide", 1977, J.Phys.D:Appl.Phys., 10, 313-21.

63. Lawson, P.A. and Lucas, J., "Electron Diffusion in Hydrogen at High Electric Fields and Low Gas Pressures", 1965, Proc.Roy.Soc., 85, 177-83.

64. Leblanc, O.H. and Devins, J.C., "Townsend Ionization Constants in N-Alkanes", 1960, Nature, 188, 219-20.

65. Limbeek, J.W., "Electron Swarm and Radiation Parameters in CO_2 Laser Gas Mixtures", 1978, Ph.D. Thesis, The University of Liverpool.

66. Linder, F. and Schmidt, H., "Experimental Study of Low Energy e-O_2 Collision Processes", 1971, Z.Naturforsch, 26a, 1617-25.

67. Lowke, J.J., "The Drift Velocity of Electrons in Hydrogen and Nitrogen", 1963, Aust.J.Phys., 16, 115-35.

68. Lowke, J.J. and Parker, J.H., "Theory of Electron Diffusion Parallel to Electric Fields II - Application to Real Gases", 1969, Phys.Rev., 181, 302-11.

69. Lucas, J., "The Amplification and Transit Time of an Electron Avalanche Traversing a Uniform Electric Field Gap", 1964, Int.J.Electronics and Control, 17, 43-48.

70. Lucas, J., "The Growth of Pre-Breakdown Current in a Uniform Electric Field Gap", 1968, Int.J.Electronics. 25, 27-36.

71. Lucas, J., "The Spatial/Time Variation of Energies of the Electrons in an Electron Swarm, Part 2", 1970, Int.J.Electronics, 29, 465-77.

72. Lucas, J. and Saelee, H.T., "A Comparison of a Monte Carlo Simulation and the Boltzmann Solution for Electron Swarm Motion in Gases", 1975, J.Phys.D: Appl.Phys., 8, 640-50.

73. Lucas, J., and Saelee, H.T., "Electron Drift Velocity in Gases at High E/N", 1975, J.Phys.D : Appl. Phys., Letter to the Editor, 8, L123-5.

74. Lucas, J., and Kucukarpaci, H.N., "A Pulse Technique for the Measurement of the Ratio of Diffusion to Mobility for Electron Swarms in Gases at High E/N", 1979, J.Phys.D : Appl.Phys., 12, 703-15.

75. Lucas,J., "Swarm Measurements in Metal Vapours and Mixtures of Inert Gases and Metal Vapours", 1981, P.231-40, Proc. of the 2nd. Int. Swarm Seminar, Oak Ridge, Tennessee, U.S.A., Edited by Loucas, G. Christophorou.

76. Masch, K., "Uber Electronenionisierung von Stickstoff", 1932, Arch.f. Electrotechnik, 26, 587-92.

77. McFarland, R.H., "Gryzinski Electron-Impact Ionization Cross-Section Computations for the Alkali Metals", 1965, Phys.Rev., 139, A40-A42.

78. Naidu, M.S. and Prasad, A.N., "Mobility Diffusion and Attachment of Electrons in Oxygen", 1970, J.Phys.D : Appl. Phys., 3, 957-64.

79. Naidu, M.S. and Prasad, A.N., "Diffusion and Drift of Electrons in SF_6", 1972, J.Phys.D : Appl.Phys., 5, 1090-95.

80 Nakamura, Y. and Lucas, J., "Electron Drift Velocities in Mercury, Sodium and Thallium Vapours : I. Experimental", 1978, J.Phys.D: Appl.Phys., 11, 325-35.

81. Nakamura, Y. and Lucas, J., "Electron Drift Velocity and Momentum Cross-Section in Mercury, Sodium and Thallium Vapours : II Theoretical", 1978, J.Phys.D : Appl. Phys., 11, 337-45.

82. Nielsen, R.A. and Bradbury, N.E., "Electron and Negative Ion Mobility in Oxygen, Air, Nitrous Oxide and Ammonia", 1937, Phys. Rev., 51, 69-75.

83. Nygaard, K.J., "Electron Impact Ionization Cross-Section in Caesium", 1968, J.Chem.Phys., 49, 5, 1995-2002.

84. Parker, J.H. and Lowke, J.J., "Theory of Electron Diffusion Parallel to Electric Field, I-Theory", 1969, Phys.Rev., 181, 290-93.

85. Pollock, W.T., "Momentum Transfer and Vibrational Cross-Sections in Non-Polar Gases", 1968, J.Chem.Soc., Faraday Trans., II, 2, 64, 2919-26.

86. Prasad, A.N. and Craggs, J.D., "Measurement of Townsend's Ionization Coefficients and Attachment Coefficients in Oxygen", 1961, Proc.Roy.Soc., London, 77, 385-98.

87. Price, D.A., Lucas, J. and Moruzzi, J.L., "Ionization in Oxygen-Hydrogen Mixtures", J.Phys.D : Appl.Phys., 5, 1249-59.

88. Ramsauer, C. and Kollath, R., "Uber den Wirkungsquerschnitt der Nichtedelgasmolekule gegenuber Elektronen unterhalb 1 Volt", 1930, Ann.Physik, 4, 91-109.

89. Ramsauer, C. and Kollath, R., "Die Winkelverteilung bei der Streuung langsamer Elektronen an Gasmolekulen", 1932, Ann.Physik, 12, 529-61.

90. Rapp, D., and Englander-Golden, P., "Total Cross-Sections for Ionization and Attachment in Gases by Electron Impact. I. Positive Ionization", 1965, J.Chem.Phys., 43, 1464-79.

91. Rapp, D., Englander-Golden, P. and Briglia, D.D., "Cross-Section for Dissociative Ionization of Molecules by Electron Impact", 1965, J.Chem.Phys., 42, 4081-85.

92. Saelee, H.T., "Monte Carlo Simulation of Electron Swarms in Gases", 1976, Ph.D. Thesis, The University of Liverpool.

93. Saelee, H.T. and Lucas, J., "Simulation of Electron Swarm Motion in Hydrogen and Carbon Monoxide for High E/N", 1977, J.Phys.D : Appl.Phys., 10, 343-54.

94. Saelee, H.T., Lucas, J. and Limbeek, J.W., "Time-of-Flight Measurements of Electron Drift Velocity and Longitudinal Diffusion Coefficient in Nitrogen, Carbon Monoxide, Carbon Dioxide and Hydrogen", 1977, Solid State and Electron Devices, 1, 4, 111-16.

95. Saelee, H.T. and Lucas, J., "Transport Properties of Metal Vapours and Gases Contaminated by Metal Vapours", 1978, Third Year Project Report, S.R.C. Ref. No. B/RG 53360.

96. Saelee, H.T. and Lucas, J., "Electron Drift Velocity and Momentum Transfer Cross-Section in Caesium Vapour", 1979, J.Phys.D : Appl.Phys., 12, 1275-83.

97. Salop, A. and Nakano. H.H., "Total Electron Scattering Cross-Sections in O_2 and Ne", 1970, Phys.Rev., 2, 127-31.

98. Schlumbohm, H., "Stossionistierungskoeffizient, Mittlere Elektronenergien und die Beweglichkeit von Elektronen in Gasen", 1965, Z.Phys., 184, 492-505.

99. Schlumbohm, H. "Elektronen lawinen bei Hohen E/p zur Bestimmung der Driftgeschwindigkeiten von Elektronen un Ionen der Elektronenstossionisierung und der Elektronenergien", 1965, Z.Phys., 182, 306-16.

100. Schlumbohm, H., "Messung der Driftgeschwindigkeiten von Elektron und Positiven Ionen in Gasen", 1965, Z.Physik, 182, 317-27.

101. Schulz, G.J., "Cross-Sections and Electron Affinity for O^- Ions from O_2, CO and CO_2 by Electron Impact", 1962, Phys.Rev., 128, 178-86.

102. Skubenich, V.V. and Zapesochny, I.P., 1967, 5th Int. Conf. on the Physics of Electronic and Atomic Collisions, Lenningrad.

103. Snelson, R.A., "Time of Flight Studies of Electron Swarms", 1974, Ph.D. Thesis, The University of Liverpool.

104. Snelson, R.A. and Lucas, J., "Measurements of the Longitudinal Diffusion Coefficient and the Drift Velocity for Electron Swarms in Hydrogen and Nitrogen using a Time-of-Flight Technique", 1975, Proc. IEE., 122, 333-36.

105. Sunshine, G., Aubbrey, B.B. and Bederson, B., "Absolute Measurements of Total Cross-Sections for the Scattering of Low Energy Electrons by Atomic and Molecular Oxygen", 1967, Phys.Rev., 154, 1-8.

106. Tholl, H., "Messung der Elektronendriftgeschwindigkeit N_2 und in CH_4", 1964, Z.Phys., 178, 183-188.

107. Thomas, R.W.L.and Thomas, W.R.L., "Monte Caro Simulation of Electrical Discharges in Gases", 1969, J.Phys., B, 2, 562-70.

108. Thomas, W.R.L., "The Determination of the Total Excitation Cross-Section in Neon by Comparison of Theoretical and Experimental Values of Townsend's Primary Ionization Coefficient", 1969, J.Phys.B., 2, 551-61.

109. Thompson, J.J., "Conduction of Electricity Through Gases", Vol. II, 1933, Cambridge University Press.

110. Townsend, J.S.E., "The Conductivity Produced in Gases by the Motion of Negatively-Charged Ions", 1900, Nature, 62, 340-1.

111. Townsend,J.S. and Bailey, V.A., "The Motion of Electrons in Gases", 1921, Phil.Mag., 42, 874-91.

112. Townsend, J.S.E., "Electrons in Gases", 1947, Hutchinson, London.

113. Trajmar, S., Cartwright, D.C. and Williams, W., "Differential and Integral Cross-Sections for the Electron-Impact Excitation of the $^1a\,\Delta_g$ and b Σ_g^+ States of O_2", 1971, Phys.Rev., 4, 1482-92.

114. Virr, L.E., "Time of Flight Studies of Electrons in Gases", 1970, Ph.D. Thesis, The University of Liverpool.

115. Virr, L.E., Lucas, J. and Kontoleon, N., "The Measurement of the Ratio of the Diffusion Coefficient to Mobility for Electrons at Low E/p", 1972, J.Phys.D.Appl.Phys., 5, 542-54.

116. Wagner, E.B., Davis, F.J. and Hurst, G.S., "Time-of-Flight Investigations of Electron Transport in some Atomic and Molecular Gases", 1967, J.Chem.Phys., 47, 3138-47.

117. Walters, H.R.J., "On the Elastic Scattering of Electrons by Lithium and the Total Cross-Sections for Electron Impact on Lithium, Sodium and Potassium", 1976, J.Phys.B. Atom.Molec.Phys., 9, 2, 227-37.

118. Webb, G.M., "The Elastic Scattering of Electrons in Molecular Hydrogen", 1935, Phys.Rev., 47, 384-88.

119. Zapesochnyi, I.P., "Absolute Cross-Sections for the Excitation of the Levels of Alkali Metal Atoms by Low-Energy Electrons", 1967, High Temperature, 5, 6-11.

120. Zapesochnyi, I.P., and Aleksakhin, I.S., "Ionization of Alkali Metal Atoms by Slow Electrons", 1969, Sov. Phys., JETP. (or Zh.Eks.Theor.Fiz.), 28, 41-45.

In addition there are the following :-

121. Crompton, R.W., Elford, M.T. and Gascoigne, J., "Precision Measurements of the Townsend Energy Ratio for Electron Swarms in Highly Uniform Electric Fields", 1965, Aust.J.Phys., 118, 409-36.

122. Dutton, J., "A Survey of Electron Swarm Data", 1975, J.Phys.Chem. Ref. Data., 4, No. 3, 577-856.

123. Lucas, J., "A Theoretical Calculation of Electron Swarm Properties in Helium", 1972, Int.J.Elec., 32, No. 4, 393-410.

124. Morgan, C.C., "Handbook of Vacuum Physics , Fundamentals of Discharges in Gases", 1965, Pergammon Press.

APPENDIX

'A'

RESULTS FOR MIXTURES :-

1. POTASSIUM AND ARGON
2. SODIUM AND ARGON
3. CAESIUM AND ARGON

PERCENTAGE IN MIXTURES OF POTASSIUM VAPOURS AND ARGON GAS FOR E/N 2.83 to 282.5 Td.										
K	0.001	0.005	0.01	0.07	0.10	0.70	1	5	10	20
Ar	99.999	99.995	99.99	99.93	99.90	99.30	99	95	90	80

PERCENTAGE IN MIXTURES OF SODIUM VAPOURS AND ARGON GAS FOR E/N 2.83 to 282.5 Td.										
Na	0.001	0.005	0.01	0.07	0.10	0.70	1	7	10	20
Ar	99.999	99.995	99.99	99.93	99.90	99.30	99	93	90	80

PERCENTAGE IN MIXTURES OF CAESIUM VAPOURS AND ARGON GAS FOR E/N 2.83 to 282.5 Td.														
Cs	0.001	0.005	0.01	0.02	0.05	0.07	0.10	0.20	0.50	0.70	1	5	10	20
Ar	99.999	99.995	99.99	99.98	99.95	99.93	99.90	99.80	99.50	99.30	99	95	90	80

and inelastic cross-sections has been collected for each gas such that the computed and experimental values gave good agreement for each swarm parameter over the entire E/N range. Electron swarm parameters have been evaluated in the range of E/N varying from 14 to 5650 Td. Theoretical values have also been computed for the electron swarm parameters by using the Boltzmann equation in a mixture of argon gas and metal vapours namely, (Ar+ k, Ar+ Na, Ar+ Cs) for E/N between 2.83 and 283 Td, and at the percentage of 0.001 % to 20%, see Appendix A. The set of metal vapour / gas cross-sections used has been obtained from the results of the previous workers in the group, as summarised in Table 1.1.

IONIZATION COEFFICIENT FOR MIXTURE OF (K + Ar)

	PERCENTAGE								
	0.001%	0.005%	0.01%	0.07%	0.1%	0.7%	1%	5%	10%
	FRACTION								
	1×10^{-5}	5×10^{-5}	1×10^{-4}	7×10^{-4}	1×10^{-3}	7×10^{-3}	1×10^{-2}	5×10^{-2}	1×10^{-1}
E/N Td	$\alpha_T/N \times 10^{-17}$ cm^2								
28.2	2.71×10^{-2}	0.10	0.18	0.50	0.46	6.47×10^{-2}	3.5×10^{-2}	2.44×10^{-4}	
56.5	0.19	0.24	0.28	0.79	0.93	0.65	0.48	3.02×10^{-2}	2.57×10^{-3}
113	1.38		1.41	1.70	1.81	2.57	2.40	0.62	0.16

	IONIZATION COEFFICIENT FOR PURE POTASSIUM (K^+) $\alpha_T/N \times 10^{-17}$ cm^2								
28.2	6.30×10^{-3}	5.57×10^{-3}	4.69×10^{-3}	5.99×10^{-4}	2.21×10^{-4}	3.47×10^{-6}	3.50×10^{-2}	2.44×10^{-4}	2.26×10^{-6}

K Ar

PERCENTAGE FRACTION	1% 1×10^{-2}		0.1% 1×10^{-3}		0.01% 1×10^{-4}	
E/N Td	$R_4 = K^+$ α_T/N $\times 10^{-17}$ cm^2	$R_6 = Ar^+$ α_T/N 10^{-17} cm^2	$R_4 = K^+$ α_T/N 10^{-17} cm^2	$R_6 = Ar^+$ α_T/N 10^{-17} cm^2	$R_4 = K^+$ α_T/N 10^{-17} cm^2	$R_6 = Ar^+$ α_T/N 10^{-17} cm^2
14.1	6.05×10^{-4}		0.07	1.32×10^{-8}	0.21	
28.3	3.55×10^{-2}	4.12×10^{-12}	0.46	2.19×10^{-4}	0.18	4.67×10^{-3}
43.0	0.19	1.04×10^{-7}	0.76	1.04×10^{-2}	0.15	4.68×10^{-2}
56.5	0.48	1.98×10^{-5}	0.86	6.58×10^{-2}	0.13	0.16
70.6	0.89	1.81×10^{-4}	0.86	1.95×10^{-1}	0.11	0.36
84.8	1.37	4.33×10^{-3}	0.84	0.41	0.10	0.62
98.9	1.87	0.20×10^{-1}	0.80	0.69	0.09	0.96
113	2.35	0.62×10^{-1}	0.76	1.04	0.09	1.33
127	2.75	1.43×10^{-1}	0.72	1.43	0.08	1.77
141	3.09	2.79×10^{-1}	0.69	1.86	0.07	2.21
155	3.37	4.74×10^{-1}	0.66	2.32	0.07	2.69
170	3.55	7.25×10^{-1}	0.63	2.80	0.07	3.17
184	3.71	10.4×10^{-1}	0.60	3.30	0.06	3.67
198	3.81	1.39	0.58	3.82	0.06	4.17
212	3.85	1.80	0.55	4.32	0.06	4.70
226	3.89	2.23	0.53	4.85	0.05	5.20
240	3.90	2.70	0.51	5.38	0.05	5.73
254	3.89	3.19	0.49	5.92	0.05	6.24
268	3.85	3.70	0.48	6.43	0.05	6.79

K Ar

0.001% 99.999%

E/N Td	$\frac{R_2 + R_3}{R_4 + R_6}$	$\frac{R_5}{R_4 + R_6}$
2.83	29.2	0.59
8.48	18.1	11.9
14.1	17.1	32.5
28.3	12.4	87
43.0	3.55	50.4
56.5	1.06	24.2
70.6	0.44	14.1
84.8	0.22	9.51
98.9	0.13	7.03
113	0.09	5.53
127	0.06	4.57
141	0.05	3.88
155	0.04	3.38
170	0.03	2.99
184	0.02	2.70
198	0.02	2.45
212	0.02	2.25
226	0.01	2.08
240	0.01	1.94
254	0.01	1.82
268	0.01	1.72

A.5

K 20%

Ar 80%

E/N Td	$\frac{R_2 + R_3}{R_4 + R_6}$ (÷ 10)	$\frac{R_5}{R_4 + R_6}$ (x 10)
28.3	3.85×10^{10}	
43.0	3.53×10^{7}	
56.5	1.05×10^{6}	
70.6	1.23×10^{5}	5.55×10^{-15}
84.8	2.86×10^{4}	1.10×10^{-12}
98.9	9.77×10^{3}	4.85×10^{-11}
113	4.34×10^{3}	8.37×10^{-10}
127	2.23×10^{3}	8.02×10^{-9}
141	1.31×10^{3}	4.77×10^{-8}
155	8.41×10^{2}	2.12×10^{-7}
170	5.73×10^{2}	7.45×10^{-7}
184	4.14×10^{2}	2.13×10^{-6}
198	3.14×10^{2}	5.23×10^{-6}
212	2.43×10^{2}	1.18×10^{-5}
226	1.94×10^{2}	2.40×10^{-5}
240	1.60×10^{2}	4.53×10^{-5}
254	1.34×10^{2}	7.94×10^{-5}
268	1.13×10^{2}	1.32×10^{-4}
283	98	2.08×10^{-4}

POTASSIUM

E/N	v_d x	$\overline{\epsilon}$	D_r/μ	α_T/N x	R_1 x	R_2 x	R_3 x	R_4 x	R_5 x	R_6 x
Td	10^7 cm/s	eV	V	10^{-17} cm^2	10^{11} s^{-1}	10^8 s^{-1}	10^7 s^{-1}	10^3 s^{-1}	10 s^{-1}	10 s^{-1}
2.83	0.9×10^{-3}	0.01	0.14		3.06	0.1×10^{-4}				
8.48	0.4×10^{-2}	0.11	0.23		3.09	0.5×10^{-3}				
14.1	0.7×10^{-2}	0.12	0.25		3.17	0.2×10^{-2}				
28.3	0.02	0.14	0.29		3.35	0.9×10^{-2}				
43.0	0.03	0.16	0.31		3.45	0.03				
56.5	0.05	0.18	0.33		3.48	0.06	0.3×10^{-5}			
70.6	0.07	0.20	0.35		3.46	0.11	0.6×10^{-4}			
84.8	0.10	0.23	0.37		3.43	0.18	0.4×10^{-3}			
98.9	0.13	0.25	0.38		3.37	0.28	0.2×10^{-2}			
113	0.17	0.27	0.40		3.31	0.41	0.6×10^{-2}			
127	0.21	0.29	0.42	1.4×10^{-8}	3.23	0.58	0.02			
141	0.25	0.31	0.43	9.8×10^{-8}	3.16	0.77	0.04			
155	0.30	0.33	0.45	5.1×10^{-7}	3.10	1.01	0.07			
170	0.35	0.35	0.46	2.1×10^{-6}	3.02	1.27	0.13	0.3×10^{-2}		
184	0.40	0.37	0.47	6.7×10^{-6}	2.93	1.57	0.21	0.95×10^{-2}		
198	0.45	0.39	0.49	1.8×10^{-5}	2.88	1.90	0.33	0.03		
212	0.51	0.41	0.50	4.5×10^{-5}	2.80	2.31	0.49	0.08		
226	0.57	0.43	0.52	9.6×10^{-5}	2.74	2.69	0.69	0.19		
240	0.64	0.46	0.53	1.95×10^{-4}	2.67	3.21	0.97	0.44		
254	0.69	0.47	0.54	3.6×10^{-4}	2.64	3.62	1.28	0.86		
268	0.77	0.51	0.56	6.9×10^{-4}	2.53	4.24	1.72	1.73		
283	0.82	0.52	0.57	1.1×10^{-3}	2.50	4.70	2.13	3.07		

ARGON

E/N	$v_d \times 10^7$	$\overline{\epsilon}$	D_r/μ	$\alpha_T/N \times 10^{-17}$	$R_1 \times 10^9$	$R_2 \times 10$	$R_3 \times 10$	$R_4 \times 10$	$R_5 \times 10^7$	$R_6 \times 10^7$
Td	cm/s	eV	V	cm^2	S^{-1}	S^{-1}	S^{-1}	S^{-1}	S^{-1}	S^{-1}
2.83	6.04	5.09	7.03		3.80				0.30×10^{-2}	
8.48	0.10	5.24	7.32	2.06×10^{-8}	3.95				0.26×10^{-1}	
14.1	0.16	5.37	7.56	2.42×10^{-5}	4.07				0.07	0.14×10^{-5}
28.3	0.29	5.65	8.02	6.84×10^{-3}	4.35				0.25	0.70×10^{-3}
43.0	0.41	5.92	8.35	0.06	4.58				0.51	0.81×10^{-2}
56.5	0.52	6.16	8.60	0.18	4.80				0.84	0.03
70.6	0.62	6.38	8.79	0.40	4.98				1.21	0.09
84.8	0.72	6.59	8.94	0.68	5.15				1.61	0.17
98.9	0.82	6.79	9.07	0.99	5.30				2.04	0.29
113	0.92	6.98	9.16	1.38	5.44				2.48	0.45
127	1.01	7.16	9.24	1.81	5.56				2.94	0.65
141	1.11	7.33	9.31	2.26	5.67				3.42	0.88
155	1.21	7.50	9.38	2.71	5.78				3.90	1.16
170	1.30	7.66	9.43	3.22	5.88				4.40	1.48
184	1.40	7.82	9.48	3.70	5.97				4.91	1.83
198	1.49	7.97	9.54	4.21	6.05				5.43	2.22
212	1.58	8.12	9.59	4.75	6.13				5.96	2.65
226	1.68	8.27	9.64	5.25	6.21				6.49	3.12
240	1.77	8.42	9.68	5.79	6.28				7.04	3.63
254	1.87	8.56	9.73	6.30	6.34				7.59	4.17
268	1.96	8.71	9.78	6.84	6.41				8.15	4.75
283	2.06	8.85	9.85	7.37	6.47				8.72	5.36

K Ar

1% 99%

E/N Td	v_d x 10^7 cm/s	$\overline{\epsilon}$ eV	D_r/μ V	α_T/N x 10^{-17} cm^2	R_1 x 10^9 s^{-1}	R_2 x 10^8 s^{-1}	R_3 x 10^8 s^{-1}	R_4 x 10^7 s^{-1}	R_5 x 10^7 s^{-1}	R_6 x 10^6 s^{-1}
2.83	0.26	0.53	0.61		2.31	0.016	0.11×10^{-4}			
8.48	0.79	0.94	0.93	6.19×10^{-6}	1.37	0.14	0.66×10^{-2}	0.17×10^{-5}		
14.1	1.12	1.22	1.21	5.96×10^{-4}	1.11	0.29	0.04	0.24×10^{-3}		
28.3	1.51	1.76	1.79	3.50×10^{-2}	1.13	0.64	0.18	0.19×10^{-1}		
43.0	1.66	2.23	2.34	18.3×10^{-2}	1.38	0.94	0.35	0.11	0.46×10^{-4}	
56.5	1.71	2.69	2.86	4.80×10^{-1}	1.72	1.21	0.52	0.29	0.16×10^{-2}	0.12×10^{-3}
70.6	1.71	3.17	3.38	0.88	2.13	1.44	0.66	0.54	0.01	0.31×10^{-2}
84.8	1.70	3.65	3.90	1.38	2.56	1.64	0.77	0.82	0.06	0.03
98.9	1.68	4.11	4.39	1.89	2.99	1.82	0.87	1.11	0.16	0.12
113	1.67	4.55	4.86	2.40	3.41	1.97	0.94	1.39	0.34	0.37
127	1.68	4.96	5.29	2.91	3.79	2.10	1.00	1.63	0.60	0.85
141	1.69	5.34	5.69	3.36	4.13	2.21	1.04	1.85	0.92	1.67
155	1.71	5.69	6.04	3.84	4.44	2.31	1.08	2.04	1.31	2.87
170	1.75	6.00	6.35	4.29	4.70	2.39	1.11	2.20	1.74	4.49
184	1.79	6.29	6.62	4.75	4.94	2.46	1.13	2.35	2.21	6.57
198	1.84	6.56	6.87	5.20	5.15	2.52	1.15	2.48	2.70	9.07
212	1.90	6.81	7.08	5.65	5.33	2.58	1.16	2.59	3.23	12.1
226	1.96	7.05	7.28	6.13	5.50	2.63	1.17	2.70	3.76	15.5
240	2.02	7.27	7.45	6.58	5.65	2.68	1.18	2.79	4.32	19.3
254	2.09	7.49	7.59	7.06	5.79	2.72	1.19	2.88	4.89	23.6
268	2.17	7.69	7.73	7.54	5.91	2.76	1.20	2.96	5.47	28.4
283	2.24	7.89	7.85	8.05	6.02	2.79	1.20	3.03	6.06	33.5

K 5% Ar 95%

E/N Td	v_d x 10^7 cm/s	$\overline{\epsilon}$ eV	D_r/μ V	α_T/N x 10^{-17} cm^2	R_1 x $10^9 s^{-1}$	R_2 x $10^8 s^{-1}$	R_3 x $10^8 s^{-1}$	R_4 x $10^7 s^{-1}$	R_5 x $10^6 s^{-1}$	R_6 x $10^6 s^{-1}$
2.83	0.05	0.23	0.38		17.1	0.3×10^{-2}				
8.48	0.25	0.37	0.49	12.4×10^{-13}	14.7	0.05	0.6×10^{-4}			
14.1	0.52	0.51	0.58	4.75×10^{-8}	12.2	0.16	0.2×10^{-2}			
28.3	1.21	0.83	0.80	24.4×10^{-5}	8.23	0.67	0.05	0.1×10^{-3}		
43.0	1.78	1.10	1.00	5.45×10^{-3}	6.01	1.33	0.20	0.3×10^{-2}		
56.5	2.21	1.34	1.19	3.02×10^{-2}	4.80	2.04	0.44	0.02		
70.6	2.55	1.58	1.38	9.29×10^{-2}	3.93	2.74	0.74	0.08	0.2×10^{-5}	
84.8	2.81	1.80	1.57	20.7×10^{-2}	3.44	3.42	1.08	0.21	0.4×10^{-4}	
98.9	2.99	2.01	1.75	3.81×10^{-1}	3.16	4.07	1.44	0.40	0.4×10^{-3}	0.2×10^{-5}
113	3.13	2.22	1.94	0.62	3.03	4.68	1.80	0.68	0.3×10^{-2}	0.3×10^{-4}
127	3.23	2.43	2.13	0.90	2.98	5.28	2.14	1.05	0.01	0.3×10^{-3}
141	3.30	2.64	2.32	1.27	2.99	5.84	2.49	1.49	0.04	0.1×10^{-2}
155	3.35	2.84	2.50	1.70	3.11	6.37	2.80	1.99	0.10	0.6×10^{-2}
170	3.38	3.06	2.70	2.15	3.18	6.88	3.11	2.56	0.23	0.02
184	3.41	3.29	2.90	2.63	3.30	7.38	3.39	3.17	0.48	0.05
198	3.41	3.51	3.10	3.16	3.45	7.84	3.66	3.81	0.87	0.11
212	3.42	3.74	3.30	3.73	3.65	8.30	3.90	4.47	1.47	0.24
226	3.42	3.97	3.51	4.27	3.84	8.71	4.13	5.15	2.32	0.45
240	3.41	4.20	3.71	4.89	4.05	9.13	4.32	5.83	3.47	0.79
254	3.41	4.44	3.92	5.51	4.18	9.53	4.49	6.52	4.97	1.30
268	3.40	4.66	4.11	6.13	4.42	9.89	4.68	7.17	6.82	2.03
283	3.40	4.90	4.32	6.75	4.59	10.2	4.82	7.83	9.04	3.01

K 10% Ar 90%

E/N Td	v_d x 10^7 cm/s	$\overline{\epsilon}$ eV	D_r/μ V	α_T/N x 10^{-17} cm^2	R_1 x 10^9 s^{-1}	R_2 x 10^9 s^{-1}	R_3 x 10^8 s^{-1}	R_4 x 10^7 s^{-1}	R_5 x 10^5 s^{-1}	R_6 x 10^4 s^{-1}
2.83	0.02	0.18	0.33		34.8	0.1×10^{-3}				
8.48	0.10	0.25	0.39		33.8	0.2×10^{-2}	0.5×10^{-6}			
14.1	0.22	0.32	0.45		31.1	0.7×10^{-2}	0.8×10^{-4}			
28.3	0.63	0.51	0.58	22.6×10^{-7}	24.5	0.04	0.9×10^{-2}	0.5×10^{-6}		
43.0	1.08	0.69	0.70	2.19×10^{-4}	19.8	0.09	0.06	0.8×10^{-4}		
56.5	1.53	0.86	0.81	2.57×10^{-3}	16.2	0.16	0.18	0.14×10^{-2}		
70.6	1.92	1.02	0.92	1.22×10^{-2}	13.8	0.24	0.37	0.83×10^{-2}		
84.8	2.30	1.19	1.03	3.67×10^{-2}	11.4	0.32	0.64	0.03		
98.9	2.61	1.33	1.14	8.33×10^{-2}	10.0	0.41	0.96	0.08		
113	2.91	1.49	1.25	1.60×10^{-1}	8.38	0.50	1.35	0.16	0.4×10^{-4}	
127	3.14	1.63	1.35	2.71×10^{-1}	7.67	0.58	1.74	0.30	0.3×10^{-3}	
141	3.35	1.78	1.46	4.21×10^{-1}	6.82	0.67	2.19	0.50	0.2×10^{-2}	
155	3.53	1.91	1.57	0.62	6.36	0.76	2.63	0.77	0.7×10^{-2}	
170	3.67	2.05	1.68	0.85	6.02	0.84	3.08	1.11	0.02	0.4×10^{-2}
184	3.81	2.20	1.79	1.13	5.56	0.92	3.58	1.53	0.07	0.02
198	3.92	2.33	1.90	1.44	5.39	1.00	4.03	2.01	0.17	0.06
212	4.03	2.49	2.02	1.81	4.98	1.08	4.48	2.58	0.37	0.18
226	4.10	2.63	2.14	2.20	5.05	1.16	4.93	3.20	0.74	0.48
240	4.17	2.78	2.26	2.63	4.96	1.23	5.37	3.89	1.38	1.15
254	4.21	2.92	2.38	3.08	5.11	1.30	5.75	4.61	2.40	2.52
268	4.26	3.07	2.50	3.59	5.23	1.37	6.17	5.39	3.94	5.01
283	4.31	3.24	2.62	4.10	4.98	1.44	6.60	6.25	6.22	9.45

K Ar

20% 80%

E/N Td	v_d x 10^7 cm/s	$\overline{\epsilon}$ eV	D_r/μ V	α_T/N x 10^{-17} cm^2	R_1 x 10^{-1} S^{-1}	R_2 x 10^{8} S^{-1}	R_3 x 10^{8} S^{-1}	R_4 x 10^{6} S^{-1}	R_5 x 10 S^{-1}	R_6 x 10 S^{-1}
2.83	0.8×10^{-2}	0.14	0.28		6.67	0.4×10^{-3}				
8.48	0.04	0.19	0.33		7.05	0.6×10^{-2}				
14.1	0.08	0.23	0.37		6.93	0.02	0.3×10^{-6}			
28.3	0.24	0.32	0.44	7.40×10^{7}	6.24	0.15	0.4×10^{-3}			
43.0	0.46	0.42	0.51	7.40×10^{7}	5.56	0.42	0.6×10^{-2}			
56.5	0.71	0.51	0.57	3.28×10^{5}	4.98	0.84	0.03	0.8×10^{-4}		
70.6	0.98	0.61	0.64	3.45×10^{4}	4.43	1.39	0.08	0.1×10^{-2}		
84.8	1.25	0.70	0.70	1.76×10^{3}	4.03	2.06	0.17	0.8×10^{-2}		
98.9	1.55	0.81	0.76	5.90×10^{3}	3.52	2.85	0.32	3.24×10^{-3}		
113	1.81	0.90	0.82	0.02	3.23	3.70	0.50	0.10		
127	2.10	1.00	0.88	0.03	2.83	4.62	0.75	0.24		
141	2.35	1.10	0.94	0.06	2.63	5.58	1.05	0.51		
155	2.57	1.18	1.00	0.10	2.36	6.53	1.37	0.94		
170	2.77	1.26	1.05	0.16	2.19	7.46	1.73	1.60		
184	3.02	1.36	1.11	0.24	1.93	8.62	2.17	2.61	0.55	
198	3.25	1.46	1.18	0.35	1.75	9.74	2.66	3.96	2.07	
212	3.37	1.52	1.23	0.48	1.75	10.6	3.06	5.60	6.59	
226	3.58	1.63	1.29	0.62	1.57	117	3.64	7.88	18.9	0.15
240	3.69	1.69	1.35	0.79	1.58	126	4.07	104	47.3	0.55
254	3.86	1.79	1.42	1.02	1.45	137	4.66	137	109	1.77
268	4.05	1.91	1.48	1.24	1.26	149	5.25	178	235	5.17
283	4.14	1.98	1.54	1.50	1.30	159	5.76	221	460	13.4

CHAPTER TWO

K Ar

0.1% 99.9 %

E/N Td	v_d x 10^7 cm/s	$\overline{\epsilon}$ eV	D_r/μ V	α_T/N x 10^{-17} cm^2	R_1 x 10^9 s^{-1}	R_2 x 10^7 s^{-1}	R_3 x 10^7 s^{-1}	R_4 x 10^6 s^{-1}	R_5 x 10^7 s^{-1}	R_6 x 10^7 s^{-1}
2.83	0.35	1.14	1.33	3.96×10^{-6}	0.39	0.20	0.01			
8.48	0.51	1.80	2.25	0.01	0.77	0.66	0.18	0.02		
14.1	0.56	2.38	3.03	0.07	1.21	1.04	0.40	0.15	0.5×10^{-4}	
28.3	0.56	3.79	4.74	0.46	2.50	1.71	0.82	0.91	0.03	4.35×10^{-5}
43.0	0.58	4.78	5.98	0.88	3.47	2.07	1.00	1.56	0.18	0.2×10^{-2}
56.5	0.64	5.40	6.79	0.93	4.07	2.26	1.08	1.95	0.45	0.01
70.6	0.72	5.83	7.30	1.07	4.48	2.38	1.13	2.19	0.81	0.05
84.8	0.80	6.16	7.66	1.24	4.77	2.47	1.15	2.37	1.21	0.12
98.9	0.89	6.44	7.89	1.50	5.01	2.54	1.17	2.51	1.64	0.22
113	0.97	6.69	8.11	1.81	5.20	2.59	1.18	2.62	2.09	0.36
127	1.06	6.91	8.26	2.15	5.37	2.64	1.20	2.72	2.56	0.54
141	1.15	7.12	8.38	2.54	5.52	2.68	1.20	2.81	3.05	0.76
155	1.24	7.31	8.47	2.97	5.65	2.72	1.21	2.88	3.55	1.02
170	1.33	7.49	8.56	3.42	5.77	2.75	1.22	2.95	4.07	1.32
184	1.42	7.66	8.62	3.90	5.87	2.79	1.22	3.02	4.58	1.66
198	1.51	7.83	8.69	4.38	5.97	2.82	1.22	3.08	5.10	2.04
212	1.61	8.00	8.74	4.86	6.06	2.84	1.23	3.14	5.64	2.46
226	1.70	8.15	8.80	5.40	6.14	2.87	1.23	3.19	6.18	2.92
240	1.79	8.31	8.86	5.88	6.22	2.89	1.23	3.24	6.73	3.41
254	1.88	8.46	8.91	6.41	6.30	2.92	1.23	3.29	7.30	3.94
268	1.98	8.61	8.96	6.92	6.36	2.94	1.23	3.34	7.86	4.51
283	2.07	8.76	9.02	7.46	6.43	2.96	1.23	3.38	8.43	5.12

K 0.7 % Ar 99.3 %

E/N Td	v_d x 10^7 cm/s	$\overline{\epsilon}$ eV	D_r/μ V	α_T/N x 10^{-17} cm^2	R_1 x 10^9 s^{-1}	R_2 x 10^8 s^{-1}	R_3 x 10^7 s^{-1}	R_4 x 10^7 s^{-1}	R_5 x 10^7 s^{-1}	R_6 x 10^7 s^{-1}
2.83	0.33	0.65	0.69	3.5×10^{-13}	1.37	0.20	0.4×10^{-3}			
8.48	0.82	1.08	1.09	3.1×10^{-5}	0.89	0.14	0.10	0.9×10^{-5}		
14.1	1.08	1.38	1.42	1.7×10^{-3}	0.85	0.27	0.43	0.7×10^{-3}		
28.3	1.36	1.97	2.12	0.06	1.10	0.55	1.77	0.03	0.1×10^{-5}	
43.0	1.44	2.53	2.78	0.03	1.50	0.78	3.21	0.15	0.4×10^{-3}	0.1×10^{-5}
56.5	1.45	3.09	3.40	0.65	1.98	0.98	4.45	0.34	0.9×10^{-2}	0.1×10^{-3}
70.6	1.44	3.65	4.03	1.13	2.49	1.15	5.46	0.58	0.05	0.2×10^{-2}
84.8	1.42	4.19	4.62	1.64	3.00	1.30	6.21	0.81	0.16	0.9×10^{-2}
98.9	1.42	4.68	5.16	2.12	3.48	1.41	6.79	1.03	0.36	0.03
113	1.43	5.13	5.65	2.57	3.89	1.51	7.19	1.22	0.65	0.08
127	1.45	5.52	6.07	2.99	4.24	1.59	7.50	1.37	1.00	0.16
141	1.49	5.87	6.43	3.39	4.55	1.66	7.72	1.51	1.41	0.28
155	1.54	6.18	6.74	3.79	4.81	1.71	7.89	1.62	1.86	0.45
170	1.59	6.47	7.01	4.21	5.04	1.76	8.04	1.72	2.35	0.66
184	1.65	6.73	7.24	4.63	5.34	1.80	8.13	1.80	2.86	0.91
198	1.72	6.97	7.43	5.06	5.42	1.83	8.22	1.88	3.38	1.21
212	1.79	7.19	7.60	5.51	5.58	1.87	8.30	1.94	3.93	1.55
226	1.86	7.41	7.75	5.96	5.72	1.90	8.35	2.00	4.48	1.93
240	1.94	7.61	7.88	6.44	5.84	1.93	8.41	2.06	5.05	2.36
254	2.01	7.81	8.00	6.92	5.96	1.95	8.43	2.11	5.62	2.82
268	2.10	8.00	8.11	7.40	6.06	1.97	8.45	2.16	6.20	3.33
283	2.17	8.18	8.20	7.91	6.16	1.99	8.50	2.21	6.80	3.88

K Ar

0.01% 99.99%

E/N	v_d x	$\overline{\epsilon}$	D_r/μ	α_T/N x	R_1 x	R_2 x	R_3 x	R_4 x	R_5 x	R_6 x
Td	10^7 cm/s	eV	V	10^{-17} cm^2	10^9 s^{-1}	10^6 s^{-1}	10^6 s^{-1}	10^5 s^{-1}	10^7 s^{-1}	10^7 s^{-1}
2.83	0.17	1.86	2.69	3.9×10^{-3}	0.78	0.70	0.20	0.02		
8.48	0.18	3.61	4.96	0.13	2.31	1.64	0.78	0.80	0.3×10^{-2}	
14.1	0.20	4.61	6.27	0.21	3.30	2.03	0.99	1.47	0.03	0.46×10^{-6}
28.3	0.31	5.43	7.36	0.18	4.12	2.29	1.10	2.01	0.20	5.13×10^{-4}
43.0	0.42	5.80	7.90	0.20	4.47	2.39	1.14	2.22	0.47	6.96×10^{-3}
56.5	0.53	6.08	8.16	0.28	4.73	2.46	1.16	2.37	0.79	0.03
70.6	0.63	6.33	8.38	0.48	4.94	2.52	1.18	2.49	1.16	0.08
84.8	0.73	6.56	8.54	0.74	5.12	2.57	1.19	2.59	1.57	0.16
98.9	0.82	6.76	8.67	1.05	5.28	2.62	1.20	2.68	1.99	0.28
113	0.92	6.96	8.73	1.41	5.42	2.66	1.20	2.76	2.44	0.43
127	1.02	7.13	8.89	1.84	5.54	2.69	1.21	2.83	2.90	0.64
141	1.12	7.31	8.99	2.29	5.66	2.73	1.22	2.90	3.38	0.87
155	1.21	7.48	9.06	2.77	5.76	2.76	1.22	2.96	3.87	1.15
170	1.30	7.64	9.12	3.25	5.86	2.79	1.22	3.02	4.37	1.46
184	1.40	7.80	9.17	3.73	5.96	2.81	1.22	3.08	4.87	1.82
198	1.49	7.96	9.14	4.24	6.05	2.84	1.23	3.14	5.40	2.20
212	1.58	8.12	9.20	4.75	6.13	2.87	1.23	3.19	5.92	2.63
226	1.68	8.26	9.26	5.25	6.21	2.89	1.23	3.24	6.47	3.09
240	1.77	8.41	9.32	5.79	6.28	2.91	1.23	3.28	7.01	3.59
254	1.87	8.56	9.41	6.30	6.34	2.93	1.23	3.33	7.57	4.13
268	1.96	8.71	9.47	6.84	6.41	2.96	1.23	3.38	8.13	4.71
283	2.06	8.85	9.54	7.37	6.47	2.98	1.24	3.42	8.69	5.32

K 0.07% Ar 99.93%

E/N	v_d	$\overline{\epsilon}$	D_r/μ	α_T/N	R_1	R_2	R_3	R_4	R_5	R_6
Td	10^7 cm/s	eV	V	10^{-17} cm^2	10^9 s^{-1}	10^7 s^{-1}	10^6 s^{-1}	10^6 s^{-1}	10^7 s^{-1}	10^7 s^{-1}
2.83	0.32	1.23	1.49	1.9×10^{-5}	0.41	0.18	0.14	0.2×10^{-4}		
8.48	0.45	1.97	2.55	0.02	0.89	0.55	1.73	0.03	0.3×10^{-6}	
14.1	0.47	2.67	3.46	0.11	1.45	0.84	3.55	0.18	0.3×10^{-3}	
28.3	0.47	4.21	5.37	0.50	2.91	1.31	6.35	0.83	0.05	0.1×10^{-3}
43.0	0.52	5.10	6.49	0.68	3.78	1.52	7.35	1.24	0.25	0.3×10^{-2}
56.5	0.60	5.62	7.16	0.79	4.29	1.63	7.77	1.46	0.55	0.02
70.6	0.69	5.99	7.60	0.90	4.63	1.70	8.00	1.60	0.92	0.06
84.8	0.77	6.29	7.89	1.10	4.89	1.75	8.16	1.71	1.32	0.13
98.9	0.86	6.55	8.11	1.36	5.10	1.79	8.26	1.80	1.75	0.24
113	0.96	6.78	8.27	1.70	5.27	1.83	8.35	1.87	2.21	0.38
127	1.05	6.99	8.40	2.06	5.43	1.86	8.41	1.93	2.67	0.57
141	1.14	7.18	8.54	2.46	5.56	1.89	8.43	1.99	3.16	0.79
155	1.23	7.36	8.63	2.91	5.68	1.91	8.48	2.03	3.65	1.07
170	1.33	7.54	8.73	3.36	5.79	1.94	8.52	2.08	4.16	1.37
184	1.42	7.70	8.79	3.84	5.90	1.96	8.54	2.12	4.67	1.72
198	1.51	7.87	8.82	4.32	6.00	1.98	8.56	2.17	5.20	2.09
212	1.60	8.03	8.87	4.83	6.08	2.00	8.59	2.21	5.73	2.52
226	1.69	8.19	8.92	5.34	6.16	2.01	8.60	2.24	6.28	2.98
240	1.78	8.34	8.97	5.59	6.24	2.03	8.59	2.28	6.82	3.48
254	1.88	8.49	9.01	6.38	6.31	2.05	8.61	2.31	7.38	4.01
268	1.97	8.64	9.05	6.89	6.38	2.06	8.64	2.35	7.95	4.58
283	2.06	8.79	9.09	7.43	6.44	2.08	8.64	2.38	8.52	5.18

K Ar

0.001% 99.999%

E/N Td	v_d x 10^7 cm/s	$\overline{\epsilon}$ eV	D_r/μ V	α_T/N x 10^{-17} cm^2	R_1 x 10^9 s^{-1}	R_2 x 10^5 s^{-1}	R_3 x 10^5 s^{-1}	R_4 x 10^4 s^{-1}	R_5 x 10^7 s^{-1}	R_6 x 10^6 s^{-1}
2.83	0.06	3.69	3.35	4.2×10^{-2}	2.38	1.68	0.80	0.85	0.5×10^{-3}	
5.65	0.08	4.73	6.67	5.7×10^{-2}	3.43	2.08	1.02	1.58	0.8×10^{-2}	
8.48	0.11	5.04	7.04	4.8×10^{-2}	3.74	2.18	1.07	1.79	0.02	
11.3	0.13	5.19	7.25	4×10^{-2}	3.89	2.22	1.08	1.89	0.04	
14.1	0.16	5.29	7.41	3.4×10^{-2}	4.00	2.26	1.10	1.96	0.06	0.1×10^{-4}
28.3	0.29	5.63	7.92	2.7×10^{-2}	4.33	2.35	1.13	2.15	0.24	0.6×10^{-2}
43.0	0.41	5.91	8.29	7×10^{-2}	4.58	2.42	1.15	2.29	0.51	0.08
56.5	0.52	6.15	8.52	0.19	4.79	2.48	1.17	2.41	0.83	0.32
70.6	0.62	6.38	8.71	0.40	4.98	2.54	1.18	2.52	1.21	0.83
84.8	0.72	6.59	8.85	0.65	5.15	2.58	1.19	2.61	1.61	1.67
98.9	0.82	6.79	8.96	0.99	5.30	2.63	1.20	2.70	2.03	2.87
113	0.92	6.98	9.07	1.38	5.44	2.66	1.21	2.78	2.48	4.45
127	1.01	7.16	9.14	1.78	5.56	2.70	1.21	2.85	2.94	6.40
141	1.11	7.34	9.23	2.23	5.68	2.73	1.22	2.91	3.42	8.77
155	1.20	7.50	9.32	2.71	5.78	2.76	1.22	2.97	3.90	11.5

K 0.005% Ar 99.995%

E/N Td	$v_d \times 10^7$ cm/s	$\overline{\epsilon}$ eV	D_r/μ V	$\alpha_T/N \times 10^{-17}$ cm^2	$R_1 \times 10^9$ s^{-1}	$R_2 \times 10^6$ s^{-1}	$R_3 \times 10^5$ s^{-1}	$R_4 \times 10^5$ s^{-1}	$R_5 \times 10^7$ s^{-1}	$R_6 \times 10^6$ s^{-1}
2.83	0.12	2.24	3.32	1.1×10^{-2}	1.07	0.48	1.75	0.5×10^{-1}	0.2×10^{-5}	
5.65	0.13	3.47	4.89	7.9×10^{-2}	2.18	0.79	3.74	0.36	0.1×10^{-2}	
8.48	0.14	4.29	5.96	0.13	2.98	0.96	4.67	0.63	0.9×10^{-2}	
11.3	0.16	4.73	6.53	0.14	3.42	1.04	5.06	0.78	0.02	
14.1	0.18	4.98	6.88	1.3×10^{-1}	3.68	1.08	5.26	0.87	0.05	0.7×10^{-5}
28.3	0.30	5.54	7.62	0.01	4.23	1.16	5.59	1.04	0.22	0.6×10^{-2}
43.0	0.41	5.86	8.04	1.29×10^{-1}	4.53	1.20	5.73	1.13	0.49	0.07
56.5	0.52	6.12	8.34	0.24	4.76	1.24	5.82	1.20	0.82	0.31
70.6	0.62	6.36	8.55	0.42	4.96	1.26	5.89	1.25	1.19	0.82
84.8	0.72	6.58	8.67	0.71	5.13	1.29	5.95	1.30	1.59	1.65

Ionization Coefficient for mixture of (Na + Ar)

	PERCENTAGE									
	0.001%	0.005%	0.01%	0.07%	0.1 %	0.7 %	1%	7%		
	FRACTION									
	1×10^{-5}	5×10^{-5}	1×10^{-4}	7×10^{-4}	1×10^{-3}	7×10^{-3}	1×10^{-2}	7×10^{-2}		
E/N Td	$\alpha_T/N \times 10^{-17}$ cm^2									
8.48	3.19×10^{-2}	11.3×10^{-2}	14.6×10^{-2}	4.04×10^{-2}	23.8×10^{-3}	17.6×10^{-5}	4.29×10^{-5}			
14.1	22.3×10^{-3}	9.86×10^{-2}	16.8×10^{-2}	19.6×10^{-2}	14.7×10^{-2}	6.05×10^{-3}	24.8×10^{-4}			
28.3	20.0×10^{-3}	7.29×10^{-2}	12.9×10^{-2}	0.52	0.56	0.16	9.27×10^{-2}	7.46×10^{-4}		
56.5	18.4×10^{-2}	21.7×10^{-2}	25.9×10^{-2}	0.65	0.82	1.11	0.90	6.58×10^{-2}		
84.8	6.61×10^{-1}	0.68	0.71	1.02	1.16	2.15	2.06	0.40		
	Ionization coefficient for pure sodium (Na^+) $\alpha_T/N \times 10^{-17}$ cm^2									
28..3	6.10×10^{-3}	5.73×10^{-3}	5.40×10^{-3}	1.81×10^{-3}	1.03×10^{-3}	2.31×10^{-7}	9.27×10^{-2}	7.46×10^{-4}		

Na Ar

PERCENTAGE FRACTION	1% 1×10^{-2}		0.1% 1×10^{-3}		0.01% 1×10^{-4}	
E/N Td	$R_5 = Na^+$ α_T/N 10^{-17} cm^2	$R_7 = Ar^+$ α_T/N 10^{-17} cm^2	$R_5 = Na^+$ α_T/N 10^{-17} cm^2	$R_7 = Ar^+$ α_T/N 10^{-17} cm^2	$R_5 = Na^+$ α_T/N 10^{-17} cm^2	$R_7 = Ar^+$ α_T/N 10^{-17} cm^2
2.83						
8.48						
14.1	2.49×10^{-3}		0.15	7.43×10^{-8}	0.17	1.08×10^{-5}
28.3	9.33×10^{-2}	1.19×10^{-8}	0.57	3.66×10^{-4}	0.13	5.37×10^{-3}
43.0	0.39	1.90×10^{-5}	0.71	7.92×10^{-3}	0.11	5.03×10^{-2}
56.5	0.91	8.38×10^{-4}	0.72	0.10	0.09	1.68×10^{-1}
70.6	1.46	8.24×10^{-3}	0.69	0.26	0.08	0.37
84.8	2.01	3.71×10^{-2}	0.66	0.48	0.07	0.63
98.9	2.51	0.11	0.63	0.80	0.07	0.97
113	2.85	0.24	0.59	1.16	0.06	1.35
127	3.12	0.42	0.57	1.55	0.06	1.77
141	3.29	0.69	0.54	2.00	0.06	2.21
155	3.42	0.99	0.52	2.48	0.05	2.66
170	3.49	1.35	0.50	2.93	0.05	3.17
184	3.53	1.77	0.48	3.45	0.05	3.68
198	3.53	2.19	0.46	3.96	0.05	4.17
212	3.54	2.68	0.44	4.45	0.05	4.70
226	3.50	3.15	0.43	5.00	0.04	5.21
240	3.47	3.66	0.42	5.52	0.04	5.57
254	3.43	4.20	0.40	6.04	0.04	6.25

Na Ar

0.001 99.999

E/N Td	$\frac{R_2 + R_3 + R_4}{R_5 + R_7}$	$\frac{R_6}{R_5 + R_7}$
2.83	17.4	1.64
8.48	12.4	20.1
14.1	11.7	52.1
28.3	7.51	119.3
4 30	1.73	55.5
56.5	0.49	25.0
70.6	0.20	14.3
84.8	0.10	9.57
98.9	6.1×10^{-2}	7.07
113	4.0×10^{-2}	5.57
127	2.8×10^{-2}	4.57
141	2.1×10^{-2}	3.90
155	1.6×10^{-2}	3.38
170	1.3×10^{-2}	2.99
184	1.0×10^{-2}	2.69
198	9.0×10^{-3}	2.45
212	7.0×10^{-3}	2.25
226	6.0×10^{-3}	2.08
240	5.0×10^{-3}	1.94
254	4.8×10^{-3}	1.82
268	4.0×10^{-3}	1.72

Na 20%

Ar 80%

E/N Td	$\frac{R_2 + R_3 + R_4}{R_5 + R_7}$	$\frac{R_6}{R_5 + R_7}$
2.83		
8.48		
14.1	1.51×10^{12}	
28.3	4.52×10^{6}	
4.30	6.47×10^{4}	
56.5	7.37×10^{3}	4.89×10^{-10}
70.6	1.89×10^{3}	4.42×10^{-8}
84.8	7.50×10^{2}	6.09×10^{-7}
98.9	3.76×10^{2}	4.02×10^{-6}
113	2.23×10^{2}	1.69×10^{-5}
127	1.46×10^{2}	5.28×10^{-5}
141	1.04×10^{2}	1.32×10^{-4}
155	0.78×10^{2}	2.84×10^{-4}
170	5 93	5.43×10^{-4}
184	49.5	9.40×10^{-4}
198	41.3	1.51×10^{-3}
212	35.4	2.31×10^{-3}
226	30.8	3.36×10^{-3}
240	27.1	4.69×10^{-3}
254	24.3	6.32×10^{-3}
268	21.9	8.27×10^{-3}

CHAPTER TWO

REVIEW OF SWARM DATA

2.1 INTRODUCTION

Many previous workers have developed basic techniques which were relevant to the development of the time of flight technique. A summary of all the relevant published data is available in several texts (Dutton, 1975 ; Laborie et al, 1968, 1971). The aim of this chapter is to summarise the techniques and methods selected or developed by the Liverpool group to be capable of covering a wide range of E/N for the measurement of these swarm parameters.

One must consider what is meant when an 'electron swarm' is referred to. A swarm of electrons is a group of electrons moving in a uniform electric field, such that there is no space charge distortion. Under the influence of the electric field, the swarm will drift and diffuse from cathode to anode, ionization and attachment taking place, creating extra electrons or absorbing them. The motion of the swarm is defined by the transport equation :-

$$\frac{\partial n}{\partial t} = -v\frac{\partial n}{\partial z} + D_L \cdot \frac{\partial^2 n}{\partial z^2} + D_r \left(\frac{\partial^2 n}{\partial x^2} + \frac{\partial^2 n}{\partial y^2} \right) + (\alpha - \eta)\, vn \,, \qquad (2.1)$$

where n = number density of electrons,

v = electron drift velocity,

z = direction of electric field,

D_L = longitudinal diffusion coefficient (parallel to the applied electric field),

D_r = radial diffusion coefficient (perpendicular to the applied electric field),

SODIUM

E/N Td	v_d $\times 10^7$ cm/s	$\overline{\epsilon}$ eV	D_r/μ V	α_T/N $\times 10^{-17}$ cm^2	R_1 $\times 10^{-1}$ S^{-1}	R_2 $\times 10^{8}$ S^{-1}	R_3 $\times 10^{6}$ S^{-1}	R_4 $\times 10^{6}$ S^{-1}	R_5 $\times 10^{6}$ S^{-1}	R_6 $\times 10^{}$ S^{-1}	R_7 $\times 10^{}$ S^{-1}
2.83	0.4×10^{-2}	0.11	0.11		3.70						
8.48	0.01	0.24	0.18		4.43	0.1×10^{-3}					
14.1	0.02	0.41	0.28		4.39	0.3×10^{-2}					
28.3	0.06	0.52	0.34	9.7×10^{-17}	4.25	0.02					
43.0	0.09	0.56	0.35	3.2×10^{-11}	4.22	0.06					
56.5	0.12	0.58	0.36	2.2×10^{-8}	4.18	0.11	0.2×10^{-4}				
70.6	0.16	0.61	0.37	1.1×10^{-6}	4.15	0.18	0.3×10^{-3}	0.7×10^{-5}			
84.8	0.20	0.64	0.39	1.6×10^{-5}	4.09	0.28	0.2×10^{-2}	0.7×10^{-4}	0.1×10^{-4}		
98.9	0.24	0.65	0.39	1.2×10^{-4}	4.05	0.40	0.9×10^{-2}	0.4×10^{-3}	0.1×10^{-3}		
113	0.29	0.68	0.41	5×10^{-4}	4.12	0.54	0.3×10^{-1}	0.1×10^{-2}	0.5×10^{-3}		
127	0.35	0.71	0.42	1.8×10^{-3}	4.04	0.73	0.7×10^{-1}	0.4×10^{-2}	0.2×10^{-2}		
141	0.40	0.73	0.43	4.7×10^{-3}	4.03	0.96	0.15	0.9×10^{-2}	0.7×10^{-2}		
155	0.46	0.76	0.45	0.01	3.99	1.18	0.30	0.2×10^{-1}	0.2×10^{-1}		
170	0.53	0.78	0.47	0.02	3.96	1.47	0.54	0.4×10^{-1}	0.4×10^{-1}		
184	0.58	0.78	0.48	0.04	3.99	1.75	0.82	0.7×10^{-1}	0.8×10^{-1}		
198	0.68	0.84	0.50	0.07	3.90	2.19	1.47	0.12	0.17		
212	0.74	0.84	0.51	0.11	3.96	2.54	2.04	0.18	0.28		
226	0.81	0.85	0.53	0.16	3.95	3.10	2.95	0.27	0.47		
240	0.93	0.91	0.57	0.25	3.82	3.72	4.48	0.44	0.82		
254	1.00	0.90	0.58	0.34	3.82	4.26	5.73	0.57	1.16		
268	1.12	0.95	0.62	0.45	3.72	4.98	8.11	0.84	1.82		
283	1.23	0.97	0.64	0.59	3.70	5.52	10.6	1.13	2.63		

Na Ar

1% 99%

E/N Td	v_d x 10^7 cm/s	$\overline{\epsilon}$ eV	D_r/μ V	α_T/N $\times 10^{-17}$ cm^2	R_1 x 10^9 S^{-1}	R_2 x 10^8 S^{-1}	R_3 x 10^7 S^{-1}	R_4 x 10^7 S^{-1}	R_5 x 10^7 S^{-1}	R_6 x 10^7 S^{-1}	R_7 x 10^7 S^{-1}
2.83	0.26	0.91	0.66	5.28×10^{-13}	0.59	0.01	0.12×10^{-6}				
8.48	0.62	1.23	0.96	4.29×10^{-5}	0.69	0.09	0.13×10^{-2}	0.50×10^{-4}	0.94×10^{-5}		
14.1	0.84	1.54	1.24	24.8×10^{-4}	0.82	0.20	0.16×10^{-1}	0.11×10^{-2}	0.74×10^{-3}		
28.3	1.09	2.25	1.97	0.09	1.27	0.48	0.16	0.17×10^{-1}	0.36×10^{-1}	0.21×10^{-4}	
43.0	1.16	2.92	2.71	0.40	1.79	0.71	0.41	0.51×10^{-1}	0.16	0.22×10^{-2}	0.78×10^{-5}
56.5	1.18	3.54	3.41	0.90	2.34	0.89	0.67	0.91×10^{-1}	0.38	0.24×10^{-1}	0.35×10^{-3}
70.6	1.20	4.11	4.07	1.50	2.87	1.03	0.91	0.13	0.62	1.00×10^{-1}	0.35×10^{-2}
84.8	1.22	4.63	4.66	2.06	3.35	1.14	1.11	0.16	0.87	0.26	0.16×10^{-1}
98.9	1.24	5.08	5.18	2.60	3.77	1.24	1.27	0.19	1.10	0.50	0.48×10^{-1}
113	1.29	5.47	5.61	3.08	4.13	1.31	1.40	0.21	1.30	0.82	0.11
127	1.34	5.82	5.99	3.56	4.43	1.37	1.51	0.23	1.48	1.20	0.20
141	1.40	6.13	6.30	3.98	4.69	1.42	1.60	0.24	1.63	1.62	0.34
155	1.46	6.42	6.57	4.41	4.92	1.46	1.67	0.26	1.77	2.08	0.51
170	1.53	6.67	6.79	4.86	5.11	1.50	1.74	0.27	1.89	2.56	0.73
184	1.60	6.91	7.00	5.28	5.29	1.54	1.79	0.28	2.00	3.07	1.00
198	1.68	7.14	7.17	5.73	5.45	1.57	1.84	0.29	2.10	3.60	1.30
212	1.75	7.35	7.33	6.22	5.59	1.59	1.89	0.29	2.19	4.14	1.66
226	1.84	7.55	7.46	6.67	5.71	1.62	1.92	0.30	2.28	4.50	2.05
240	1.92	7.74	7.58	7.15	5.83	1.64	1.96	0.31	2.36	5.26	2.49
254	2.00	7.93	7.70	7.63	5.93	1.66	1.99	0.31	2.43	5.83	2.97
268	2.09	8.11	7.81	8.11	6.03	1.68	2.02	0.32	2.50	6.41	3.48
283	2.17	8.28	7.91	8.59	6.12	1.70	2.05	0.32	2.56	7.00	4.03

Na Ar

7% 93%

E/N Td	v_d $\times 10^7$ cm/s	$\overline{\epsilon}$ eV	D_r/μ V	α_T/N $\times 10^{-17}$ cm^2	R_1 $\times 10^9 S^{-1}$	R_2 $\times 10^8 S^{-1}$	R_3 $\times 10^7 S^{-1}$	R_4 $\times 10^7 S^{-1}$	R_5 $\times 10^7 S^{-1}$	R_6 $\times 10^7 S^{-1}$	R_7 $\times 10^6 S^{-1}$
2.83	0.07	0.60	0.39	6.24×10^{-21}	2.99	3.4×10^{-3}					
8.48	0.23	0.70	0.45	16.1×10^{-12}	2.92	0.33	0.6×10^{-6}				
14.1	0.40	0.79	0.51	3.28×10^{-7}	2.85	0.96	0.1×10^{-3}	0.2×10^{-5}			
28.3	0.87	1.01	0.66	7.46×10^{-4}	2.67	0.41	0.01	0.6×10^{-3}	0.2×10^{-3}		
43.0	1.32	1.26	0.84	13.4×10^{-3}	2.53	0.92	0.09	0.7×10^{-2}	0.6×10^{-2}		
56.5	1.72	1.52	1.03	0.07	2.44	1.57	0.31	0.03	0.04	0.2×10^{-6}	
70.6	2.05	1.81	1.25	0.20	2.41	2.28	0.68	0.07	0.14	0.9×10^{-5}	
84.8	2.30	2.09	1.47	0.40	2.43	2.98	1.18	0.13	0.32	0.1×10^{-3}	0.5×10^{-5}
98.9	2.50	2.37	1.70	0.71	2.49	3.66	1.80	0.22	0.62	0.7×10^{-3}	0.79×10^{-4}
113	2.64	2.65	1.94	1.07	2.58	4.30	2.47	0.31	1.02	0.3×10^{-2}	0.6×10^{-3}
127	2.75	2.93	2.19	1.55	2.69	4.88	3.20	0.42	1.52	0.9×10^{-2}	0.4×10^{-2}
141	2.84	3.20	2.43	2.09	2.82	5.45	3.92	0.53	2.11	0.02	0.1×10^{-1}
155	2.90	3.47	2.67	2.71	2.98	5.94	4.65	0.64	2.77	0.05	0.4×10^{-1}
170	2.95	3.72	2.91	3.36	3.14	6.43	5.35	0.75	3.49	0.10	0.10
184	2.98	3.98	3.16	4.04	3.31	6.87	6.05	0.86	4.25	0.16	0.23
198	3.01	4.24	3.39	4.77	3.49	7.27	6.70	0.96	5.04	0.26	0.45
212	3.04	4.49	3.64	5.51	3.66	7.66	7.34	1.07	5.85	0.39	0.81
226	3.06	4.74	3.87	6.24	3.84	8.03	7.93	1.16	6.65	0.56	1.35
240	3.09	4.98	4.10	7.01	4.01	8.35	8.49	1.26	7.46	0.76	2.11
254	3.12	5.22	4.32	7.77	4.18	8.69	9.02	1.34	8.25	1.00	3.16
268	3.14	5.46	4.55	8.53	4.35	8.97	9.52	1.43	9.04	1.28	4.52
283	3.17	5.70	4.75	9.29	4.50	9.24	10.0	1.51	9.80	1.60	6.24

Na 10% Ar 90%

E/N Td	v_d x 10^7 cm/s	$\overline{\epsilon}$ eV	D_r/μ V	α_T/N $\times 10^{-17}$ cm^2	R_1 x 10^9 S^{-1}	R_2 x 10^8 S^{-1}	R_3 x 10^7 S^{-1}	R_4 x 10^7 S^{-1}	R_5 x 10^7 S^{-1}	R_6 x 10^6 S^{-1}	R_7 x 10^7 S^{-1}
2.83	0.05	0.57	0.37		4.24						
8.48	0.17	0.64	0.41	14.6×10^{-14}	4.19	0.02					
14.1	0.29	0.71	0.43	16.4×6^{-9}	4.10	0.07	0.19×10^{-4}	0.18×10^{-6}			
28.3	0.66	0.88	0.56	16.5×0^{-5}	3.87	0.31	0.43×10^{-2}	0.17×10^{-3}	0.38×10^{-4}		
43.0	1.05	1.06	0.68	4.75×10^{-3}	3.65	0.74	0.04	0.28×10^{-2}	0.18×10^{-2}		
56.5	1.44	1.25	0.82	0.03	3.47	1.34	0.17	0.01	0.02		
70.6	1.81	1.46	0.98	0.10	3.32	2.05	0.43	0.04	0.06	0.48×10^{-5}	
84.8	2.14	1.69	1.15	0.23	3.19	2.84	0.84	0.09	0.17	0.92×10^{-4}	
98.9	2.42	1.92	1.32	0.43	3.12	3.67	1.39	0.16	0.37	0.80×10^{-3}	0.37×10^{-6}
113	2.66	2.16	1.51	0.71	3.09	4.49	2.06	0.24	0.67	0.42×10^{-2}	0.43×10^{-5}
127	2.85	2.40	1.70	1.07	3.08	5.28	2.83	0.35	1.08	0.16×10^{-1}	0.31×10^{-4}
141	3.01	2.64	1.89	1.50	3.11	6.06	3.64	0.47	1.60	0.47×10^{-1}	0.15×10^{-3}
155	3.14	2.87	2.09	2.01	3.16	6.78	4.50	0.59	2.22	0.12	0.56×10^{-3}
170	3.25	3.11	2.29	2.54	3.23	7.48	5.58	0.72	2.93	0.25	0.17×10^{-2}
184	3.33	3.34	2.49	3.16	3.31	8.11	6.26	0.86	3.72	0.48	0.44×10^{-2}
198	3.40	3.58	2.70	2.81	3.41	8.73	7.15	0.99	4.58	0.84	0.01
212	3.45	3.80	2.89	4.49	3.53	9..28	8.00	1.13	5.50	1.37	0.02
226	3.50	4.02	3.09	5.23	3.65	9.84	8.83	1.26	6.43	2.11	0.04
240	3.54	4.25	3.29	5.96	3.78	10.4	9.63	1.39	7.41	3.09	0.07
254	3.57	4.48	3.50	6.75	3.91	10.8	10.4	1.52	8.42	4.36	0.11
268	3.61	4.69	3.69	7.51	4.04	11.3	11.2	1.64	9.42	5.90	0.17
283	3.64	4.91	3.89	8.28	4.17	11.7	11.9	1.75	10.4	7.76	0.25

Na 20% Ar 80%

E/N Td	v_d x 10^7 cm/s	$\overline{\epsilon}$ eV	D_r/μ V	α_T/N $\times 10^{-17}$ cm^2	R_1 x 10^9 S^{-1}	R_2 x 10^7 S^{-1}	R_3 x 10^6 S^{-1}	R_4 x 10^6 S^{-1}	R_5 x 10^6 S^{-1}	R_6 x 10^5 S^{-1}	R_7 x 10^4 S^{-1}
2.83	0.03	0.51	0.34		8.48	0.01					
8.48	0.08	0.57	0.37	11.9×10^{-20}	8.42	0.12					
14.1	0.15	0.62	0.39	4.46×10^{-12}	8.34	0.35					
28.3	0.33	0.71	0.44	2.97×10^{-6}	8.07	1.57	0.26×10^{-2}				
43.0	0.55	0.80	0.50	3.11×10^{-4}	7.78	3.88	0.52×10^{-1}	0.22×10^{-2}			
56.5	0.79	0.89	0.56	3.64×10^{-3}	7.49	7.48	0.30	0.18×10^{-1}	0.10×10^{-1}		
70.6	1.06	0.99	0.64	17.6×10^{-3}	7.21	12.4	1.01	0.75×10^{-1}	0.66×10^{-1}		
84.8	1.34	1.10	0.72	0.05	6.94	18.6	2.46	0.21	0.25		
98.9	1.64	1.22	0.81	0.12	6.63	26.2	4.97	0.47	0.71	0.3×10^{-4}	
113	1.93	1.35	0.91	0.23	6.37	34.8	8.63	0.87	1.60	0.3×10^{-3}	
127	2.23	1.49	1.02	0.40	6.12	44.5	13.8	1.48	3.15	0.17×10^{-2}	
141	2.51	1.64	1.13	0.62	5.93	54.4	20.1	2.26	5.47	0.72×10^{-2}	0.5×10^{-3}
155	2.78	1.80	1.25	0.90	5.71	65.3	27.8	3.26	8.79	0.25×10^{-1}	0.3×10^{-2}
170	3.03	1.96	1.37	1.24	5.53	74.0	36.8	4.46	13.2	0.72×10^{-1}	0.1×10^{-1}
184	3.26	2.13	1.49	1.61	5.38	87.0	46.6	5.81	18.6	0.18	0.52×10^{-1}
198	3.49	2.31	1.62	2.06	5.20	98.4	57.7	7.36	25.4	0.38	0.16
212	3.67	2.48	1.75	2.54	5.10	109	68.9	8.98	33.1	0.76	0.43
226	3.84	2.65	1.88	3.08	5.00	120	80.0	10.7	41.9	1.4	1.0
240	4.00	2.84	2.02	3.67	4.91	130	93.7	12.6	52.1	2.4	2.30
254	4.15	3.02	2.16	4.29	4.84	141	106	14.5	63.1	4.0	4.7
268	4.27	3.20	2.30	4.94	4.80	151	119	16.5	74.9	6.2	8.6
283	4.38	3.37	2.44	5.65	4.78	161	132	18.5	87.4	9.2	15

Na Ar

0.1% 99.9 %

E/N Td	v_d x 10^7 cm/s	$\overline{\epsilon}$ eV	D_r/μ V	α_T/N $\times 10^{-17}$ cm^2	R_1 x 10^9 S^{-1}	R_2 x 10^7 S^{-1}	R_3 x 10^6 S^{-1}	R_4 x 10^5 S^{-1}	R_5 x 10^6 S^{-1}	R_6 x 10^7 S^{-1}	R_7 x 10^7 S^{-1}
2.83	0.25	1.39	1.64	2.2×10^{-5}	0.49	0.12	0.22×10^{-2}	0.90×10^{-3}	0.20×10^{-4}		
8.48	0.36	2.26	2.77	0.02	1.11	0.48	0.15	0.16	0.03	0.43×10^{-5}	
14.1	0.38	0.31	3.79	0.15	1.80	0.75	0.46	0.59	0.20	0.11×10^{-2}	0.1×10^{-7}
28.3	0.41	4.53	5.68	0.56	3.22	1.13	1.09	1.57	0.82	0.07	0.15×10^{-3}
43.0	0.48	5.28	6.65	0.73	3.96	1.29	1.37	2.04	1.21	0.28	0.38×10^{-2}
56.5	0.57	5.73	7.20	0.82	4.39	1.37	1.52	2.30	1.45	0.59	0.02
70.6	0.67	6.07	7.55	0.95	4.69	1.43	1.62	2.47	1.63	0.95	0.06
84.8	0.76	6.35	7.80	1.16	4.93	1.47	1.70	2.60	1.77	1.36	0.13
98.9	0.85	6.60	8.00	1.44	5.13	1.51	1.76	2.70	1.89	1.79	0.24
113	0.95	6.82	8.16	1.75	5.30	1.54	1.81	2.79	1.99	2.24	0.39
127	1.04	7.02	8.29	2.12	5.45	1.57	1.85	2.87	2.08	2.71	0.57
141	1.13	7.21	8.39	2.54	5.58	1.59	1.89	2.94	2.17	3.19	0.80
155	1.22	7.39	8.50	2.99	5.70	1.61	1.93	3.00	2.25	3.68	1.07
170	1.32	7.56	8.58	3.45	5.81	1.63	1.96	3.05	2.32	4.19	1.37
184	1.41	7.73	8.66	3.93	5.91	1.65	1.99	3.10	2.39	4.70	1.72
198	1.50	7.89	8.73	4.41	6.00	1.67	2.02	3.15	2.45	5.22	2.10
212	1.60	8.05	8.80	4.92	6.08	1.69	2.04	3.20	2.51	5.75	2.52
226	1.69	8.20	8.86	5.42	6.16	1.71	2.07	3.24	2.57	6.30	2.99
240	1.78	8.36	8.92	5.93	6.24	1.72	2.09	3.28	2.62	6.85	3.48
254	1.88	8.51	8.99	6.47	6.31	1.74	2.11	3.32	2.68	7.41	4.02
268	1.97	8.65	9.03	6.98	6.37	1.75	2.13	3.35	2.73	7.97	4.59
283	2.06	8.80	9.09	7.49	6.44	1.77	2.15	3.39	2.78	8.54	5.20

Na Ar

0.2% 99.8%

E/N Td	v_d x 10^7 cm/s	$\overline{\epsilon}$ eV	D_r/μ V	α_T/N $\times 10^{-17}$ cm^2	R_1 x 10^9 S^{-1}	R_2 x 10^7 S^{-1}	R_3 x 10^6 S^{-1}	R_4 x 10^5 S^{-1}	R_5 x 10^6 S^{-1}	R_6 x 10^7 S^{-1}	R_7 x 10^7 S^{-1}
2.83	0.28	1.24	1.25	5.88×10^{-24}	0.44	0.14	0.50×10^{-3}	0.11×10^{-3}	0.55×10^{-6}	0.1×10^{-24}	0.6×10^{-54}
8.48											
14.1	0.52	2.48	2.79	0.06	1.30	1.12	0.45	0.50	0.12	0.49×10^{-4}	0.24×10^{-9}
28.3	0.54	3.80	4.43	0.49	2.51	1.92	1.56	2.15	0.95	0.02	0.33×10^{-4}
43.0	0.58	4.73	5.62	0.90	3.42	2.35	2.32	3.39	1.84	0.15	0.18×10^{-2}
56.5	0.64	5.34	6.38	1.17	4.00	2.59	2.77	4.13	2.48	0.41	0.01
70.6	0.72	5.77	6.88	1.33	4.41	2.75	3.05	4.60	2.93	0.74	0.05
84.8	0.80	6.11	7.23	1.53	4.71	2.86	3.25	4.95	3.29	1.13	0.11
98.9	0.89	6.40	7.50	1.78	4.96	2.95	3.40	5.21	3.57	1.56	0.21
113	0.98	6.65	7.70	2.09	5.16	3.02	3.53	5.42	3.81	2.01	0.34
127	1.07	6.88	7.87	2.46	5.33	3.08	3.63	5.60	4.02	2.47	0.52
141	1.16	7.08	8.01	2.83	5.48	3.15	3.72	5.76	4.21	2.95	7.39
155	1.25	7.28	8.13	3.25	5.61	3.19	3.80	5.90	4.38	3.45	1.00
170	1.34	7.46	8.23	3.70	5.73	3.23	3.87	6.02	4.54	3.95	1.30
184	1.43	7.64	8.32	4.15	5.84	3.28	3.94	6.14	4.69	4.46	1.64
198	1.52	7.81	8.41	4.63	5.94	3.32	4.00	6.24	4.83	4.99	2.01
212	1.61	7.97	8.49	5.14	6.03	3.36	4.05	6.34	4.95	5.52	2.43
226	1.70	8.14	8.56	5.60	6.12	3.39	4.10	6.43	5.08	6.07	2.89
240	1.80	8.29	8.63	6.13	6.20	3.43	4.15	6.51	5.19	6.61	3.38
254	1.89	8.45	8.69	6.64	6.27	3.46	4.20	6.59	5.30	7.17	3.91
268	1.98	8.60	8.76	7.18	6.34	3.49	4.24	6.67	5.41	7.73	4.48
283	2.07	8.74	8.81	7.63	6.40	3.52	4.28	6.74	5.51	8.30	5.09

Na Ar

0.7% 99.3%

E/N Td	v_d x 10^7 cm/s	$\overline{\epsilon}$ eV	D_r/μ V	α_T/N $\times 10^{-17}$ cm^2	R_1 x 10^9 S^{-1}	R_2 x 10^8 S^{-1}	R_3 x 10^7 S^{-1}	R_4 x 10^6 S^{-1}	R_5 x 10^7 S^{-1}	R_6 x 10^7 S^{-1}	R_7 x 10^7 S^{-1}
2.83	0.28	0.98	0.76	2.99×10^{-11}	0.50	0.01					
8.48	0.62	1.36	1.14	1.76×10^{-4}	0.65	0.09	0.26×10^{-2}	0.12×10^{-2}	0.4×10^{-4}		
14.1	0.79	1.71	1.50	6.05×10^{-3}	0.84	0.18	0.02	0.02	0.17×10^{-2}		
28.3	0.95	2.54	2.40	0.16	1.43	0.41	0.18	0.21	0.05	0.18×10^{-3}	
43.0	0.99	3.30	3.28	0.56	2.09	0.57	0.40	0.52	0.20	0.89×10^{-2}	0.48×10^{-4}
56.5	1.00	3.99	4.09	1.11	2.73	0.70	0.60	0.84	0.39	0.06	0.13×10^{-2}
70.6	1.02	4.58	4.79	1.67	3.29	0.80	0.77	1.11	0.59	0.21	0.89×10^{-2}
84.8	1.06	5.08	5.38	2.15	3.77	0.87	0.89	1.32	0.77	0.45	0.03
98.9	1.11	5.51	5.87	2.57	4.16	0.92	0.99	1.49	0.92	0.77	0.08
113	1.16	5.87	6.25	2.97	4.48	0.97	1.07	1.62	1.05	1.15	0.17
127	1.23	6.19	6.57	3.33	4.74	1.00	1.13	1.73	1.16	1.58	0.29
141	1.30	6.47	6.83	3.73	4.97	1.03	1.19	1.82	1.26	2.04	0.45
155	1.37	6.72	7.05	4.12	5.17	1.06	1.23	1.89	1.34	2.53	0.66
170	1.45	6.96	7.24	4.52	5.34	1.08	1.27	1.96	1.42	3.04	0.91
184	1.53	7.17	7.40	4.97	5.49	1.10	1.30	2.01	1.49	3.56	1.20
198	1.61	7.38	7.55	5.40	5.63	1.12	1.33	2.07	1.55	4.09	1.54
212	1.70	7.57	7.67	5.85	5.75	1.14	1.36	2.11	1.61	4.64	1.91
226	1.78	7.76	7.79	6.33	5.86	1.15	1.38	2.15	1.66	5.19	2.33
240	1.87	7.94	7.80	6.81	5.96	1.17	1.40	2.19	1.71	5.75	2.79
254	1.96	8.12	7.99	7.29	6.06	1.18	1.42	2.23	1.76	6.33	3.29
268	2.05	8.29	8.09	7.77	6.14	1.19	1.44	2.26	1.80	6.90	3.83
283	2.13	8.45	8.17	8.28	6.22	1.21	1.46	2.29	1.84	7.49	4.40

A:30

Na Ar

0.01% 99.99 %

E/N Td	v_d x 10^7 cm/s	$\overline{\epsilon}$ eV	D_r/μ V	α_T/N $\times 10^{-17}$ cm^2	R_1 x 10^9 S^{-1}	R_2 x 10^6 S^{-1}	R_3 x 10^5 S^{-1}	R_4 x 10^4 S^{-1}	R_5 x 10^5 S^{-1}	R_6 x 10^7 S^{-1}	R_7 x 10^7 S^{-1}
2.83	0.12	2.34	3.51	9.41×10^{-3}	1.15	0.51	0.17	0.19	0.04	0.18×10^{-5}	
8.48	0.13	4.28	6.08	0.15	1.97	1.08	1.00	1.42	0.69	0.83×10^{-2}	
14.1	0.18	4.96	6.96	0.17	3.66	1.23	1.28	1.89	1.05	0.04	
28.3	0.30	5.53	7.69	0.13	4.22	1.34	1.48	2.23	1.36	0.22	0.57×10^{-3}
43.0	0.41	5.85	8.11	0.16	4.52	1.40	1.58	2.39	1.53	0.48	0.73×10^{-2}
56.5	0.52	6.12	8.36	0.26	4.76	1.44	1.65	2.51	1.66	0.81	0.03
70.6	0.62	6.36	8.57	0.45	4.96	1.48	1.71	2.62	1.78	1.18	0.08
84.8	0.72	6.57	8.72	0.72	5.13	1.51	1.76	2.71	1.89	1.59	0.16
98.9	0.82	6.78	8.84	1.05	5.29	1.54	1.81	2.79	1.98	2.01	0.28
113	0.92	6.97	8.96	1.41	5.43	1.56	1.85	2.86	2.07	2.46	0.44
127	1.02	7.15	9.05	1.84	5.55	1.58	1.87	2.93	2.15	2.92	0.64
141	1.11	7.32	9.13	2.27	5.67	1.61	1.92	2.98	2.23	3.39	0.87
155	1.21	7.49	9.21	2.74	5.78	1.63	1.95	3.04	2.30	3.88	1.14
170	1.30	7.65	9.29	3.22	5.87	1.65	1.98	3.09	2.36	4.38	1.46
184	1.39	7.81	9.36	3.73	5.97	1.66	2.01	3.14	2.43	4.89	1.81
198	1.49	7.97	9.43	4.24	6.05	1.68	2.03	3.18	2.49	5.41	2.20
212	1.58	8.12	9.49	4.75	6.13	1.70	2.06	3.22	2.54	5.93	2.63
226	1.68	8.27	9.55	5.25	6.21	1.71	2.08	3.26	2.60	6.48	3.10
240	1.77	8.42	9.60	5.79	6.28	1.73	2.10	3.30	2.65	7.02	3.60
254	1.87	8.56	9.68	6.33	6.34	1.74	2.12	3.33	2.70	7.58	4.14
268	1.96	8.71	9.73	6.84	6.41	1.76	2.14	3.37	2.75	8.14	4.71
283	2.05	8.85	9.78	7.66	6.47	1.77	2.16	3.40	2.80	8.70	5.53

Na Ar

0.07% 99.93%

E/N Td	v_d $\times 10^7$ cm/s	$\overline{\epsilon}$ eV	D_r/μ V	α_T/N $\times 10^{-17}$ cm^2	R_1 $\times 10^9 s^{-1}$	R_2 $\times 10^7 s^{-1}$	R_3 $\times 10^6 s^{-1}$	R_4 $\times 10^5 s^{-1}$	R_5 $\times 10^6 s^{-1}$	R_6 $\times 10^7 s^{-1}$	R_7 $\times 10^7 s^{-1}$
2.83	0.23	1.48	1.87	8.42×10^{-5}	0.54	0.11	0.38×10^{-2}	0.19×10^{-2}	0.69×10^{-4}		
8.48	0.31	2.51	3.21	0.04	1.30	0.40	0.16	0.19	0.04	0.33×10^{-4}	
14.1	0.32	3.42	4.39	0.02	2.13	0.60	0.43	0.57	0.22	0.34×10^{-2}	
28.3	0.37	4.83	6.23	0.05	3.51	0.84	0.85	1.24	0.68	0.11	0.24×10^{-3}
43.0	0.46	5.46	7.04	0.06	4.14	0.93	1.01	1.51	0.92	0.34	0.47×10^{-2}
56.5	0.55	5.86	7.50	0.07	4.51	0.98	1.09	1.66	1.07	0.66	0.02
70.6	0.65	6.17	7.80	0.08	4.78	1.01	1.16	1.76	1.18	1.03	0.07
84.8	0.75	6.42	8.03	1.02	5.00	1.04	1.20	1.84	1.27	1.43	0.14
98.9	0.84	6.66	8.20	1.30	5.18	1.06	1.24	1.91	1.34	1.86	0.25
113	0.94	6.87	8.34	1.64	5.34	1.08	1.28	1.97	1.41	2.31	0.40
127	1.03	7.06	8.46	2.03	5.48	1.10	1.31	2.02	1.47	2.78	0.59
141	1.12	7.25	8.56	2.46	5.61	1.12	1.33	2.07	1.53	3.26	0.82
155	1.22	7.42	8.65	2.91	5.72	1.13	1.36	2.11	1.58	3.75	1.09
170	1.31	7.59	8.73	3.36	5.83	1.15	1.38	2.15	1.63	4.25	1.40
184	1.40	7.76	8.81	3.84	5.93	1.16	1.40	2.18	1.68	4.76	1.75
198	1.50	7.92	8.88	4.35	6.02	1.17	1.42	2.21	1.73	5.29	2.14
212	1.59	8.07	8.95	4.86	6.10	1.18	1.43	2.24	1.77	5.82	2.56
226	1.69	8.23	9.00	5.37	6.18	1.20	1.45	2.27	1.81	6.36	3.02
240	1.78	8.38	9.06	5.88	6.25	1.21	1.47	2.30	1.84	6.91	3.52
254	1.87	8.53	9.12	6.41	6.32	1.22	1.48	2.33	1.88	7.46	4.06
268	1.97	8.67	9.17	6.92	6.39	1.23	1.49	2.35	1.92	8.02	4.63
283	2.06	8.82	9.22	7.46	6.45	1.24	1.51	2.37	1.95	8.59	5.24

α = ionization coefficient,

η = attachment coefficient.

It is not always possible to measure both α and v when ionization is present (Lucas and Saelee, 1975). Other coefficients are measured which are closely related to α and v, but involve a factor $\frac{\alpha D_L}{v}$, e.g. a steady state measurement of ionization measures α_T (Townsend's ionization coefficient) where :-

$$\alpha_T = \lambda - u \ ,$$

with $$\lambda = \frac{v}{2 D_L} \ , \quad u^2 = \lambda^2 - 2\alpha\lambda \ .$$

If $\frac{\alpha}{\lambda} \ll 1$ then $\alpha_T = \alpha$.

Measurement of the drift velocity gives v_d and v_{exp} where :-

$$v_d = \frac{uv}{\lambda} \ ,$$

and $$v_{exp} = \tfrac{1}{2}\left(\frac{u}{\lambda} + 1\right) v \ .$$

2.2 UNIFORM ELECTRIC FIELDS

One of the prime requirements of experimental apparatus designed to measure these five swarm parameters, which define the swarm motion, is that a uniform field region must exist. There are two basic electrode geometries which may create a uniform electric field region. The first type, which may be used to measure α and η when secondary ionization currents are present, uses two electrodes with Rogowski profiles to maintain a homogeneous field in the centre of the electrodes. A study of such electrodes was performed by Harrison (1967) who designed a modified form of the Rogowski profile to

Na 0.001% Ar 99.999%

E/N Td	v_d x 10^7 cm/s	$\overline{\epsilon}$ eV	D_r/μ V	α_T/N $\times 10^{-17}$ cm^2	R_1 x $10^9 S^{-1}$	R_2 x $10^5 S^{-1}$	R_3 x $10^4 S^{-1}$	R_4 x $10^3 S^{-1}$	R_5 x $10^4 S^{-1}$	R_6 x $10^7 S^{-1}$	R_7 x $10^6 S^{-1}$
2.83	0.04	4.29	6.27	4.38×10^{-2}	2.97	1.09	1.00	1.43	0.69	0.11×10^{-2}	
5.65	0.07	4.95	7.01	4.10×10^{-2}	3.65	1.24	1.29	1.90	1.04	0.94×10^{-2}	
8.48	0.10	5.14	7.24	3.19×10^{-2}	3.84	1.27	1.36	2.02	1.15	0.02	
11.3	0.13	5.25	7.39	2.61×10^{-2}	3.95	1.29	1.40	2.09	1.21	0.04	
14.1	0.16	5.33	7.53	2.23×10^{-2}	4.04	1.31	1.42	2.13	1.26	0.07	0.91×10^{-5}
28.3	0.29	5.65	8.00	2×10^{-2}	4.34	1.37	1.52	2.30	1.43	0.24	0.62×10^{-2}
43	0.41	5.91	8.34	6.41×10^{-2}	4.58	1.41	1.60	2.43	1.56	0.51	0.76×10^{-1}
56.5	0.51	6.16	8.58	0.18	4.80	1.45	1.66	2.54	1.69	0.84	0.31
70.6	0.62	6.39	8.77	0.38	4.99	1.48	1.72	2.63	1.80	1.21	0.82
84.8	0.72	6.60	8.93	0.66	5.15	1.51	1.77	2.72	1.90	1.61	1.66
98.9	0.82	6.80	9.05	0.99	5.31	1.54	1.81	2.80	1.99	2.04	2.86
113	0.92	6.98	9.15	1.37	5.44	1.57	1.85	2.87	2.08	2.48	4.43
127	1.01	7.16	9.24	1.80	5.57	1.59	1.89	2.93	2.16	2.94	6.41
141	1.11	7.34	9.39	2.24	5.68	1.61	1.93	2.99	2.23	3.42	8.74

Na 0.005% Ar 99.995%

E/N Td	v_d x 10^7 cm/s	$\bar{\epsilon}$ eV	D_r/μ V	α_T/N $\times 10^{-17}$ cm^2	R_1 x 10^9 S^{-1}	R_2 x 10^5 S^{-1}	R_3 x 10^4 S^{-1}	R_4 x 10^4 S^{-1}	R_5 x 10^4 S^{-1}	R_6 x 10^7 S^{-1}	R_7 x 10^6 S^{-1}
2.83	0.08	2.86	4.31	0.23	1.60	3.45	1.87	0.23	0.69	0.4×10^{-4}	
5.65	0.09	4.16	6.01	0.95	2.84	5.27	4.72	0.67	3.15	0.3×10^{-2}	
8.48	0.11	4.72	6.73	1.13	3.41	5.92	5.93	0.87	4.59	0.01	
11.3	0.14	5.00	7.07	1.08	3.70	6.21	6.48	0.96	5.35	0.03	
14.1	0.17	5.17	7.28	0.99	3.87	6.37	6.79	1.01	5.81	0.05	0.8×10^{-5}
28.3	0.29	5.60	7.88	0.73	4.29	6.77	7.51	1.13	6.99	0.23	0.6×10^{-2}
43	0.41	5.89	8.22	1.05	4.56	7.02	7.93	1.21	7.74	0.50	0.7×10^{-1}
56.5	0.52	6.14	8.48	2.17	4.78	7.23	8.28	1.26	8.38	0.83	0.31
70.6	0.62	6.37	8.67	4.12	4.97	7.39	8.57	1.31	8.95	1.20	0.82
84.8	0.72	6.59	8.82	6.84	5.15	7.54	8.83	1.36	9.47	1.60	1.65

IONIZATION COEFFICIENT FOR MIXTURE OF (Cs+Ar)

	PERCENTAGE									
	0.001%	0.005%	0.01%	0.02%	0.05%	0.1%	0.2%	0.5%	1%	5%
	FRACTION									
	1×10^{-5}	5×10^{-5}	1×10^{-4}	2×10^{-4}	5×10^{-4}	1×10^{-3}	2×10^{-3}	5×10^{-3}	1×10^{-2}	5×10^{-2}
E/N Td	$\alpha_T/N \times 10^{-17}$ cm^2									
14.1	3.33×10^{-2}	1.41×10^{-1}	2.22×10^{-1}	2.65×10^{-1}	1.83×10^{-1}	9.58×10^{-2}	3.79×10^{-2}	6.30×10^{-3}	8.19×10^{-4}	9.27×10^{-9}
28.3	2.68×10^{-2}	1.03×10^{-3}	1.85×10^{-1}	0.34	0.54	0.54	0.37	1.37×10^{-1}	4.29×10^{-2}	9.52×10^{-5}
56.5	1.89×10^{-1}	2.37×10^{-1}	0.29	0.40	0.68	0.99	1.21	0.99	0.55	1.88×10^{-2}
84.8	6.64×10^{-1}	6.92×10^{-1}	0.73	0.82	1.02	1.30	1.72	2.01	1.55	1.57×10^{-1}
	IONIZATION COEFFICIENT FOR PURE ARGON (Ar^+) $\alpha_T/N \times 10^{-17}$ cm^2									
28.3	6.25×10^{-3}	5.72×10^{-3}	4.94×10^{-3}	3.53×10^{-3}	1.22×10^{-3}	1.88×10^{-4}	6.42×10^{-6}	2.06×10^{-9}		
84.8	0.65	0.64	0.64	0.60	0.52	0.41	0.25	4.47×10^{-2}		

Cs Ar

Percentage	1%		0.1%		0.01%	
Fraction	$1x10^{-2}$		$1x10^{-3}$		$1x10^{-4}$	
E/N Td	$R_4=Cs^+$ α_T/N 10^{-17} cm^2	$R_6=Ar^+$ α_T/N 10^{-17} cm^2	$R_4=Cs^+$ α_T/N 10^{-17} cm^2	$R_6=Ar^+$ α_T/N 10^{-17} cm^2	$R_4=Cs^+$ α_T/N 10^{-17} cm^2	$R_6=Ar^+$ α_T/N 10^{-17} cm^2
14.1	$8.23x10^{-4}$		0.10		0.22	
28.3	$4.29x10^{-2}$		0.54	$1.88x10^{-4}$	0.19	$4.94x10^{-4}$
43.0	0.22	$1.34x10^{-9}$	0.84	$9.99x10^{-3}$	0.15	$4.76x10^{-2}$
56.5	0.55	$5.41x10^{-6}$	0.92	$0.65x10^{-1}$	0.13	0.16
70.6	1.01	$2.21x10^{-4}$	0.93	0.20	0.12	0.36
84.8	1.55	$2.49x10^{-3}$	0.90	0.41	0.11	0.64
98.9	2.10	$1.35x10^{-2}$	0.86	0.70	0.10	0.96
113	2.65	$4.63x10^{-2}$	0.83	1.04	0.09	1.35
127	3.13	$1.17x10^{-1}$	0.78	1.43	0.08	1.74
141	3.53	0.24	0.75	1.86	0.08	2.21
155	3.82	0.42	0.72	2.32	0.08	2.66
170	4.08	0.66	0.69	2.80	0.07	3.15
184	4.26	0.95	0.67	3.31	0.07	3.65
198	4.40	1.30	0.64	3.82	0.07	4.17
212	4.48	1.69	0.62	4.34	0.06	4.70
226	4.55	2.11	0.60	4.85	0.06	5.21
240	4.56	2.57	0.58	5.38	0.06	5.75
254	4.57	3.06	0.57	5.92	0.06	6.25
268	4.56	3.55	0.55	6.46	0.06	6.79

Cs Ar

0.001% 99.999%

E/N Td	$\frac{R_2 + R_3}{R_4 + R_6}$	$\frac{R_5}{R_4 + R_6}$
14.1	21.4	33.6
28.3	15.4	88.6
43.0	4.34	50.5
56.5	1.30	24.2
70.6	0.54	14.1
84.8	0.28	9.50
98.9	0.17	7.02
113	0.11	5.55
127	7.6×10^{-2}	4.57
141	5.7×10^{-2}	3.88
155	4.4×10^{-2}	3.38
170	3.5×10^{-2}	2.99
184	2.8×10^{-2}	2.69
198	2.3×10^{-2}	2.45
212	2.0×10^{-2}	2.25
226	1.70×10^{-2}	2.08
240	1.50×10^{-2}	1.94
254	1.30×10^{-2}	1.82
268	1.10×10^{-2}	1.72
283	1.0×10^{-2}	1.63

Cs 20%

Ar 80%

E/N Td	$\frac{R_2 + R_3}{R_4 + R_6}$ (÷10^3)	$\frac{R_5}{R_4 + R_6}$ (x10^7)
4.30	6.33×10^{9}	
56.5	4.46×10^{7}	
70.6	2.68×10^{6}	
84.8	4.14×10^{5}	
98.9	1.04×10^{5}	
113	3.60×10^{4}	
127	1.57×10^{4}	
141	7.94×10^{3}	
155	4.48×10^{3}	
170	2.76×10^{3}	
184	1.82×10^{3}	
198	1.27×10^{3}	4.29×10^{-9}
212	9.27×10^{2}	9.18×10^{-8}
226	6.87×10^{2}	2.56×10^{-7}
240	5.34×10^{2}	7.55×10^{-7}
254	4.24×10^{2}	1.71×10^{-6}
268	3.43×10^{2}	3.56×10^{-6}
283	2.84×10^{2}	6.89×10^{-6}

CAESIUM

E/N Td	v_d x 10^6 cm/s	$\overline{\epsilon}$ eV	D_r/μ V	α_T/N x 10^{-17} cm^2	R_1 x 10^{10} S^{-1}	R_2 x 10^7 S^{-1}	R_3 x 10^7 S^{-1}	R_4 x 10^{-1} S^{-1}	R_5 x 10^{-1} S^{-1}	R_6 x 10^{-1} S^{-1}
14.1	0.06	0.16	0.23		31.1	0.01				
28.3	0.15	0.19	0.26		33.1	0.06	0.04			
43.0	0.26	0.22	0.28		33.2	0.14	0.12			
56.5	0.39	0.24	0.29		32.8	0.26	0.27			
70.6	0.53	0.26	0.30		32.3	0.43	0.49			
84.8	0.69	0.28	0.31		31.6	0.64	0.80			
98.9	0.86	0.30	0.32		30.9	0.90	1.20			
113	1.05	0.31	0.33		30.2	1.22	1.70			
127	1.25	0.33	0.34		29.5	1.60	2.32			
141	1.45	0.34	0.35		28.8	2.04	3.04			
155	1.67	0.36	0.35		28.1	2.54	3.89			
170	1.90	0.38	0.36		27.5	3.10	4.86			
184	2.13	0.39	0.37		26.8	3.73	5.97			
198	2.38	0.40	0.38		26.2	4.43	7.20			
212	2.62	0.42	0.39		25.6	5.20	8.56			
226	2.88	0.43	0.39	1.2×10^{-7}	25.0	6.03	10.1	0.12		
240	3.14	0.45	0.40	5.8×10^{-7}	24.5	6.93	11.7	0.64		
254	3.40	0.46	0.41	2.0×10^{-6}	23.9	7.90	13.5	2.36		
268	3.67	0.47	0.41	5.4×10^{-6}	23.4	8.94	15.4	7.04		
283	3.94	0.49	0.42	1.2×10^{-5}	22.9	10.1	17.5	16.7		

Cs 1% Ar 99%

E/N Td	v_d x 10^7 cm/s	$\overline{\epsilon}$ eV	D_r/μ V	α_T/N x 10^{-17} cm^2	R_1 x $10^9 S^{-1}$	R_2 x $10^8 S^{-1}$	R_3 x $10^8 S^{-1}$	R_4 x $10^7 S^{-1}$	R_5 x $10^7 S^{-1}$	R_6 x $10^7 S^{-1}$
2.83	0.22	0.50	0.47	1.86×10^{-14}	2.27	0.01	0.01			
5.65	0.48	0.69	0.59	6.05×10^{-8}	1.71	0.02	0.04			
8.48	0.70	0.83	0.70	9.61×10^{-6}	1.42	0.05	0.10			
11.3	0.88	0.96	0.80	1.44×10^{-4}	1.27	0.08	0.16			
14.1	1.02	1.07	0.90	8.19×10^{-4}	1.20	0.12	0.24	0.3×10^{-3}		
28.3	1.39	1.63	1.43	0.04	1.23	0.32	0.65	0.21×10^{-2}		
43.0	1.50	2.15	1.97	0.22	1.52	0.51	1.03	0.12	0.13×10^{-4}	
56.5	1.52	2.66	2.52	0.55	1.90	0.67	1.38	0.30	0.73×10^{-3}	0.29×10^{-5}
70.6	1.52	3.16	3.06	1.01	2.33	0.81	1.68	0.54	0.82×10^{-2}	0.12×10^{-3}
84.8	1.50	3.65	3.59	1.55	2.78	0.94	1.95	0.82	0.4×10^{-1}	0.13×10^{-2}
98.9	1.49	4.12	4.10	2.13	3.24	1.05	2.18	1.11	0.12	0.71×10^{-2}
113	1.49	4.57	4.58	2.70	3.66	1.14	2.39	1.40	0.28	0.02
127	1.50	4.98	5.00	3.25	4.05	1.22	2.56	1.66	0.51	0.06
141	1.52	5.35	5.38	3.76	4.40	1.28	2.70	1.90	0.81	0.13
155	1.56	5.69	5.72	4.27	4.71	1.34	2.83	2.11	1.17	0.23
170	1.60	6.00	6.02	4.75	4.98	1.39	2.94	2.31	1.58	0.37
184	1.65	6.28	6.28	5.23	5.21	1.43	3.03	2.49	2.03	0.55
198	1.70	6.55	6.51	5.68	5.42	1.47	3.11	2.65	2.51	0.78
212	1.76	6.79	6.71	6.16	5.61	1.50	3.18	2.79	3.01	1.05
226	1.82	7.02	6.89	6.64	5.78	1.53	3.25	2.93	3.53	1.36
240	1.89	7.24	7.05	7.12	5.93	1.56	3.31	3.05	4.07	1.72
254	1.96	7.44	7.20	7.63	6.07	1.59	3.36	3.17	4.62	2.12
268	2.03	7.64	7.33	8.11	6.19	1.61	3.41	3.28	5.18	2.55
283	2.10	7.83	7.46	8.62	6.31	1.63	3.46	3.38	5.75	3.03

A.40

Cs 5% Ar 95%

E/N Td	v_d x 10^7 cm/s	$\overline{\epsilon}$ eV	D_r/μ V	α_T/N x 10^{-17} cm^2	R_1 x $10^9 s^{-1}$	R_2 x $10^8 s^{-1}$	R_3 x $10^7 s^{-1}$	R_4 x $10^7 s^{-1}$	R_5 x $10^6 s^{-1}$	R_6 x $10^5 s^{-1}$
2.83	0.39	0.26	0.31		16.1		0.01			
5.65	0.96	0.33	0.34	1.42×10^{-21}	14.9		0.08			
8.48	1.69	0.39	0.38	6.53×10^{-14}	13.9	0.01	0.21			
11.3	2.50	0.44	0.41	9.97×10^{-11}	12.4	0.03	0.43			
14.1	0.34	0.49	0.43	9.27×10^{-9}	11.4	0.04	0.74			
28.3	0.78	0.71	0.57	9.52×10^{-5}	8.07	0.19	3.57	0.26×10^{-4}		
43.0	1.19	0.91	0.69	2.82×10^{-3}	6.23	0.43	8.22	1.17×10^{-3}		
56.5	1.52	1.10	0.83	0.02	5.19	0.72	14.1	10.1×10^{-3}		
70.6	1.79	1.30	0.97	0.06	4.54	1.04	20.8	4.11×10^{-2}		
84.8	2.01	1.50	1.12	0.20	4.16	1.39	27.9	0.11		
98.9	2.17	1.70	1.28	0.31	3.93	1.74	35.2	0.24		
113	2.31	1.90	1.44	0.53	3.80	2.09	42.5	0.43		
127	2.41	2.10	1.60	0.81	3.76	2.43	49.6	0.69	1.48×10^{-3}	
141	2.49	2.31	1.77	1.16	3.80	2.77	56.6	1.02	6.34×10^{-3}	
155	2.55	2.52	1.94	1.56	3.86	3.09	63.4	1.41	0.02	4.59×10^{-3}
170	2.60	2.73	2.12	2.02	3.95	3.40	70.0	1.86	0.06	19.9×10^{-3}
184	2.64	2.94	2.30	2.53	4.08	3.70	76.4	2.36	0.13	6.80×10^{-2}
198	2.67	3.15	2.48	3.08	4.23	3.99	82.6	2.91	0.28	0.20
212	2.69	3.37	2.66	3.67	4.39	4.27	88.5	3.50	0.53	0.48
226	2.71	3.58	2.85	4.29	4.56	4.53	94.2	4.11	0.91	1.06
240	2.73	3.80	3.04	4.94	4.75	4.79	99.7	4.75	1.48	2.12
254	2.74	4.02	3.22	5.62	4.95	5.03	105	5.41	2.28	3.90
268	2.75	4.24	3.41	6.30	5.14	5.26	110	6.08	3.32	6.67
283	2.77	4.46	3.59	7.01	5.34	5.49	115	6.76	4.65	10.8

Cs Ar

10% 90%

E/N Td	v_d x 10^7 cm/s	$\overline{\epsilon}$ eV	D_r/μ V	α_T/N x 10^{-17} cm^2	R_1 x $10^9 s^{-1}$	R_2 x $10^8 s^{-1}$	R_3 x $10^8 s^{-1}$	R_4 x $10^7 s^{-1}$	R_5 x $10^4 s^{-1}$	R_6 x s^{-1}
2.83	0.17	0.22	0.28		33.1	0.7×10^{-3}	0.5×10^{-3}			
5.65	0.40	0.26	0.30		32.4	2.8×10^{-3}	2.8×10^{-3}			
8.48	0.68	0.29	0.32		31.2	6.5×10^{-3}	7.9×10^{-3}			
11.3	1.02	0.32	0.34		29.9	12×10^{-3}	1.6×10^{-2}			
14.1	0.14	0.35	0.35		28.6	0.01	0.03			
28.3	0.36	0.49	0.43	9.1×10^{-8}	22.9	0.09	0.16			
43.0	0.61	0.61	0.50	3.3×10^{-6}	18.8	0.23	0.42	0.72×10^{-5}		
56.5	0.87	0.72	0.56	5.73×10^{-4}	15.9	0.42	0.79	0.18×10^{-3}		
70.6	1.11	0.83	0.63	3.59×10^{-3}	13.8	0.66	1.27	0.14×10^{-2}		
84.8	1.33	0.94	0.70	0.01	12.2	0.95	1.85	0.62×10^{-2}		
98.9	1.54	1.04	0.77	0.03	11.0	1.27	2.50	0.02		
113	1.74	1.15	0.84	0.08	9.89	1.62	3.22	0.05		
127	1.91	1.27	0.92	0.14	9.13	2.00	4.00	0.10		
141	2.07	1.38	1.00	0.23	8.54	2.39	4.79	0.17		
155	2.21	1.50	1.08	0.37	8.00	2.79	5.62	0.29		
170	2.33	1.62	1.17	0.54	7.61	3.20	6.47	0.45		
184	2.45	1.74	1.26	0.76	7.30	3.62	7.34	0.66	0.03	
198	2.55	1.86	1.35	1.01	7.11	4.03	8.20	0.91	0.08	
212	2.64	1.99	1.44	1.31	6.89	4.45	9.07	1.23	0.24	7.92
226	2.73	2.11	1.53	1.65	6.73	4.87	9.94	1.59	0.59	70.00
240	2.80	2.24	1.63	2.03	6.68	5.28	10.8	2.01	1.31	286.6
254	2.87	2.37	1.73	2.45	6.58	5.69	11.7	2.49	2.66	889.0
268	2.92	2.50	1.83	2.91	6.56	6.09	12.5	3.01	5.06	22×10^2
283	2.98	2.64	1.93	3.42	6.55	6.48	13.4	3.59	9.09	90.9×10^3

بِسْمِ اللّٰهِ الرَّحْمٰنِ الرَّحِيْمِ ۝

سَنُرِيْهِمْ اٰيٰتِنَا فِى الْاٰفَاقِ وَفِىْٓ
اَنْفُسِهِمْ حَتّٰى يَتَبَيَّنَ لَهُمْ اَنَّهُ الْحَقُّ ؕ

"We will show them Our Signs on the horizons and within themselves, until it becomes manifest unto them that this (The Qur'ān) is the truth . . ."

(Al-Qur'ān, 41:53)

facilitate the study of strongly attaching gases. For this profile the field on all parts of the curved section were less than on the flat central area.

The second type of electrode geometry was used for measurements of the diffusion coefficients and the electron drift velocity. This geometry relies upon a thick guard ring structure to produce the uniform field. This geometry produced a larger volume of uniform electric field and also prevented any stray electrons entering the gap. It also formalised the boundary conditions since all electrons reaching the walls were absorbed, (Crompton et al, 1965).

2.3 ELECTRON SOURCES

The main types of electron sources used were heated filaments and back-illuminated thin metal films. The initial electron current required determines the type of electron source used. For steady-state measurements of the ionization coefficient and the radial diffusion coefficient, which do not require a large initial current, then back-illumination of a thin gold film by ultra-violet light will give a maximum current of the order of 10^{-9} amps. However, for time of flight measurements of the electron drift velocity and longitudinal and radial diffusion coefficient, which usually require a greater magnitude of emission current, a heated filament is used which will give an emission current of the order of a few microamps.

2.4 MEASUREMENT OF PARAMETERS

2.4.1 The Electron Drift Velocity, v

In 1936, Bradbury and Nielsen described a method for measuring the electron drift velocity in gases. An electrical shutter was employed in

Cs Ar

20% 80%

E/N	v_d x	$\overline{\epsilon}$	D_r/μ	α_T/N x	R_1 x	R_2 x	R_3 x	R_4 x	R_5 x	R_6 x
Td	10^7 cm/s	eV	V	10^{-17} cm^2	10^9 S^{-1}	10^8 S^{-1}	10^8 S^{-1}	10^8 S^{-1}	10 S^{-1}	10 S^{-1}
2.83	0.71	0.19	0.25		65.9	0.4×10^{-3}	0.1×10^{-3}			
5.65	1.68	0.22	0.27		66.4	1.4×10^{-3}	0.9×10^{-3}			
8.48	2.78	0.24	0.29		66.0	3.1×10^{-3}	2.7×10^{-3}			
11.3	4.04	0.25	0.30		65.1	5.6×10^{-3}	5.7×10^{-3}			
14.1	0.05	0.27	0.31		64.0	8.9×10^{-3}	0.01			
28.3	0.14	0.35	0.35		57.3	0.04	0.06			
43.0	0.26	0.42	0.39		51.0	0.10	0.17			
56.5	0.38	0.49	0.42		45.7	0.20	0.34			
70.6	0.51	0.55	0.46		41.2	0.32	0.58			
84.8	0.65	0.61	0.49		37.4	0.48	0.88	32.9×10^{-4}		
98.9	0.79	0.67	0.53		34.3	0.67	1.25	18.4×10^{-4}		
113	0.92	0.73	0.56		31.6	0.89	1.68	71.5×10^{-4}		
127	1.05	0.79	0.60		29.3	1.14	2.18	0.02		
141	1.18	0.84	0.63	0.01	27.3	1.41	2.73	0.05		
155	1.31	0.90	0.67	0.02	25.5	1.71	3.33	0.11		
170	1.44	0.96	0.70	0.04	23.9	2.04	3.98	0.22		
184	1.55	1.01	0.74	0.07	22.4	2.38	4.68	0.39		
198	1.67	1.07	0.78	0.11	21.3	2.75	5.42	0.65		
212	1.78	1.13	0.82	0.16	20.1	3.13	6.19	1.02	0.09	
226	1.89	1.19	0.86	0.23	19.1	3.52	7.00	1.53	0.39	
240	2.00	1.26	0.90	0.31	18.0	3.95	7.86	2.21	1.67	
254	2.09	1.32	0.94	0.42	17.6	4.35	8.70	3.08	5.28	
268	2.18	1.38	0.98	0.54	16.8	4.79	9.61	4.19	14.9	0.01
283	2.27	1.45	1.03	0.69	16.1	5.23	10.5	5.55	38.2	0.10

Cs 0.1% Ar 99.9%

E/N Td	v_d x 10^7 cm/s	$\overline{\epsilon}$ eV	D_r/μ V	α_T/N x 10^{-17} cm^2	R_1 x $10^9 S^{-1}$	R_2 x $10^7 S^{-1}$	R_3 x $10^7 S^{-1}$	R_4 x $10^7 S^{-1}$	R_5 x $10^7 S^{-1}$	R_6 x $10^7 S^{-1}$
14.1	0.53	2.41	2.95	0.10	1.26	0.60	1.22	0.02	2.5×10^{-5}	
28.3	0.51	3.90	4.87	0.54	2.63	1.01	2.10	0.10	0.02	3.4×10^{-5}
43.0	0.54	4.89	6.14	0.85	3.61	1.22	2.56	0.16	0.17	1.9×10^{-3}
56.5	0.61	5.48	6.85	0.99	4.18	1.32	2.79	0.20	0.45	0.01
70.6	0.69	5.89	7.33	1.13	4.56	1.39	2.94	0.23	0.80	0.05
84.8	0.77	6.21	7.63	1.30	4.84	1.44	3.05	0.25	1.20	0.11
98.9	0.86	6.48	7.86	1.55	5.07	1.48	3.13	0.26	1.63	0.21
113	0.95	6.71	8.03	1.86	5.26	1.51	3.20	0.28	2.08	0.35
127	1.05	6.93	8.17	2.23	5.42	1.54	3.27	0.29	2.55	0.53
141	1.14	7.13	8.28	2.63	5.56	1.56	3.32	0.30	3.04	0.75
155	1.23	7.32	8.40	3.05	5.69	1.59	3.37	0.31	3.53	1.01
170	1.32	7.49	8.49	3.50	5.80	1.61	3.41	0.32	4.04	1.31
184	1.41	7.66	8.56	3.98	5.90	1.63	3.46	0.33	4.55	1.65
198	1.50	7.83	8.63	4.46	6.00	1.65	3.50	0.34	5.08	2.03
212	1.59	7.99	8.72	4.96	6.09	1.66	3.53	0.35	5.61	2.44
226	1.69	8.15	8.78	5.45	6.17	1.68	3.57	0.36	6.15	2.90
240	1.78	8.30	8.83	5.96	6.25	1.70	3.60	0.37	6.70	3.39
254	1.87	8.46	8.88	6.50	6.32	1.71	3.63	0.37	7.26	3.92
268	1.96	8.61	8.93	7.01	6.39	1.73	3.67	0.38	7.83	4.48
283	2.06	8.76	8.97	7.51	6.46	1.74	3.70	0.39	8.40	5.08

Cs 0.2% Ar 99.8%

E/N Td	v_d x 10^7 cm/s	$\overline{\epsilon}$ eV	D_r/μ V	α_T/N x 10^{-17} cm^2	R_1 x 10^9 s^{-1}	R_2 x 10^7 s^{-1}	R_3 x 10^7 s^{-1}	R_4 x 10^6 s^{-1}	R_5 x 10^7 s^{-1}	R_6 x 10^7 s^{-1}
14.1	0.74	1.91	2.12	0.04	0.92	0.85	1.72	0.10		
28.3	0.73	3.05	3.56	0.37	1.86	1.58	3.25	0.94	0.20×10^{-2}	0.17×10^{-5}
43.0	0.71	4.07	4.83	0.85	2.84	2.08	4.35	2.14	0.05	0.57×10^{-2}
56.5	0.73	4.84	5.77	1.21	3.60	2.41	5.05	3.14	0.22	0.57×10^{-2}
70.6	0.78	5.40	6.44	1.53	4.13	2.61	5.50	3.87	0.51	0.03
84.8	0.84	5.82	6.88	1.72	4.52	2.75	5.81	4.42	0.87	0.07
98.9	0.92	6.16	7.22	1.98	4.82	2.86	6.04	4.85	1.28	0.16
113	1.00	6.45	7.49	2.26	5.06	2.94	6.23	5.21	1.72	0.28
127	1.08	6.70	7.70	2.60	5.27	3.01	6.38	5.52	2.19	0.44
141	1.17	6.93	7.86	2.94	5.44	3.07	6.51	5.80	2.67	0.64
155	1.25	7.14	7.99	3.36	5.59	3.12	6.63	6.04	3.16	0.88
170	1.34	7.33	8.11	3.79	5.72	3.17	6.73	6.27	3.67	1.17
184	1.43	7.52	8.23	4.24	5.84	3.22	6.83	6.48	4.19	1.49
198	1.52	7.70	8.32	4.69	5.95	3.26	6.91	6.68	4.71	1.86
212	1.61	7.87	8.40	5.20	6.05	3.30	7.00	6.86	5.25	2.26
226	1.69	8.03	8.47	5.68	6.14	3.33	7.07	7.04	5.79	2.70
240	1.78	8.20	8.54	6.19	6.23	3.37	7.15	7.21	6.34	3.18
254	1.87	8.35	8.60	6.70	6.31	3.40	7.22	7.37	6.89	3.70
268	1.97	8.51	8.66	7.20	6.38	3.43	7.28	7.53	7.46	4.25
283	2.06	8.66	8.70	7.71	6.45	3.46	7.35	7.68	8.03	4.84

Cs 0.5% Ar 99.5%

E/N Td	v_d x 10^7 cm/s	$\overline{\epsilon}$ eV	D_r/μ V	α_T/N x 10^{-17} cm^2	R_1 x $10^9 s^{-1}$	R_2 x $10^7 s^{-1}$	R_3 x $10^7 s^{-1}$	R_4 x $10^7 s^{-1}$	R_5 x $10^7 s^{-1}$	R_6 x $10^7 s^{-1}$
14.1	1.00	1.40	1.31	6.3×10^{-3}	0.80	1.17	2.32	0.22×10^{-2}		
28.3	1.13	2.16	2.17	0.14	1.26	2.55	5.20	0.55×10^{-1}	0.63×10^{-5}	
43.0	1.13	2.88	3.01	0.48	1.85	3.68	7.59	0.19	0.15×10^{-2}	0.42×10^{-5}
56.5	1.10	3.57	3.82	0.99	2.48	4.61	9.57	0.38	0.23×10^{-1}	0.30×10^{-3}
70.6	1.09	4.21	4.57	1.53	3.10	5.35	11.2	0.58	0.11	0.35×10^{-2}
84.8	1.10	4.77	5.21	2.01	3.65	5.92	12.4	0.76	0.29	0.02
98.9	1.12	5.24	5.73	2.43	4.10	6.36	13.4	0.92	0.57	0.05
113	1.17	5.65	6.16	2.82	4.47	6.70	14.2	1.05	0.92	0.12
127	1.22	5.99	6.51	3.19	4.78	6.98	14.8	1.16	1.33	0.22
141	1.28	6.30	6.80	3.56	5.04	7.21	15.3	1.25	1.78	0.36
155	1.35	6.57	7.04	3.96	5.26	7.40	15.7	1.34	2.26	0.55
170	1.42	6.82	7.24	4.35	5.45	7.57	16.0	1.41	2.75	0.78
184	1.50	7.04	7.41	4.77	5.62	7.72	16.4	1.48	3.27	1.05
198	1.57	7.26	7.55	5.23	5.76	7.85	16.7	1.54	3.80	1.36
212	1.65	7.46	7.69	5.65	5.90	7.97	16.9	1.60	4.34	1.72
226	1.73	7.65	7.81	6.13	6.02	8.09	17.2	1.65	4.89	2.11
240	1.81	7.83	7.92	6.61	6.13	8.19	17.4	1.70	5.44	2.54
254	1.90	8.01	8.01	7.09	6.23	8.29	17.6	1.75	6.01	3.02
268	1.98	8.18	8.10	7.57	6.32	8.38	17.8	1.79	6.58	3.53
283	2.07	8.35	8.18	8.08	6.41	8.47	18.0	1.83	7.16	4.08

Cs 0.7% Ar 99.3%

E/N Td	v_d x 10^7 cm/s	$\overline{\epsilon}$ eV	D_r/μ V	α_T/N x 10^{-17} cm^2	R_1 x 10^9 s^{-1}	R_2 x 10^7 s^{-1}	R_3 x 10^7 s^{-1}	R_4 x 10^7 s^{-1}	R_5 x 10^7 s^{-1}	R_6 x 10^7 s^{-1}
14.1	1.04	1.24	1.09	2.53×10^{-3}	0.90	1.22	2.42	0.93×10^{-3}		
28.3	1.28	1.89	1.78	0.08	1.18	2.91	5.90	3.71×10^{-1}	0.29×10^{-6}	
43.0	1.31	2.51	2.47	0.34	1.63	4.36	8.95	0.16	0.19×10^{-3}	0.27×10^{-6}
56.5	1.30	3.10	3.15	0.76	2.14	5.60	11.6	0.36	0.53×10^{-2}	0.43×10^{-4}
70.6	1.28	3.69	3.81	1.30	2.69	6.64	13.8	0.59	0.04	0.88×10^{-3}
84.8	1.27	4.24	4.42	1.84	3.21	7.51	15.7	0.83	0.13	0.62×10^{-2}
98.9	1.27	4.73	4.97	2.37	3.69	8.22	17.3	1.05	0.31	0.02
113	1.29	5.17	5.44	2.85	4.11	8.79	18.5	1.25	0.58	0.06
127	1.33	5.56	5.84	3.31	4.47	9.26	19.5	1.42	0.92	0.14
141	1.37	5.90	6.19	3.76	4.77	9.64	20.4	1.58	1.31	0.24
155	1.43	6.21	6.48	4.15	5.04	9.97	21.1	1.71	1.75	0.39
170	1.49	6.48	6.73	4.58	5.26	10.3	21.7	1.83	2.22	0.58
184	1.55	6.74	6.94	5.03	5.46	10.5	22.2	1.94	2.72	0.82
198	1.62	6.97	7.12	5.45	5.63	10.7	22.7	2.03	3.24	1.10
212	1.69	7.19	7.29	5.90	5.79	10.9	23.1	2.12	3.77	1.42
226	1.76	7.40	7.43	6.38	5.93	11.1	23.5	2.21	4.31	1.78
240	1.84	7.59	7.56	6.86	6.06	11.3	23.9	2.28	4.86	2.18
254	1.92	7.78	7.67	7.35	6.17	11.4	24.2	2.36	5.42	2.63
268	2.00	7.97	7.78	7.83	6.27	11.6	24.5	2.42	6.00	3.11
283	2.08	8.14	7.88	8.31	6.37	11.7	24.8	2.49	6.58	3.63

Cs 0.01%

Ar 99.99%

E/N Td	v_d x 10^7 cm/s	$\overline{\epsilon}$ eV	D_r/μ V	α_T/N x 10^{-17} cm^2	R_1 x $10^9 s^{-1}$	R_2 x $10^6 s^{-1}$	R_3 x $10^6 s^{-1}$	R_4 x $10^5 s^{-1}$	R_5 x $10^7 s^{-1}$	R_6 x $10^7 s^{-1}$
14.1	0.19	4.71	6.52	0.22	3.40	1.19	2.49	1.49	0.03	0.50×10^{-6}
28.3	0.30	5.46	7.45	0.19	4.16	1.33	2.80	1.99	0.20	0.53×10^{-3}
43.0	0.42	5.82	7.87	0.15	4.49	1.39	2.93	2.22	0.47	0.71×10^{-2}
56.5	0.52	6.09	8.16	0.29	4.74	1.43	3.03	2.40	0.79	0.03
70.6	0.62	6.34	8.43	0.48	4.94	1.46	3.10	2.55	1.16	0.08
84.8	0.72	6.56	8.55	0.74	5.12	1.49	3.17	2.69	1.57	0.16
98.9	0.82	6.76	8.67	1.05	5.28	1.52	3.23	2.82	1.99	0.28
113	0.92	6.96	8.77	1.44	5.42	1.55	3.28	2.93	2.44	0.44
127	1.02	7.14	8.85	1.84	5.55	1.57	3.33	3.04	2.90	0.63
141	1.11	7.31	8.94	2.29	5.67	1.59	3.38	3.14	3.38	0.87
155	1.21	7.48	9.00	2.74	5.77	1.61	3.42	3.24	3.87	1.14
170	1.30	7.65	9.05	3.22	5.87	1.63	3.46	3.33	4.37	1.45
184	1.40	7.80	9.10	3.73	5.96	1.65	3.50	3.41	4.88	1.81
198	1.49	7.96	9.14	4.24	6.05	1.66	3.53	3.49	5.40	2.20
212	1.58	8.11	9.19	4.78	6.13	1.68	3.56	3.57	5.92	2.63
226	1.68	8.26	9.23	5.28	6.20	1.69	3.60	3.65	6.46	3.10
240	1.77	8.41	9.28	5.79	6.28	1.71	3.63	3.73	7.00	3.60
254	1.87	8.56	9.33	6.33	6.34	1.72	3.66	3.80	7.55	4.14
268	1.96	8.70	9.37	6.84	6.41	1.74	3.69	3.87	8.12	4.71
283	2.05	8.85	9.43	7.37	6.47	1.75	3.72	3.94	8.69	5.32

Cs 0.02%

Ar 99.98%

E/N Td	v_d x 10^7 cm/s	$\overline{\epsilon}$ eV	D_r/μ V	α_T/N x 10^{-17} cm^2	R_1 x $10^9 S^{-1}$	R_2 x $10^6 S^{-1}$	R_3 x $10^6 S^{-1}$	R_4 x $10^5 S^{-1}$	R_5 x $10^7 S^{-1}$	R_6 x $10^7 S^{-1}$
14.1	0.23	4.12	5.60	0.27	2.81	2.12	4.42	2.20	0.01	
28.3	0.32	5.26	7.09	0.34	3.96	2.58	5.45	3.70	0.16	$4x10^{-4}$
43.0	0.43	5.71	7.61	0.28	4.39	2.74	5.79	4.30	0.42	$6.18x10^{-3}$
56.5	0.53	6.03	7.94	0.40	4.68	2.83	6.00	4.70	0.75	$2.80x10^{-2}$
70.6	0.63	6.29	8.24	0.57	4.90	2.91	6.17	5.04	1.12	$7.56x10^{-2}$
84.8	0.73	6.52	8.39	0.82	5.09	2.98	6.31	5.33	1.52	0.16
98.9	0.83	6.73	8.51	1.13	5.26	3.03	6.43	5.59	1.95	0.27
113	0.92	6.93	8.62	1.50	5.40	3.08	6.55	5.83	2.40	0.43
127	1.02	7.12	8.71	1.89	5.54	3.13	6.65	6.05	2.86	0.62
141	1.11	7.29	8.81	2.32	5.65	3.17	6.74	6.25	3.34	0.85
155	1.21	7.46	8.88	2.80	5.76	3.21	6.82	6.45	3.83	1.13
170	1.30	7.63	8.94	3.25	5.86	3.25	6.91	6.63	4.33	1.44
184	1.40	7.79	8.99	3.76	5.96	3.29	6.98	6.81	4.84	1.79
198	1.49	7.95	9.03	4.27	6.04	3.32	7.05	6.97	5.36	2.18
212	1.58	8.10	9.08	4.77	6.13	3.35	7.12	7.13	5.89	2.61
226	1.68	8.25	9.12	5.28	6.20	3.38	7.19	7.29	6.42	3.07
240	1.77	8.40	9.16	5.82	6.27	3.41	7.25	7.44	6.97	3.57
254	1.87	8.55	9.20	6.33	6.34	3.44	7.31	7.59	7.52	4.11
268	1.96	8.69	9.24	6.86	6.41	3.47	7.37	7.73	8.09	4.69
283	2.05	8.84	9.29	7.40	6.47	3.50	7.43	7.87	8.66	5.30

Cs 0.05% Ar 99.95%

E/N Td	v_d x 10^7 cm/s	$\overline{\epsilon}$ eV	D_r/μ V	α_T/N x 10^{-17} cm^2	R_1 x $10^9 S^{-1}$	R_2 x $10^7 S^{-1}$	R_3 x $10^7 S^{-1}$	R_4 x $10^7 S^{-1}$	R_5 x $10^7 S^{-1}$	R_6 x $10^7 S^{-1}$
14.1	0.37	3.08	4.00	0.18	1.82	0.40	0.82	0.02	9.56×10^{-4}	
28.3	0.38	4.68	6.10	0.54	3.38	0.59	1.23	0.07	0.08	1.64×10^{-4}
43.0	0.46	5.40	7.02	0.59	4.09	0.66	1.39	0.10	0.31	4.06×10^{-3}
56.5	0.56	5.82	7.48	0.68	4.49	0.69	1.46	0.11	0.62	2.18×10^{-2}
70.6	0.65	6.14	7.85	0.79	4.78	0.72	1.52	0.12	0.99	6.40×10^{-2}
84.8	0.75	6.40	8.06	1.02	5.00	0.74	1.56	0.13	1.40	0.14
98.9	0.84	6.64	8.22	1.30	5.19	0.75	1.59	0.14	1.83	0.25
113	0.93	6.85	8.35	1.64	5.35	0.77	1.62	0.14	2.28	0.40
127	1.03	7.05	8.46	2.01	5.49	0.78	1.65	0.15	2.74	0.59
141	1.12	7.23	8.56	2.43	5.62	0.79	1.68	0.15	3.22	0.81
155	1.22	7.41	8.66	2.88	5.74	0.80	1.70	0.16	3.72	1.08
170	1.31	7.58	8.73	3.36	5.84	0.81	1.72	0.16	4.22	1.39
184	1.40	7.74	8.80	3.84	5.94	0.82	1.74	0.17	4.73	1.73
198	1.49	7.90	8.86	4.35	6.03	0.83	1.76	0.17	5.25	2.12
212	1.59	8.06	8.90	4.83	6.11	0.84	1.78	0.18	5.79	2.54
226	1.68	8.21	8.95	5.37	6.19	0.84	1.79	0.18	6.32	3.01
240	1.77	8.36	9.00	5.88	6.27	0.85	1.81	0.19	6.87	3.50
254	1.87	8.51	9.04	6.38	6.34	0.86	1.82	0.19	7.43	4.04
268	1.96	8.66	9.09	6.92	6.40	0.87	1.84	0.19	7.99	4.61
283	2.06	8.81	9.12	7.43	6.46	0.87	1.85	0.20	8.56	5.22

Cs 0.07%

Ar 99.93%

E/N Td	v_d x 10^7 cm/s	$\overline{\epsilon}$ eV	D_r/μ V	α_T/N x 10^{-17} cm^2	R_1 x 10^9 s^{-1}	R_2 x 10^7 s^{-1}	R_3 x 10^7 s^{-1}	R_4 x 10^7 s^{-1}	R_5 x 10^7 s^{-1}	R_6 x 10^7 s^{-1}
14.1	0.44	2.73	3.47	0.14	1.52	0.49	1.00	0.02		
28.3	0.43	4.33	5.54	0.57	3.04	0.77	1.62	0.09	0.05	
43.0	0.49	5.19	6.65	0.73	3.89	0.89	1.88	0.13	0.25	0.30×10^{-2}
56.5	0.57	5.68	7.21	0.82	4.37	0.95	2.01	0.15	0.55	0.02
70.6	0.66	6.04	7.63	0.93	4.69	0.99	2.10	0.17	0.91	0.06
84.8	0.76	6.33	7.88	1.13	4.94	1.02	2.16	0.18	1.32	0.13
98.9	0.85	6.57	8.07	1.41	5.14	1.05	2.22	0.19	1.75	0.23
113	0.94	6.80	8.21	1.72	5.31	1.07	2.26	0.20	2.20	0.38
127	1.03	7.00	8.33	2.09	5.46	1.08	2.30	0.21	2.67	0.56
141	1.13	7.19	8.44	2.51	5.60	1.10	2.34	0.21	3.15	0.79
155	1.22	7.37	8.55	2.94	5.72	1.12	2.37	0.22	3.64	1.05
170	1.31	7.55	8.63	3.42	5.83	1.13	2.40	0.23	4.15	1.36
184	1.40	7.71	8.70	3.90	5.93	1.14	2.43	0.24	4.66	1.70
198	1.50	7.87	8.76	4.38	6.02	1.16	2.46	0.24	5.18	2.08
212	1.60	8.03	8.82	4.89	6.10	1.17	2.48	0.25	5.72	2.50
226	1.68	8.19	8.87	5.40	6.19	1.18	2.50	0.25	6.26	2.96
240	1.78	8.34	8.92	5.90	6.26	1.19	2.53	0.26	6.81	3.46
254	1.87	8.49	8.96	6.44	6.33	1.20	2.55	0.26	7.36	3.99
268	1.96	8.64	9.01	6.95	6.40	1.21	2.57	0.27	7.93	4.56
283	2.06	8.79	9.04	7.49	6.46	1.22	2.59	0.27	8.49	5.16

Cs Ar

0.001% 99.999%

E/N Td	v_d x 10^7 cm/s	$\overline{\epsilon}$ eV	D_r/μ V	α_T/N x 10^{-17} cm^2	R_1 x 10^9 s^{-1}	R_2 x 10^6 s^{-1}	R_3 x 10^6 s^{-1}	R_4 x 10^5 s^{-1}	R_5 x 10^6 s^{-1}	R_6 x 10^6 s^{-1}
14.1	0.16	5.31	7.45	0.03	4.01	0.13	0.28	0.19	0.64	
28.3	0.29	5.64	7.94	0.03	4.33	0.14	0.29	0.21	2.43	0.06
43.0	0.41	5.91	8.29	0.07	4.58	0.14	0.30	0.23	5.09	0.88
56.5	0.51	6.16	8.52	0.19	4.79	0.14	0.30	0.24	8.35	3.20
70.6	0.62	6.38	8.70	0.39	4.98	0.15	0.31	0.26	12.1	8.30
84.8	0.72	6.59	8.84	0.66	5.15	0.15	0.32	0.27	16.1	1.66

Cs Ar

0.005% 99.995%

E/N Td	v_d x 10^7 cm/s	$\overline{\epsilon}$ eV	D_r/μ V	α_T/N x 10^{-17} cm^2	R_1 x 10^9 s^{-1}	R_2 x 10^6 s^{-1}	R_3 x 10^6 s^{-1}	R_4 x 10^6 s^{-1}	R_5 x 10^6 s^{-1}	R_6 x 10^6 s^{-1}
14.1	0.17	5.04	7.02	0.14	3.74	0.63	1.32	0.09	0.47	
28.3	0.30	5.56	7.67	0.10	4.25	0.67	1.42	0.10	2.25	6.08×10^{-3}
43.0	0.41	5.87	8.04	0.13	4.54	0.70	1.48	0.11	4.90	7.55×10^{-3}
56.5	0.52	6.13	8.32	0.24	4.77	0.72	1.52	0.12	8.16	0.32
70.6	0.62	6.36	8.56	0.43	4.96	0.73	1.56	0.13	11.7	0.82
84.8	0.72	6.58	8.66	0.70	5.14	0.75	1.59	0.14	15.9	1.64

which the shutters had the form of two fine wire grids, alternate wires of which were connected to a high frequency alternating potential. Electrons passed through the grids only when the potential between adjacent grid wires was zero, and only electrons which crossed the gap in a whole number of half cycles were received at the anode. A sharp maximum was thus observed in the electrometer current when the drift velocity of the electrons multiplied by one half cycle was equal to the distance between the grids. The values of v obtained from this experiment were taken to be the most accurate up to that date, and the method itself opened up a new era in time of flight studies. However, the method was restricted to measurements of low E/N, corresponding to low mean electron energies. This restriction on the energy is due to the grids, which have to be able to stop the electrons. At high energies (the onset energy for ionization may be used as a guideline) the grids cannot effectively stop electrons, and so the method begins to break down.

In 1960, Frommhold measured the current growth of a single avalanche as a function of time. The chamber was basically a Townsend discharge chamber with a spark light source to release a short pulse of electrons. The growth of anode current was amplified and observed on an oscilloscope. Semi-logarithmic plots were then drawn of the anode current variation with time. The growth was described by the following equation :-

$$n = n_o \exp(\alpha v t) \quad , \tag{2.2}$$

where α = ionization coefficient,

v = electron drift velocity.

The charge induced on the anode by the avalanche is then given by (Morgan 1965) :-

APPENDIX

·B·

VALUES OF CROSS-SECTIONS

1. OXYGEN
2. METHANE
3. ARGON
4. POTASSIUM
5. SODIUM
6. CAESIUM

COLLISION CROSS-SECTION IN OXYGEN

TOTAL

MW 3.200E+01 7 NO.OF C.S.

NQ	ENERGY
2.48E+03	0.17E+00
1.95E+03	0.20E+00
1.56E+03	0.30E+00
1.95E+03	0.40E+00
1.95E+03	0.50E+00
2.12E+03	0.60E+00
2.16E+03	0.70E+00
2.21E+03	0.90E+00
1.98E+03	1.00E+00
2.23E+03	2.00E+00
2.34E+03	3.00E+00
2.37E+03	4.00E+00
2.38E+03	5.00E+00
2.66E+03	6.00E+00
2.87E+03	7.00E+00
3.15E+03	8.00E+00
3.56E+03	9.00E+00
3.43E+03	10.00E+00
3.47E+03	15.50E+00
3.55E+03	16.00E+00
3.29E+03	19.50E+00
3.52E+03	20.00E+00
3.55E+03	21.00E+00
3.24E+03	25.00E+00
3.40E+03	30.00E+00
3.36E+03	36.00E+00
3.29E+03	40.00E+00
3.40E+03	49.00E+00
3.19E+03	50.00E+00
2.90E+03	64.00E+00
2.73E+03	81.00E+00
2.48E+03	1.00E+02
1.58E+03	2.00E+02
1.10E+03	3.00E+02
9.00E+02	4.00E+02
7.60E+02	5.00E+02
6.60E+02	6.00E+02
6.00E+02	7.00E+02
5.40E+02	8.00E+02
5.00E+02	9.00E+02
4.60E+02	1.00E+03
STOP -1.00E+00	3.00E+03
3.40E-05	1.00E+00

EXCITATION

0.00E+00	0.00E+00
0.00E+00	4.40E+00
21.24E-02	4.88E+00
56.64E-02	5.20E+00
15.93E-01	5.60E+00
38.94E-01	6.40E+00
42.48E-01	6.56E+00
44.25E-01	6.70E+00
42.48E-01	7.00E+00
34.34E-01	7.50E+00
20.18E-01	8.00E+00
10.62E-01	8.50E+00
56.64E-02	9.00E+00
0.00E+00	1.00E+01
0.00E+00	1.00E+04
-1.00E+00	5.00E+04
4.40E+00	1.50E+00
0.00E+00	0.00E+00
0.00E+00	8.00E+00
81.42E+00	8.50E+00
16.64E+01	9.00E+00
22.13E+01	9.50E+00
24.78E+01	1.00E+01
26.20E+01	1.10E+01
26.20E+01	1.20E+01
21.77E+01	1.40E+01
12.59E+01	2.00E+01
0.00E+00	5.00E+01
0.00E+00	1.00E+04
-1.00E+00	5.00E+04
8.00E+00	1.50E+00
0.00E+00	0.00E+00
0.00E+00	9.70E+00
26.55E+00	1.00E+01
70.80E+00	1.05E+01
99.12E+00	1.10E+01
11.86E+01	1.15E+01
13.27E+01	1.20E+01
15.58E+01	1.30E+01
18.58E+01	1.50E+01
21.24E+01	1.80E+01
22.30E+01	2.00E+01
53.10E+01	1.00E+02
49.97E+01	2.00E+02
43.06E+01	3.00E+02
37.13E+01	4.00E+02
32.99E+01	5.00E+02
29.43E+01	6.00E+02
26.47E+01	7.00E+02
24.30E+01	8.00E+02
22.32E+01	9.00E+02
20.74E+01	1.00E+03
-1.00E+00	3.00E+04
9.70E+00	1.50E+00

DISSOCIATION

0.00E+00	0.00E+00
0.00E+00	1.73E+01
0.00E+00	2.00E+01
7.08E+00	2.20E+01
1.72E+01	2.60E+01
3.54E+01	3.00E+01
42.48E+00	3.40E+01
77.88E+00	3.80E+01
9.91E+01	4.00E+01
12.62E+01	4.50E+01
15.33E+01	5.00E+01
20.82E+01	6.00E+01

24.78E+01	7.00E+01
28.14E+01	8.00E+01
30.69E+01	9.00E+01
32.57E+01	1.00E+02
36.11E+01	1.50E+02
34.69E+01	2.00E+02
28.52E+01	3.00E+02
23.72E+01	4.00E+02
20.18E+01	5.00E+02
17.49E+01	6.00E+02
15.33E+01	7.00E+02
14.16E+01	8.00E+02
12.99E+01	9.00E+02
12.28E+01	1.00E+03
-1.00E+00	5.00E+04
17.50E+00	1.00E+00

IONIZATION

0.00E+00	0.00E+00
0.00E+00	1.22E+01
3.54E+00	1.25E+01
19.12E+00	1.40E+01
30.09E+00	1.50E+01
35.93E+00	1.70E+01
10.86E+01	2.00E+01
14.00E+01	2.20E+01
21.47E+01	2.60E+01
28.21E+01	3.00E+01
36.46E+01	3.40E+01
40.36E+01	3.80E+01
42.13E+01	4.00E+01
47.56E+01	4.50E+01
51.22E+01	5.00E+01
60.00E+01	6.00E+01
59.47E+01	7.00E+01
61.07E+01	8.00E+01
62.06E+01	9.00E+01
61.95E+01	1.00E+02
59.12E+01	1.50E+02
54.87E+01	2.00E+02
48.85E+01	3.00E+02
42.83E+01	4.00E+02
38.94E+01	5.00E+02
35.30E+01	6.00E+02
32.11E+01	7.00E+02
29.38E+01	8.00E+02
27.01E+01	9.00E+02
24.89E+01	1.00E+03
-1.00E+00	5.00E+04
1.22E+01	1.00E+00

VIBRATION

8

0.00E+00	0.00E+00
0.00E+00	0.19E+00
14.16E-01	0.35E+00
49.56E+00	0.37E+00
49.56E+00	0.45E+00
0.00E+00	0.47E+00
0.00E+00	0.10E+05
-1.06E+00	3.00E+04
3.70E-01	
0.00E+00	0.00E+00
0.00E+00	0.38E+00
28.32E-02	0.54E+00
33.28E+01	0.56E+00
33.28E+01	0.64E+00
0.00E+00	0.66E+00
0.00E+00	0.10E+05
-1.00E+00	3.00E+04
5.60E-01	
0.00E+00	0.00E+00
0.00E+00	0.57E+00
14.16E-02	0.73E+00
20.35E+00	0.75E+00
20.35E+00	0.83E+00
0.00E+00	0.85E+00
0.00E+00	0.10E+05
-1.00E+00	3.00E+04
7.50E-01	
0.00E+00	0.00E+00
0.00E+00	0.75E+00
70.80E-05	0.91E+00
42.48E+00	0.93E+00
42.48E+00	1.01E+00
0.00E+00	1.05E+00
0.00E+00	0.10E+05
-1.00E+00	5.00E+04
9.30E-01	
0.00E+00	0.00E+00
0.00E+00	0.94E+00
10.62E-02	1.10E+00
38.41E+00	1.12E+00
38.41E+00	1.20E+00
0.00E+00	12.20E-01
0.00E+00	0.10E+05
-1.00E+00	5.00E+04
1.12E+00	
0.00E+00	0.00E+00
0.00E+00	1.12E+00
3.54E-02	1.28E+00
42.48E+00	1.30E+00
42.48E+00	1.38E+00
0.00E+00	1.40E+00
0.00E+00	1.00E+04
-1.00E+00	5.00E+04
1.30E+00	
0.00E+00	0.00E+00
0.00E+00	1.29E+00
21.24E-05	1.45E+00
28.32E+00	1.47E+00
28.32E+00	1.55E+00
0.00E+00	1.57E+00
0.00E+00	1.00E+04
-1.00E+00	5.00E+04
1.47E+00	
0.00E+00	0.00E+00
0.00E+00	1.46E+00

28.52E-03 1.62E+00
19.47E+00 1.64E+00
19.47E+00 1.72E+00
10.62E+00 1.89E+00
0.00E+00 2.80E+00
0.00E+00 1.00E+04
-1.00E+00 3.00E+04
1.64E+00

ANGULAR SCATTERING

16 NO. OF SETS

0.00 ENERGY ANGLES AT PROBABILITY

56.2 59.0 59,4 67,0 73.5 79,4 85,0 90,2 95,1 99,7
104.2 108,6 113,1 117,5 121.9 126,7 132,2 139,1 148,3 180,0

0.74

36,2 59,0 59,4 67,0 73,5 79,4 85,0 90,2 95,1 99,7
104,2 108,6 113,1 117,5 121,9 126,7 132,2 139,1 148,3 180,0

0.96

34,7 47,6 56,1 63,1 69,3 74,9 80,0 84,7 89,2 93,5
97,7 101,9 106,1 110,4 115,1 120,6 127,2 135,3 146,2 180,0

1.50

35,8 44,5 52,6 59,3 65,2 70,4 75,4 80,3 84,8 89,1
95,4 97,7 102,1 106,6 111,3 116,9 123,8 132,4 144,1 180,0

2,00

31,9 42,6 50,3 56,6 62,2 67,5 72,1 76,7 81,3 85,9
90,6 95,4 100,3 105,5 110,9 116,6 122,9 130,8 142,4 180,0

3,00

28,1 37,6 44,8 50,8 56,1 61,1 65,8 70,4 74,9 79,5
83,7 88,4 93,4 99,1 105,1 111,4 118,8 128,1 140,9 180,0

4,00

19,8 28,4 35,2 41,0 46,4 51,5 56,3 61,1 65,8 70,6
75,5 80,6 86,1 92,1 99,0 106,8 116,0 127,1 142,1 180,0

5,00

19,8 28,8 36,0 42,2 47,9 53,3 58,4 63,3 68,3 73,3
78,5 84,0 89,9 96,3 103,3 111,2 120,1 130,8 144,8 180,0

7,00

15,9 23,4 29,3 34,9 39,8 44,5 49,0 53,5 57,9 62,5
67,5 72,4 77,7 83,6 90,1 97,8 107,0 118,5 134,5 180,0

10,00

11,0 16,9 22,2 27,1 31,9 36,7 41,4 46,3 51,3 56,5
62,1 68,0 74,3 81,3 89,3 98,0 108,4 121,0 137,8 180,0

15,00

8,9 13,4 17,5 21,3 25,0 28,8 32,5 36,5 40,7 45,2
50,2 55,8 62,0 69,3 78,4 88,5 100,2 114,4 135,2 180,0

20,00

9,1 13,4 17,1 20,3 23,8 27,1 30,4 33,8 37,3 41,0
45,0 49,5 54,4 60,0 66,6 74,4 84,4 98,0 116,7 180,0

45,00

5,1 7,6 9,7 11,6 13,5 15,4 17,3 19,3 21,4 23,7
26,1 28,8 31,8 35,4 39,6 45,1 53,0 65,5 88,4 180,0

300,00

2,1 3,5 4,5 5,6 6,5 7,3 8,5 9,6 10,7 11,9
13,4 15,0 17,0 19,7 23,2 28,1 34,7 44,4 64,6 180,0

400,00

2,1 3,4 4,3 5,3 6,2 7,1 8,2 9,6 9,7 9,7
12,9 17,0 19,0 23,4 27,8 33,1 40,0 50,4 72,0 180,0

500,00

2,0 3,3 4,2 5,1 6,0 7,0 7,9 9,0 10,1 11,5
13,0 15,0 17,7 21,1 25,1 29,6 35,4 44,9 65,2 180,0

COLLISION CROSS-SECTION IN METHANE

TOTAL

1.604E+01	6
9.91E+02	0.15E+00
6.98E+02	0.20E+00
5.20E+02	0.30E+00
4.60E+02	0.40E+00
4.18E+02	0.50E+00
4.96E+02	0.60E+00
5.49E+02	0.70E+00
6.20E+02	0.80E+00
6.90E+02	0.90E+00
7.43E+02	1.00E+00
10.62E+02	1.40E+00
21.24E+02	2.00E+00
28.32E+02	2.50E+00
39.65E+02	5.00E+00
60.18E+02	4.00E+00
70.80E+02	4.80E+00
77.88E+02	5.00E+00
86.92E+02	6.00E+00
88.56E+02	7.00E+00
86.73E+02	8.00E+00
84.96E+02	9.00E+00
81.42E+02	10.00E+00
70.80E+02	15.00E+00
61.95E+02	20.00E+00
51.33E+02	30.00E+00
42.48E+02	40.00E+00
35.40E+02	50.00E+00
24.00E+02	10.00E+01
17.00E+02	20.00E+01
14.00E+02	30.00E+01
12.00E+02	40.00E+01
11.00E+02	50.00E+01
10.00E+02	60.00E+01
9.50E+02	70.00E+01
9.00E+02	80.00E+01
8.50E+02	90.00E+01
8.00E+02	10.00E+02
-1.00E+00	3.00E+03
6.78E-05	1.00E+00

VIBRATION

0.00E+00	0.00E+00
0.00E+00	1.62E-01
13.10E+01	0.20E+00
21.95E+01	0.26E+00
21.95E+01	0.30E+00
21.24E+01	0.35E+00
20.00E+01	0.40E+00
14.16E+01	0.46E+00
10.62E+01	0.50E+00
7.79E+01	0.55E+00
7.08E+01	0.60E+00
6.37E+01	0.70E+00

6.37E+01	0.80E+00
6.73E+01	0.90E+00
7.08E+01	1.00E+00
8.50E+01	1.50E+00
10.02E+01	2.00E+00
10.97E+01	3.00E+00
11.53E+01	4.00E+00
11.55E+01	5.00E+00
9.00E+01	1.00E+01
6.80E+01	2.00E+01
5.40E+01	3.00E+01
4.70E+01	5.00E+01
3.50E+01	7.00E+01
2.60E+01	1.00E+02
2.60E+01	1.00E+03
-1.00E+00	5.00E+02
1.62E-01	1.00E+00
0.00E+00	0.00E+00
0.00E+00	5.74E-01
10.62E+01	0.40E+00
17.70E+01	0.44E+00
21.24E+01	0.47E+00
22.66E+01	0.50E+00
21.24E+01	0.60E+00
17.70E+01	0.65E+00
14.16E+01	0.68E+00
10.62E+01	0.70E+00
7.08E+01	0.80E+00
6.73E+01	0.90E+00
6.37E+01	1.00E+00
7.08E+01	1.45E+00
9.45E+01	2.00E+00
10.62E+01	2.70E+00
10.97E+01	3.00E+00
11.33E+01	4.00E+00
11.33E+01	5.00E+00
9.00E+01	1.00E+01
6.80E+01	2.00E+01
5.40E+01	3.00E+01
4.10E+01	5.00E+01
3.50E+01	7.00E+01
2.60E+01	1.00E+02
2.60E+01	1.00E+03
-1.00E+00	5.00E+02
3.74E-01	1.00E+00

EXCITATION

0.00E+00	0.00E+00
0.00E+00	7.50E+00
4.60E+01	8.00E+00
7.08E+01	9.00E+00
10.62E+01	1.00E+01
13.45E+01	1.10E+01
14.16E+01	1.20E+01
13.45E+01	1.30E+01
12.74E+01	1.35E+01
13.45E+01	1.40E+01
14.87E+01	1.45E+01
1.70E+02	2.00E+01
2.60E+02	4.00E+01
3.00E+02	6.00E+01
3.20E+02	7.00E+01
3.10E+02	8.00E+01
3.00E+02	9.00E+01
2.95E+02	1.00E+02
2.20E+02	2.00E+02
1.80E+02	3.00E+02
1.40E+02	4.00E+02
1.20E+02	5.00E+02
1.00E+02	6.00E+02
9.00E+01	7.00E+02
8.00E+01	8.00E+02
7.00E+01	9.00E+02
6.20E+01	1.00E+03
-1.00E+00	1.00E+04
7.50E+00	3.00E+00

DISSOCIATION

0.00E+00	0.00E+00
0.00E+00	25.00E+00
1.77E+01	30.00E+00
6.37E+01	40.00E+00
10.62E+01	50.00E+00
14.62E+01	60.00E+00
16.99E+01	70.00E+00
18.30E+01	80.00E+00
19.12E+01	90.00E+00
19.69E+01	10.00E+01
18.87E+01	15.00E+01
17.84E+01	15.00E+01
15.61E+01	20.00E+01
14.16E+01	23.00E+01
12.39E+01	27.50E+01
11.51E+01	30.00E+01
88.50E+00	40.00E+01
73.63E+00	50.00E+01
61.95E+00	60.00E+01
53.10E+00	70.00E+01
49.56E+01	80.00E+01
44.96E+01	90.00E+01
43.19E+01	10.00E+02
-1.00E+00	3.00E+03
0.25E+02	1.00E+00

IONIZATION

0.00E+00	0.00E+00
0.00E+00	15.40E+00
12.04E+01	13.50E+00
26.20E+00	14.00E+00
70.09E+00	15.00E+00
12.78E+01	16.00E+00
18.80E+01	17.00E+00
24.99E+01	18.00E+00
31.15E+01	19.00E+00
43.99E+01	21.00E+00
50.27E+01	22.00E+00
55.56E+01	23.00E+00
60.89E+01	24.00E+00
69.58E+01	26.00E+00
82.13E+01	30.00E+00
87.69E+01	32.00E+00
92.18E+01	34.00E+00
95.97E+01	36.00E+00
10.05E+02	40.00E+00
10.83E+02	50.00E+00
11.14E+02	60.00E+00
11.26E+02	70.00E+00
11.25E+02	80.00E+00
11.23E+02	85.00E+00
11.17E+02	90.00E+00
11.03E+02	10.00E+01
10.23E+02	14.00E+01
90.94E+01	20.00E+01
76.64E+01	30.00E+01
65.14E+01	40.00E+01
57.42E+01	50.00E+01
51.51E+01	60.00E+01
46.73E+01	70.00E+01
42.48E+01	80.00E+01
39.40E+01	90.00E+01
37.45E+01	10.00E+02
-1.00E+00	5.00E+03
13.29E+00	1.00E+00

ANGULAR SCATTERING

```
10
  0.00
 25.8   36.9   45.6   53.1   60.0   66.4   72.5   78.5   84.3   90.0
 95.7  101.5  107.5  113.6  120.0  126.9  134.4  145.1  154.1  180.0
  4.00
 17.9   26.2   33.4   39.9   46.0   52.0   57.4   62.4   67.4   72.2
 76.8   81.4   86.2   91.4   97.2  104.0  112.7  123.7  139.1  180.0
  6.00
 14.0   19.3   24.0   28.6   35.1   37.7   42.4   47.6   53.0   58.8
 64.9   71.5   78.4   85.4   92.5  100.3  109.9  122.2  138.6  180.0
 10.00
 10.2   15.8   20.2   24.2   28.3   32.3   36.3   40.4   45.1   50.7
 57.2   64.4   72.0   80.5   90.9  103.6  119.3  134.6  150.3  180.0
 20.00
  5.9   11.0   15.7   19.7   23.2   26.3   29.3   32.2   35.3   38.7
 42.8   48.9   56.8   67.3   78.1   90.5  105.9  122.6  141.3  180.0
 30.00
  3.3    6.4   10.6   15.1   19.1   22.8   26.5   30.5   36.7   42.7
 50.5   59.8   71.0   85.1  101.1  114.6  126.3  138.1  151.4  180.0
 84.00
  2.2    3.4    4.2    5.2    6.3    7.4    8.8   10.5   12.6   15.3
 18.5   22.8   29.6   40.6   53.1   77.4   94.4  117.1  138.1  180.0
205.00
  1.4    2.4    3.3    4.1    5.2    6.3    7.7    9.3   11.2   13.6
 16.6   20.1   24.3   29.5   36.4   47.6   64.5   86.5  106.8  180.0
410.00
  0.8    1.5    2.1    2.9    3.8    5.7    6.6    8.5   10.7   13.1
 19.8   19.0   22.5   26.8   31.8   38.4   48.2   62.6   88.9  180.0
820.00
  0.3    0.7    1.2    1.6    2.0    2.6    3.2    4.0    5.2    6.9
  9.3   12.0   15.0   18.5   22.6   28.0   37.8   56.2   86.3  180.0
```

COLLISION CROSS-SECTION IN ARGON

MOMENTUM	TRANSFER
28.50E+02	4
21.59E+02	0.01E+00
15.23E+02	0.02E+00
9.91E+02	0.03E+00
8.11E+02	0.04E+00
6.52E+02	0.05E+00
4.04E+02	0.07E+00
1.98E+02	0.09E+00
1.21E+02	0.11E+00
0.83E+02	0.14E+00
0.69E+02	0.17E+00
0.63E+02	0.20E+00
0.55E+02	0.25E+00
0.54E+02	0.32E+00
0.64E+02	0.40E+00
1.00E+02	0.50E+00
1.66E+02	0.65E+00
2.41E+02	0.80E+00
3.72E+02	0.10E+01
6.16E+02	1.50E+00
8.78E+02	0.20E+01
14.41E+02	0.30E+01
20.53E+02	0.40E+01
30.80E+02	0.60E+01
41.42E+02	0.80E+01
48.85E+02	1.00E+01
51.33E+02	1.20E+01
46.73E+02	1.50E+01
36.82E+02	2.00E+01
29.38E+02	2.60E+01
25.49E+02	3.00E+01
20.89E+02	4.00E+01
17.88E+02	5.00E+01
16.24E+02	6.00E+01
15.52E+02	7.00E+01
15.07E+02	8.00E+01
14.54E+02	9.00E+01
13.89E+02	1.00E+02
11.72E+02	1.50E+02
10.22E+02	2.00E+02
8.84E+02	2.50E+02
7.86E+02	3.00E+02
6.02E+02	4.00E+02
5.45E+02	5.00E+02
-1.00E+00	6.00E+02
2.69E-05	1.00E+00

EXCITATION

0.00E+00	0.00E+00
0.00E+00	1.16E+01
0.45E+02	1.30E+01
0.93E+02	1.50E+01
1.45E+02	1.75E+01
1.85E+02	2.00E+01
2.40E+02	2.50E+01
2.65E+02	3.00E+01
2.75E+02	3.50E+01
2.78E+02	4.00E+01
2.72E+02	5.00E+01
2.64E+02	6.00E+01
2.60E+02	7.00E+01
2.54E+02	8.00E+01
2.47E+02	1.00E+02
2.28E+02	1.50E+02
1.90E+02	2.00E+02
1.44E+02	3.00E+02
1.19E+02	4.00E+02
0.99E+02	5.00E+02
0.89E+02	6.00E+02
0.78E+02	7.00E+02
-1.00E+00	1.00E+03
1.16E+01	1.50E+00

IONIZATION

0.00E+00	0.00E+00
0.00E+01	1.58E+01
0.71E-01	1.60E+01
2.57E-01	1.65E+01
4.74E-01	1.70E+01
1.04E+00	1.80E+01
2.22E+00	2.00E+01
3.30E+00	2.20E+01
4.60E+00	2.50E+01
5.66E+00	2.80E+01
6.37E+00	3.00E+01
6.94E+00	3.20E+01
7.47E+00	3.40E+01
7.93E+00	3.60E+01
8.25E+00	3.80E+01
8.46E+00	4.00E+01
8.81E+00	4.50E+01
8.99E+00	5.00E+01
9.20E+00	5.50E+01
9.42E+00	6.00E+01
9.81E+00	7.00E+01
1.01E+01	8.00E+01
1.01E+01	9.00E+01
1.01E+01	1.00E+02
9.95E+00	1.20E+02
9.66E+00	1.40E+02
9.27E+00	1.60E+02
8.46E+00	2.00E+02
7.68E+00	2.50E+02
7.01E+00	3.00E+02
6.41E+00	3.50E+02
5.95E+00	4.00E+02
5.17E+00	5.00E+02
-1.00E+00	6.00E+02
1.58E+01	1.00E+02

COLLISION CROSS-SECTION IN POTASSIUM

MOMENTUM TRANSFER	
3.910E+01	4
1.21E+06	0.00E+00
1.21E+06	0.03E+00
1.45E+06	0.04E+00
1.83E+06	0.06E+00
2.05E+06	0.08E+00
2.22E+06	0.10E+00
2.40E+06	0.13E+00
2.45E+06	0.16E+00
2.13E+06	0.20E+00
1.37E+06	0.25E+00
0.75E+06	0.30E+00
0.34E+06	0.35E+00
0.13E+06	0.40E+00
0.80E+05	0.45E+00
0.45E+05	0.50E+00
0.24E+05	0.60E+00
0.17E+05	0.70E+00
0.16E+05	0.80E+00
0.15E+05	1.00E+00
1.45E+04	1.50E+00
1.40E+04	2.00E+00
1.35E+04	4.00E+00
1.30E+04	1.00E+01
1.25E+04	1.00E+02
-1.45E+04	1.01E+02
27.82E-06	1.00E+00

EXCITATION

0.00E+00	0.00E+00
0.00E+00	1.61E+00
3.34E+03	1.65E+00
4.73E+03	1.70E+00
6.97E+03	1.80E+00
1.13E+04	2.00E+00
1.29E+04	2.25E+00
1.36E+04	2.50E+00
1.49E+04	2.75E+00
1.62E+04	3.00E+00
1.81E+04	3.50E+00
1.89E+04	4.00E+00
1.92E+04	6.00E+00
1.88E+04	1.00E+01
1.79E+04	1.50E+01
1.66E+04	2.00E+01
1.41E+04	3.00E+01
1.21E+04	4.00E+01
1.06E+04	5.00E+01
9.24E+03	6.33E+01
6.83E+03	9.90E+01
6.82E+03	1.00E+02
-0.01E+00	1.01E+02
1.61E+00	1.00E+00

0.00E+00	0.00E+00
0.00E+00	2.50E+00
3.11E+03	2.67E+00
5.01E+03	2.83E+00
6.52E+03	3.00E+00
1.00E+04	3.50E+00
1.15E+04	4.00E+00
1.19E+04	4.50E+00
1.16E+04	5.00E+00
1.08E+04	6.00E+00
9.94E+03	7.00E+00
9.13E+03	8.00E+00
8.43E+03	9.00E+00
7.83E+03	1.00E+01
5.42E+03	1.50E+01
4.22E+03	2.00E+01
3.01E+03	3.00E+01
2.49E+03	4.00E+01
2.01E+03	5.00E+01
8.03E+02	1.00E+02
-0.01E+00	1.01E+02
2.60E+00	1.00E+00

IONIZATION

0.00E+00	0.00E+00
0.00E+00	4.34E+00
7.02E+02	5.00E+00
1.65E+03	6.00E+00
2.56E+03	6.82E+00
2.75E+03	8.55E+00
2.66E+03	1.00E+01
2.46E+03	1.25E+01
2.32E+03	1.50E+01
2.24E+03	1.80E+01
2.29E+03	2.00E+01
2.52E+03	2.25E+01
2.63E+03	2.50E+01
2.68E+03	3.00E+01
2.09E+03	5.00E+01
1.59E+03	1.00E+02
1.24E+03	2.00E+02
9.56E+02	3.00E+02
8.14E+02	4.00E+02
7.43E+02	5.00E+02
-0.01E+00	1.01E+02
4.34E+00	1.00E+00

COLLISION CROSS-SECTION IN SODIUM

MOMENTUM TRANSFER	
2.500E+0?	5
4.05E+04	0.00E+00
3.54E+04	1.40E-04
3.40E+04	2.70E-04
3.07E+04	6.80E-04
2.76E+04	1.36E-03
2.45E+04	2.72E-03
2.24E+04	6.80E-03
2.58E+04	1.36E-02
3.22E+04	2.00E-02
4.28E+04	2.72E-02
6.96E+04	4.08E-02
1.06E+05	5.44E-02
1.50E+05	6.80E-02
2.16E+05	8.00E-02
2.51E+05	9.00E-02
2.60E+05	1.00E-01
2.72E+05	1.50E-01
2.21E+05	2.00E-01
1.55E+05	3.00E-01
1.22E+05	4.00E-01
8.99E+04	6.00E-01
7.51E+04	8.00E-01
6.36E+04	1.00E+00
4.51E+04	1.20E+00
3.24E+04	1.40E+00
2.48E+04	1.60E+00
1.59E+04	2.00E+00
1.61E+04	2.05E+00
1.42E+04	2.13E+00
1.23E+04	2.16E+00
1.07E+04	2.20E+00
8.85E+03	2.30E+00
7.43E+03	2.50E+00
6.49E+03	2.70E+00
5.24E+03	3.00E+00
2.72E+03	4.00E+00
2.64E+03	5.00E+00
2.55E+03	5.50E+00
2.32E+03	6.00E+00
2.35E+03	7.00E+00
2.13E+03	8.00E+00
2.22E+03	9.00E+00
2.42E+03	1.00E+01
2.09E+03	2.00E+01
1.84E+03	5.00E+01
1.55E+03	6.00E+01
1.47E+03	7.00E+01
1.40E+03	8.00E+01
1.29E+03	9.00E+01
1.25E+03	1.00E+02
0.86E+03	2.00E+02
0.66E+03	3.00E+02
0.58E+03	4.00E+02
=1.00E+00	4.00E+01
4.74E-03	1.00E+00

EXCITATION	
0.00E+0?	0.00E+00
0.00E+00	2.10E+00
2.27E+03	2.15E+00
5.16E+03	2.16E+00
3.79E+03	2.40E+00
4.53E+03	2.30E+00
6.66E+03	2.50E+00
8.35E+03	2.70E+00
9.59E+03	3.00E+00
1.07E+04	3.40E+00
11.00E+03	3.60E+00
11.00E+03	3.80E+00
11.10E+03	4.00E+00
11.10E+03	4.50E+00
10.90E+03	5.00E+00
10.90E+03	5.50E+00
11.00E+03	6.00E+00
11.40E+03	7.00E+00
11.40E+03	8.00E+00
11.50E+03	1.05E+01
10.80E+03	1.56E+01
9.77E+03	2.38E+01
9.03E+03	3.00E+01
8.00E+03	4.00E+01
7.50E+03	5.00E+01
6.60E+03	6.00E+01
6.20E+03	7.00E+01
5.70E+03	8.00E+01
5.20E+03	9.00E+01
4.90E+03	1.00E+02
3.00E+03	2.00E+02
2.28E+03	3.00E+02
1.80E+03	4.00E+02
1.50E+03	5.00E+02
=1.00E+00	4.00E+01
2.10E+00	1.00E+00
0.00E+00	0.00E+00
0.00E+00	3.62E+00
2.12E+02	3.92E+00
4.24E+02	4.17E+00
6.37E+02	4.43E+00
8.49E+02	4.63E+00
1.06E+03	4.89E+00
1.27E+03	5.09E+00
1.31E+03	5.14E+00
1.35E+03	5.30E+00
1.40E+03	5.40E+00
1.44E+03	5.45E+00
1.48E+03	5.65E+00
1.52E+03	5.81E+00
1.57E+03	5.96E+00
1.61E+03	6.47E+00
1.62E+03	7.00E+00
1.62E+03	8.00E+00
1.61E+03	8.86E+00
1.57E+03	1.01E+01
1.52E+03	1.14E+01
1.48E+03	1.25E+01
1.44E+03	1.39E+01

$$n' = \frac{1}{d} \int_0^d n(z, t)\, dz \quad ,$$

$$\text{i.e.} \quad n' = \frac{n_o}{\alpha d} \left\{ \exp(\alpha v t) - 1 \right\} \quad . \tag{2.3}$$

Since $\exp(\alpha v t) \gg 1$, then equation (2.3) reduces to :-

$$n' = \frac{n_o}{\alpha d} \exp(\alpha v t) = n'_o \exp(\alpha v t) \quad . \tag{2.4}$$

It appears that the source has an effective strength of $\frac{n_o}{\alpha d}$, which is a constant and has no effect on the slope of the logarithmic plot. The maximum value of n at the anode, distance α, is :-

$$n = n_o \exp(\alpha_T d) \quad . \tag{2.5}$$

If $t = t_e$, the mean arrival time of the electrons then :-

$$\alpha v t_e = \alpha_T d \quad ,$$

$$\text{i.e.} \quad t_e = \frac{d\,\alpha_T}{\alpha v} = \frac{d}{v_{exp}} \quad , \tag{2.6}$$

$$\text{where} \quad v_{exp} = \frac{\alpha v}{\alpha_T} \quad .$$

From the logarithmic plots, the slope gives αv, and the time to the plateau is t_e. Hence, by using equation (2.6), v_{exp} and hence α_T may be calculated.

It was observed that the curve of the logarithmic plot rounded near the start of the plateau. This was due to the diffusion of the electrons affecting α and v, this was studied theoretically by Lucas (1964). His explanation was that the electrons at the back of the avalanche will be in the gas longer than those at the front before being collected at the anode. This meant that the electrons at the tail would cause more ionization during the extra time in the gas. Lucas (1964) showed that :-

1.40E+03	1.50E+01
1.35E+03	1.61E+01
1.31E+03	1.72E+01
1.27E+03	1.84E+01
1.20E+03	2.00E+01
1.31E+03	2.20E+01
1.09E+03	2.40E+01
1.05E+03	2.60E+01
1.02E+03	2.80E+01
1.00E+03	3.00E+01
8.45E+02	4.00E+01
7.40E+02	5.00E+01
6.50E+02	6.00E+01
5.90E+02	7.00E+01
5.40E+02	8.00E+01
5.00E+02	9.00E+01
4.79E+02	1.00E+02
3.00E+02	2.00E+02
2.25E+02	3.00E+02
1.85E+02	4.00E+02
1.58E+02	5.00E+02
-1.00E+00	4.00E+01
3.62E+00	1.00E+00
0.00E+00	0.00E+00
0.00E+00	4.12E+00
4.25E+01	4.50E+00
1.22E+02	5.00E+00
1.55E+02	5.20E+00
1.88E+02	5.40E+00
2.12E+02	5.60E+00
2.34E+02	5.80E+00
2.46E+02	6.00E+00
2.54E+02	6.20E+00
2.58E+02	6.40E+00
2.60E+02	6.60E+00
2.62E+02	6.80E+00
2.63E+02	7.00E+00
2.64E+02	7.20E+00
2.64E+02	7.60E+00
2.63E+02	7.80E+00
2.63E+02	8.00E+00
2.60E+02	8.50E+00
2.58E+02	9.00E+00
2.54E+02	1.00E+01
2.43E+02	1.20E+01
2.28E+02	1.50E+01
2.04E+02	2.00E+01
1.83E+02	2.50E+01
1.67E+02	3.00E+01
1.50E+02	4.00E+01
1.35E+02	5.00E+01
1.25E+02	6.00E+01
1.18E+02	7.00E+01
1.10E+02	8.00E+01
1.06E+02	9.00E+01
1.00E+02	1.00E+02
-1.00E+00	4.00E+01
4.12E+00	1.00E+00

IONIZATION

0.00E+00	0.00E+00
0.00E+00	5.14E+00
7.08E+01	5.27E+00
1.41E+02	5.33E+00
2.12E+02	5.45E+00
2.85E+02	5.53E+00
3.54E+02	5.64E+00
4.24E+02	5.73E+00
4.95E+02	5.81E+00
5.66E+02	5.91E+00
6.37E+02	6.00E+00
7.08E+02	6.07E+00
7.78E+02	6.17E+00
8.49E+02	6.28E+00
9.20E+02	6.36E+00
9.92E+02	6.44E+00
1.06E+03	6.55E+00
1.13E+03	6.65E+00
1.20E+03	6.76E+00
1.27E+03	6.87E+00
1.34E+03	6.93E+00
1.41E+03	7.05E+00
1.48E+03	7.19E+00
1.55E+03	7.32E+00
1.62E+03	7.43E+00
1.69E+03	7.60E+00
1.77E+03	7.73E+00
1.84E+03	7.91E+00
1.91E+03	8.13E+00
1.98E+03	8.39E+00
2.05E+03	8.67E+00
2.12E+03	9.00E+00
2.19E+03	9.47E+00
2.26E+03	1.01E+01
2.30E+03	1.05E+01
2.33E+03	1.12E+01
2.35E+03	1.19E+01
2.36E+03	1.20E+01
2.38E+03	1.25E+01
2.39E+03	1.30E+01
2.40E+03	1.35E+01
2.40E+03	1.45E+01
2.39E+03	1.50E+01
2.37E+03	1.60E+01
2.34E+03	1.80E+01
2.30E+03	2.00E+01
2.26E+03	2.20E+01
2.21E+03	2.40E+01
2.17E+03	2.60E+01
2.12E+03	2.80E+01
2.07E+03	3.00E+01
1.45E+03	5.00E+01
1.03E+03	1.00E+02
0.74E+03	2.00E+02
6.02E+02	3.00E+02
0.51E+03	4.00E+02
0.46E+03	5.00E+02
-1.00E+00	4.00E+01
5.14E+00	1.00E+00

CF = 3·5E5

σ x CF = TOTAL

COLLISION CROSS-SECTION IN CAESIUM

MOMENTUM TRANSFER

1.329E+02	4
1.27E+06	0.00E+00
1.27E+06	0.05E+00
1.45E+06	0.04E+00
1.85E+06	0.06E+00
2.05E+06	0.08E+00
2.22E+06	0.10E+00
2.40E+06	0.13E+00
2.45E+06	0.16E+00
2.15E+06	0.20E+00
1.57E+06	0.25E+00
0.75E+06	0.30E+00
0.54E+06	0.35E+00
0.15E+06	0.40E+00
0.95E+05	0.45E+00
0.78E+05	0.50E+00
0.62E+05	0.60E+00
0.54E+05	0.70E+00
0.49E+05	0.80E+00
0.44E+05	1.00E+00
0.40E+05	1.50E+00
0.38E+05	2.00E+00
0.34E+05	4.00E+00
0.30E+05	1.00E+01
1.49E+04	1.00E+02
-1.45E+04	1.01E+02
82.57E-07	1.00E+00

EXCITATION

0.00E+00	0.00E+00
0.00E+00	1.59E+00
7.08E+05	2.00E+00
7.78E+05	2.50E+00
8.49E+05	3.00E+00
9.91E+05	4.00E+00
1.10E+04	5.00E+00
1.15E+04	6.00E+00
1.13E+04	8.00E+00
1.10E+04	1.00E+01
1.06E+04	1.50E+01
1.05E+04	2.00E+01
9.20E+05	3.00E+01
9.20E+05	1.00E+02
-9.20E+03	1.01E+02
1.59E+00	1.00E+00
0.00E+00	0.00E+00
0.00E+00	1.45E+00
1.45E+04	2.00E+00
1.56E+04	2.50E+00
1.77E+04	3.00E+00
2.05E+04	4.00E+00
2.27E+04	5.00E+00
2.57E+04	6.00E+00
2.42E+04	8.00E+00
2.47E+04	1.00E+01
2.25E+04	1.50E+01
2.18E+04	2.00E+01
1.91E+04	3.00E+01
1.91E+04	1.00E+02
-1.91E+04	1.01E+02
1.45E+00	1.00E+00

IONIZATION

0.00E+00	0.00E+00
0.00E+00	5.89E+00
9.76E+02	5.00E+00
1.77E+03	6.00E+00
2.08E+03	7.00E+00
2.32E+03	8.00E+00
2.56E+03	9.00E+00
2.62E+03	1.00E+01
2.81E+03	1.10E+01
2.99E+03	1.20E+01
3.17E+03	1.30E+01
3.34E+03	1.40E+01
3.60E+03	1.50E+01
3.48E+03	1.60E+01
3.56E+03	1.70E+01
3.17E+03	1.80E+01
3.11E+03	1.90E+01
3.17E+03	2.00E+01
3.56E+03	2.20E+01
3.48E+03	2.40E+01
3.54E+03	2.60E+01
3.54E+03	3.00E+01
3.54E+03	1.00E+02
-3.54E+03	1.01E+02
3.89E+00	1.00E+00

APPENDIX C

COMPUTER PROGRAMS

1. MONTE CARLO A (Molecular Gas)
2. MONTE CARLO AH (Inert Gas)
3. BOLTZMANN

COMPUTER PROGRAM FOR THE CALCULATION OF SWARM PARAMETERS BY THE MONTE CARLO COMPUTER SIMULATION METHOD

```
JOB  :RMHEP,EE26C??,CP76(T500,P3000,SP)
ATTACH(JACK,EE59MOLECHUX,ST=S6A)
ATTACH(LOCAL,LIBNAGFTNSCM,ID=LIBAPPL)
LIBRARY(LOCAL)
FTN(I=JACK)
ATTACH(FRED,EE26CORTAN,ST=S6A)
COPYS(FRED,BOTH)
COPY(INPUT,BOTH)
REWIND (BOTH)
LDSET(MAP=B/ZZZZMP,PRESET=NGINF)
LGO(BOTH,PL=5000)
####S
    1.0    0.5   11.0    1.0    1.0
 0.2000E+01 0.1000E+00 2.0000E+04
 0.2000E+00 0.1000E-07
0.1500E-01   10
0.10000000
      10.00
        470       10000          -1
****
```

Monte Carlo A

(Molecular Gas)

```
      PROGRAM MOLE(INPUT,OUTPUT,TAPE5=INPUT,TAPE6=OUTPUT)
      INTEGER W,WW
      DIMENSION K1(200),K2(200),W(10),WW(10),NW(10),UH(10),K3(10,200)
     9,RAT(10)
     1,MT(100),M2(100),UUA(20),UUB(20),ZS(20),TS(20),STOZS(20)
     4,TVE(20),SIG2(20),NES(20)
     3,NCL(20),ZS2(20),ZS2M(20),UR(20),URM(20),AN1S(20)
     2,N1S(20),UBS(20),UAS(20),ZSM(20),TSM(20)
     8,QT(10,50),EN(10,50),Q(10,500),QP(10)
     6,XU(2000),XZ(2000),XT(2000),XCSS(2000),NS(2000),XPHI(2000)
     7,RS(20),RSM(20)
     6,ONSET(10),XY(2000),XX(2000)
     C,NP(10,20),NC(10),FACT(10),ANG(20,21),ENG(21),NAVA(100)
     D,VEN(10,50),VIB(10,50)
      COMMON/VT/VSET(10),LEV,QV(10,500),UCELL
      COMMON/ION/XX,XZ,XY,XT,XU,XCSS,XPHI,NS
      LEVEL 2,XX,XY,XZ,XT,XU,XCSS,XPHI,NS
      READ(5,65) UTM,NXS
65    FORMAT(E10.3,I5)
      DO 47 J=1,NXS
      IF(J-2) 247,47,247
247   CONTINUE
      DO 66 I=1,150
      READ(5,46) QT(J,I),EN(J,I)
46    FORMAT(2E10.2)
      IF(QT(J,I) ) 147,66,66
66    CONTINUE
147    READ(5,48) ONSET(J),FACT(J)
48    FORMAT(2E10.2)
 47   CONTINUE
      READ(5,400) LEV
400   FORMAT(I4)
      DO 401 J=1,LEV
      DO 402 I=1,50
      READ(5,403) VIB(J,I),VEN(J,I)
403   FORMAT(2E10.2)
      IF(VIB(J,I).LT.0.0) GOTO 401
402   CONTINUE
401   READ(5,405) VSET(J)
405   FORMAT(E10.2)
      READ(5,238) NANG
  238 FORMAT(I4)
      DO 245 K=1,NANG
      READ(5,239) ENG(K)
  239 FORMAT(F7.2)
      ANG(K,1)=0.0
      DO 240 J=1,2
      J1=(J-1)*10 + 2
      J2=J*10 + 1
  240 READ(5,241) (ANG(K,JJ),JJ=J1,J2)
  241 FORMAT(10F6.1)
```

```
  243 CONTINUE
55    WRITE(6,15)
      ONSET(2)=VSET(1)
      READ(5,55) (FACT(J),J=1,NXS)
   55 FORMAT(20F6.1)
15    FORMAT(51H1ELECTRON SWARM MOTION IN GASES)
      READ(5,2) U,F,E
2     FORMAT(3E11.4)
      READ(5,2) UCELL ,ZCELL
      READ(5,16) TMAX,JSTEP
16    FORMAT(E11.4,I4)
      READ(5,3) RN
3     FORMAT(F10.8)
      READ(5,172) AVE
172   FORMAT(F10.2)
      READ(5,4) NPRINT,NSTOP,NREP
4     FORMAT(3I10)
      WRITE(6,7) U,F,E
7     FORMAT(/11H INPUT ENG=,E11.4,5X,5HSTEP=,E11.4
     9,5X,10HEL. FIELD=,E11.4)
      WRITE(6,8) TMAX,JSTEP
8     FORMAT(/13H FLIGHT TIME=,E11.4,5X,6HJSTEP=,I4)
      WRITE(6,9) UCELL,ZCELL
9     FORMAT(/7H UCELL=,E11.4,5X,6HZCELL=,E11.4)
      WRITE(6,175) AVE
175   FORMAT(/23H AVERAGE AVALANCHE NO.=,F6.2/)
      WRITE(6,17) RN
17    FORMAT(/15H RANDOM NUMBER=,F10.8)
      WRITE(6,18) NPRINT,NSTOP,NREP
18    FORMAT(/10H PRINTING=,I10,5X,5HSTOP=,I10,5X,7HREPEAT=,I10)
      WRITE(6,19) WTM,ONSET(1)
19    FORMAT(/18H MOLECULAR WEIGHT=,E9.3,5X,13HELASTIC LOSS=,E8.2)
      WRITE(6,54) (ONSET(J),J=2,NXS)
54    FORMAT(/6H ONSET,9X,10E11.3)
      WRITE(6,199) (FACT(J),J=1,NXS)
199   FORMAT(5H FACT,F9.2,10F11.2)
      DO 72 J=1,NXS
      IF(J-2) 272,72,272
272   CONTINUE
      KI=1
      Q(J,1)=QT(J,1)*FACT(J)
      NLU=500
      NLU2=498
      DO 75 I=2,NLU
      AI=I-1
      AI=AI*UCELL
      DO 74 K=KI,100
      IF(EN(J,K).GT.AI) GOTO 75
74    CONTINUE
```

```
75      Q(J,I)=QT(J,K-1)+(QT(J,K)-QT(J,K-1))*(AI-EN(J,K-1))/
     1(EN(J,K)-EN(J,K-1))
        Q(J,I)=Q(J,I)*FACT(J)
73      KI=K-1
72      CONTINUE
        DO 150 J=1,LEV
        KI=1
        QV(J,1)=VIB(J,1)
        DO 151 I=2,NLU
        AI=I-1
        AI=AI*UCELL
        DO 152 K=KI,100
        IF(VEN(J,K).GT.AI) GOTO 153
152     CONTINUE
153     QV(J,I)=VIB(J,K-1)+(VIB(J,K)-VIB(J,K-1))*(AI-VEN(J,K-1))/
     1(VEN(J,K)-VEN(J,K-1))
        QV(J,I)=QV(J,I)*FACT(2)
151     KI=K-1
150     CONTINUE
        DO 155 I=1,NLU
        Q(2,I)=0.0
        DO 156 J=1,LEV
156     Q(2,I)=Q(2,I)+QV(J,1)
155     CONTINUE
        DO 501 K=1,NLU,10
        WRITE(6,500) K,(Q(J,K),J=1,NXS)
500     FORMAT(I4,10E11.3)
501     CONTINUE
        WRITE(6,54) (VSET(J),J=1,LEV)
        DO 1136 K=1,NLU,10
1136     WRITE(6,500) K,(QV(J,K),J=1,LEV)
        WRITE(6,244)
244     FORMAT(10H1ANGULAR SCATTER)
        DO 246 K=1,NANG
        WRITE(6,248) ENG(K)
246     WRITE(6,245) (ANG(K,J),J=1,21)
245     FORMAT(21F6.1)
248     FORMAT(F8.2)
        NE=0
        UD=0
        DO 6 J=1,200
        K1(J)=0
        DO 666 L=1,JSTEP
  666   K3(L,J)=0
6       K2(J)=0
        LPRINT=NPRINT
        DO 69 K=1,JSTEP
        DO 106 J=1,NXS
106     NP(J,K)=0
        NES(K)=0
        ZS2M(K)=0.0
```

```
      URM(K)=0.0
      ANTS(K)=0.0
      NCL(K)=0
      ZS2(K)=0.0
      UR(K)=0.0
      TS(K)=0.0
      N1S(K)=0
      ZS(K)=0.0
      STOZS(K)=0.0
      UUA(K)=0.0
      UBS(K)=0.0
      UAS(K)=0.0
      ZSM(K)=0.0
      TSM(K)=0.0
69    UUB(K)=0.0
      DO 25 J=1,20
      RS(J)=0.0
25    RSM(J)=0.0
      EBM=1.6022E+12/9.1096
      MAXZ=10
      NMAX=10
      MAXR=10
      DO 171 J=1,100
171   NAVA(J)=0
      CALL GUSCBF(RN)
65    NE=NE+1
      DO 553 J=1,100
      XCSS(J)=0.0
      XU(J)=0.0
      XZ(J)=0.0
      XT(J)=0.0
      XY(J)=0.0
      XX(J)=0.0
      XPHI(J)=0.0
553   NS(J)=0
      U=UD
      NSTEP=1
      Z=0.0
      NION=0
      NVAR=0
      NRUN=0
      X=0.0
      Y=0.0
      SPHI=0.0
      CSS=1.0
      SNN=0.0
       PHI=0.0
      T=0.0
      AJS=JSTEP
      TN=TMAX/AJS
```

```
      TERM=1,0-EXP(-F)
200   DO 150 J=1,NXS
150   NC(J)=0
      N1=0
      UB=0,0
      UA=0,0
20    V=SQRT(2,0*EBM*ABS(U))
      VZ=V*CSS
      VR=V*SNN
11    TER=1,0
      U=ABS(U)
      I=U/UCELL
      IF(I-NLU2) 700,701,701
701   Q1=Q(1,NLU)
      GOTO 705
700   AI=I
      AI=AI*UCELL
      I=I+1
      Q1=Q(1,I)*(Q(1,I+1)-Q(1,I))*(U-AI)/UCELL
705   S=F/Q1
      RN=GUSCAP(Q)
      IF(RN,LE,TERM) TER=RN/TERM
      DT=(S/V)*TER
      DVZ=EBM*DT*E
      DZ=VZ*DT+0,5*EBM*DT*DT*E
      DX=VR*DT*COS(SPHI)
      DY=VR*DT*SIN(SPHI)
      VZ=VZ+DVZ
      Z=Z+DZ
      X=X+DX
      Y=Y+DY
      T=T+DT
      U=U+DZ*E
      V=SQRT(2,0*EBM*ABS(U))
162   IF(Z,GE,TN) GOTO 62
      IF(RN,GT,TERM) GOTO 11
      N1=N1+1
      CSS=VZ/V
      SNN=SQRT(ABS(1,0-CSS*CSS))
      UU=U
      UB=UB+U
      I=ABS(U)/UCELL
      SUM=0,0
      IF(I-NLU2) 704,705,705
705   DO 707 J=1,NXS
      QP(J)=Q(J,NLU)
707   SUM=SUM+QP(J)
      GOTO 706
704   AI=I
      AI=AI*UCELL
```

```
      I=I+1
      DO 120 J=1,NXS
      QP(J)=Q(J,I)+(Q(J,I+1)-Q(J,1))*(U-AI)/UCELL
120   SUM=SUM+QP(J)
706   CONTINUE
      SUM=SUM-QP(1)
      CHECK=SUM/QP(1)
      RN=GUSCAF(Q)
      IF(RN.LE.CHECK) GOTO 121
      NC(1)=NC(1)+1
      RN=GUSCAF(Q)
      CALL DIFANG(RN,U,ANG,ENG,CS,SN)
      RN=GUSCAF(Q)
      CALL ETA (RN,PHI,SPHI)
      CSS=CSS*CS+SNN*SN*COS(PHI)
      SNN=SQRT(ABS(1.0-CSS*CSS))
      DELU=U*(1.0-CS)*ONSET(1)
      U=U-DELU
      UA=UA+U
      GOTO 20
121   CHECK=QP(2)/QP(1)
      IF(RN.GT.CHECK) GOTO 122
      NC(2)=NC(2)+1
      PP=RN/CHECK
      QVT=QP(2)
      CALL VIBRAT(PP,U,QVT,DELU)
      GOTO 126
122   NXSS=NXS-2
      DO 123 K=3,NXSS
      CHECK=CHECK+QP(K)/QP(1)
      IF(RN.LE.CHECK) GOTO 124
123   CONTINUE
      CHECK=CHECK+QP(NXS-1)/QP(1)
      LXS=NXS
      IF(RN.LE.CHECK) LXS=NXS-1
      GOTO 125
124   DELU=ONSET(K)
      NC(K)=NC(K)+1
      GOTO 126
125   CONTINUE
      NC(LXS)=NC(LXS)+1
      DELU=(U+ONSET(LXS))/2.0
      NION=NION+1
      J=NION
      XZ(J)=Z
      XY(J)=Y
      XX(J)=X
      XU(J)=(U-ONSET(LXS))/2.0
      XT(J)=T
      XCSS(J)=CSS
```

$$v_{exp} = \left(\frac{u+\lambda}{2\lambda} \right) v \quad , \tag{2.7}$$

and

$$n = n_o \frac{u}{\lambda} \exp\left\{ (\lambda - u)\, d \right\} = \frac{n_o u}{\lambda} \exp(\alpha_T d) \quad , \tag{2.8}$$

where $\lambda = \frac{v}{2D}$ and $u^2 = \lambda^2 - 2\alpha\lambda$.

This method can give values of v at high E/N where the electron mean energy is above the onset energy for ionization by applying the correction shown in equation (2.7) to the measured values of drift velocity, v_{exp} .

Snelson (1974) developed a time of flight technique to measure electron swarm parameters. This consisted of a Townsend discharge chamber with a thick guard ring construction, a heated filament electron source and a movable, screened anode. Screening the anode meant that the anode current was measured as opposed to the integrated anode current by the Frommhold technique. The solution of the transport equation (2.1) in the presence of ionization and attachment processes is :-

$$n(z,t) = \frac{n_o}{\sqrt{4\pi D t}} \exp\left\{ \frac{-(z - vt)^2}{4 D t} + (\alpha - \eta)\, vt \right\} . \tag{2.9}$$

For a fixed E/N, the anode current time distribution was measured for a series of gap separations. Referring to the time of flight characteristic shown in Fig. 2.1, by measuring the time t_{max} (the time elapsed before maximum anode current was observed) the electron drift velocity was calculated as :-

$$v_d = \frac{d}{t_{max}} \quad , \tag{2.10}$$

where d = gap separation.

```
      XPHI(J)=SPHI
      NS(J)=NSTEP
      NVAR=NVAR+1
126   CONTINUE
      RN=GUSCAF(Q)
      CALL DIFANG(RN,U,ANG,ENG,CS,SN)
      RN=GUSCAF(Q)
      CALL ETA (RN,PHI,SPHI)
      CSS=CSS*CS+SNN*SN*COS(PHI)
      SNN=SQRT(ABS(1.0-CSS*CSS))
      U=U-DELU
      UA=UA+U
      GOTO 20
62    CONTINUE
      NES(NSTEP)=NES(NSTEP)+1
      DO 151 J=1,NXS
151   NP(J,NSTEP)=NC(J)+NP(J,NSTEP)
      CTERM=(Z-TN)/DZ
      CT=T-UT*CTERM
      CX=X-DX*CTERM
      CY=Y-DY*CTERM
      TS(NSTEP)=TS(NSTEP)+CT
      R2=CX*CX+CY*CY
      RS(NSTEP)=RS(NSTEP)+R2
      ZS(NSTEP)=ZS(NSTEP)+Z
      ZS2(NSTEP)=ZS2(NSTEP)+CT*CT
      CU=U-DZ*E*CTERM
      UR(NSTEP)=UR(NSTEP)+CU
      UBS(NSTEP)=UBS(NSTEP)+UB
      UAS(NSTEP)=UAS(NSTEP)+UA
      N1S(NSTEP)=N1+N1S(NSTEP)
      AN1S(NSTEP)=N1S(NSTEP)
      LLL=SQRT(R2)*100.0/TMAX+1
      IF(LLL.GT.200) LLL=200
      IF(LLL.GT.MAXR) MAXR=LLL
      K3(NSTEP,LLL)=K3(NSTEP,LLL)+1
      NSTEP=NSTEP+1
      ANS=NSTEP
      TN=TMAX*(ANS/AJS)
61    IF(NSTEP-JSTEP) 162,162,21
21    L=U+1
      LL=T/ZCELL+1
      IF(L.GT.200) L=200
      IF(L.GT.NMAX) NMAX=L
      K1(L)=K1(L)+1
      IF(LL.GT.200) L=200
      IF(LL.GT.MAXZ) MAXZ=LL
      K2(LL)=K2(LL)+1
      IF(NVAR) 45,45,64
64    NRUN=NRUN+1
```

```
      J=N+UN
      U=XU(J)
      Z=XZ(J)
      Y=XY(J)
      X=XX(J)
      T=XT(J)
      CSS=XCSS(J)
      SPHI=XPHI(J)
      SNN=SQRT(ABS(1.0-CSS*CSS))
      RN=GOBCAR(Q)
      CALL DIFANG(RN,U,ANG,ENG,CS,SN)
      CSS=CSS*CS+SNN*SN*COS(SPHI)
      NSTEP=NS(J)
      ANS=NSTEP
      TN=TMAX*(ANS/AJS)
      NVAR=NVAR+1
      GOTO 200
   45 CONTINUE
      NAV=NION+1
      JJ=NAV*10.0/AVE
      JJ=JJ+1
      IF(JJ.GT.100) JJ=100
      NAVA(JJ)=NAVA(JJ)+1
      IF(NE.LT.NPRINT) GOTO 65
   68 VEL=Z/T
      NPRINT=NPRINT+LPRINT
      DO 105 J=1,JSTEP
      ANE=NES(J)
      TSM(J)=TS(J)/ANE
      ZSM(J)=ZS(J)/ANE
      ZS2M(J)=ZS2(J)/ANE
      RSM(J)=RS(J)/ANE
      URM(J)=UR(J)/ANE
      UUB(J)=UBS(J)/AN1S(J)
      SIGZ(J)=(ZS2M(J)-(TSM(J)**2))
      TVEL(J)=ZSM(J)/TSM(J)
      UUA(J)=UAS(J)/AN1S(J)
  105 CONTINUE
      WRITE(6,110) NE
  110 FORMAT(1H1NO. OF ELECTRONS,5X,I6)
      WRITE(6,138)
  138 FORMAT(//20H TYPES OF COLLISIONS)
      WRITE(6,107)
  107 FORMAT(/6H TOTAL)
      DO 140 K=1,JSTEP
      WRITE(6,139) N1S(K),(NP(J,K),J=1,NXS)
  139 FORMAT(1118)
  140 CONTINUE
      WRITE(6,111)
  111 FORMAT(/4X,11H ENG BEFORE,5X,10H ENG AFTER,5X,9H MEAN ENG)
```

```
      DO 78 K=1,JSTEP
78    WRITE(6,112) UUP(K),UUA(K),URM(K)
112   FORMAT(3E15.4)
      WRITE(6,113)
113   FORMAT(/13X,2H Z,11X,4H Z*Z,13X,2H T)
      DO 79 K=1,JSTEP
79    WRITE (6,114) ZSM(K),ZS2M(K),TSM(K),NES(K)
114   FORMAT(3E18.5,I8)
      WRITE(6,300)
300   FORMAT(/5X,4H VEL,8X,5H SIG2,13X,5H RAD2)
      DO 302 K=1,JSTEP
302   WRITE(6,301) TVEL(K),SIG2(K),RSM(K)
301   FORMAT(3E15.6)
29    WRITE (6,82)
82    FORMAT(5H     N,16X,37HELECTRON ENERGY DISTRIBUTION FUNCTION)
      IF(NMAX-100) 51,51,52
52    NMAX=100
51    NMAX=NMAX
      DO 70 J=1,NMAX,10
      DO 71 K=1,10
      JK=J+K-1
71    W(K)=K1(JK)
70    WRITE(6,83) J,(W(K),K=1,10)
83    FORMAT(1H ,I4,5X,10I6)
      WRITE(6,104)
104   FORMAT(3H1 Z,8X,25HDISPLACEMENT DISTRIBUTION)
      DO 90 J=1,MAXZ,10
      DO 92 K=1,10
      JK=J+K-1
92    WW(K)=K2(JK)
90    WRITE (6,89) J,(WW(K),K=1,10)
89    FORMAT(1H ,I4,5X,10I6)
      WRITE(6,158)
158   FORMAT(25H1AVALANCHE DISTRIBUTION/)
      DO 159 J=1,100,10
      N10=J+9
159   WRITE(6,153) J,(NAVA(K),K=J,N10)
153   FORMAT(I4,5X,10I6)
      DO 1101 L=1,JSTEP
      AL=L
      IF (NREP.EQ.-10) GO TO 1162
      WRITE(6,160) ZSM(L)
160   FORMAT(23H1 RADIAL    DISTRIBUTION,5X,6H GAP =,E11.4)
      NSUM=0
      DO 161 J=1,MAXR,10
      DO 160 K=1,10
      JK=J+K-1
      AJK=JK
      NW(K)=K3(L,JK)
      NSUM=NSUM+NW(K)
```

```
      R=AJX*TMAX*0.07
      D=TMAX*0.1*AL
      R=SQRT(D*D+R*R)
      A1=NSUM
      A2=NES(L)
      JK=K
      RAT(JK)=A1/A2
      UH(JK)=0.0
      IF (RAT(JK).GE.1.0) GOTO1161
      UH(JK)=-ALOG(R/D*(1.0-RAT(JK)))/(R-D)
      UH(JK)=E/(2.0*UH(JK))
  166 CONTINUE
      WRITE(6,163) J,(NW(K),K=1,10)
  163 FORMAT(I5,2X,10(I8))
      WRITE(6,164) (RAT(K),K=1,10)
  164 FORMAT(6X,10(F8.5))
      WRITE(6,165) (UH(K),K=1,10)
  165 FORMAT(6X,10(F6.3)///)
  161 CONTINUE
 1161 CONTINUE
 1162 WRITE(6,85) RN
   85 FORMAT(/5H RN =,F10.8)
      IF(NE-NSTOP) 65,22,22
   22 IF(NREP) 50,50,53
   50 WRITE (6,84)
   84 FORMAT(13H RUN COMPLETE)
      CALL EXIT
      END
*FORTRAN
      SUBROUTINE THETA (RN,EP,CS,SN)
      CS=(-1.0+SQRT(ABS(1.0+EP*EP-EP*(4.0*P-2.0))))/EP
      SN=SQRT(ABS(1.0-CS*CS))
      RETURN
      END
*FORTRAN
      SUBROUTINE ETA (RN,PHI,SPHI)
      PHI=6.28318530*RN
      SPHI=SPHI+PHI
      NPHI=SPHI/6.28318530
      A=NPHI
      SPHI=SPHI-A*6.28318530
      RETURN
      END
*FORTRAN
      SUBROUTINE TROPIC (RN,CS,SN)
      CS=1.0-2.0*RN
      SN=SQRT(ABS(1.0-CS*CS))
      RETURN
      END
*FORTRAN
```

```
      SUBROUTINE DIFANG(RN,U,ANG,ENG,CS,SN)
      DIMENSION ANG(20,21),ENG(21)
      U=ABS(U)
      IF(U.GT.780.0) U=780.0
      NP=RN*20.0
      ANP=NP
      NP=NP+1
      NPP=NP+1
      DO 1 J=1,21
      CHECK=U-ENG(J)
      IF(CHECK) 2,2,1
    1 CONTINUE
    2 NC=J-1
      NCC=J
      DEG1=ANG(NC,NP)+(RN*20.0-ANP)*(ANG(NC,NPP)-ANG(NC,NP))
      DEG2=ANG(NCC,NP)+(RN*20.0-ANP)*(ANG(NCC,NPP)-ANG(NCC,NP))
      DEG=DEG1+(DEG2-DEG1)*(U-ENG(NC))/(ENG(NCC)-ENG(NC))
      DEG=DEG/57.2958
      CS=COS(DEG)
      SN=SIN(DEG)
      RETURN
      END
*FORTRAN
      SUBROUTINE VIBRAT(PP,U,QVT,DELU)
      COMMON/VT/VSET(10),LEV,QV(10,500),UCELL
      CON=U.U
      U=ABS(U)
      I=U/UCELL
      AI=I
      AI=AI*UCELL
      DO 120 J=1,LEV
      IF(I.LT.498) GOTO 1
      Q=QV(J,500)
      GOTO 2
    1 I=I+1
      Q=QV(J,I)+(QV(J,I+1)-QV(J,I))*(U-AI)/UCELL
                I=I-1
    2 CONTINUE
      CON=CON*Q/QVT
      DELU=VSET(J)
      IF(PP.LE.CON) GOTO 5
  120 CONTINUE
    5 CONTINUE
      RETURN
      END
```

A SAMPLE PRINTOUT

```
ELECTRON SWARM MOTION IN GASES

INPUT ENG=   .1000E+01        STEP=   .1000E+00        EL. FIELD=   .2000E+05

GAP SEPARATION =   .1500E-01        JSTEP=  10

UCELL=   .2000E+00        TCELL=   .1000E-07

AVERAGE AVALANCHE NO,= 10.00


RANDOM NUMBER= .98765432

PRINTING=        470      STOP=        9000      REPEAT=          -1

MOLECULAR WEIGHT= .280E+02        ELASTIC LOSS= .38E-04

ONSET                .250E+00    .772E+01    .224E+02    .140E+02
FACT       1.00           .50        11.00        1.00         1.00
  1    .100E+04   0.             0.             0.             0.
 11    .122E+05    .208E+04   0.             0.             0.
 21    .525E+04    .750E+02   0.             0.             0.
 31    .425E+04   0.             0.             0.             0.
 41    .410E+04   0.              .481E+02   0.             0.
 51    .400E+04   0.              .396E+03   0.             0.
 61    .390E+04   0.              .660E+03   0.             0.
 71    .403E+04   0.              .799E+03   0.             0.
 81    .414E+04   0.              .887E+03   0.              .400E+02
 91    .422E+04   0.              .922E+03   0.              .900E+02
101    .430E+04   0.              .957E+03   0.              .150E+03
111    .426E+04   0.              .966E+03   0.              .210E+03
121    .422E+04   0.              .975E+03    .479E+01    .265E+03
131    .416E+04   0.              .975E+03    .127E+02    .315E+03
141    .408E+04   0.              .966E+03    .265E+02    .363E+03
151    .400E+04   0.              .957E+03    .354E+02    .410E+03
161    .394E+04   0.              .944E+03    .443E+02    .440E+03
171    .388E+04   0.              .931E+03    .531E+02    .470E+03
181    .382E+04   0.              .917E+03    .619E+02    .493E+03
191    .376E+04   0.              .904E+03    .734E+02    .524E+03
201    .370E+04   0.              .891E+03    .849E+02    .550E+03
211    .364E+04   0.              .882E+03    .906E+02    .563E+03
221    .358E+04   0.              .873E+03    .963E+02    .580E+03
231    .352E+04   0.              .865E+03    .104E+03    .602E+03
241    .346E+04   0.              .856E+03    .113E+03    .616E+03
251    .340E+04   0.              .847E+03    .123E+03    .630E+03
261    .336E+04   0.              .838E+03    .129E+03    .640E+03
271    .332E+04   0.              .829E+03    .135E+03    .650E+03
281    .328E+04   0.              .821E+03    .141E+03    .660E+03
291    .324E+04   0.              .812E+03    .150E+03    .670E+03
301    .320E+04   0.              .803E+03    .159E+03    .680E+03
311    .317E+04   0.              .795E+03    .164E+03    .684E+03
321    .314E+04   0.              .786E+03    .169E+03    .688E+03
331    .311E+04   0.              .780E+03    .174E+03    .692E+03
341    .308E+04   0.              .772E+03    .179E+03    .696E+03
351    .305E+04   0.              .765E+03    .184E+03    .700E+03
361    .302E+04   0.              .757E+03    .187E+03    .703E+03
371    .299E+04   0.              .749E+03    .190E+03    .706E+03
381    .296E+04   0.              .741E+03    .194E+03    .709E+03
391    .293E+04   0.              .734E+03    .197E+03    .712E+03
401    .290E+04   0.              .726E+03    .200E+03    .715E+03
411    .288E+04   0.              .719E+03    .203E+03    .716E+03
421    .286E+04   0.              .713E+03    .206E+03    .716E+03
431    .284E+04   0.              .706E+03    .209E+03    .717E+03
```

SAMPLE (CONTINUED)

451	.280E+04	0.	.695E+03	.215E+03	.713E+03
461	.278E+04	0.	.680E+03	.217E+03	.715E+03
471	.275E+04	0.	.680E+03	.219E+03	.719E+03
481	.274E+04	0.	.673E+03	.221E+03	.719E+03
491	.272E+04	0.	.667E+03	.223E+03	.726E+03

ONSET	.250E+00	.450E+00	.700E+00	.120E+01
1 0.	0.	0.	0.	
11 .208E+04	.575E+00	.250E+00	.375E+00	
21 .750E+02	0.	0.	0.	
31 0.	0.	0.	0.	
41 0.	0.	0.	0.	
51 0.	0.	0.	0.	
61 0.	0.	0.	0.	
71 0.	0.	0.	0.	
81 0.	0.	0.	0.	
91 0.	0.	0.	0.	
101 0.	0.	0.	0.	
111 0.	0.	0.	0.	
121 0.	0.	0.	0.	
131 0.	0.	0.	0.	
141 0.	0.	0.	0.	
151 0.	0.	0.	0.	
161 0.	0.	0.	0.	
171 0.	0.	0.	0.	
181 0.	0.	0.	0.	
191 0.	0.	0.	0.	
201 0.	0.	0.	0.	
211 0.	0.	0.	0.	
221 0.	0.	0.	0.	
231 0.	0.	0.	0.	
241 0.	0.	0.	0.	
251 0.	0.	0.	0.	
261 0.	0.	0.	0.	
271 0.	0.	0.	0.	
281 0.	0.	0.	0.	
291 0.	0.	0.	0.	
301 0.	0.	0.	0.	
311 0.	0.	0.	0.	
321 0.	0.	0.	0.	
331 0.	0.	0.	0.	
341 0.	0.	0.	0.	
351 0.	0.	0.	0.	
361 0.	0.	0.	0.	
371 0.	0.	0.	0.	
381 0.	0.	0.	0.	
391 0.	0.	0.	0.	
401 0.	0.	0.	0.	
411 0.	0.	0.	0.	
421 0.	0.	0.	0.	
431 0.	0.	0.	0.	
441 0.	0.	0.	0.	
451 0.	0.	0.	0.	
461 0.	0.	0.	0.	
471 0.	0.	0.	0.	
481 0.	0.	0.	0.	
491 0.	0.	0.	0.	

SAMPLE (CONTINUED)

NO. OF ELECTRONS 470

TYPES OF COLLISIONS

TOTAL					
10978	9867	291	770	1	49
27121	23958	568	2343	10	242
49465	43504	901	4521	23	516
77047	69139	1401	7506	42	909
122658	107152	2123	11823	76	1484
185551	160104	3109	17955	118	2245
267252	232826	4468	26469	183	3306
386864	336837	6524	38320	274	4909
555893	483842	9347	55224	415	7065
796228	692950	13338	79177	591	10172

ENG BEFORE	ENG AFTER	MEAN ENG
.8472E+01	.7841E+01	.1576E+02
.1011E+02	.9250E+01	.1637E+02
.1064E+02	.9704E+01	.1664E+02
.1093E+02	.9941E+01	.1683E+02
.1110E+02	.1009E+02	.1649E+02
.1117E+02	.1014E+02	.1670E+02
.1126E+02	.1021E+02	.1685E+02
.1127E+02	.1022E+02	.1672E+02
.1128E+02	.1022E+02	.1675E+02
.1126E+02	.1020E+02	.1669E+02

Z	Z*Z	T	
.150000E-02	.11584E-16	.30372E-08	520
.30000E-02	.42913E-16	.61060E-08	722
.45000E-02	.92644E-16	.91152E-08	1009
.60000E-02	.15428E-15	.11913E-07	1421
.75000E-02	.23480E-15	.14800E-07	2030
.90000E-02	.33110E-15	.17670E-07	2833
.10500E-01	.44323E-15	.20538E-07	3959
.12000E-01	.57329E-15	.23427E-07	5653
.13500E-01	.71871E-15	.26288E-07	7950
.15000E-01	.88311E-15	.29195E-07	11253

VEL	SIGZ	RADZ
.493873E+06	.235968E-17	.974239E-06
.491320E+06	.562968E-17	.245176E-05
.493681E+06	.955760E-17	.390017E-05
.503667E+06	.123658E-16	.500807E-05
.506765E+06	.157676E-16	.613228E-05
.509343E+06	.188850E-16	.746254E-05
.511244E+06	.214099E-16	.892340E-05
.512234E+06	.244791E-16	.104010E-04
.513552E+06	.276743E-16	.117033E-04
.513780E+06	.307565E-16	.130304E-04

ELECTRON ENERGY DISTRIBUTION FUNCTION

N										
1	0	12	60	116	163	264	328	384	536	535
11	613	653	753	634	606	585	480	479	426	401
21	355	317	318	241	219	202	181	146	156	122
31	110	67	106	75	73	64	48	43	38	35
41	26	23	17	24	21	24	11	10	8	5
51	4	7	11	10	3	7	6	6	4	7
61	4	3	6	0	2	1	0	1	3	2
71	0	0	0	1	0	0	0	4	2	2
81	0	0	1	0	0	0	0	0	0	0
91	0	0	0	0	0	0	0	0	0	0

Monte Carlo AH

(Inert Gas)

```
      PROGRAM CALC(INPUT,OUTPUT,TAPE5=INPUT,TAPE6=OUTPUT)
      INTEGER W,WW
      DIMENSION K1(200),K2(200),W(10),WW(10)
     9,RAT(10),NW(10),UH(10),K3(10,200)
     1,M1(100),M2(100),UUA(20),UUB(20),ZS(20),TS(20),STOZS(20)
     4,TVEL(20),SIG2(20),NES(20)
     3,NCL(20),ZS2(20),ZS2M(20),UR(20),URM(20),AN1S(20)
     2,N1S(20),UBS(20),UAS(20),ZSM(20),TSM(20)
     9,QT(6,75),EN(6,75),J(6,500),QP(6)
     6,XU(2000),XZ(2000),XT(2000),XCSS(2000),NS(2000),XPHI(2000)
     7,RS(20),RSM(20)
     8,ONSET(6),XY(2000),XX(2000)
     5,NP(6,10),NC(6),FACT(6),ANG(30,21),ENG(30)
     A,NAVA(100)
      COMMON XX,XZ,XY,XT,XU,XCSS,XPHI,NS
      LEVEL2,XX,XZ,XY,XT,XU,XCSS,XPHI,NS
      READ(5,65) WTM,NXS
65    FORMAT(E10.3,I5)
      DO 47 J=1,NXS
      DO 66 I=1,150
      READ(5,46) QT(J,I),EN(J,I)
46    FORMAT(2E10.2)
      IF(QT(J,I) ) 47,66,66
66    CONTINUE
47    READ(5,48) ONSET(J),FACT(J)
48    FORMAT(2E10.2)
      READ(5,238) NANG
  238 FORMAT(I4)
      DO 243 K=1,NANG
      READ(5,239) ENG(K)
  239 FORMAT(F7.2)
      ANG(K,1)=0.0
      DO 240 J=1,2
      J1=(J-1)*10 + 2
      J2=J*10 + 1
  240 READ(5,241) (ANG(K,JJ),JJ=J1,J2)
  241 FORMAT(10F6.1)
  243 CONTINUE
53    WRITE(6,13)
      READ (5,33) (FACT(J),J=1,NXS)
   33 FORMAT (20F6.1)
13    FORMAT(31H1ELECTRON SWARM MOTION IN GASES)
      READ(5,2) U,F,E
2     FORMAT(3E11.4)
      READ(5,2) UCELL ,ZCELL
      READ(5,16) TMAX,JSTEP
16    FORMAT(E11.4,I4)
      READ(5,3) RN
3     FORMAT(F10.8)
      READ(5,172) AVE
172   FORMAT(F10.2)
      READ(5,4) NPRINT,NSTOP,NREP
4     FORMAT(3I10)
      WRITE(6,7) U,F,F
7     FORMAT(/11H INPUT ENG=,E11.4,5X,5HSTEP=,F11.4
     9,5X,10HEL. FIELD=,E11.4)
```

```
      WRITE(6,8) TMAX,JSTEP
8     FORMAT(//9H MAX GAP=,E11.4,5X,12HNO. OF GAPS=,I4)
      WRITE(6,9) UCELL,ZCELL
9     FORMAT(/7H UCELL=,E11.4,5X,8HZCELL=,E11.4)
      WRITE(6,173) AVE
173   FORMAT(//22HAVERAGE AVALANCHE NO.=,F6.2//)
      WRITE(6,17) RN
17    FORMAT(/15H RANDOM NUMBER=,F10.8)
      WRITE(6,18) NPRINT,NSTOP,NREP
18    FORMAT(/10H PRINTING=,I10,5X,5HSTOP=,I10,5X,7HREPEAT=,I10)
      WRITE(6,19) WTM,ONSET(1)
19    FORMAT(/18H MOLECULAR WEIGHT=,E9.3,5X,13HELASTIC LOSS=,E8.2)
      WRITE(6,54) (ONSET(J),J=2,NXS)
54    FORMAT(/6H ONSET,14X,5F15.3)
      WRITE(6,199) (FACT(J),J=1,NXS)
199   FORMAT(7H FACTOR,5F15.2)
      DO 72 J=1,NXS
      KI=1
      Q(J,1)=QT(J,1)*FACT(J)
      DO 73 I=2,500
      AI=I-1
      AI=AI*UCELL
      DO 74 K=KI,100
      IF(EN(J,K).GT.AI) GOTO 75
74    CONTINUE
75    Q(J,I)=QT(J,K-1)+(QT(J,K)-QT(J,K-1))*(AI-EN(J,K-1))/
     1(EN(J,K)-EN(J,K-1))
      Q(J,I)=Q(J,I)*FACT(J)
73    KI=K-1
72    CONTINUE
      DO 501 K=1,500,10
      WRITE(6,500) K,(Q(J,K),J=1,NXS)
500   FORMAT(I4,6F15.3)
501   CONTINUE
      WRITE(6,244)
244   FORMAT(16H1ANGULAR SCATTER)
      DO 246 K=1,NANG
      WRITE(6,248) ENG(K)
246   WRITE(6,245) (ANG(K,J),J=1,21)
245   FORMAT(21F6.1)
248   FORMAT(F8.2)
      NE=0
      UD=U
      DO 6 J=1,200
      K1(J)=0
      DO 666 L=1,JSTEP
  666 K3(L,J)=0
6     K2(J)=0
      LPRINT=NPRINT
      DO 69 K=1,JSTEP
      DO 106 J=1,NXS
106   NP(J,K)=0
      NES(K)=0
      ZS2M(K)=0.0
      URM(K)=0.0
```

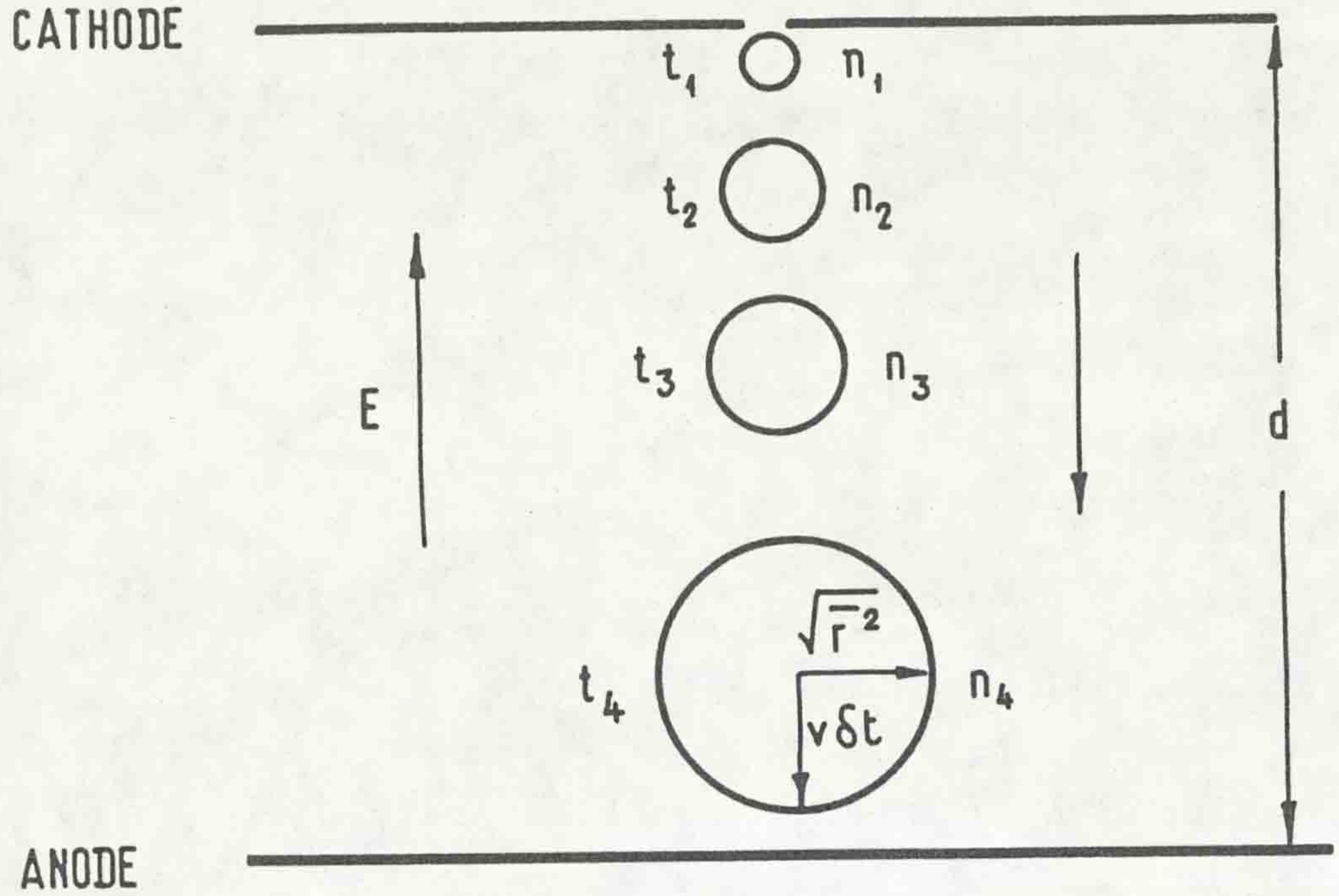

where d is gap separation

$t_4 > t_3 > t_2 > t_1$ t = time

for amplification

$n_4 > n_3 > n_2 > n_1$

for attachment

$n_4 < n_3 < n_2 < n_1$

n = electron number density

$\bar{r}^2$ = Radial variance

$2 v\delta t$ = Half width

Fig.(2.1) SCHEMATIC DIAGRAM SHOWING DRIFT AND DIFFUSION OF ELECTRONS IN A UNIFORM ELECTRIC FIELD

```
      ANIS(K)=0.0
      NCL(K)=0
      ZS2(K)=0.0
      UR(K)=0.0
      TS(K)=0.0
      N1S(K)=0
      ZS(K)=0.0
      STOZS(K)=0.0
      UUA(K)=0.0
      UBS(K)=0.0
      UAS(K)=0.0
      ZSM(K)=0.0
      TSM(K)=0.0
69    UUB(K)=0.0
      DO 25 J=1,20
      RS(J)=0.0
25    RSM(J)=0.0
      FBM=1.6022E+1279.1096
      MAXZ=10
      NMAX=10
      MAXR=10
      DO 171 J=1,100
171   NAVA(J)=0
      CALL G05CBF(RN)
63    NE=NE+1
      DO 553 J=1,100
      XCSS(J)=0.0
      XU(J)=0.0
      XZ(J)=0.0
      XT(J)=0.0
      XV(J)=0.0
      XX(J)=0.0
      XPHI(J)=0.0
553   NS(J)=0
      U=UD
      NSTEP=1
      DELZ=0.0
      STOZ=0.0
      Z=0.0
      NTON=0
      NVAR=0
      NRUN=0
      X=0.0
      Y=0.0
      SPHI=0.0
      CSS=1.0
      SNN=0.0
       PHI=0.0
      T=0.0
      SU=0.0
      AJS=JSTEP
      TN=TMAX/AJS
      TERM=1.0-EXP(-F)
200   DO 150 J=1,NXS
150   NC(J)=0
```

```
      N1=0
      UB=0.0
      UA=0.0
20    V=SQRT(2.0*EBM*ABS(U))
      VZ=V*CSS
      VR=V*SNN
11    TER=1.0
      I=ABS(U)/UCELL
      IF(I-498) 700,701,701
701   Q1=Q(1,500)
      GOTO 703
700   AI=I
      AI=I
      AI=AI*UCELL
      I=I+1
      Q1=Q(1,I)+(Q(1,I+1)-Q(1,I))*(U-AI)/UCELL
703   S=F/Q1
      RN=G05CAF(QQ)
      IF(RN-TERM) 14,14,12
14    TER=RN/TERM
12    DT=(S/V)*TER
      DVZ=EBM*DT*E
      DZ=VZ*DT+0.5*EBM*DT*DT*E
      DX=VR*DT*COS(SPHI)
      DY=VR*DT*SIN(SPHI)
      DELZ=DELZ+DZ
      VZ=VZ+DVZ
      Z=Z+DZ
      X=X+DX
      Y=Y+DY
      T=T+DT
      U=U+DZ*E
      V=SQRT(2.0*EBM*ABS(U))
162   IF(Z.GE.TN) GOTO 62
      IF(RN-TERM) 10,10,11
10    CONTINUE
      N1=N1+1
      CSS=VZ/V
      DELZ=0.0
      SNN=SQRT(ABS(1.0-CSS*CSS))
      UU=U
      UB=UB+U
      DELU=0.0
      RN=G05CAF(QQ)
      I=ABS(U)/UCELL
      SUM=0.0
      IF(I-498) 704,705,705
705   DO 707 J=1,NX8
      QP(J)=Q(J,500)
707   SUM=SUM+QP(J)
      GOTO 706
704   AI=I
      AI=AI*UCELL
      I=I+1
```

```
      DO 120 J=1,NXS
      QP(J)=Q(J,I)+(Q(J,I+1)-Q(J,I))*(U-AI)/UCELL
120   SUM=SUM+QP(J)
706   CONTINUE
      SUM=SUM-QP(1)
      CHECK=SUM/QP(1)
      IF(RN.LE.CHECK) GOTO 121
      NC(1)=NC(1)+1
      RN=G05CAF(QQ)
      CALL DIFANG(RN,U,ANG,ENG,CS,SN)
      RN=G05CAF(QQ)
      CALL ETA (RN,PHI,SPHI)
      CSS=CSS*CS+SNN*SN*COS(PHI)
      SNN=SQRT(ABS(1.0-CSS*CSS))
      DELU=U*(1.0-CS)*ONSET(1)
      U=U-DELU
      UA=UA+U
      GOTO 20
121   NXSS=NXS-1
      CHECK=0.0
      DO 123 K=2,NXSS
      CHECK=CHECK+QP(K)/QP(1)
      IF(RN.LE.CHECK) GOTO 124
123   CONTINUE
      GOTO 125
124   DELU=ONSET(K)
      NC(K)=NC(K)+1
      GOTO 126
125   CONTINUE
      NC(NXS)=NC(NXS)+1
      DELU=(U+ONSET(NXS))/2.0
      NION=NION+1
      J=NION
      XZ(J)=Z
      XY(J)=Y
      XX(J)=X
      XU(J)=(U-ONSET(NXS))/2.0
      XT(J)=T
      XCSS(J)=CSS
      XPHI(J)=SPHI
      NS(J)=NSTEP
      NVAR=NVAR+1
126   CONTINUE
      RN=G05CAF(QQ)
      CALL DIFANG(RN,U,ANG,ENG,CS,SN)
      RN=G05CAF(QQ)
      CALL ETA (RN,PHI,SPHI)
      CSS=CSS*CS+SNN*SN*COS(PHI)
      SNN=SQRT(ABS(1.0-CSS*CSS))
      U=U-DELU
      UA=UA+U
      GOTO 20
62    CONTINUE
      NES(NSTEP)=NES(NSTEP)+1
```

```
      DO 151 J=1,NXS
151   NP(J,NSTEP)=NC(J)+NP(J,NSTEP)
      CTERM=(Z-TN)/DZ
      CT=T-DT*CTERM
      CX=X-DX*CTERM
      CY=Y-DY*CTERM
      TS(NSTEP)=TS(NSTEP)+CT
      R2=CX*CX+CY*CY
      RS(NSTEP)=RS(NSTEP)+R2
      ZS(NSTEP)=ZS(NSTEP)+Z
      ZS2(NSTEP)=ZS2(NSTEP)+CT*CT
      CU=U-DZ*E*CTERM
      UR(NSTEP)=UR(NSTEP)+CU
      UBS(NSTEP)=UBS(NSTEP)+UB
      UAS(NSTEP)=UAS(NSTEP)+UA
      N1S(NSTEP)=N1+N1S(NSTEP)
      AN1S(NSTEP)=N1S(NSTEP)
      LLL=SQRT(R2)*100.0/TMAX+1
      IF(LLL.GT.200) LLL=200
      IF(LLL.GT.MAXR) MAXR=LLL
      K3(NSTEP,LLL)=K3(NSTEP,LLL)+1
      NSTEP=NSTEP+1
      ANS=NSTEP
      TN=TMAX*(ANS/AJS)
61    IF(NSTEP-JSTEP) 162,162,21
21    L=U/UCELL+1
      LL=T/ZCELL+1
      IF(L-NMAX) 95,95,96
96    NMAX=L
95    NMAX=NMAX
      IF(L-100) 40,40,41
41    L=100
40    K1(L)=K1(L)+1
      IF(LL-MAXZ) 100,100,101
101   MAXZ=LL
100   MAXZ=MAXZ
      IF(LL-100) 102,103,103
103   LL=100
      MAXZ=LL
102   K2(LL)=K2(LL)+1
      IF(NVAR) 45,45,64
64    NRUN=NRUN+1
      J=NRUN
      U=XU(J)
      Z=XZ(J)
      Y=XY(J)
      X=XX(J)
      T=XT(J)
      CSS=XCSS(J)
      SPHI=XPHI(J)
      SNN=SQRT(ABS(1.0-CSS*CSS))
      RN=GO5CAF(QQ)
      CALL DIFANG(RN,U,ANG,ENG,CS,SN)
      CSS=CSS*CS+SNN*SN*COS(SPHI)
      NSTEP=NS(J)
```

```
      ANS=NSTEP
      TN=TMAX*(ANS/AJS)
      NVAR=NVAR-1
      GOTO 200
45    CONTINUE
      NAV=NION+1
      JJ=NAV*10.0/AVE
      JJ=JJ+1
      IF(JJ.GT.100) JJ=100
      NAVA(JJ)=NAVA(JJ)+1
      IF(NE.LT.NPRINT) GOTO 65
68    VEL=Z/T
      NPRINT=NPRINT+LPRINT
      DO 105 J=1,JSTEP
      ANE=NES(J)
      TSM(J)=TS(J)/ANE
      ZSM(J)=ZS(J)/ANE
      ZS2M(J)=ZS2(J)/ANE
      RSM(J)=RS(J)/ANE
      URM(J)=UR(J)/ANE
      UUB(J)=UBS(J)/AN1S(J)
      SIG2(J)=(ZS2M(J)-(TSM(J)**2))
      TVEL(J)=ZSM(J)/TSM(J)
      UUA(J)=UAS(J)/AN1S(J)
105   CONTINUE
      WRITE(6,110) NE
110   FORMAT(17H1NO. OF ELECTRONS,5X,I6)
      WRITE(6,138)
138   FORMAT(//20H TYPES OF COLLISIONS)
      WRITE(6,107)
107   FORMAT(/6H TOTAL)
      DO 140 K=1,JSTEP
      WRITE(6,139) N1S(K),(NP(J,K),J=1,NXS)
139   FORMAT(7I8)
140   CONTINUE
      WRITE(6,111)
111   FORMAT(/4X,11H ENG BEFORE,5X,10H ENG AFTER,5X,9H MEAN ENG)
      DO 78 K=1,JSTEP
78    WRITE(6,112) UUB(K),UUA(K),URM(K)
112   FORMAT(3E15.4)
      WRITE(6,113)
113   FORMAT(/13X,2H Z,11X,4H Z*2,13X,2H T)
      DO 79 K=1,JSTEP
79    WRITE (6,114) ZSM(K),ZS2M(K),TSM(K),NES(K)
114   FORMAT(3E18.5,I8)
      WRITE(6,300)
300   FORMAT(/5X,4H VEL,8X,5H SIG2,13X,5H RAD2)
      DO 302 K=1,JSTEP
302   WRITE(6,301) TVEL(K),SIG2(K),RSM(K)
301   FORMAT(3E15.6)
29    WRITE (6,82)
82    FORMAT(5H     N,16X,37HELECTRON ENERGY DISTRIBUTION FUNCTION)
      IF(NMAX-100) 51,51,52
52    NMAX=100
51    NMAX=NMAX
      DO 70 J=1,NMAX,10
```

```
      DO 71 K=1,10
      JK=J+K-1
71    W(K)=K1(JK)
70    WRITE(6,83) J,(W(K),K=1,10)
83    FORMAT(1H ,I4,5X,10I6)
      WRITE(6,104)
104   FORMAT(3H1 Z,8X,25HDISPLACEMENT DISTRIBUTION)
      DO 90 J=1,MAXZ,10
      DO 92 K=1,10
      JK=J+K-1
92    WW(K)=K2(JK)
90    WRITE (6,89) J,(WW(K),K=1,10)
89    FORMAT(1H ,I4,5X,10I6)
      WRITE(6,158)
158   FORMAT(23H1AVALANCHE DISTRIBUTION/)
      DO 159 J=1,100,10
      N10=J+9
159   WRITE(6,153) J,(NAVA(K),K=J,N10)
153   FORMAT(I4,5X,10I6)
      DO 1161 L=1,JSTEP
      AL=L
      IF (NREP.EQ.-10) GOTO1162
      WRITE(6,160) ZSM(L)
160   FORMAT(23H1 RADIAL    DISTRIBUTION,5X,6H GAP =,E11.4)
      NSUM=0
      DO 161 J=1,MAXR,10
      DO 166 K=1,10
      JK=J+K-1
      AJK=JK
      NW(K)=K3(L,JK)
      NSUM=NSUM+NW(K)
      R=AJK*TMAX*0.01
      D=TMAX*0.1*AL
      R=SQRT(D*D+R*R)
      A1=NSUM
      A2=NES(L)
      JK=K
      RAT(JK)=A1/A2
      UH(JK)=0.0
      IF(RAT(JK).GE.1.0) GOTO1161
      UH(JK)=-ALOG(R/D*(1.0-RAT(JK)))/(R-D)
      UH(JK)=E/(2.0*UH(JK))
166   CONTINUE
      WRITE(6,163) J,(NW(K),K=1,10)
163   FORMAT(I5,2X,10(I8))
      WRITE(6,164) (RAT(K),K=1,10)
```

```
 164  FORMAT(6X,10(F8.5))
      WRITE(6,165) (QH(K),K=1,10)
 165  FORMAT(6X,10(F8.3)///)
 161  CONTINUE
1161  CONTINUE
1162   WRITE(6,85) RN
 85    FORMAT(/5H RN =,F10.8)
       IF(NE-NSTOP) 63,22,22
 22    IF(NREP) 50,50,53
 50    WRITE (6,84)
 84    FORMAT(13H RUN COMPLETE)
       CALL EXIT
       END
*FORTRAN
       SUBROUTINE ETA (RN,PHI,SPHI)
       PHI=6.283185307*RN
       SPHI=SPHI+PHI
       NPHI=SPHI/6.283185307
       A=NPHI
       SPHI=SPHI-A*6.283185307
       RETURN
       END
*FORTRAN
       SUBROUTINE TROPIC (RN,CS,SN)
       CS=1.0-2.0*RN
       SN=SQRT(ABS(1.0-CS*CS))
       RETURN
       END
*FORTRAN
       SUBROUTINE DIFANG(RN,U,ANG,ENG,CS,SN)
       DIMENSION ANG(30,21),ENG(30)
       U=ABS(U)
       IF(U.GT.900.0) U=900.0
       NP=RN*20.0
       ANP=NP
       NP=NP+1
       NPP=NP+1
       DO 1 J=1,30
       CHECK=U-ENG(J)
       IF(CHECK) 2,1,1
     1 CONTINUE
     2 NC=J-1
       NCC=J
       DEG1=ANG(NC,NP)+(RN*20.0-ANP)*(ANG(NC,NPP)-ANG(NC,NP))
       DEG2=ANG(NCC,NP)+(RN*20.0-ANP)*(ANG(NCC,NPP)-ANG(NCC,NP))
       DEG=DEG1+(DEG2-DEG1)*(U-ENG(NC))/(ENG(NCC)-ENG(NC))
       DEG=DEG/57.2958
       CS=COS(DEG)
       SN=SIN(DEG)
       RETURN
       END
```

Boltzmann

```
      PROGRAM BOLTZ(INPUT,OUTPUT,TAPE5=INPUT,TAPE6=OUTPUT)
      DIMENSION EX(10,151),SQ(510),R(10,510),F(510),QT(10,151)
     A,EN(10),ONSET(15),L(10),Q(10,310),SCALE(10)
     B,FACT(10),S(10),AL(10),MM(10)
      COMMON/ABC/U(510),DF(510)/ARRAY/SIMF(510),USTEP
C     SOLUTION OF BOLTZMANN EQUATION STEADY STATE SOLUTION
C     PROGRAM TITLE
      WRITE(6,99)
   99 FORMAT(44H1BOLTZMANN STEADY STATE EQUATION PHELPS SOLN)
C     INPUT X-SECTION
      READ(5,65) JTM,NXS
65    FORMAT(E10.3,I5)
      DO 47 J=1,NXS
      WRITE(6,25) J
   25 FORMAT(I5)
      DO 66 I=1,150
      READ(5,40) QT(J,I),EX(J,I)
40    FORMAT(2E10.2)
      WRITE(6,26) QT(J,I),EX(J,I)
   26 FORMAT(2E11.4)
      IF(QT(J,I)) 470,66,66
66    CONTINUE
470   CONTINUE
      READ(5,48) ONSET(J),FACT(J)
      WRITE(6,26) ONSET(J),FACT(J)
   48 FORMAT(2E10.2)
   47 CONTINUE
      ONSET(9)=ONSET(6)
      ONSET(10)=ONSET(7)
      ONSET(11)=ONSET(8)
      NSTORE=NXS
      READ(5,2154)(SCALE(J),J=1,NXS)
2154  FORMAT(10F6.3)
      WRITE(6,2155)(SCALE(J),J=1,NXS)
2155  FORMAT(11H SCALING IS,10F10.5)
      DO 2143 J=1,NXS
2143  FACT(J)=FACT(J)*SCALE(J)
63    READ(5,105) E,T
105   FORMAT(2E11.4)
      WRITE(6,303) E,T
303   FORMAT(11H1EL. FIELD=,E11.4,4H V/M,10X,12HTEMPERATURE=,E11.4,
     12H K)
      READ(5,104) UMAX,NMAX,NPRINT
104   FORMAT(E11.4,2I10)
      WRITE(6,301) UMAX,NMAX,NPRINT
  301 FORMAT(6H UMAX=,F7.2,5X,5HNMAX=,I6,5X,7HNPRINT=,I4)
      NXS=NSFORE
      NXSS=NXS+1
      ONSET(6)=ONSET(9)
      ONSET(7)=ONSET(10)
      ONSET(8)=ONSET(11)
```

```
      ANMAX=NMAX
      USTEP=UMAX/ANMAX
      PETSU=1.0/USTEP
      N1=NMAX+1
C     TRANSFER
      GM=UNSET(1)
      NS=NMAX+3
      DO 4 I=1,NS
      J=I-1
      AJ=J
      U(I)=AJ*USTEP
2     SQ(I)=SQRT(U(I))
      DO 8 J=1,NXS
8     Q(J,1)=QT(J,1)*FACT(J)
      DO 17 J=1,NXS
      KI=1
      DO 4 I=2,N1
      AI=I-1
      AI=AI*USTEP
      DO 5 K=KI,100
      IF(EX(J,K).GT.AI) GOTO 6
5     CONTINUE
6     Q(J,I)=QT(J,K-1)+(QT(J,K)-QT(J,K-1))*(AI-EX(J,K-1))/
     1(EX(J,K)-EX(J,K-1))
      Q(J,I)=Q(J,I)*FACT(J)
4     KI=K-1
17    CONTINUE
      DO 1000 I=1,N1
      Q(1,I)=Q(1,I)+Q(6,I)
      Q(6,I)=Q(7,I)
1000  Q(7,I)=Q(8,I)
      NXS=NXS-1
      NXSS=NXSS-1
      GM=UNSET(1)*FACT(1)*UNSET(6)*FACT(6)/100.0
      UNSET(6)=UNSET(7)
      UNSET(7)=UNSET(8)
      DO 1 J=2,NXS
      I=J+1
1     EN(I)=UNSET(J)
      DO 7 J=3,NXSS
      AL(J)=EN(J)*PETSU
7     L(J)=AL(J)
998   L(2)=1
      L(1)=1
      DO 70 J=3,NXSS
70    AL(J)=L(J)
      DO 9 I=1,N1
      B(1,I)=E*E/(3.0*Q(1,I))
      B(2,I)=GM*U(I)*Q(1,I)
      DO 71 J=3,NXSS
71    B(J,I)=U(I)*Q(J-1,I)
```

```
9       CONTINUE
C       STARTING ENERGY DISTRIBUTION
        IJIM=0
        DF(NMAX+2)=0.0
        DF(NMAX+3)=0.0
        F(NMAX+1)=1.00E-7
        F(NMAX)=1.00E-7
C       BOUNDRY CONDITIONS
        READ(5,501) ASTOP,JREP,JSTOP
501     FORMAT(E11.4,2I4)
        WRITE(6,505) ASTOP,JREP,JSTOP
  505   FORMAT(7H ASTOP=,E11.4,5X,5HJREP=,I4,5X,6HJSTOP=,I4)
        JIM=0
        SUMFJ=1.0
        G=3.95095E+05
C       CYCLE POSITION
100     SSF=0.0
        Z=0.0
        DO 10 M=1,NMAX
        I=NMAX-M+2
        AI=I
        DO 72 J=3,NXSS
72      MM(J)=L(J)+I
        M6=MM(NXSS)
        IF(M6.GE.NMAX+1) GOTO 199
        K=NXSS
        Z=Z+B(K,M6)*F(M6)/AI
       1+(B(K,M6+1)*F(M6+1)-B(K,M6)*F(M6))
       2*(EN(K)*PETSU-AL(K))/AI
199     SF=Z
        DO 75 J=3,NXSS
75      SF=SF-F(I)*B(J,I)
        MN=NXSS-1
202     MC=MM(MN)
        IF(MC.LT.NMAX+1) GOTO 201
        MN=MN-1
        IF(MN-2) 205,205,202
201     DO 74 J=3,MN
        MD=MM(J)
        SF=SF+B(J,MD)*F(MD)
       1+(B(J,MD+1)*F(MD+1)-B(J,MD)*F(MD))*(EN(J)*PETSU-AL(J))
74      CONTINUE
  205   SF=SF*USTEP
        SSF=SSF+SF
        DF(I)=(-B(2,I)*U(I)*F(I)*SSF)
       1/(U(I)*F(I)*(B(1,I)*B(2,I)*8.61705E-05*T))
        IF(IJIM.GT.0) GOTO 10
C       BACKWARD PROLONGATION
        F(I-1)=F(I)*EXP(-(3.0*DF(I)-DF(I+1))*0.5*USTEP)
10      CONTINUE
        DF(1)=0.0
```

In this case the relationship between v_d and v is given by (Lucas and Saelee, 1975) :-

$$v_d = \frac{u}{\lambda} v \quad , \tag{2.11}$$

where u and λ have their usual definitions.

The Snelson technique may be used at high E/N, since it also takes into account the effect of ionization at electron energies higher than the ionization onset energy.

2.4.2 The Longitudinal Diffusion Coefficient, D_L

Wagner, Davis and Hurst (1967) developed an apparatus to measure the diffusion coefficient and drift velocity by a time of flight method. This method brought to light the first set of data for the diffusion coefficient which varied from Townsend's measurements. The Townsend method measured the diffusion in the direction perpendicular to the applied electric field, while the time of flight method measured the diffusion in the direction parallel to the applied field. This gave rise to the idea that the diffusion coefficient is a tensor quantity. Their apparatus comprised of a three section chamber containing a swarm region, transition region and a detection region. The electron swarms were generated by a pulsed ultraviolet light, which also triggered a time of flight analyser. The electron detection system consisted of an electron multiplier operating in a pulse counting mode. After passing through high gain amplifiers, the signal was fed directly into a time of flight analyser, which developed a time of flight characteristic of those particular experimental conditions.

```
      IJIM=IJIM+1
C     GAUSS-SEIDEL ITERATION
      F(2)=EXP((DF(1)+DF(2))*0.5*USTEP)
      F(3)=EXP(USTEP*(DF(1)+4.0*DF(2)+DF(3))/3.0)
      DO 32 I=5,N1,2
32    F(I)=F(I-2)*EXP(USTEP*(DF(I-2)+4.0*DF(I-1)+DF(I))/3.0)
      DO 33 I=4,NMAX,2
33    F(I)=F(I-2)*EXP(USTEP*(DF(I-2)+4.0*DF(I-1)+DF(I))/3.0)
C     NORMALIZATION
      DO 11 J=1,N1
11    SIMF(J)=F(J)*SQ(J)
      CALL SIMP(NMAX,SUM)
      FMUS=1.0/SUM
      DO 12 I=1,N1
12    F(I)=F(I)*FMUS
      ADD=ABS(1.0-SUM/SUMPJ)
      SUMPJ=SUM
      JIM=JIM+1
      WRITE(6,20) JIM,FMUS
20    FORMAT(I4,E11.4)
      IF(JSTOP.LT.JIM) GOTO 25
      IF(ADD.GE.ASTOP) GOTO 100
25    CONTINUE
      WRITE(6,109)
109   FORMAT(2X,2HNU,9X,4HF(U),9X,9HSQ(U)F(U),9X,5HDF(U))
      DO 16 I=1,NMAX,NPRINT
      FNIII=F(I)*SQ(I)
16    WRITE(6,110) U(I),F(I),FNIII,DF(I)
110   FORMAT(F6.2,5X,E11.4,5X,E11.4,5X,E11.4)
      WRITE(6,503) JIM
503   FORMAT(5H JIM=,I4///)
      DO 55 J=1,N1
55    SIMF(J)=-B(1,J)*DF(J)*U(J)*F(J)
      CALL SIMP(NMAX,SUM)
      VEL=SUM*G/E
      WRITE(6,56) VEL
56    FORMAT(//16H DRIFT VELOCITY=,E11.4,4H M/S)
      DO 53 J=1,N1
53    SIMF(J)=U(J)*F(J)*B(1,J)
      CALL SIMP(NMAX,SUM)
      DIFF=SUM*G/(E*E)
      WRITE(6,54) DIFF
54    FORMAT(//13H DIFF COEFF.=,E11.4,6H MSQ/S)
      DO 50 J=1,N1
50    SIMF(J)=F(J)*SQ(J)*U(J)
      CALL SIMP(NMAX,SUM)
      EMEAN=SUM
      WRITE(6,51) EMEAN
51    FORMAT(//13H MEAN ENERGY=,E11.4,14H ELECTRON-VOLT)
      DU=DIFF*E/VEL
      WRITE(6,62) DU
62    FORMAT(//5H D/U=,E11.4)
```

```
      DO 57 I=2,NXSS
      DO 58 J=1,N1
58    SIMF(J)=B(I,J)*F(J)
      CALL SIMP(NMAX,SUM)
57    S(I)=SUM*6
      S(2)=S(2)/GM
      WRITE(6,59)
59    FORMAT(//19H RATE OF COLLISIONS)
      DO 60 J=1,NXS
      N=J+1
      WRITE(6,61) J,S(N)
61    FORMAT(/I5,5X,E11.4)
60    CONTINUE
      IF(JREP.GE.0) GOTO 63
502   WRITE(6,112)
 112  FORMAT(19H RUN COMPLETE)
      CALL EXIT
      END
*FORTRAN
      SUBROUTINE SIMP(NMAX,SUM)
      COMMON/ARRAY/SIMF(510),USTEP
      ODD=0.0
      EVEN=0.0
      DO 1 I=2,NMAX,2
1     ODD=ODD+SIMF(I)
      NO=NMAX-1
      DO 2 I=3,NO,2
2     EVEN=EVEN+SIMF(I)
      SUM=USTEP*(SIMF(1)+SIMF(NMAX+1)+4.0*ODD+2.0*EVEN)/3.0
      RETURN
      END
*FORTRAN
      SUBROUTINE EXTRA(I,AREA)
      COMMON/ABC/U(510),DF(510)
      X0=U(I-1)
      X1=U(I)
      X2=U(I+1)
      X3=U(I+2)
      Y1=DF(I)
      Y2=DF(I+1)
      Y3=DF(I+2)
      AA=((Y1-Y2)*(X2-X3)-(Y2-Y3)*(X1-X2))/
     B(X1-X2)*(X2-X3)*((X1+X2)-(X2+X3))
      BB=((Y1-Y2)-AA*(X1*X1-X2*X2))/(X1-X2)
      CC=Y1-AA*X1*X1-BB*X1
      AREA=AA*(X1**3-X0**3)/3.0
     C+BB*(X1**2-X0**2)/2.0+CC*(X1-X0)
      RETURN
      END
```

APPENDIX

D

1. PRESSURE CALIBRATION
2. SPECIFICATION OF GASES
3. SPECIFICATION OF EQUIPMENT

TABLE A : PRESSURE CALIBRATION

Pressure, p_o, (torr)		
Mcleod Gauge	Baratron Gauge	Pressure Range of Baratron (x 100)
0.106	0.105	0.001
0.0478	0.0477	0.001
0.453	0.454	0.01
4.57	4.60	0.1
7.69	7.81	0.1
9.00	9.19	0.1

TABLE B : SPECIFICATION OF GASES

Gas	Supplier's Grading	Main Contents	
O_2	B.O.C. Ltd. CP Crade	99.5 % < 5 v.p.m. ≃ 50 v.p.m. < 0.5 %	O_2 CO_2 H_2 Ar
CH4	B.O.C. Ltd. CP Grade	99.2% 0.7% 2 v.p.m. 1 v.p.m.	CH4 N_2 O_2 CO_2
SF_6	B.O.C. Ltd. CP Grade	99.9% < 900 ppm < 15 ppm	SF_6 air + non-condensables water

TABLE C

SPECIFICATION OF EQUIPMENT

Description	Information	Model
Pressure gauge	M.K.S. Baratron Full scales : 0.1, 1, 10 and 100 torr	94 AH - 100 170 M - 7A
Digital voltmeter	Solartron digital 0-1000 volts, input impedance 10 M	LM 1420.2
Voltage supply	Fluke, 0 - 3100 V	415 B
Filament supply	Farnell Range 0 - 30 V, 0 - 5 A Range 0 - 12 V, 0 - 10 A	 L30E L30F
Filament	Vacuum Generators Thoriated iridium	V1G21 Filament
Differential ac amplifier	Brookdeal 0.1 Hz - 2 MHz. I/P 20.MΩ, 20 pF O/P 1 KΩ, 10 μF Gain 20 - 100 dB	 9454
Pulse Generator	Lyons Instruments O/P 50	PG 71N
X-Y Recorder	Bryans	26000A4
Box-car detector	Brookdeal Linear gate and scan delay generator	9415 9425A
Ionization gauge	Mullard	10G 12
Oil diffusion pump	Edwards Speedivac Speed : 70-80 L/sec	203B
Pirani gauge	Edwards Full scale 0.005 or 10 torr	8 - 2
Rotary pumps	Metrovac Displacement 1 L/sec Ultimate pressure 5×10^{-4} torr	G DR 2
Oscilloscope	Tektronix 15 MHz Bandwidth	555

Since the electron multiplier was required to count single electrons, this placed a severe restriction on the range of E/N and the gases to be studied. At high E/N, corresponding to high electron energies compared to the onset energy of ionization, the counter would be triggered by the first electron to reach it. This meant that low E/N and high pressures had to be used to prevent ionization so that single electrons could be counted accurately.

The time of flight method of Snelson, however, could be used to measure the longitudinal diffusion coefficient at high E/N in the presence of ionization. Referring once again to equation (2.9) and Fig. 2.1, the anode current/time distribution was analysed to determine the half width $2\delta t$. The diffusion coefficient was then determined by using the equation :-

$$(D_L)_d = \frac{d^2 (\delta t)^2}{4\, t_{max}^2} \quad . \tag{2.12}$$

It is also worthwhile to note that by obtaining the distribution for different gap separations and measuring the half width and t_{max} as a function of gap separation, the Snelson method can eliminate electrode effects and time delays inherent to the electrical circuit by using a difference technique. The Wagner, Davis and Hurst (1967) method does not do this, rather the effect is enhanced by the circuitry employed.

As before, the experimental value of the longitudinal coefficient $(D_L)_d$ is related to the value obtained from the transport equation by the relationship :-

$$(D_L)_d = \frac{u}{\lambda} D_L \quad . \tag{2.13}$$

2.4.3 The Radial Diffusion Coefficient, D_r

Using a method developed by Townsend-Huxley (1947), Lawson and Lucas (1965) reported on the measurement of the radial distribution of a stream of electrons drifting through a gas in a uniform electric field in the presence of ionization. The earlier work by Townsend in measuring this coefficient employed a technique of admitting an electron stream to the diffusion gap through a pinhole at the centre of the cathode and to measure the fraction F, of the current collected by an insulated disc at the centre of the anode. The relationship between F, and the diffusion coefficient was calculated from the steady state diffusion equation for electrons drifting in a uniform electric field.

The solution (Huxley and Crompton, 1955) is :-

$$1 - F = \frac{d}{R} \exp \left\{ - \lambda \, (R - d) \right\} \quad , \qquad (2.14)$$

where $\lambda = \frac{v}{2D}$,

d = gap separation,

v = electron drift velocity,

D_r = radial diffusion coefficient,

r = radius of disc,

$R = \sqrt{d^2 + r^2}$.

Lawson and Lucas (1965) showed the solution of the diffusion equation in the presence of ionization to be :-

$$1 - F = \frac{d}{R} \left\{ \exp - u(R - d) \right\} \quad , \qquad (2.15)$$

where $u^2 = \lambda^2 - 2 \alpha \lambda$.

Equation (2.15) shows that an experimental determination of F, will give a value of u, but to analyse the diffusion experiment to give values of D_r/μ (the ratio of radial diffusion coefficient to mobility for electrons) the coefficient λ , is required. When there is no ionization, $u = \lambda$ and equation (2.15) reduces to equation (2.14), the empirical solution obtained by other workers. When ionization is present $u \neq \lambda$, and to obtain values of λ , and hence D_r/μ from the diffusion experiment, it is necessary to measure the variation of current amplification, A(x), with electrode separation x, (Huxley, 1959 ; Lucas, 1964). In this case :-

$$\lambda - u = \frac{1}{d} \ell n \left\{ \frac{A(x+d)}{A(x)} \right\} \quad , \tag{2.16}$$

and $$D_r/\mu = \frac{E}{2\{u + (\lambda - u)\}} \quad , \tag{2.17}$$

where E = electric field strength.

To obtain equations (2.14) and (2.15) it has been necessary to consider electrode boundary conditions. The usual condition is to assume that the electron concentration is zero at the electrode surface. Equations (2.14) and (2.15) have only assumed the presence of an anode boundary condition and are often referred to as a 'pole' solution. In the presence of both an anode and cathode boundary condition, another solution is found, the 'dipole' solution. However, experimental results tend to fit the pole solution. A method developed by Virr et al (1972) employs a difference technique which eliminates the boundary conditions from the solution. In this method, $\overline{r^2}$, the mean radial position of the anode current is measured where :

$$\overline{r^2} = 4 D_r \bar{t} \quad ,$$

$$\text{or} \qquad \overline{r^2} = \frac{2}{u}(d - d_o) \quad , \tag{2.18}$$

where d_o = electrode effect.

Considering two gap separations (d) and (d + a)

$$\overline{r^2}_{d+a} - \overline{r^2}_{d} = \frac{2a}{u} \quad ,$$

$$\text{i.e.} \qquad u = \frac{2a}{\overline{r^2}_{d+a} - \overline{r^2}_{d}} \quad . \tag{2.19}$$

In this paper, Virr et al show that the influence of an electrode is to effectively reduce the gap separation by $\frac{1}{2}\lambda$ and since λ may be related to the mean swarm energy, $\bar{\epsilon}$, then :-

$$\frac{1}{\lambda d} = \frac{4}{3} \cdot \bar{\epsilon} \cdot \frac{1}{V} \quad , \tag{2.20}$$

where V = gap voltage .

Equation (2.20) implies that the influence of the electrodes is negligible provided that $V \gg \bar{\epsilon}$.

Whereas the Huxley-Crompton analysis applies only at low E/N where there is no ionization, the method of Kontoleon (1971) is valid at high E/N where ionization is present, and can also take into account secondary ionization processes by positive ions and photons. The radial distribution of anode current was measured by splitting the anode up into a central disc surrounded by nine concentric annuli. The total current was also measured as a function of gap separation. The solution to the steady state transport equation :-

ELECTRONS SWARMS IN GASES AND METAL VAPOURS

by

SAMI AMIN JALIL AL-AMIN

Thesis submitted in accordance with the requirements
of The University of Liverpool for the degree of
Doctor in Philosophy

JANUARY, 1984

$$-v \cdot \frac{\partial n}{\partial z} + D_L \frac{\partial^2 n}{\partial z^2} + D_r \left(\frac{\partial^2 n}{\partial x^2} + \frac{\partial^2 n}{\partial y^2} \right) + \alpha v n = 0 \quad , \qquad (2.21)$$

takes the form of a Bessel function of the form :-

$$n(z,r) = \sum_s A_s e^{g_s z} J_o (\theta_s r) \quad , \qquad (2.22)$$

where A_s = constant,

θ_s = R_s/b ,

R_s = Bessel roots,

b = wall radius.

However, α is not directly measureable but $\alpha_T (= \lambda - u)$ the Townsend ionization coefficient is easily measured and is a close approximation to α.

Therefore the Lucas method measures a parameter D_r / μ_{exp} such that :-

$$\frac{D_r}{\mu_{exp}} = \frac{\alpha_T E}{\theta_m^2} \quad ,$$

with

$$\frac{D_r}{\mu_{exp}} = \frac{2\lambda}{(\lambda + u)} \frac{D_r}{\mu}$$

This is to be compared with

$$\left(\frac{D_r}{\mu} \right)_d = \frac{\lambda}{u} \frac{D_r}{\mu} \quad .$$

Kontoleon expressed the experimental current distribution as a Bessel series :-

$$j(d,r) = \sum_s B_s J_o (\theta_s r) \quad . \qquad (2.23)$$

Comparing equations (2.22) and (2.23) :-

$$B_s = A_s e^{g_s z} \quad . \qquad (2.24)$$

By plotting logarithmic graphs, the slope gave values of g_s (using the Kruithof and Penning three point method to eliminate electrode effects, assuming a constant secondary ionization coefficient). Combining equations (2.21) and (2.22) gave :-

$$- vg_s + D_L g_s^2 - D_r \theta_s^2 + \alpha v = 0 \quad . \qquad (2.25)$$

Hence, by plotting g_s as a function of θ_s^2 , and determining the value of θ_s^2 which made g_s equal to zero, the value of D_r was found from equation (2.25) to be given as :

$$D_r = \frac{\alpha v}{\theta_m^2} \quad ,$$

where αv = rate of ionization.

Since $\alpha v = \alpha_T v_{exp}$, $\frac{D_r}{v_{exp}} = \frac{\alpha_T}{\theta_m^2}$

where α_T = the Townsend ionization coefficient.

v_{exp} = measured drift velocity.

The method has been used at high E/N where secondary ionization existed, assuming that the secondary ionization coefficient was constant. Electrode effects were removed by the difference technique, but the results for D_r are limited by the accuracy of the measurement of α_T .

The Kontoleon et al method uses analysis to separate the primary electrons from the secondary electrons. Kucukarpaci and Lucas (1979) have also achieved this by using a time of flight technique. They used an unscreened, segmented anode to collect the primary electron current. This current is made up of the steady state electron I_e (d, r) current and the space charge current I_{sc}(d, r), i.e.

$$I(d, r) = I_e(d, r) + I_{sc}(d, r) \qquad (2.26)$$

A Bessel series analysis is used, and this method directly measured $(D_r/\mu)_d$. When d_o effects are present, then the effective gap separation is $d - d_o$ so that (2.26) is replaced by :-

$$I(d - d_o, r) = I_e(d - d_o, r) + I_{sc}(d - d_o, r). \qquad (2.27)$$

(2.27) gives the current collected by a central anode disc of radius r when a pulse of electrons has been released from the cathode. It is important to realise that this current does not have the same magnitude as the steady state current received from a continuous source when expressed as a fraction of the total anode current. This is because it contains an extra term $\{ I_{sc}(d - d_o, r)\}$ created by the space charge fields of the ions . In order to use (2.27) to analyse experimental data it is necessary to operate with a pulse duration which is larger than the electron transit time but which is much smaller than the ion transit time. In the experimental investigation a pulse duration that is just greater than the electron transit time has been maintained. This short time duration reduces the formation of secondary electrons which are mainly formed by positive ion bombardment of the cathode surface.

Experimentally, the pulsed current collected by a central disc may be measured and analysed by (2.26) to give $(D_r/\mu)_d$ provided the Townsend ionization coefficient α_T is known and a reasonable estimation of D_r/D_L is available.

2.4.4 The Ionization and Attachment Coefficients, α and η

In 1936, Kruithof and Penning developed an apparatus to measure α using a d.c. technique. The apparatus consisted of a variable gap with an ultraviolet illuminated cathode as the electron source. Anode current was

measured as a function of gap separation. The Townsend equation for current amplification in the presence of primary and secondary ionization for a discharge chamber with large electrodes is given by :-

$$J(d,\alpha) = \frac{J_o \exp \{ \alpha_T (d - d_o) \}}{1 - \gamma \{ \exp \alpha_T (d - d_o) - 1 \}} \quad , \qquad (2.28)$$

where d = gap separation,

J_o = initial electron current ,

α_T = primary ionization coefficient (Townsend 's coefficient),

γ = secondary ionization coefficient.

The distance d_o is included to account for electrode effects and is the distance an electron must travel to reach an equilibrium energy characteristic of the operating E/N.

If equation (2.28) is re-arranged, since d is variable, d_o can be eliminated from the analysis to give :-

$$\frac{J_o}{J_d} = \frac{1 - \gamma (\exp \alpha_T d - 1)}{\exp \alpha_T d} \quad , \qquad (2.29)$$

and hence

$$\frac{J_o}{J_d} = (1 + \gamma) \exp (- \alpha_T d) - \gamma \quad . \qquad (2.30)$$

Now, the Kruithof and Penning three point method utilised the values of J_d at three gap separations such that :-

$$d_3 - d_2 = d_2 - d_1 = a \quad .$$

Substitution in equation (2.30) gives the expression :

$$\alpha = \frac{1}{a} \ell n \left\{ \frac{J_3(J_2 - J_1)}{J_1 (J_3 - J_2)} \right\} \quad . \qquad (2.31)$$

At low values of E/N, γ is very small or effectively zero, but becomes more important as E/N increases. The value of γ may be found by using the known value of α and either curve fitting to the J(d) versus d plot or by measuring the breakdown distance, d_B. At breakdown the denominator of (2.28) reduces to zero, such that :-

$$\gamma = \frac{1}{\exp \alpha_T (d_B - d_o) - 1} \quad . \qquad (2.32)$$

In 1953, Harrison and Geballe studied the anode current in the presence of ionization and attachment. Simultaneous measurements of the two coefficients were made using an apparatus which was basically the same as that of Kruithof and Penning (1936). The steady state solution for the total current collected was found to be :-

$$J(d) = J_o \left\{ \frac{\alpha}{\alpha - \eta} \exp (\alpha - \eta) d \right\} - \frac{J_o \eta}{\alpha - \eta} \quad , \qquad (2.33)$$

where η = the attachment coefficient.

This expression assumes that detachment is negligible and can be reduced to :-

$$J(d) = J_o \exp \{ (\alpha - \eta) d \} \quad . \qquad (2.34)$$

If η is very small and as η tends to zero, equation (2.34) reduces to the Townsend amplification equation.

The value of $(\alpha - \eta)$ is obtained from the experimental curve which represents the variation of the total current collected by the anode as a function of electrode separation using the relationship derived by Harrison and Geballe (1953) :-

$$\alpha - \eta = \frac{1}{a} \ell n \left\{ \frac{J_3 - J_2}{J_2 - J_1} \right\} , \qquad (2.35)$$

where J_1 , J_2 and J_3 are the total currents which correspond to gap settings d, (d + a) and (d + 2a). Individual values of α and η can be obtained by using the ($\alpha - \eta$) value and curve fitting to the J(d) versus d curve (Prasad and Craggs, 1961).

CHAPTER THREE

CHAPTER THREE

THE TIME OF FLIGHT EXPERIMENT

3.1 INTRODUCTION

The aim of this experiment is to determine the values of the electron drift velocity, the ratio of longitudinal diffusion coefficient to mobility and the ratio of radial diffusion coefficient to mobility by using a modified form of the time of flight method developed by Snelson and Lucas (1974), and Kucukarpaci and Lucas (1979). A narrow pulse of electrons is injected at the cathode and thereupon they drift and diffuse across a uniform electric field region to be collected at the anode. From the variation of anode current with time, one can deduce the drift velocity, longitudinal and radial diffusion coefficient. The experiment was originally developed by Snelson and Lucas (1974). However, the present system is a modified form of the u.h.v. system designed by Saelee, Lucas and Limbeek (1977). Using this method, the electron drift velocity and longitudinal and radial diffusion coefficient have been deduced in oxygen, methane and sulphur hexafluoride over a wide range of E/N.

3.2 EXPERIMENTAL APPARATUS OF DRIFT VELOCITY AND LONGITUDINAL DIFFUSION COEFFICIENT

3.2.1 The Vacuum Chamber

The apparatus is shown in the photograph and the schematic diagram of Fig. 3.1 has the following salient features :-

1. Thoriated iridium filament.
2. Electron injection grid.

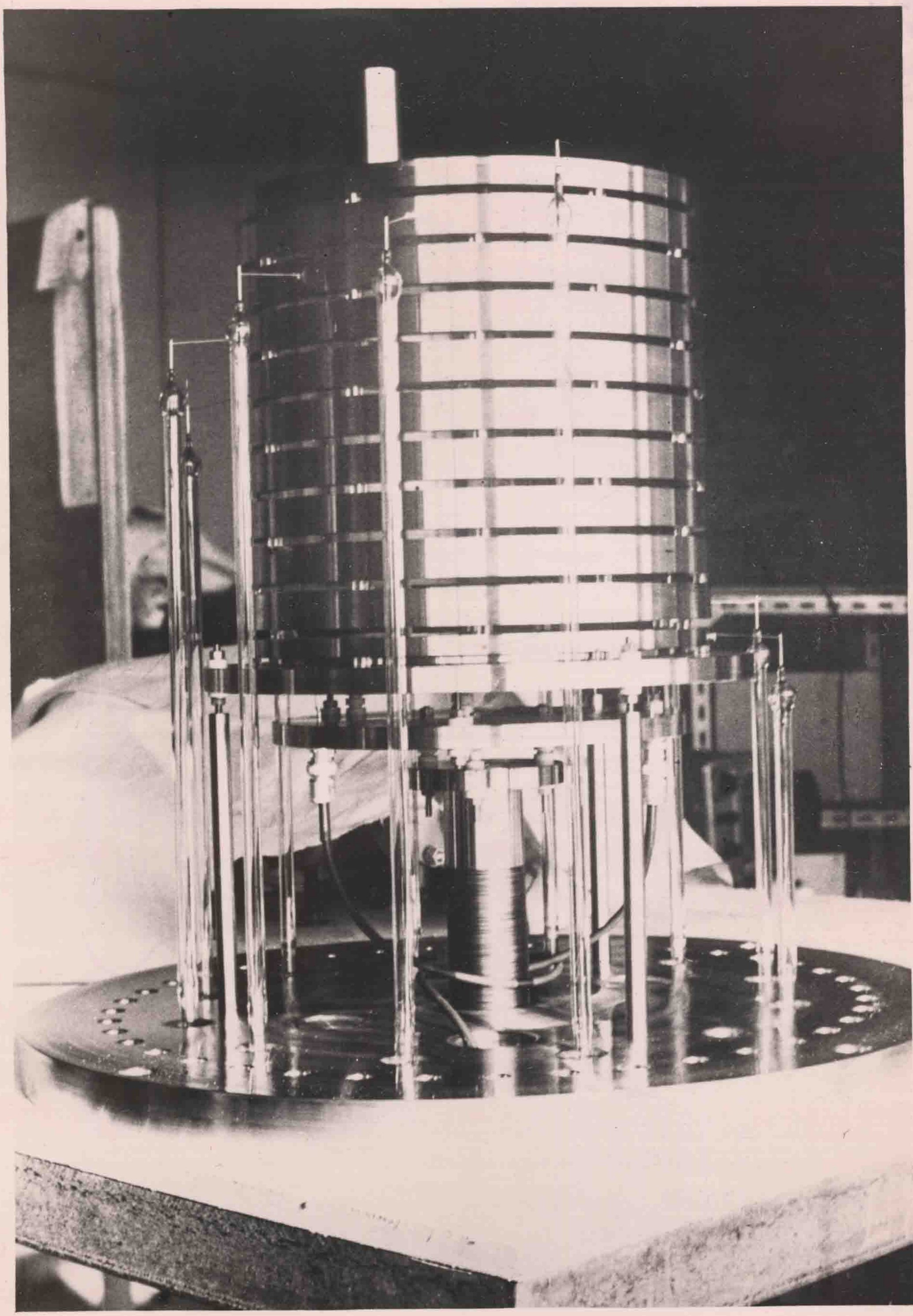

The TOF Chamber

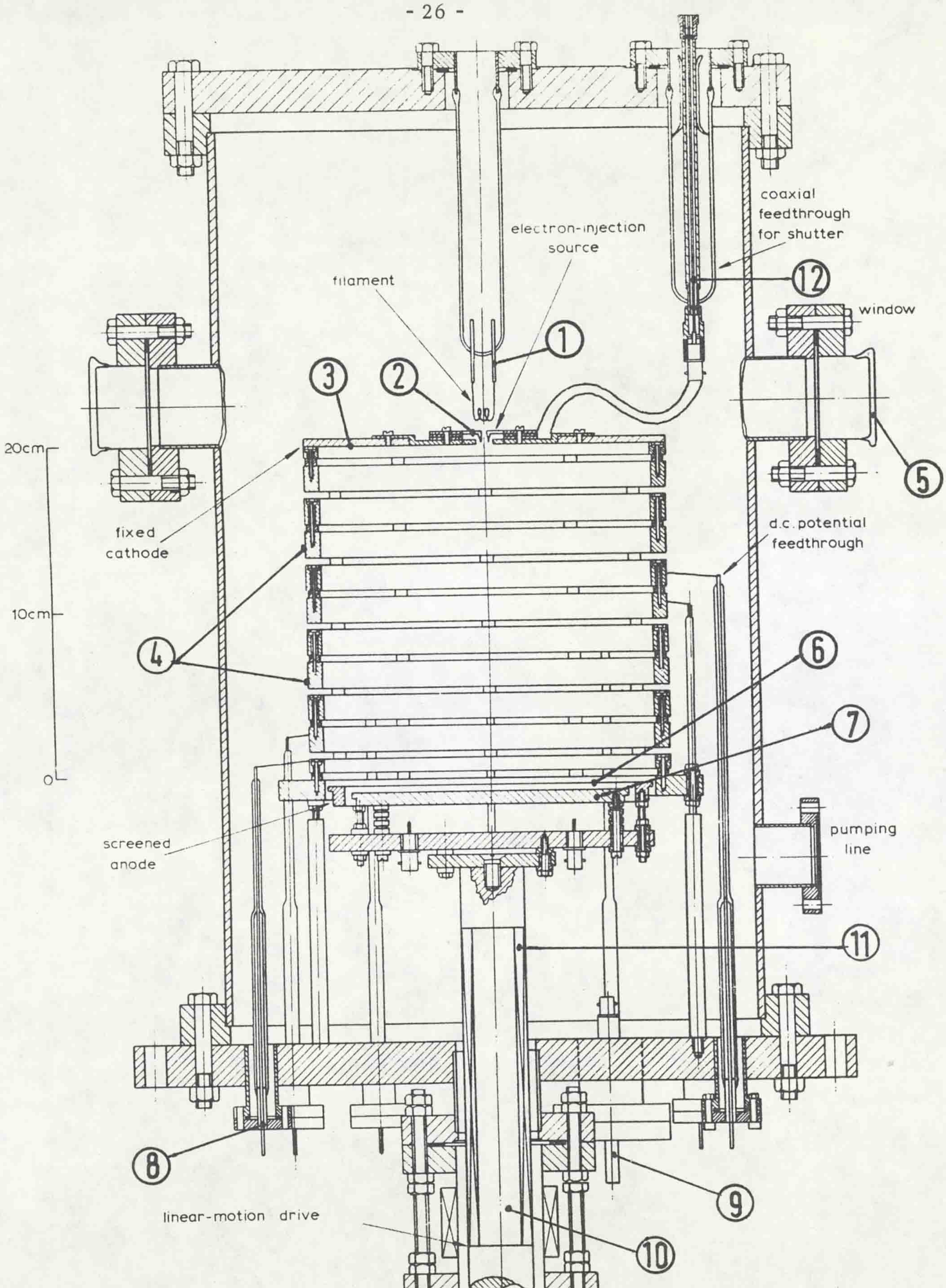

Fig.(3·1) VACUUM CHAMBER

ACKNOWLEDGEMENTS

The work described in this thesis was performed in the Department of Electrical Engineering and Electronics of the University of Liverpool. I wish to thank all brothers for the provision of their studentship, especially the MSS (I regret I am unable to mention your name). I am greatly indebted to Dr. J. Lucas for his continued interest and for giving me the opportunity to carry out the research. I have great pleasure in expressing my deep sense of gratitude and sincere thanks to him for supervising the project, for his expert guidance, kind advice, constant encouragement and most inspiring discussions during the course of the work and in the orientation as well as the comments on the draft for the preparation of this thesis. His considerable attention and care towards the individual research students will remain in my mind.

I should also like to thank Dr. A. Parker who read the manuscript and made many helpful comments - special regards to him. To my dear brother, Hassan Necdet Kücükarpaci, I extend special acknowledgement and appreciation to him for the help and assistance rendered in most stages of the experimental and theoretical work, which I hope I will never forget.

My thanks and acknowledgement are due to Mrs. Brenda Lussey for her patient work in the typing of this thesis and to Mrs. Sandra Collins for drafting the figures. I also extend my thanks for the assistance provided by the Technical Staff of the Mechanical, Electronics, Glass, Vacuum and Instrument Workshops and Members of the Stores and Design Office.

Deep thanks and special appreciation is extended to Mrs. Oliver C. Wilson who is my landlady, in fact it is impossible for me to say how much my ideas are owed to the help, care and advice given to me over a number of years, which I shall not forget. In addition, I would also like to take this opportunity

3. Fixed cathode.

4. Thick guard ring assembly, consisting of rings with an outer diameter (O.D.) 22 cm and an inner diameter (I.D.) of 19.7 cm, each being 1.6 cm thick and separated by glass spacers.

5. Observation window.

6. Anode screen with approximately 84% transmission.

7. Anode plate, 17.8 cm diameter.

8. Glass-metal feedthrough for electrical connections to guard rings.

9. Special design coaxial glass-metal feedthrough for electrical connection to the anode assembly.

10. Shaft driven by geared electric motor to move the anode assembly vertically.

11. Bellows, length variable over 20.4 cm.

12. Special design coaxial glass-metal feedthrough for input pulse signal to the injection grid.

The source of initial electrons is a heated thoriated iridium filament. The pulse of electrons is released into the main gap by the injection grid mounted in the centre of the fixed cathode. A uniform electric field with equipotential planes at 2 cm intervals is maintained by a thick guard ring structure. The anode consists of a highly polished stainless steel plate protected by a fine mesh screen. The screen is included to prevent induced charges collecting on the anode itself. The anode mesh screen is separated from the anode itself by a 2 mm gap, the resultant capacitance between screen and anode being 180 pF. The anode assembly is movable and can move within

the guard ring structure by means of a bellows and shaft which is driven by a geared electric motor. The gap separation is infinitely variable between 0 and 20 cm and may be measured accurately to within 0.01 cm by means of a dial gauge. The whole system is made of stainless steel and was electro-polished prior to assembly.

The chamber is evacuated by a trapped oil diffusion pump backed by a rotary pump, as shown in Fig. 3.2. Knife edge seals with copper gaskets and u.h.v. taps are used throughout. The top and base flanges of the chamber are flat flanges with soft lead gaskets. Background pressures of the order of 10^{-7} torr may be obtained without baking, with a leak rate of less than 2.5×10^{-5} torr/hour. Gas pressures are measured by a M.K.S. Baratron pressure transducer, with the reference side of the transducer continuously pumped by an oil diffusion pump. The Baratron pressure transducer having four pressure ranges of 100, 10, 1 and 0.1 torr full scale deflection (f s d). The accuracy was ($\pm$ 3% f s d) on all ranges. The Baratron gauge was checked against McLeod gauge and was in fact shown to be accurate to $\pm$ 1%, (see Appendix D and Table A).

Evacuation pressures are measured by an ionization gauge. Filling gas is introduced via leak valve V_3 and u.h.v. tap V_1, which may be used to isolate the system in an emergency. The gas handling line is normally kept evacuated by rotary pump until a new change of gas is required, u.h.v. tap V_2 isolates the vacuum chamber and pressure gauges from the pumping system.

3.2.2 The Electrical System

A schematic diagram of the electrical system is shown in Fig. 3.3.

A high signal gain is required so the importance of reducing pick-up and

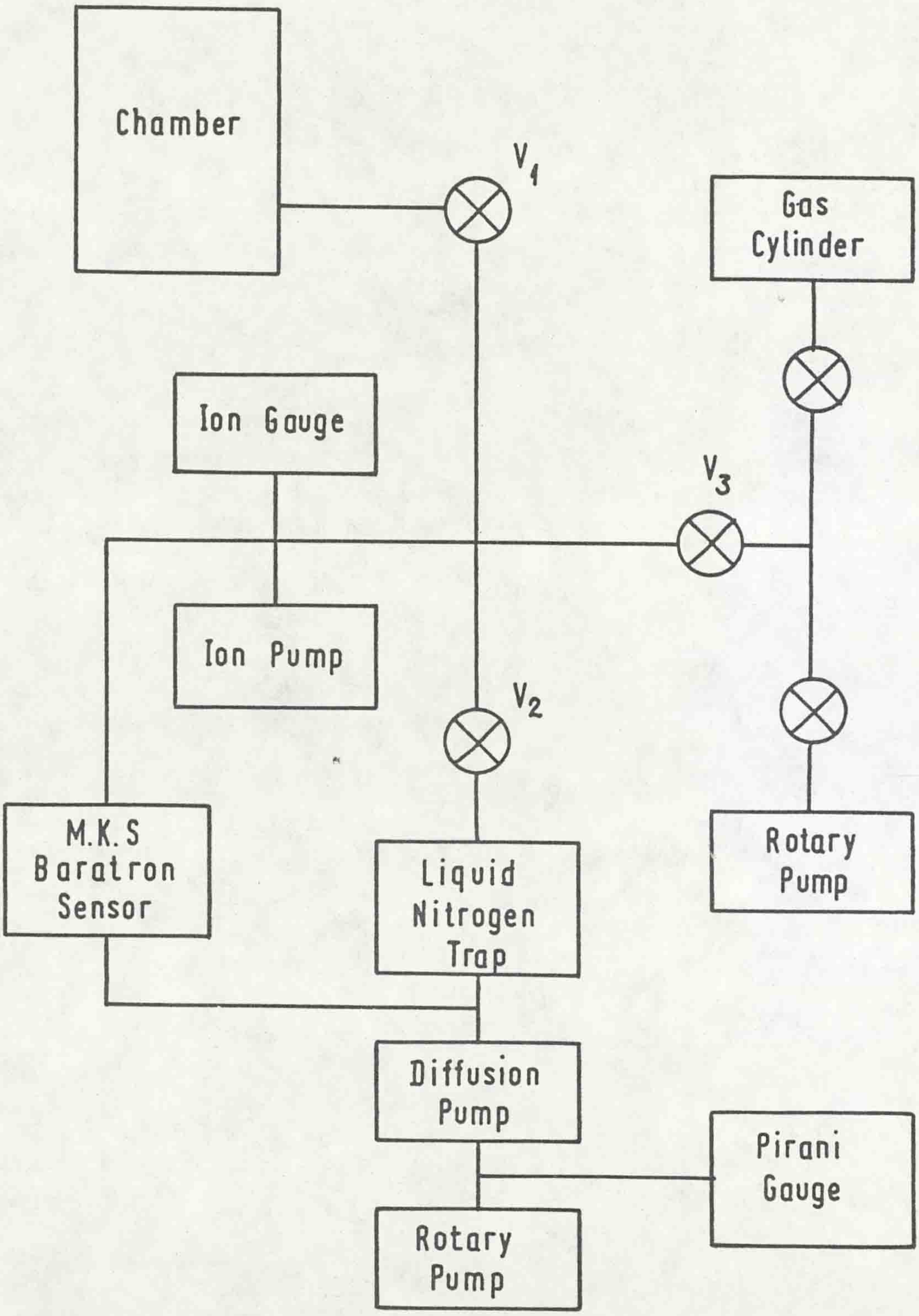

V_1 and V_2 U.H.V. Taps

V_3 Leak Valve

Fig.(3.2) VACUUM SYSTEM

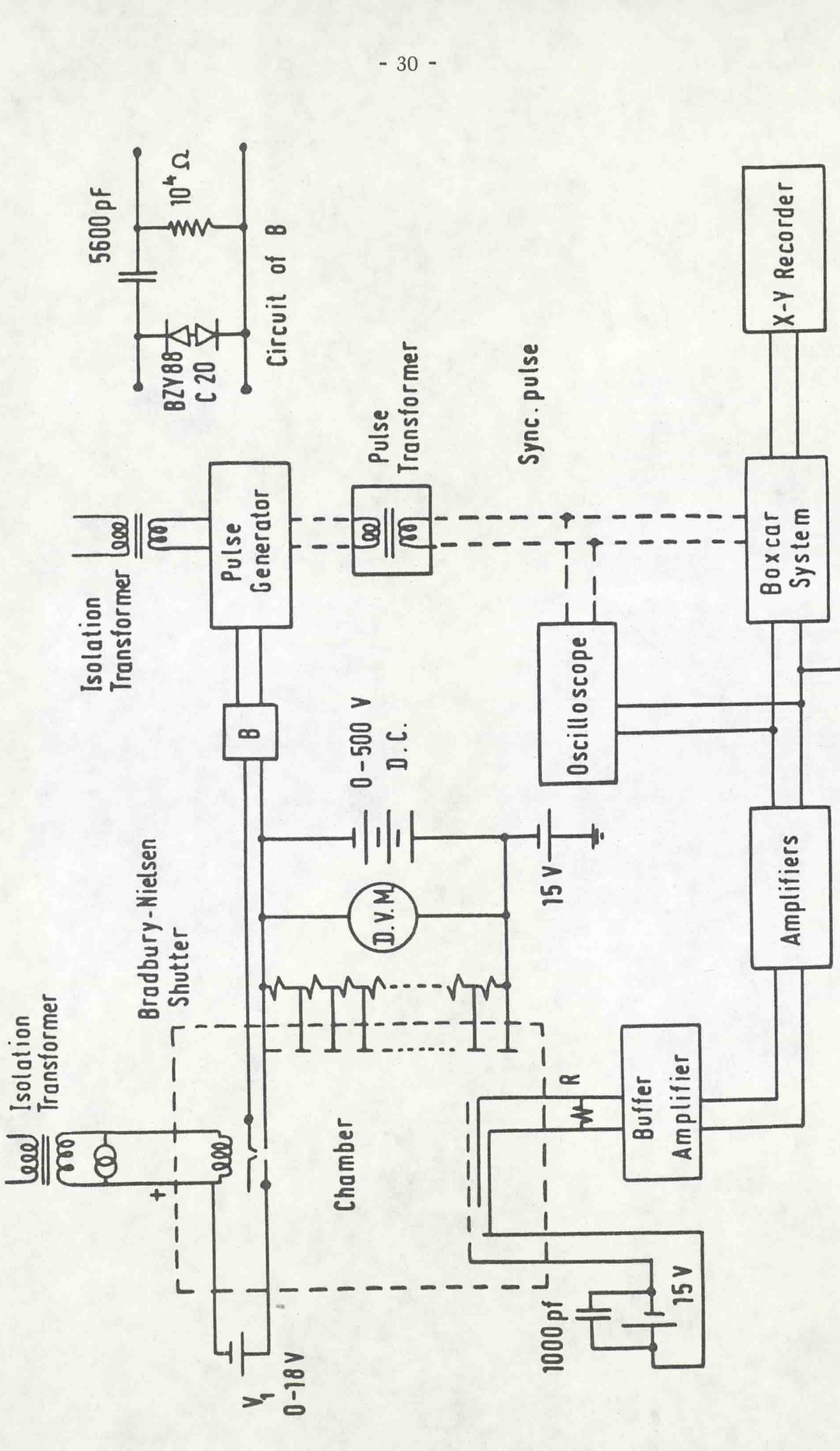

Fig.(3.3) ELECTRICAL SYSTEM

earth loops cannot be over-emphasised. Therefore, all cables are shielded and all terminations are matched to 50 Ω. The pulse generator and D.C. filament supply are floated by means of isolation transformers so that they may be operated at negative D.C. potential. In this way the anode is kept effectively at earth potential and negative voltage is applied to the cathode. The pulse generator opens the injection grid with a positive pulse with pulse width between 50 and 200 nsec, depending on the operating E/N. Optimum voltage conditions are obtained by adjusting the filament-cathode acceleration voltage. Circuit B protects the pulse generator from the filament current by using protective diodes. The filament supply is operated in a constant current mode.

The screen of the anode is kept at a potential of 15 volts negative with respect to earth. This sweep field ensures that all electrons will pass through the screen to the anode plate, thus eliminating the danger of induced charges being recorded. The anode current collected is passed through the resistor R(= 50 to 500 Ω, depending upon operating conditions) and the resultant voltage signal is amplified. The value of the resistor is chosen to keep the time constant of the anode circuit to a minimum, but still giving sufficient voltage signal. Potentials for the guard rings are tapped off a resistor chain consisting of 250 KΩ, 1 watt, 0.5 % high stability resistors.

The voltage signal developed across R is fed into the impedance converter which has an input impedance of 10 MΩ and an output impedance of 50 Ω, Fig. 3.4 . It is then amplified by two cascaded amplifiers (total gain $\leq$ 60 dB) before being processed by the 'box-car' detector system. The box-car consists of a scan delay generator and a high speed linear gate, it can extract

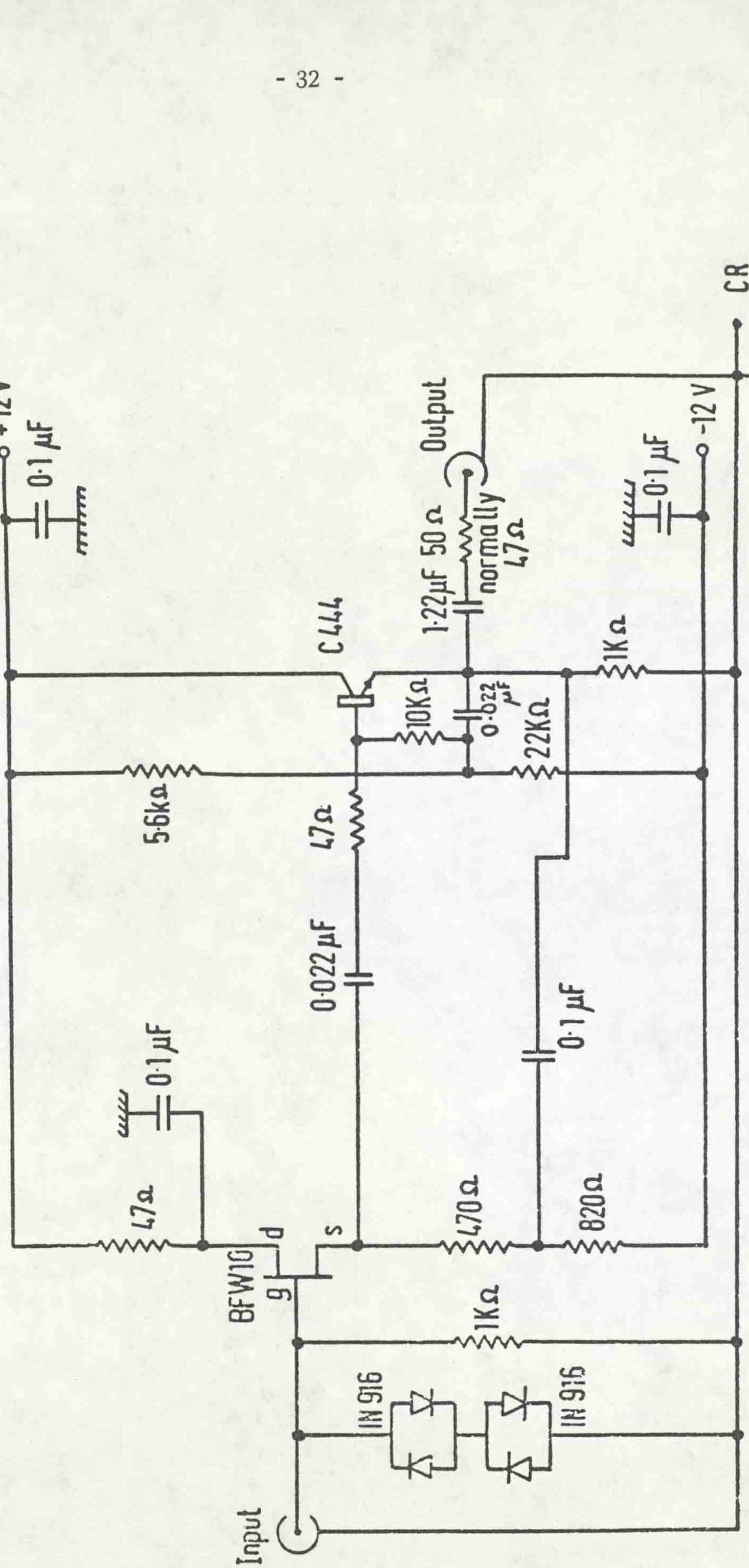

Fig.(3·4) IMPEDANCE CONVERTER

the voltage signal from a large noise signal and also allows the signal to be read out on a slow time scale. The signal is recorded on an X-Y chart recorder.

In an operating region of high E/N, ionization creates gas amplification, so a lower amplifier gain may be used. In this case the impedance converter is bypassed and R is 50 Ω, the input impedance of the amplifier. This gives the shortest possible rise time of the anode circuit ($\simeq$ 10 nsec) for the present apparatus. A specification of the manufacturer's equipment used in time of flight (TOF) experiment is given in Appendix D.

3.3. EXPERIMENTAL APPARATUS OF RADIAL DIFFUSION COEFFICIENT

The u.h.v. apparatus of Saelee et al (1977) for measuring TOF electron drift velocities and the longitudinal diffusion coefficient has been adapted to measure the radial diffusion coefficient (Kucukarpaci and Lucas, 1979). Only the anode has been modified. It is no longer screened and has been split into three parts, an inner disc of radius 4 cm, an annulus of O.D. 16.6 cm and a screening annulus of O.D. 19.6 cm, as shown in Fig. 3.5.

The electrical measuring system was also redesigned to give improved accuracy over the method of Kucukarpaci and Lucas. The circuit is shown in Fig. 3.6 and uses annul output technique. The two currents, i_1 and i_2 whose values are to be measured are fed via resistors R_1 and R_2 to channels A and B of an ortec-Brooken 9454 differential ac amplifier (having 2 MHz band width and up to 60 dB gain), R_1 is a fixed resistance 510 Ω, whilst R_2 is a potentiometer (0 - 2 KΩ) resistance, the input voltage V_A and V_B are arranged to be equal by varying R_2 such that the following condition is achieved :

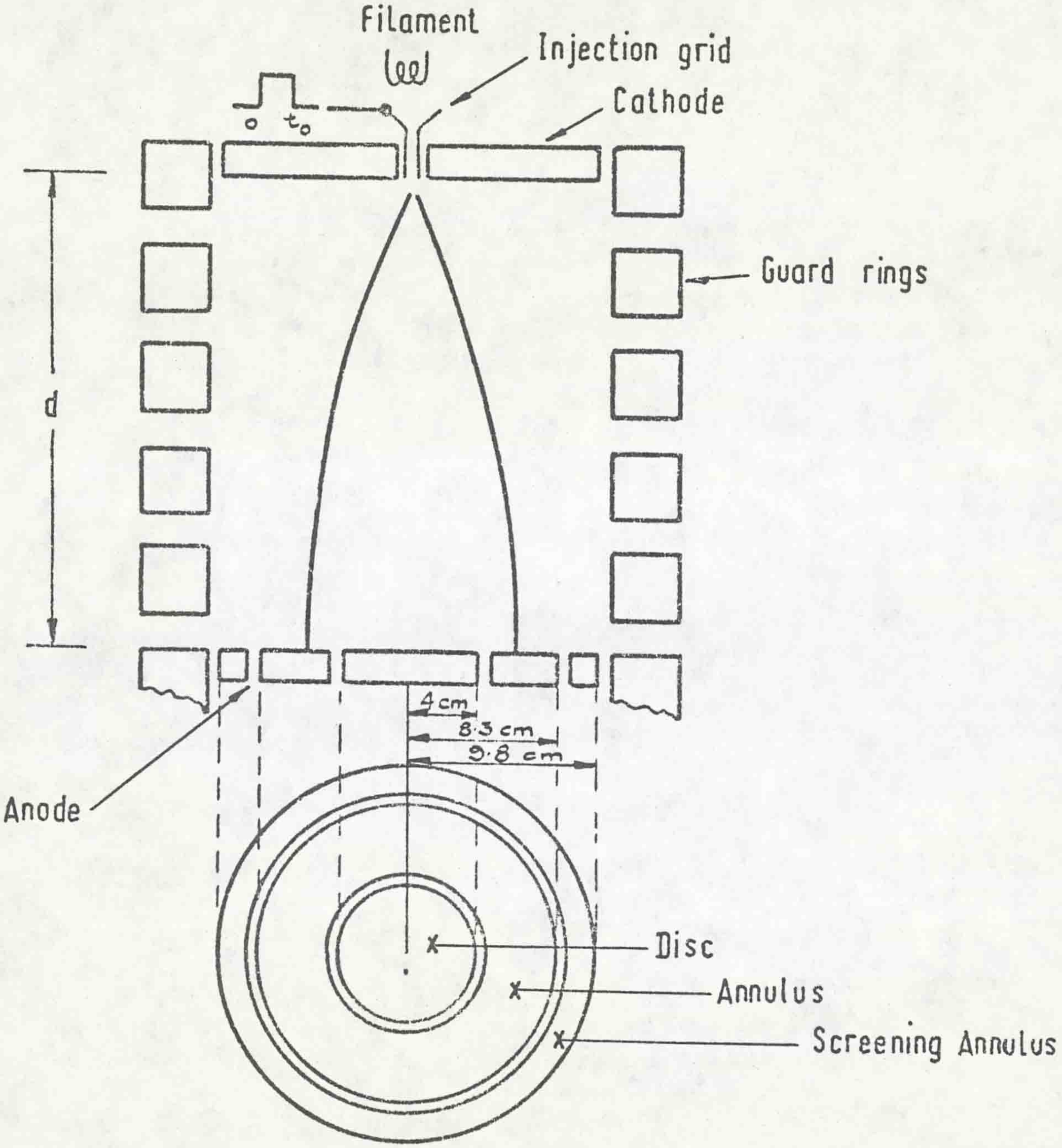

Fig.(3·5) THE TOF APPARATUS MODIFIED FOR MEASUREMENT OF RADIAL DIFFUSION

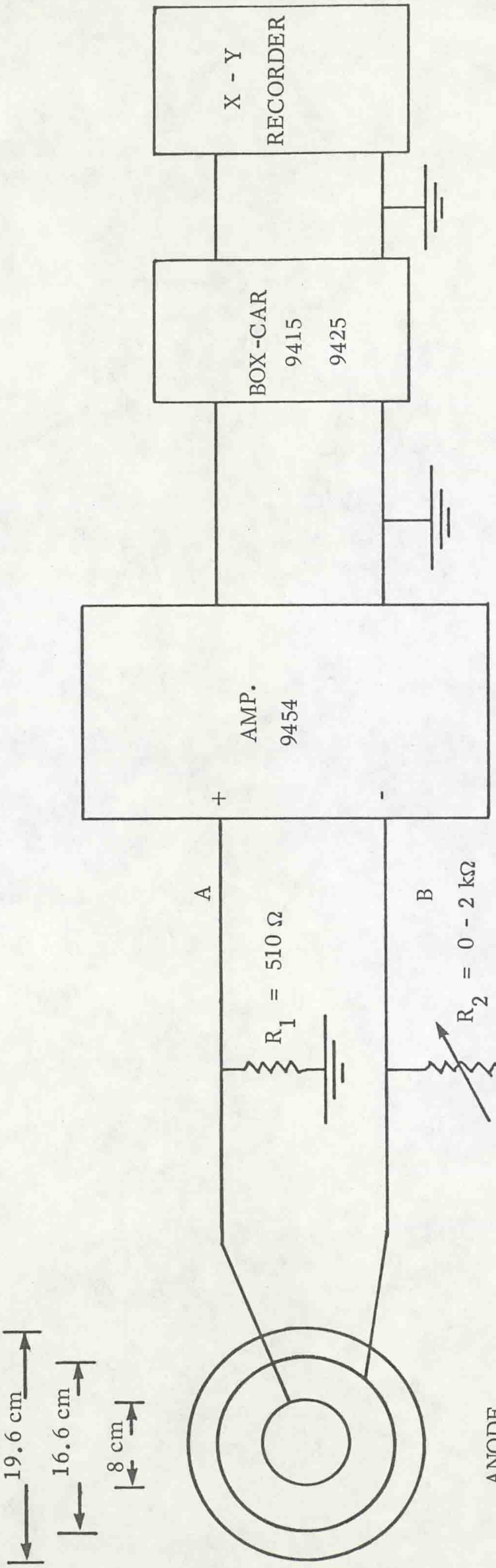

Fig. (3.6) THE ELECTRICAL RECORDING SYSTEM

$$V_A = V_B$$

$$i_1 R_1 = i_2 R_2$$

$$\text{current ratio} = \frac{i_1}{i_1 + i_2} = \frac{1}{1 + R_1/R_2} \quad .$$

The balanced output voltage is signal averaged by using an Ortec-Brookden Box car integrator (9425 and 9415) in order to remove random noise and the output is displayed on an X-Y recorder.

The electron source was a heated thoriated iridium filament, the electrons were injected into the gap through a central hole in the cathode for a short time duration between 0.4 and 5 μs. The pulse duration was arranged to be of the order of the electron transit time between the cathode and anode.

to express my indebtedness and gratitude to those who helped and guided me through the different stages in my education, especially from the following :-

I am also indebted to my late Father - may Allah (God) forgive him and bless his soul (Amin) - Who was very kind and gentle with me and who encouraged me to proceed to higher studies. Extra thanks and special appreciation are due to my Mother who decided to remain living with my brothers and sisters in order to offer a better future for her son by allowing him to study abroad even though this meant her making many sacrifices. Credit must go to my Brothers, Jalil, Raad and Makky and to my two Sisters, Hanna and Jennan, since without their encouragement, assistance, patience and much understanding, this study could not have been seen in its present form - special regards, with my warm compliments to them.

May Allah guide us to remain in his way and to forgive and bless all of us for he is the Merciful and most Beneficent.

3.4 EXPERIMENTAL RESULTS IN OXYGEN

A time of flight technique (TOF) has been used to measure the drift velocity, v_d, the ratio of longitudinal diffusion coefficient to mobility $(D_L/\mu)_d$, and the ratio of radial diffusion coefficient to mobility $(D_r/\mu)_d$ in oxygen. Results have been made and tabulated in Table 3.1 and Table 3.2 respectively. The experimental range is between $25.4 \leq E/N \leq 848$ Td for v_d and $(D_L/\mu)_d$, while for $(D_r/\mu)_d$, the experimental range is between $14.1 \leq E/N \leq 5650$ Td. The oxygen gas was supplied by BOC Ltd. and had a purity of 99.5% minimum with impurities $CO_2 < 5$ v.p.m., $H_2 \simeq 50$ v.p.m. and Ar $< 0.5\%$. Fig. 3.7 shows the variation of v_d with E/N. The maximum drift velocity measured is 76.5×10^6 cm/sec and this is close to the limitation of the TOF apparatus. The results of $(D_L/\mu)_d$ against E/N are illustrated in Fig. 3.8. The value of $(D_L/\mu)_d$ is between 1.50 to 13.1 V and the maximum value of $(D_L/\mu)_d$ is much less than the maximum gap voltage set just before breakdown occurs in the system. Values of $(D_r/\mu)_d$ as a function of E/N are shown in Fig. 3.9 This figure shows that the values of $(D_r/\mu)_d$ increase with the increasing of E/N up to ($\leq$ 1695 Td) at which it reaches a peak value of 16.5 V. The comparison of the experimental results with the theoretical results and other available data will be described in Chapter Four.

TABLE 3.1 : EXPERIMENTAL RESULTS IN OXYGEN

E / P_o V/cm, torr	E / N Td	v_d $\times 10^7$ cm/s	$(D_L / \mu)_d$ V
9	25.4	0.58	1.50
15	42.4	1.02	1.95
25	70.6	1.30	2.18
35	98.9	1.69	2.95
50	141	2.03	4.03
70	198	2.70	4.11
100	283	3.11	5.18
140	396	4.21	6.60
200	565	4.99	9.59
250	706	6.00	11.0
300	848	7.65	13.1

TABLE 3.2 : RADIAL DIFFUSION COEFFICIENT RESULTS IN OXYGEN

E / P_o V /cm, torr	E / N Td	$(D_r / \mu)_d$ V
5	14.1	1.01
10	28.3	2.18
30	84.8	3.26
50	141	4.04
70	198	4.70
100	283	6.11
200	565	7.33
300	848	10.8
350	989	11.3
500	1413	13.5
600	1695	16.5
700	1978	15.5
800	2260	15.2
900	2543	15.0
1000	2825	14.7
1500	4238	12.0
2000	5650	11.0

O_2

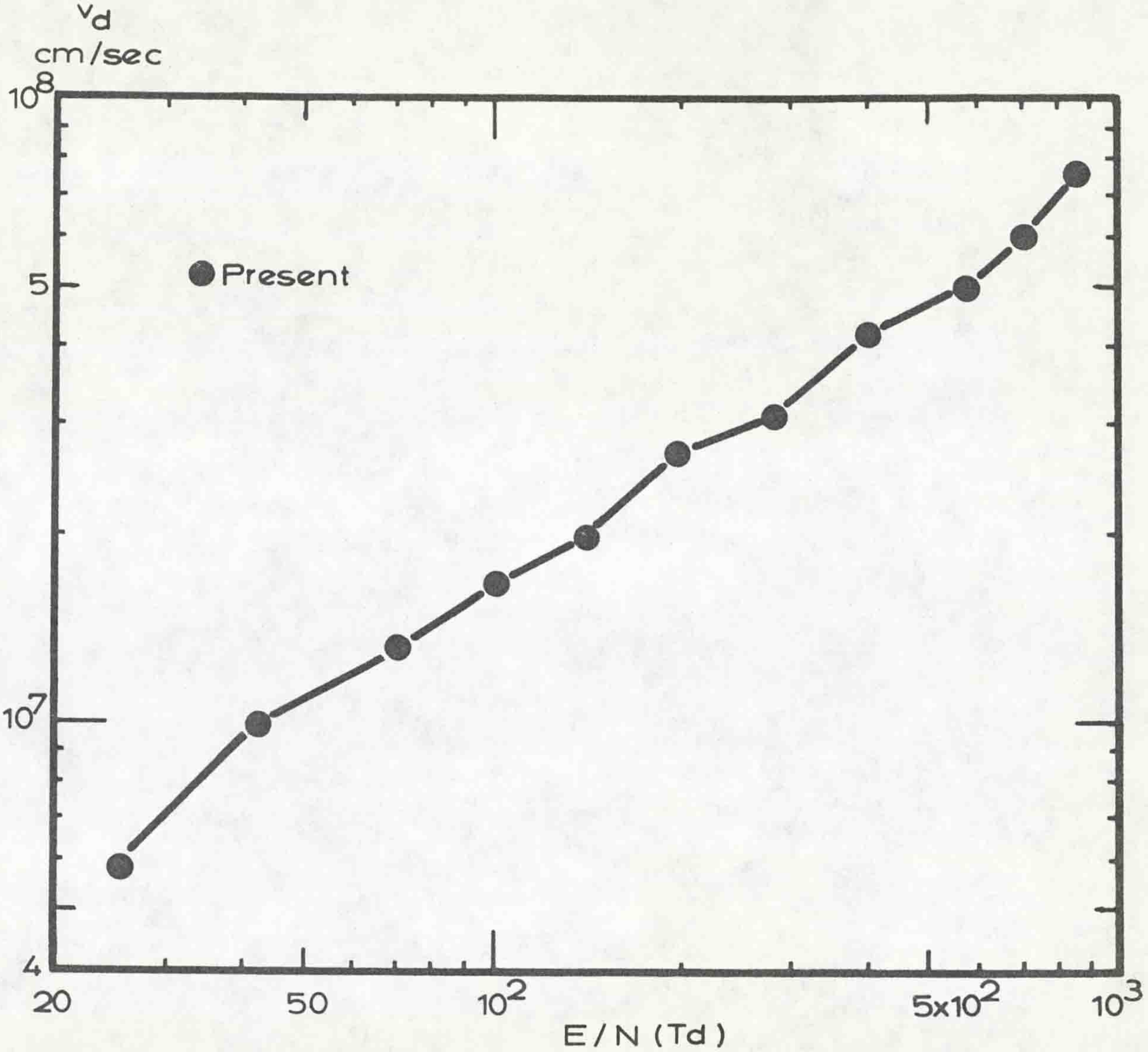

Fig.(3.7) Drift velocity in Oxygen.

O_2

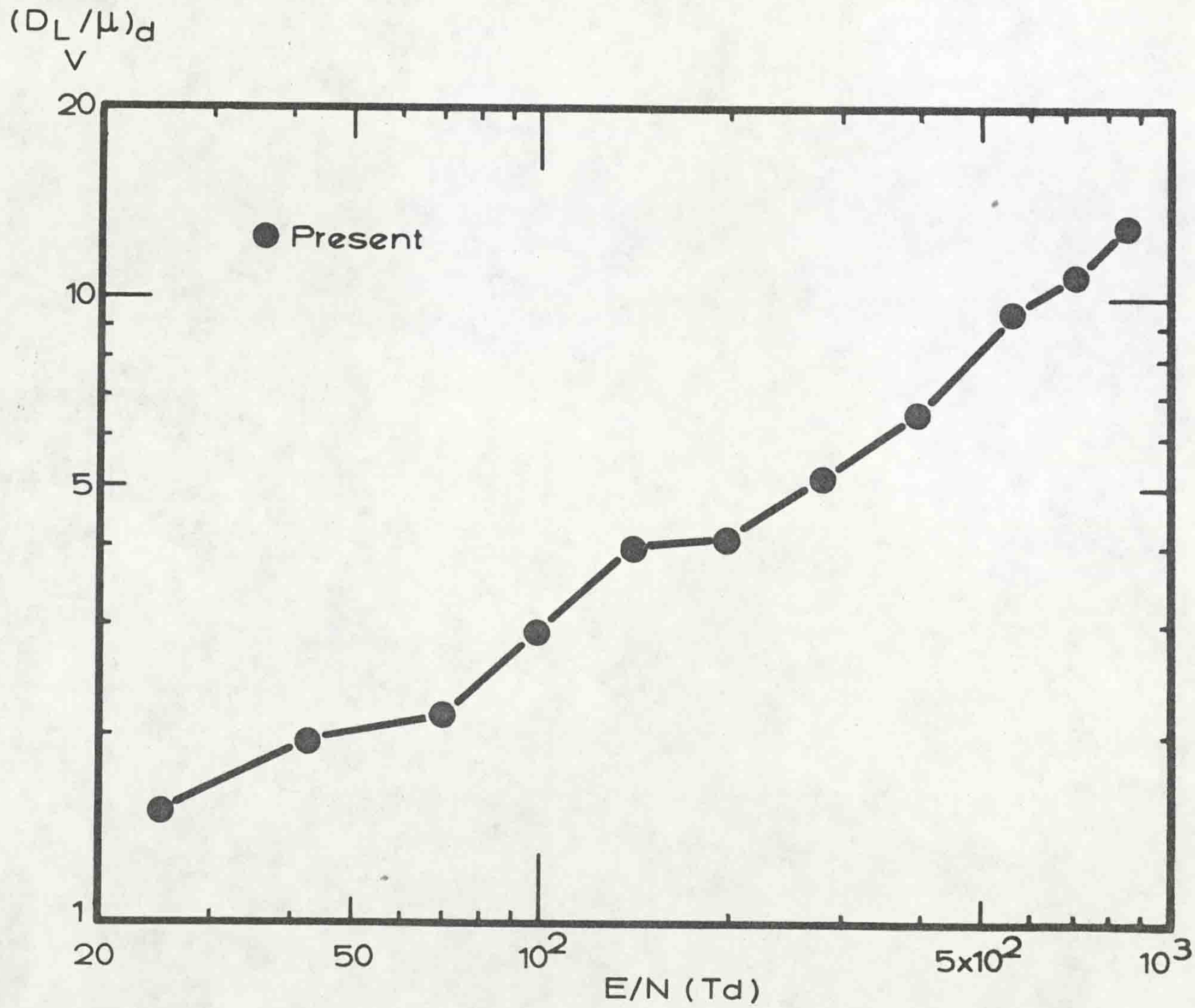

Fig.(3-8) Ratio of Longitudinal Diffusion Coefficient to Mobility in Oxygen.

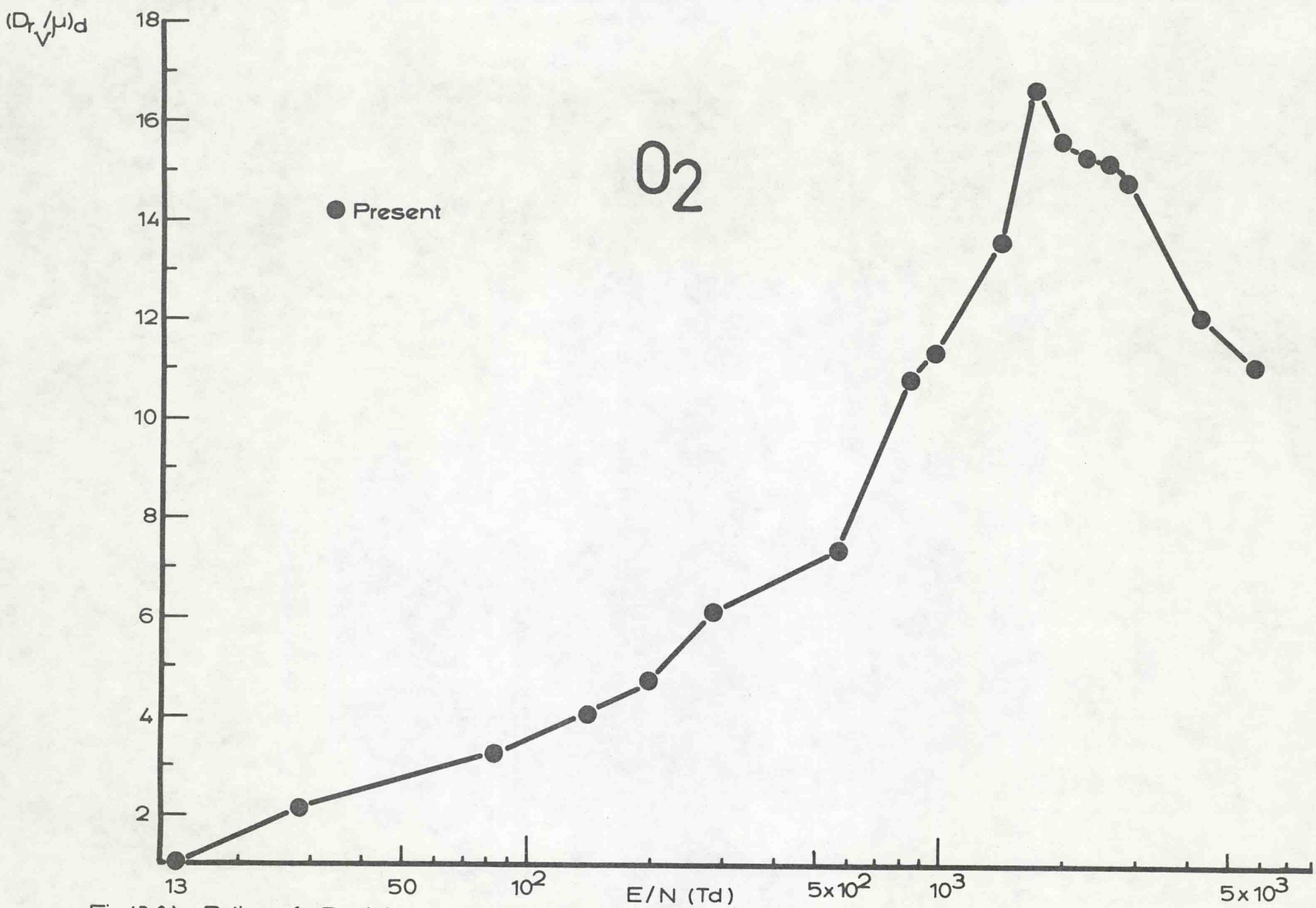

Fig(3.9) Ratio of Radial Diffusion Coefficient to Mobility in Oxygen.

3.5 EXPERIMENTAL RESULTS IN METHANE

A pulse technique has been developed for the measurement of swarm electron parameters at high E/N. These parameters, namely drift velocity v_d, ratio of both longitudinal and radial diffusion coefficient to mobility $(D_L/\mu)_d$ and $(D_r/\mu)_d$ respectively have been measured in methane. The methane gas purity was 99.2% with 0.7% for N_2, 2 v.p.m. for O_2 and 1 v.p.m. for CO_2. The gas was supplied by BOC Ltd. Over the range of $0.28 \leq E/N \leq 848$ Td, results for v_d and $(D_L/\mu)_d$ have been obtained and the experimental values of these two parameters are tabulated together in Table 3.3 and illustrated in Fig. 3.10. This figure shows that the drift velocity varies from 0.86 to 58.2×10^6 cm/sec. The curve of v_d has a peak ($\simeq 10.2 \times 10^6$ cm/sec) at E/N = 4.24 Td, then there is a rapid fall in value of v_d to 6×10^6 cm/sec occurring at E/N $\simeq$ 56.5 Td. As the range of E/N is increased, the value of v_d increases until it reaches a maximum value of 58.2×10^6 cm/sec at E/N = 848 Td. This figure also shows that the experimental values of $(D_L/\mu)_d$ are changing from 0.20 to 8.58 V for the range of $14.1 \leq E/N \leq 848$ Td. The curve of $(D_L/\mu)_d$ has also small peak ($\simeq$ 3.52 V) at E/N $\simeq$ 169 Td. The values of $(D_r/\mu)_d$ for the range of E/N varying between $84.8 \leq E/N \leq 5650$ Td have also been made experimentally and these are tabulated in Table 3.4 and shown in Fig. 3.11 as a function of E/N. The maximum value of $(D_r/\mu)_d$ is 12.6 V and corresponds to E/N = 2825 Td. The present results in methane, together with other available data, will be discussed in Chapter Four.

TABLE 3.3 : EXPERIMENTAL RESULTS IN METHANE

E/P_o V/cm, torr	E/N Td	v_d $x10^6$ cm/s	$(D_L/\mu)_d$ V
0.1	0.28	0.86	
0.2	0.56	2.24	
0.3	0.85	3.76	
0.5	1.41	6.80	
0.7	1.98	8.27	
1.0	2.83	9.82	
1.5	4.24	10.2	
2.0	5.65	9.75	
3.0	8.48	8.31	
5.0	14.1	7.11	0.20
10	28.3	6.03	0.38
20	56.5	6.00	0.72
40	113	8.63	2.77
50	141	10.9	3.31
60	169	12.6	3.52
80	226	16.4	2.80
100	283	19.6	3.20
150	424	29.6	4.67
200	565	38.1	5.70
250	706	48.0	6.68
300	848	58.2	8.58

TABLE 3.4 : RADIAL DIFFUSION COEFFICIENT RESULTS IN METHANE

E / P_o V/cm, torr	E / N Td	$(D_r / \mu)_d$ V
30	84.8	4.64
40	113	5.28
50	141	4.29
70	198	4.40
100	283	4.41
150	424	4.57
200	565	5.36
300	848	5.50
400	1130	7.64
500	1413	7.86
700	1978	10.4
1000	2825	12.6
1500	4238	11.2
2000	5650	10.6

CH_4

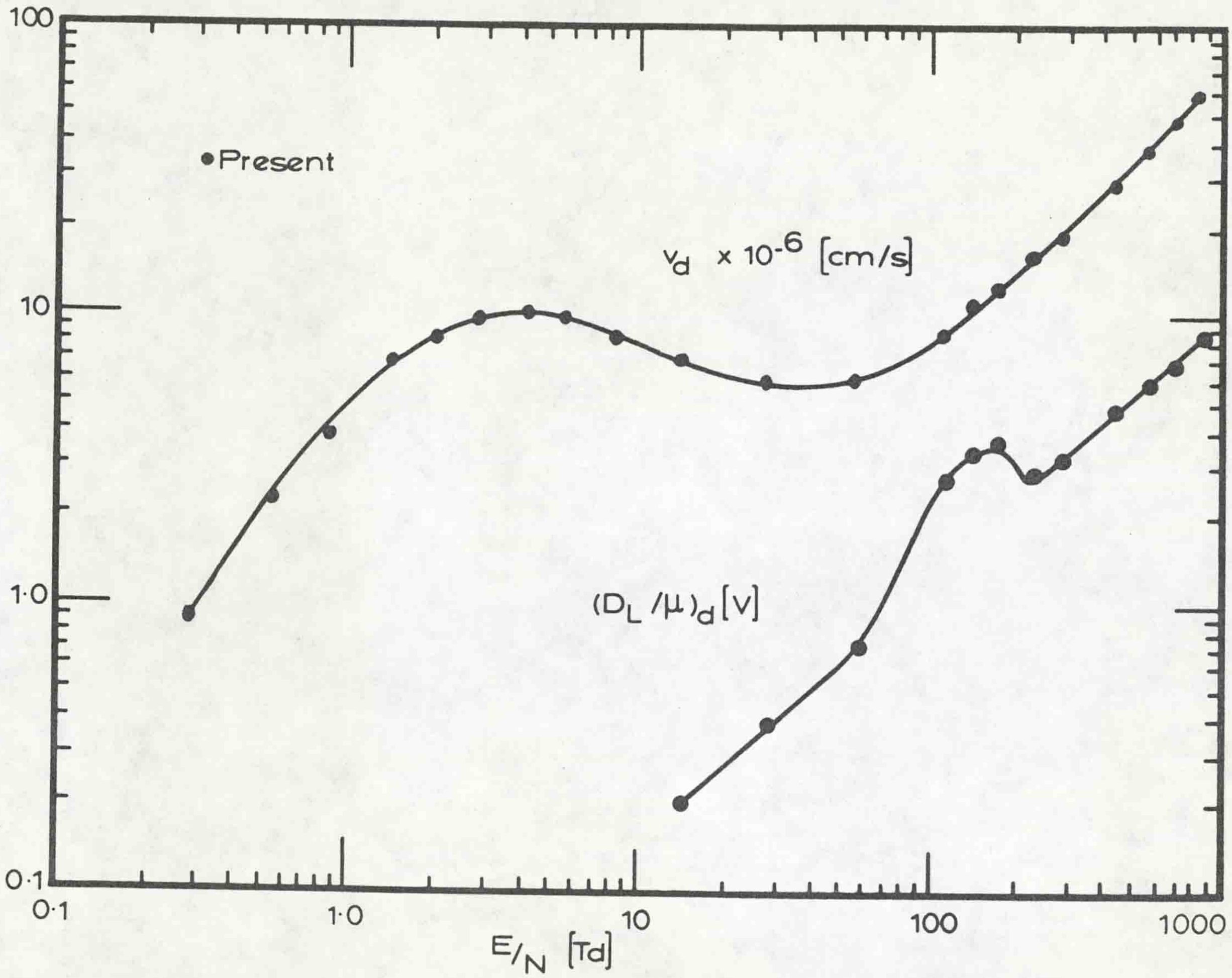

Fig.(3.10) Drift Velocity and Ratio of Longitudnal Diffusion Coefficient to Mobility in Methane

ABSTRACT

A time of flight (TOF) technique has been used to measure the drift velocity, v_d, the ratio of longitudinal diffusion coefficient to mobility $(D_L/\mu)_d$, and the ratio of radial diffusion coefficient to mobility $(D_r/\mu)_d$, over a wide range of E/N (where E/N is the ratio of the electric field to gas number density). Time of flight measurements of the electron drift velocity and the ratio of longitudinal diffusion coefficient to mobility have been made for the first time in oxygen and methane for the region of E/N from 0.28 to 848 Td (1 Td = 10^{-17} V cm^2). TOF technique has also been applied for the first time to measure the ratio of radial diffusion coefficient to mobility in oxygen, methane and sulphur hexafluoride for a wide range of E/N from 13 to 5650 Td. The present results in oxygen, methane and sulphur hexafluoride have been compared with experimental values obtained by a dc technique and they show good agreement with the results of Naidu and Prasad (1970), Kontoleon (1971) and Lakshminarasimha (1977) for E/N varying from 28 to 5650 Td.

The Monte Carlo technique has been used to simulate three-dimensional motion of electron swarms in gases. This investigation has given more insight into the validity of the swarm parameters and has resulted in giving a set of cross-sections which is compatible to the measured swarm parameters. Electron swarm motion in oxygen and methane has been simulated in the region of E/N varying from 14 to 5650 Td. The swarm parameters calculated from the simulation are also compared with existing experimental values. By adjusting the cross-sections, a close fit between the swarm parameters has been obtained.

For the first time theoretical results have been calculated for the electron swarm parameters by using the Boltzmann equation in a mixture of argon gas

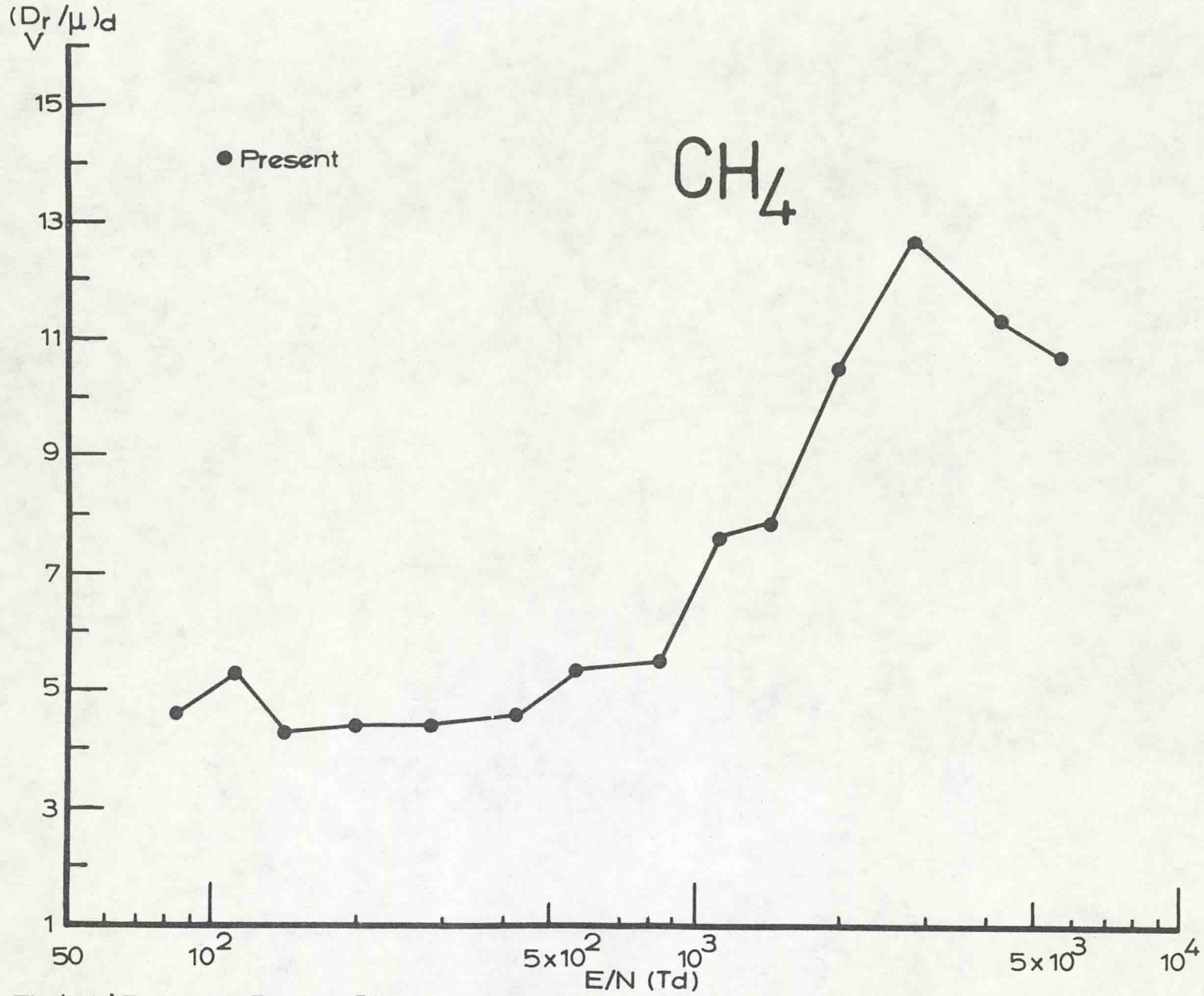

Fig.(3.11) Ratio of Radial Diffusion Coefficient to Mobility in Methane.

3.6 EXPERIMENTAL RESULTS IN SULPHUR HEXAFLUORIDE

A measurement of the ratio of radial diffusion coefficient to mobility $(D_r/\mu)_d$ has been made in sulphur hexafluoride. The gas purity was 99.9% with air + non-condensables < 900 ppm, water < 15 ppm. The gas was also supplied by BOC Ltd. Current ratios have been recorded between 848 $\leq$ E/N $\leq$ 5650 Td for gap voltages variable from 100 V up to just below breakdown voltage. The experimental results for $(D_r/\mu)_d$ are summarised in Table 3.5, the values of the ratio, $(D_r/\mu)_d$ against E/N is illustrated in Fig. 3.12 . For comparison experimental values of Naidu and Prasad (1972) are also plotted over the experimental range of 340 $\leq$ E/N $\leq$ 600 Td. The value of $(D_r/\mu)_d$ varies with increasing value of E/N until it reaches a maximum value of 18.2 V at E/N $\simeq$ 4238 Td.

TABLE 3.5 : RADIAL DIFFUSION COEFFICIENT RESULTS IN SULPHUR HEXAFLUORIDE

E / P_o V / cm, torr	E / N Td	$(D_r / \mu)_d$ V
300	848	6.75
400	1130	7.38
500	1413	9.33
600	1695	10.3
700	1978	12.9
1500	4238	18.2
2000	5650	14.1

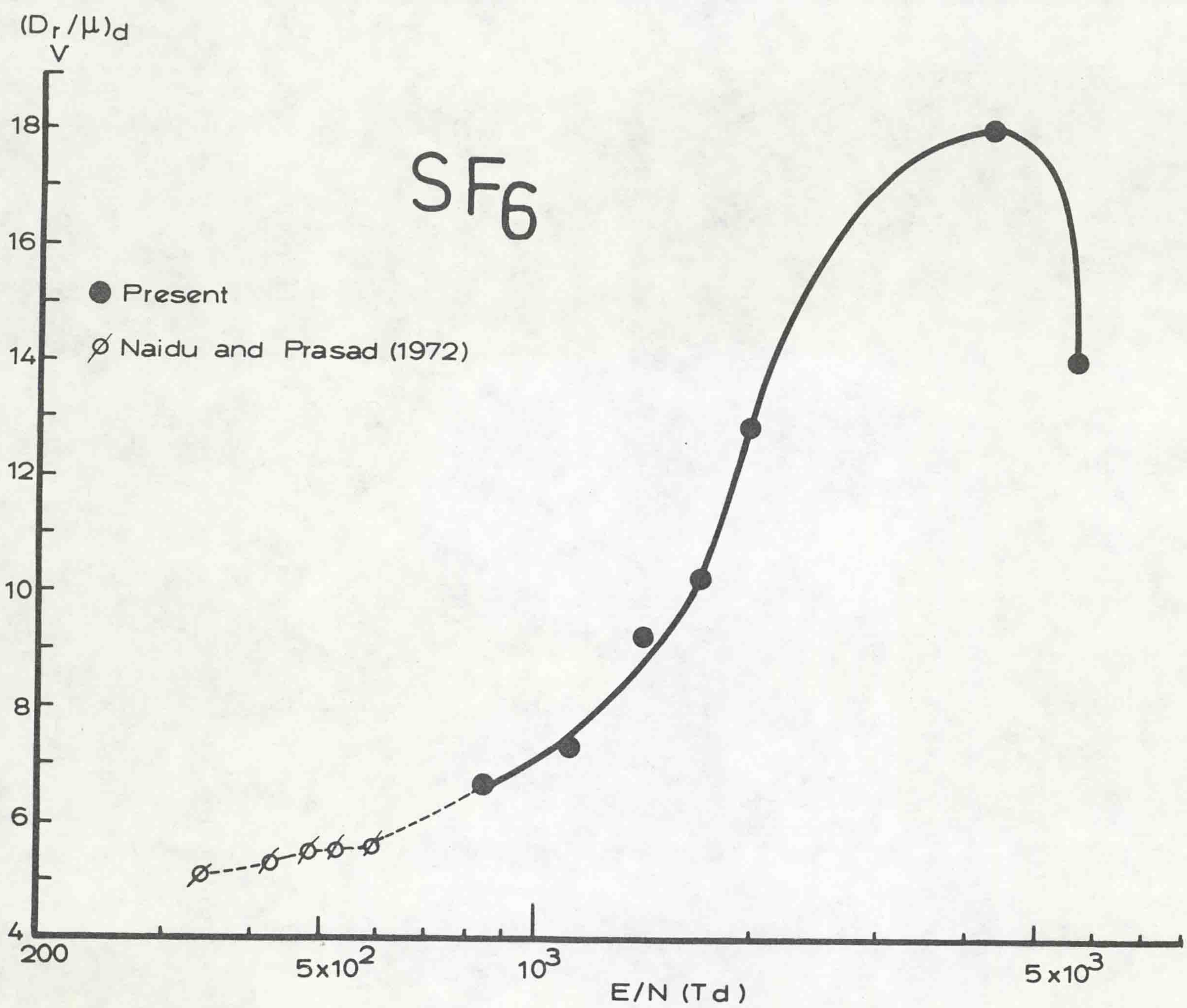

Fig.(3.12) Ratio of Radial Diffusion Coefficient to Mobility in sulphur Hexafluoride

CHAPTER FOUR

CHAPTER FOUR

THE MONTE CARLO COMPUTER TECHNIQUE

4.1 INTRODUCTION

The Monte Carlo Technique (MCT) has been used to simulate electron swarm motion across uniform electric field in the presence of both elastic and inelastic collisions by a number of workers (Itoh and Musha, 1960, Thomas and Thomas, 1969, Lucas, 1972 and Saelee and Lucas, 1977). Itoh and Musha approximated the electron trajectory by small linear steps, Δs. The mean free path, L , within the step was considered to be constant and the probability of colliding within the step to be

$$P = \Delta s/L \quad .$$

If there was no collision the momentum was balanced after each step so as to represent the parabolic trajectory of the electron in the electric field. If a collision occurred the electron lost a small amount of energy and was scattered isotropically. In the case of an ionizing collision, only one electron, arbitrarily chosen, was traced. The drift velocity and ionization coefficient in helium were calculated by assuming that the behaviour of a single electron averaged over a period of time is the same as the behaviour of a number of electrons at an instant of time.

Thomas and Thomas (1969) considered this hypothesis to be invalid when ionization was present, as electron diffusion and the production of slow electrons by ionization had an influence on the energy distribution. They then did a similar simulation in neon, but with the collision probability as :

$$P = 1 - \exp (- \Delta s/L).$$

They observed the electron swarm as a whole and traced both the electrons in an event of an ionizing collision. The energy relaxation time, back diffusion, drift velocity and ionization coefficient were investigated.

Lucas (1972) used a Monte Carlo-Boltzmann method to simulate the electron swarm motion. This method required less computations and was thus faster in terms of computer time. However, the method was valid only when the mean energy change by the electric field between collisions was much smaller than the mean energy of the swarm. This condition is only applicable at low E/N ($\simeq$ 300 Td) in all gases but has the added advantage that it may be used at a much lower E/N range than the technique of Thomas and Thomas.

The Saelee and Lucas (1977) Monte Carlo method starts from the basic techniques of Itoh and Musha and Thomas and Thomas, but because of the vast improvement in computer speed it is possible to simulate more realistically the swarm motion. The electron is traced in three-dimensional geometry. This is necessary to simulate the actual drift tube and to investigate the radial and longitudinal diffusion. In model gases, the electrons are scattered isotropically and in real gases the electrons are scattered according to the probability distribution determined from the differential scattering cross-sections. The rest of this chapter describes the Monte Carlo Techniques employed and the results obtained in oxygen and methane. The pseudo-random number generator which is required in the Monte Carlo technique is provided by the ICL 1906S NAG Library. The interpolation routines used are also provided by this library.

of the electron (z, r) (ϵ is the energy of the electron ; r is the radial position ; z is the distance from the cathode), mean energy before and after the collision, the number of collisions and the number, A, of electrons produced by ionization are stored. The electron is allowed to continue its motion until it reaches another termination, say a fixed time, 2t. The process is repeated for a series of terminations with equal time intervals. At the last termination, ϵ , z and A are stored into histograms and the electrons which were produced by ionization are traced.

A swarm is represented by a number of test electrons traced in a similar manner. The mean state of all the electrons at the terminations are analysed to give the swarm parameters, i.e. drift velocity (v), radial diffusion coefficient (D_r), longitudinal diffusion coefficient (D_L) and ionization coefficient (α). For fixed time (t) termination, the results can be analysed as follows :-

$$v = \frac{\bar{z}}{t} \quad ,$$

$$\frac{D_r}{\mu} = \frac{\overline{r^2}}{t} \cdot \frac{E}{4v} \quad ,$$

$$\frac{D_L}{\mu} = \frac{(\overline{z^2} - \bar{z}^2)}{t} \cdot \frac{E}{2v} \quad , \qquad (4.1)$$

$$\alpha = \frac{\overline{Ln(A)}}{t} \cdot \frac{1}{v} \quad .$$

A bar indicates the mean value. Knowing the mean states at equal time intervals a difference technique can be used to obtain the above swarm parameters without the need to consider in detail the electrode and energy relaxation time.

Similarly for fixed distance (d) termination, the results can be analysed as follows :-

$$v_d = \frac{d}{t} \quad ,$$

$$\left(\frac{D_r}{\mu}\right)_d = \frac{\overline{r^2}}{d} \cdot \frac{E}{4} \quad ,$$

$$\left(\frac{D_L}{\mu}\right)_d = \frac{(\overline{t^2} - \bar{t}^2)}{d} \cdot \frac{E}{2} v_d^2 \quad , \qquad (4.2)$$

$$\alpha_T = \frac{\mathrm{Ln}(\bar{A})}{d} \quad .$$

In the presence of ionization ; Lucas (1964) has shown that

$$\bar{t} = \frac{\lambda}{u} \frac{d}{v} \quad , \qquad (4.3)$$

where $\lambda = \frac{v}{2D_L}$ and $u^2 = \lambda^2 - 2\alpha\lambda$,

by solving the transport equation with the proper boundary conditions.

Therefore, the parameters calculated from fixed time and fixed distance are related as follows :-

$$v_d = \frac{u}{\lambda} v \quad ,$$

$$\left(\frac{D_r}{\mu}\right)_d = \frac{\lambda}{u} \cdot \frac{D_r}{\mu} \quad , \qquad (4.4)$$

$$\left(\frac{D_L}{\mu}\right)_d = \frac{u}{\lambda} \cdot \frac{D_L}{\mu} \quad ,$$

$$\alpha_T = \lambda - u \quad .$$

If there is no ionization, $u = \lambda$ and the two sets of parameters are equal. The statistical sampling error causes a standard deviation of $100/\sqrt{N_e}$ % on the mean and $100/\sqrt{N_{e/2}}$ % on the variance, where N_e is the number of electrons.

4.2 MONTE CARLO METHOD

The physical processes to be simulated are outlined below. The conditions assumed as in swarm experiments in the regions of relatively high E/N are

(a) uniform electric field,

(b) low charge density, i.e. no interaction of charged particles,

(c) atoms are stationary,

(d) no collision of the second kind, i.e. super-elastic.

The test electron is injected from an infinitesimal pinhole source at the cathode with an initially selected energy. The electron moves freely under the action of the electric field until it hits a gas atom. At a collision the electron loses an amount of energy associated with the type of collision. In an event of an ionizing collision the resulting energy is shared equally between the two electrons and the state of the new electron is stored. The electron is then scattered isotropically or according to a probability distribution and again moves the free path under the electric field. The electron is traced in this way until a fixed time or distance is reached. The latter condition is equivalent to an anode without reflection. The electrons produced by ionization are individually brought from the store and their motion is traced in the same manner. The swarm is represented by considering many test electrons in order to reduce statistical fluctuations, and swarm parameters are given by the average state of all these electrons.

4.3 SWARM PARAMETERS

A test electron is injected from the cathode and is traced until it reaches a termination, say a fixed time, t. At the termination, the position

and metal vapours of potassium (K), sodium (Na) and Caesium (Cs), (Ar + K, Ar + Na, Ar + Cs) for E/N ranging from 2.83 to 283 Td and at the percentage of 0.001 % to 20 %. These results have been discussed. There are currently no experimental values for comparison with theory in these mixtures.

It is useful to illustrate the range of properties of the electrons arriving at the anode by means of histograms. The variables are transit time (t), energy (E), total number of electrons (N) and radial position (r). These use cells denoted by T CELL, U CELL, AV. NUMBER and D/100 respectively. The histograms give detailed insight into the swarm behaviour. Of special interest is the radial histogram because it may be used to compute another definition of the ratio of radial diffusion coefficient to mobility by Lucas (1968) given by D_r/μ_{exp}, which has been widely measured for high E/N.

4.4 THEORETICAL DISCUSSION

The Monte Carlo method is used to simulate the electron swarm motion in gases by using a set of cross-sections compiled from the available experimental data. The calculated swarm parameters are then compared with swarm parameters which are given in Chapter 3. Adjustment of the cross-sections used are made so that the fit is good. The set of cross-sections can then be obtained so that agreement exists between experimental and theoretical swarm parameters. These cross-sections, however, are sufficient but not unique. The types of cross-section used are the total cross-section $Q_{Tot.}$, the vibration cross-section $Q_{Vib.}$, the excitation cross-section $Q_{Ex.}$, the dissociative ionization cross-section, $Q_{Dis.}$, and the ionization cross-section, $Q_{Ion.}$. The probability of collision is determined by the total cross-section. The electron, after a collision, is scattered anisotropically according to a probability distribution which is determined from the differential scattering cross-sections. It is often found that the differential scattering cross-sections are not satisfactorily defined, therefore it is necessary to adopt three limiting

cases in the simulation, represented by curves A, B and C in the figures, for example, in oxygen, Fig. 4.2. In case A, both the elastic and inelastic scatterings are according to the elastic differential cross-section and in case B, the elastic scattering is according to the elastic differential cross-section and the inelastic scattering is isotropic. In case C, both the elastic and inelastic scatterings are according to isotropic scattering. The true scattering is expected to be between these cases. Another uncertainty arises in the case of excitation cross-sections and therefore it has often been necessary to scale the cross-section or to modify the energy range in order to provide a good overall fit to the experimental data. The excitation cross-section is chosen for scaling because both the total and the ionization cross-sections are more accurately measured by electron beam techniques (Laborie et al, 1968, 1971).

It is important therefore to check the measured values for drift velocity, v_d, the ratio of both longitudinal and radial diffusion coefficients to mobility, $(D_L/\mu)_d$ and $(D_r/\mu)_d$ respectively, against the theoretical values. At high E/N, the preferred method is the Monte Carlo Technique because it directly simulates the experimental method and also provides a check upon whether equilibrium has been attained. The method has been documented fully by Saelee and Lucas (1977) and Kucukarpaci and Lucas (1979). Using (MCT), v_d, $(D_L/\mu)_d$ and $(D_r/\mu)_d$ as well as α_T/N and $\bar{\epsilon}$ have been calculated for oxygen and methane for E/N up to 5650 Td.

4.5 SIMULATION RESULTS IN OXYGEN

There are five varieties of electron-oxygen molecule collisions, namely elastic, vibration, excitation, dissociative ionization and ionization. The sources of these cross-section measurements are given in Table 4.1. The cross-sections for various values of electron energy are tabulated together with the scattering probability in Appendix B. The set of cross-sections used in the simulation is shown in Fig. 4.1, in the form of the number of collisions per cm (NQ) for gas pressure of 1 torr at 0^{o}C. The results for $NQ_{Tot.}$, given by Bruche (1927), Ramsauer and Kollath (1930), Salop and Nakano (1970) for energies up to 50 eV are used together with those of Sunshine et al (1967) for higher energies. The vibrations cross-section, $NQ_{Vib.}$, used are those of Hake and Phelps (1967) with the vibration cross-section being divided into eight main vibrational levels with onset energies of 0.37, 0.56, 0.75, 0.93, 1.12, 1.30, 1.47 and 1.64 eV consecutively. The total ionization cross-section $NQ_{Ion.}$, has an onset energy of 12.2 eV and is given by Rapp and Englander-Golden (1965). The dissociative ionization cross-section $NQ_{Dis.}$, with an onset energy of 20 eV is by Rapp et al (1965). Three types of excitation cross-sections $NQ_{Ex.}$ were demonstrated by Hake and Phelps (1967), who give the onset energies of 4.4, 8.0 and 9.7 eV respectively. The excitation cross-sections are adjusted so that the computed ionization coefficient fitted those measured by Kontoleon (1971), Lakshminarasimha (1974) and others data, as shown in Fig. 4.2. To achieve this a scaling factor of 1.5 was used with the excitation cross-section. The elastic differential cross-sections are given by Linder and Schmidt (1971) for energies up to 4 eV and by Trajmer et al (1971) for energies up to 300 eV and for the higher energy region to about 500 eV were obtained privately from Dr. J.A. Rees.

Electron swarm motion in oxygen has been simulated for the range of $28.3 \leq E/N \leq 5650$ Td. The results for α_T/N, v_d, $(D_L/\mu)_d$, $(D_r/\mu)_d$ and $\bar{\epsilon}$ are tabulated in Table 4.2 for A and B condition. The results for C condition in the range of $14.1 \leq E/N \leq 2825$ Td are tabulated in Table 4.3. The swarm data which are most accurately computed are the ionization coefficient, the drift velocity, and the ratio of both longitudinal and radial diffusion coefficient to mobility and we have adjusted the selected cross-section in order to produce as good a fit as possible with the experimental data.

The ionization coefficient (α_T/N) is shown in Fig. 4.2 as a function of E/N. The agreement is excellent over the entire E/N range. The computed result agrees with the data of Kontoleon (1971), Lakshminarasimha (1974), Harrison and Geballe (1953) and Naidu and Prasad (1970) up to $E/N \geq 1000$ Td and for the higher E/N it agrees with Schlumbohm (1965). This figure illustrates that case A conditions are lower than both case B and C conditions.

The computed drift velocity, v_d, has been plotted against E/N and shown in Fig. 4.3. This figure shows that the present experimental values show good fit at low E/N, while at high E/N the experimental data generally lie lower than either of the A or B conditions. The better fit is given by theoretical condition C which represents isotropic scattering during inelastic and elastic conditions. The reason for this is that the computation is very sensitive to the mean electron energy which is changing rapidly as shown in Fig. 4.6. Comparison with the other experimental values of drift velocity is also shown in Fig. 4.3.

Fig. 4.4 compares the theoretical and the present experimental values of the ratio of longitudinal diffusion coefficient to mobility $(D_L/\mu)_d$. The present values agree well with the theoretical values at low E/N, while for

higher E/N, the theoretical values fall below the experimental values which seem to agree best with the case A condition. Data from Schlumbohm (1965) and Lowke and Parker (1969) are also shown in the figure.

The variation of radial diffusion coefficient to mobility $(D_r/\mu)_d$ with E/N is shown in Fig. 4.5. The theoretical values are generally lower over the entire range of E/N than the present results and also with the other experimental data such as those of Kontoleon (1971) and Lakshminarasimha (1974). To obtain a better agreement in the middle range of E/N it would be necessary to have more backward scattering of the electron in a collision. Condition C, which assumes the isotropic scattering, seems to give the better fit to the present results.

The graph of the computed mean electron energy as a function of E/N is shown in Fig. 4.6. The mean electron energy for case A condition rises from 5.29 to 160 eV in the range of $28.3 \leq E/N \leq 5650$ Td. For case B condition, the range of mean electron energy is between 8.44 to 115 eV for E/N increasing from 141 to 5650 Td, while for case C condition, the mean electron energy increases from 4 to 56.7 eV for the range of E/N between 14.1 to 2825 Td. This figure shows clearly that case A condition is higher than both B and C conditions.

TABLE 4.1 : SOURCES OF OXYGEN COLLISION CROSS-SECTIONS

CROSS-SECTION	ENERGY-RANGE OR ONSET-ENERGY e V	SOURCE
* TOTAL	$\frac{2m}{M} = 3.40 \times 10^{-5}$	Bruche (1927) Ramsauer and Kollath (1930) Sunshine et al (1967) Salop and Nakano (1970)
VIBRATION	0.37, 0.56, 0.75, 0.93, 1.12, 1.30, 1.47, 1.64	Hake and Phelps (1967)
EXCITATION	4.4, 8.0, 9.7	Hake and Phelps (1967)
DISSOCIATIVE IONIZATION	20	Rapp et al (1965)
IONIZATION	12.2	Rapp et al (1965)
* DIFFERENTIAL ELASTIC	0.74, 4.0 45, 300 500	Linder and Schmidt (1971) Trajmar et al (1971) Private communication from Dr. Rees

* modified

TABLE 4.2 : CALCULATED SWARM PARAMETERS IN OXYGEN

E / P_o V/cm, torr	E / N Td	CASE	α_T / N $\times 10^{-17}$ cm^2	v_d $\times 10^7$ cm/s	$(D_L/\mu)_d$ V	$(D_r/\mu)_d$ V	$\bar{\epsilon}$ eV
10	28.3	A		0.71	2.08	1.84	5.29
30	84.8	A	0.06	1.83	2.49	2.15	6.90
50	141	A	0.42	2.81	2.93	2.41	8.50
		B	0.40	2.72	2.90	2.53	8.44
100	283	A	2.70	5.07	4.66	2.82	13.2
200	565	A	8.85	8.97	7.93	3.71	22.0
300	848	A	13.7	12.0	10.1	4.58	30.1
		B	13.7	9.50	7.27	5.80	27.9
500	1413	A	20.3	16.6	12.7	5.89	44.1
700	1978	A	24.4	20.2	15.4	7.27	57.4
		B	27.1	13.9	10.6	12.4	49.4
1000	2825	A	28.0	25.6	20.2	9.02	78.5
		B	33.3	16.1	13.3	17.9	64.0
1500	4238	A	29.5	32.1	26.9	11.2	118
		B	43.8	18.3	17.6	28.1	88.2
2000	5650	A	29.3	38.4	36.4	14.0	160
		B	42.1	19.6	21.3	39.4	115

TABLE 4.3 : COMPUTED OXYGEN SWARM PARAMETERS (ALL CASE C)

E / P_o V/cm, torr	E / N Td	α_T / N $\times 10^{-17}$ cm^2	v_d $\times 10^7$ cm/s	$(D_L/\mu)_d$ V	$(D_r/\mu)_d$ V	$\bar{\epsilon}$ eV
5	14.1		0.36	1.25	1.68	4.00
10	28.3		0.59	1.73	2.29	4.96
30	84.8	0.06	1.29	2.77	3.41	6.96
50	141	0.52	1.85	2.82	3.83	8.49
300	848	15.8	5.79	7.24	10.7	24.5
1000	2825	39.3	10.8	15.5	25.3	56.7

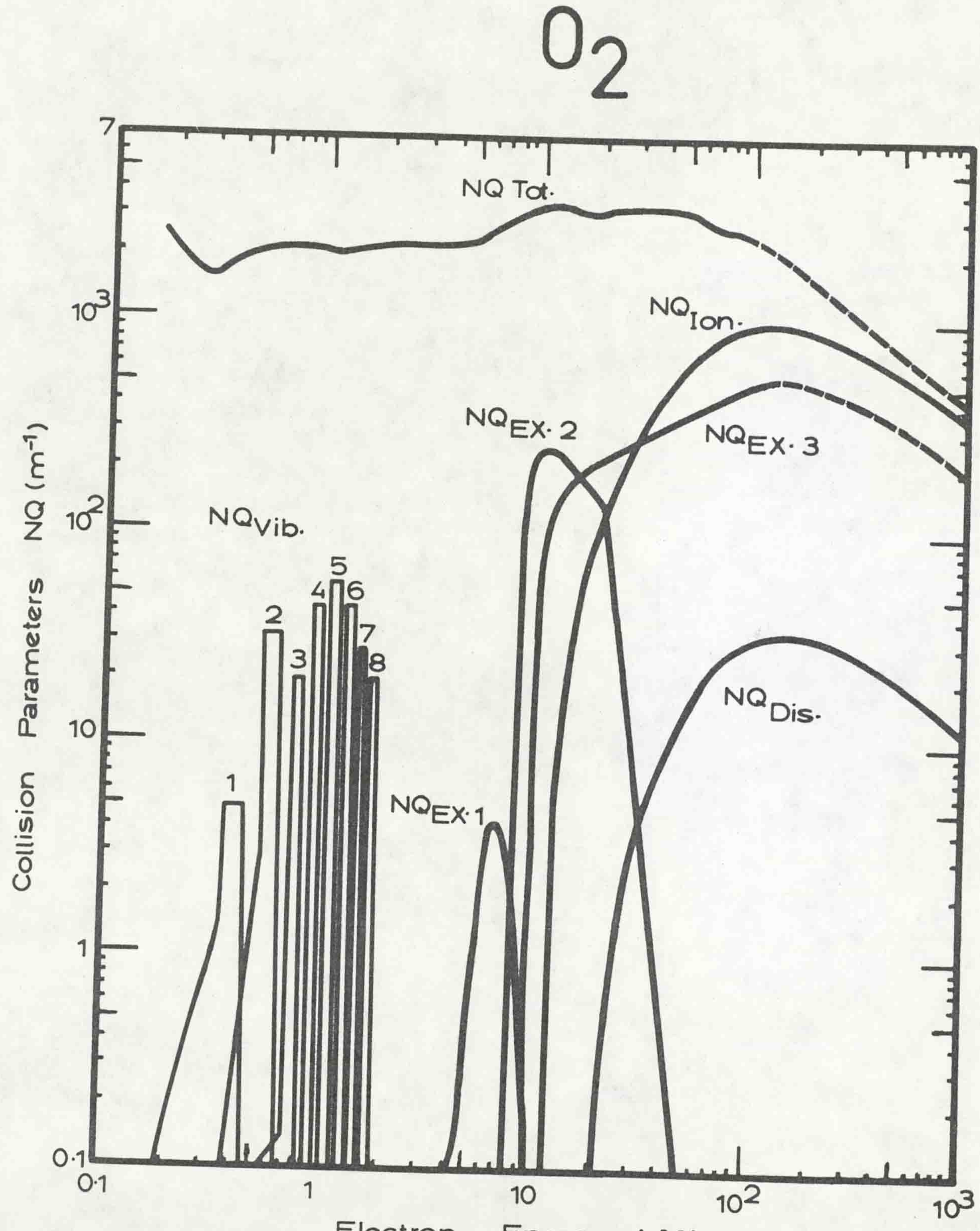

Fig.(4.1) Oxygen Cross-section NQ ($N = 3.54 \times 10^{16}$ cm^{-3})

(------ Estimated)

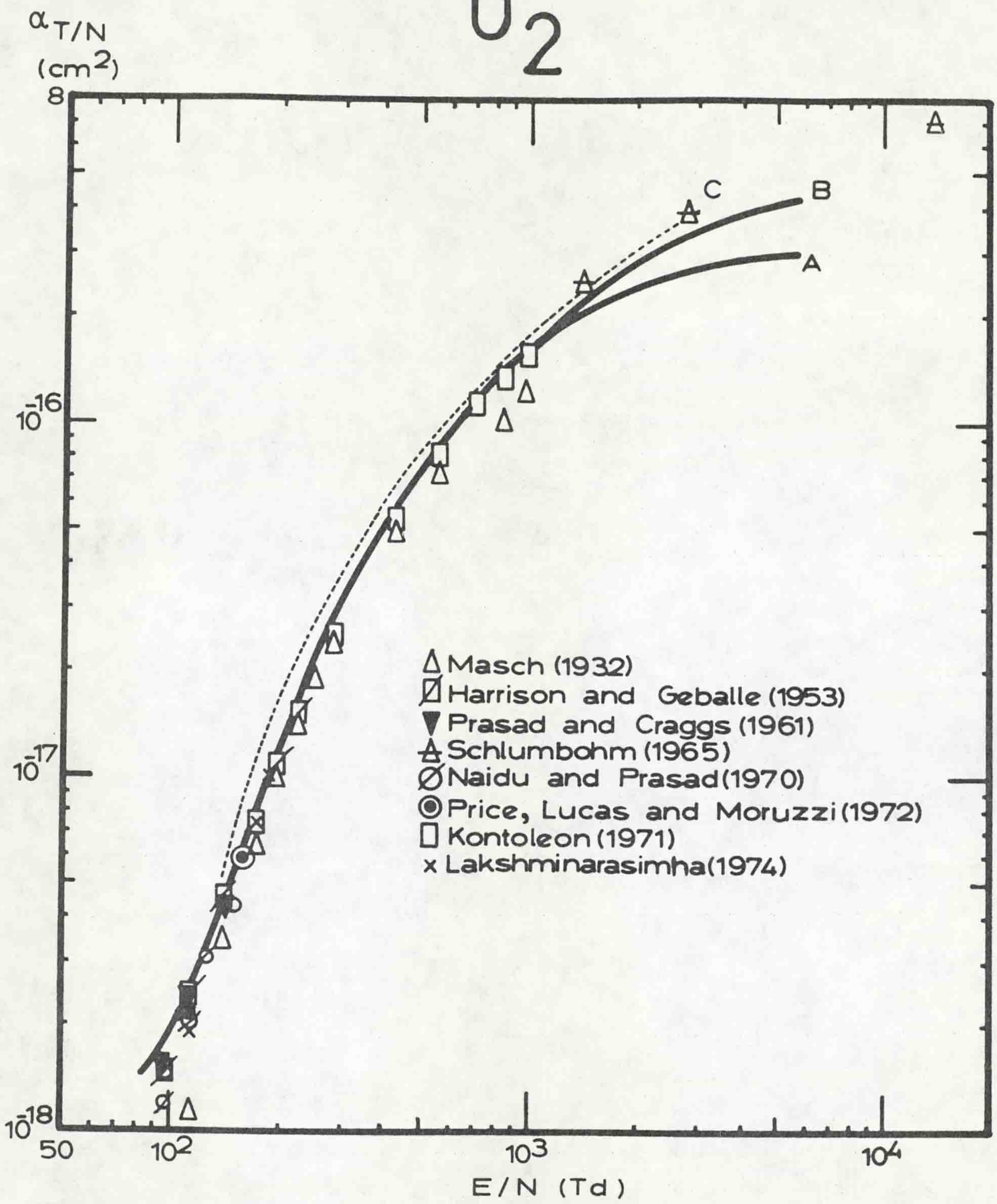

Fig. (4.2) Ionization Coefficient in Oxygen.

CONTENTS

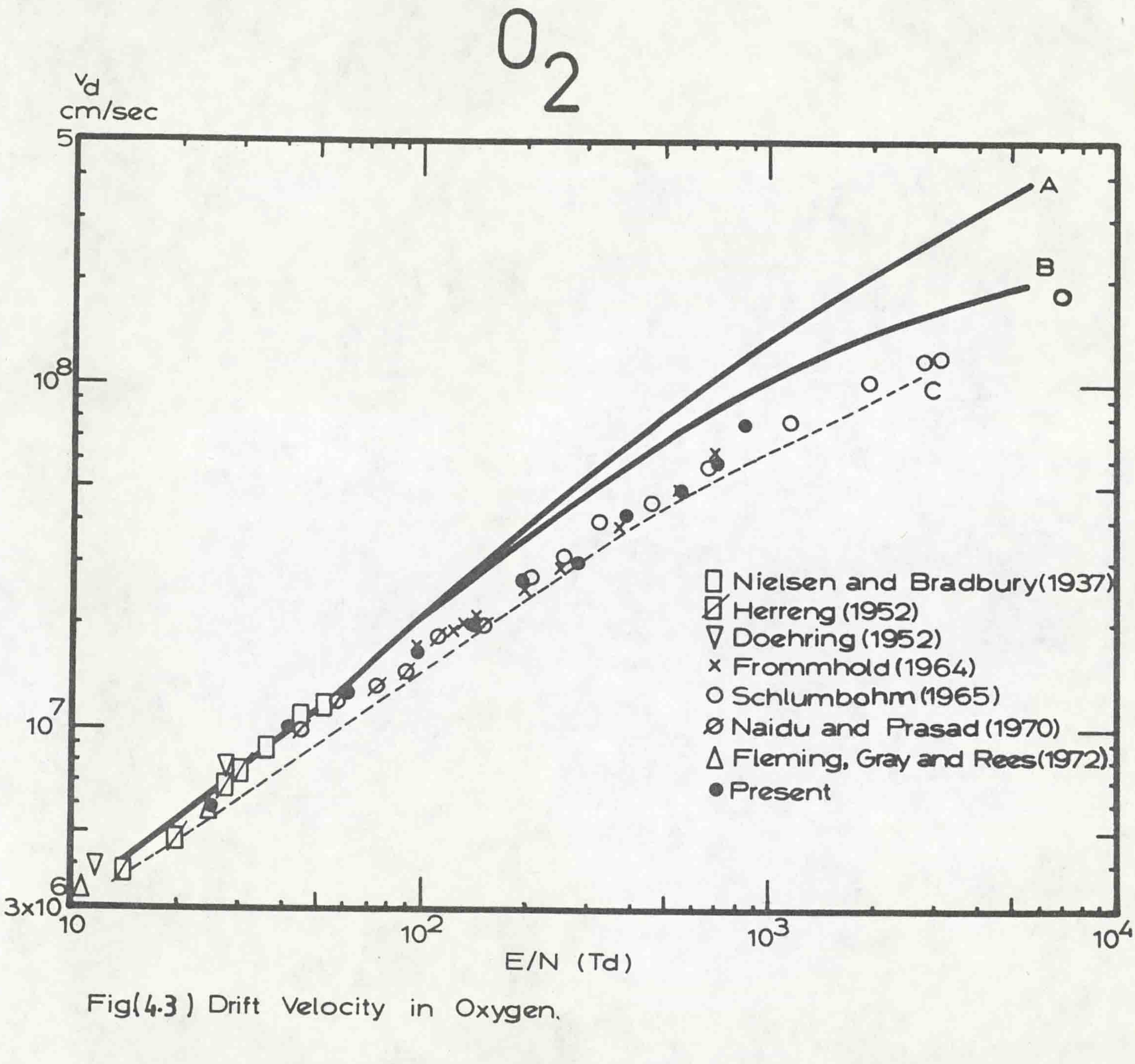

Fig(4.3) Drift Velocity in Oxygen.

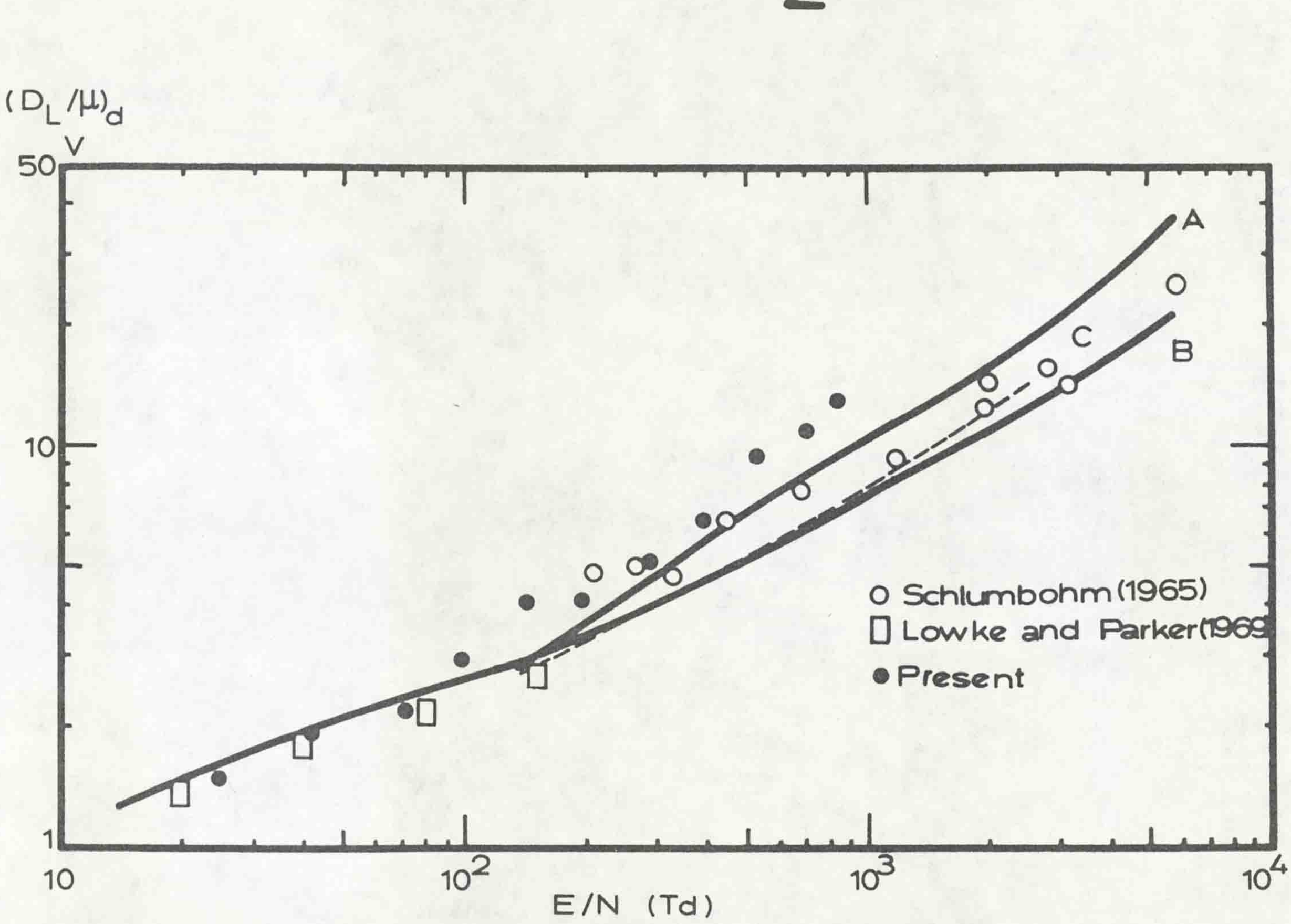

Fig.(4.4) Ratio of Longitudinal Diffusion Coefficient to Mobility in Oxygen.

O_2

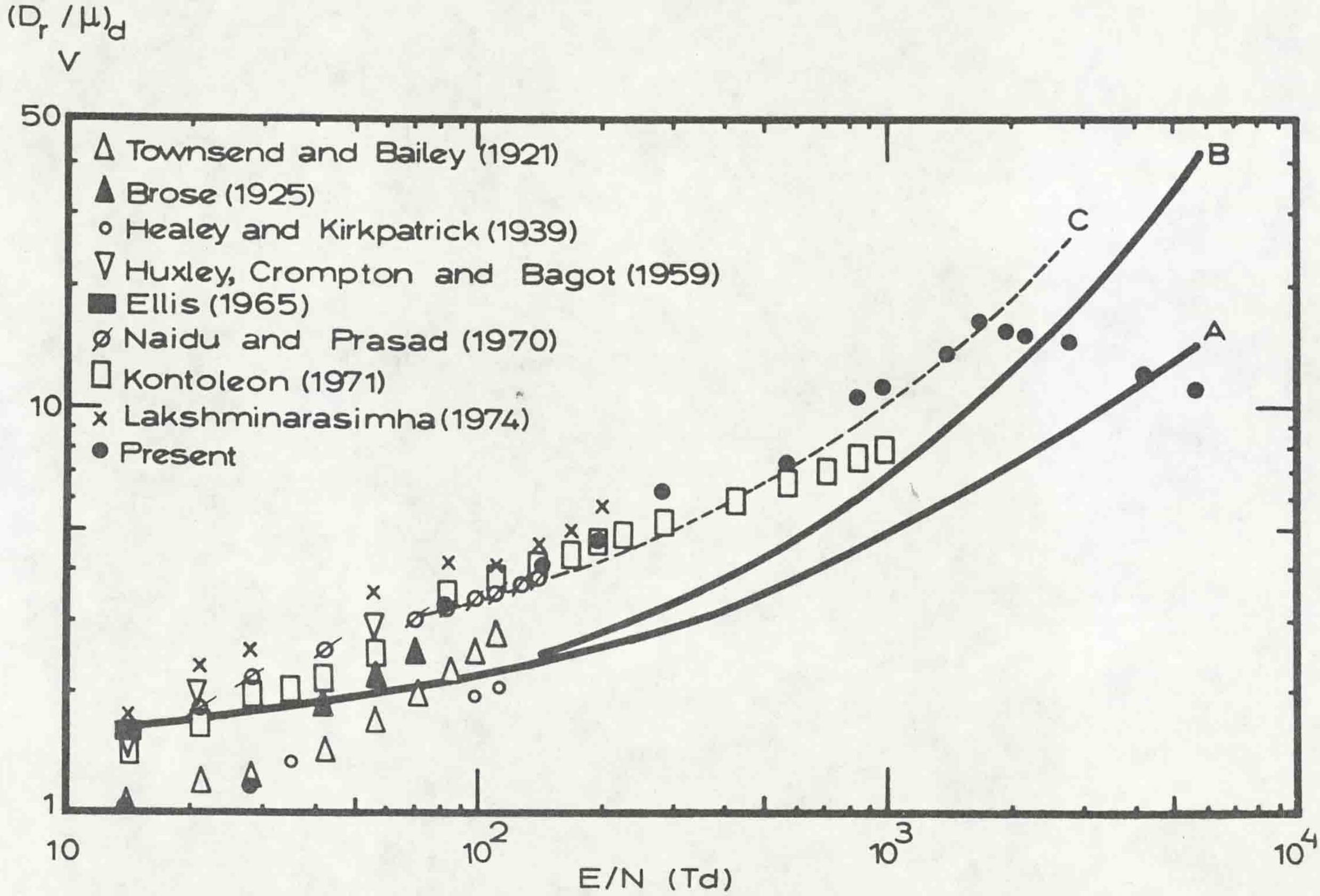

Fig.(4.5) Ratio of Radial Diffusion Coefficient to Mobility in Oxygen.

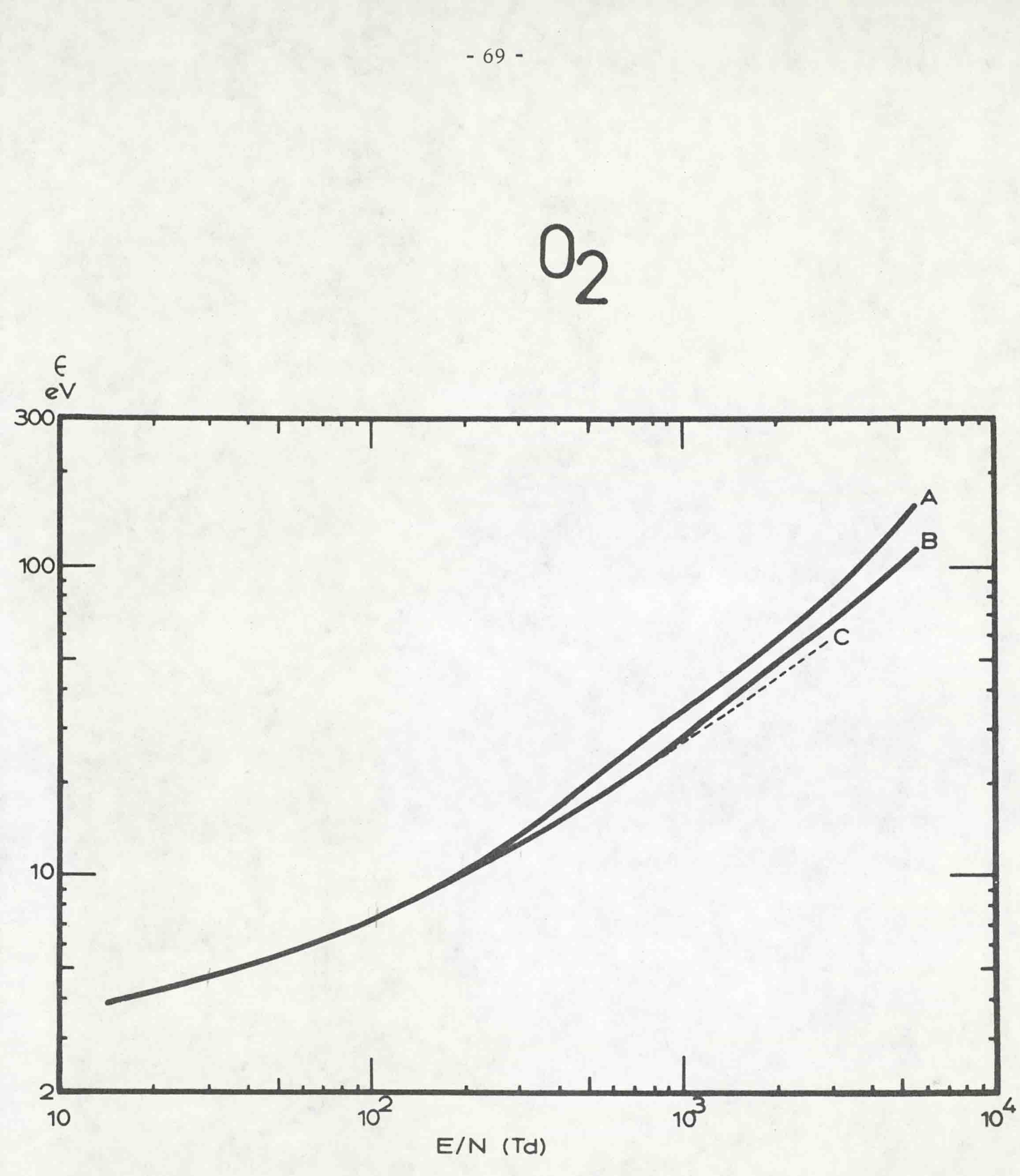

Fig (4.6) Mean Electron Energy in Oxygen

4.6 SIMULATION RESULTS IN METHANE

A set of cross-sections representing electron collision in methane has been taken from the references given in Table 4.4. To obtain the best agreement with the experimental swarm data it was necessary to use a scaling factor for some of these cross-sections.

The set of cross-sections has also been plotted in Fig. 4.7 in the form of the number of collisions per cm (NQ) for a gas pressure of 1 torr at 0^{o}C. The energy range has been extrapolated up to 1000 eV. The total cross-sections $NQ_{Tot.}$, used at lower energies up to 0.90 eV, are those published by Ramsauer and Kollath (1930), and then follows the values given by Bruche (1930) at the higher energy region (1-50 eV) extrapolated to 1000 eV. These cross-sections were slightly modified by curve smoothing to obtain a good fit to experimental measurements.

A modification was also made to the only two vibration cross-section $NQ_{Vib.}$, which are taken from Duncan and Walker (1972). The onset energy of 0.16 and 0.37 eV has been given to both vibration cross-sections.

The shape of the excitation cross-section $NQ_{Ex.}$ is obtained from Bowman and Miller (1965). The onset energy of excitation is taken to be 7.50 eV. A scaling factor of 3 for the excitation cross-section was necessary in order to get an acceptable ionization coefficient and drift velocity.

The dissociative ionization cross-section, $NQ_{Dis.}$ of Rapp and Englander-Golden (1965) was used with an onset energy of 25 eV. The values of cross-section for ionization, $NQ_{Ion.}$, by collision with electrons have also been taken from Rapp et al (1965). The onset energy of ionization is assumed to be 13.2 eV. The scattering probabilities used are derived from the elastic

differential cross-sections given by Bullard and Massey (1931) for low energy range between 4-30 eV, and for higher energies up to 820 eV by Arnote (1931). The set of cross-sections together with the scattering probability distribution are tabulated in Appendix B.

The Monte Carlo Technique has been used to simulate the electron swarm motion in methane. Electron swarm parameters have been evaluated in the range of E/N varying from 28.3 to 5650 Td. Comparison has been made also with the experimental results for the ionization coefficient α_T/N, the drift velocity, v_d, and both the longitudinal $(D_L/\mu)_d$ and radial $(D_r/\mu)_d$ diffusion coefficient to mobility.

The results for A and B condition are obtained from (MCT) and tabulated in Table 4.5. The ionization coefficient is shown in Fig. 4.8 over a wide range of E/N. This figure compares the computed to the recent experimental values of α_T/N. It can be seen that the computed values are in excellent agreement with the experimental results of Lablanc and Devins (1960), Heylen (1963), Schlumbohm (1965), and Lakshminarasimha (1977).

The results of simulation for drift velocity are shown in Fig. 4.9. This figure illustrates a very good agreement with the present experimental data, especially at middle of E/N. Comparison with the other experimental data is also shown in this figure. There is a good fit with those of Pollock (1968), and Fink and Huber (1965) at the low E/N region. The results of Franke (1960), and Frommhold (1960) at the middle of E/N are compatible with both present results and simulation results. The present results seem to agree best with the case A condition.

The present and simulation results for $(D_L/\mu)_d$ as a function of E/N are compared in Fig. 4.10. The experimental results are lower than the theoretical simulation except in the region $424 \leq E/N \leq 706$ Td at which the agreement is very good. The better degree of fit to the present values are given also by case A condition whilst the values of Frommhold (1960), Fink and Huber (1965) and Schlumbohm (1965) at high E/N lie well below the case B condition.

The theoretical and experimental values of $(D_r/\mu)_d$ with E/N are illustrated in Fig. 4.11. This figure also shows that the present values and the values of Lakshminarasimha (1977), are always higher than the simulation results except at $E/N \geq 2000$ Td, at which both the experimental results fall below the simulation results. Condition B appears to give the best fit to the experimental results.

The variation of the mean electron energy against E/N is shown in Fig. 4.12. The value of mean electron energy for case A condition increases from 3.94 to 119 eV while for case B condition the value of mean electron energy increases from 7.54 to 87.2 eV over the range of $141 \leq E/N \leq 5650$ Td.

TABLE 4.4 : SOURCES OF METHANE COLLISION CROSS-SECTIONS

CROSS-SECTION	ENERGY-RANGE OR ONSET-ENERGY eV	SOURCE
* TOTAL	$\frac{2m}{M} = 6.78 \times 10^{-5}$	Ramsauer and Kollath (1930) Bruche (1930)
* VIBRATION	0.16 , 0.37	Duncan and Walker (1972)
* EXCITATION	7.50	Bowman and Miller (1965)
DISSOCIATIVE IONIZATION	25.0	Rapp et al (1965)
IONIZATION	13.2	Rapp et al (1965)
DIFFERENTIAL ELASTIC	4 - 30 30 - 820	Bullard and Massey (1931) Arnot (1931)

* modified

TABLE 4.5 : CALCULATED SWARM PARAMETERS IN METHANE

E/P_o V/cm,torr	E/N Td	CASE	α_T/N $x10^{-17}cm^2$	v_d $x10^7$ cm/s	$(D_L/\mu)_d$ V	$(D_r/\mu)_d$ V	$\bar{\epsilon}$ eV
10	28.3	A		0.52	0.53	1.99	3.94
30	84.8	A	0.03	0.86	2.56	2.54	7.10
50	141	A	0.34	1.25	2.77	2.71	7.44
		B	0.34	1.23	2.69	2.59	7.54
100	283	A	3.37	2.35	4.31	2.73	10.3
200	565	A	11.6	4.24	5.54	3.40	15.0
300	848	A	18.7	5.88	6.91	4.39	19.1
		B	18.5	5.35	6.19	4.64	18.7
500	1413	A	28.0	8.34	9.58	5.75	27.4
		B	28.9	7.42	7.79	6.91	25.9
700	1978	A	34.3	10.7	12.3	7.50	36.3
		B	36.2	9.23	9.89	9.25	33.4
1000	2825	A	38.9	14.4	18.2	9.76	53.0
		B	43.6	11.5	12.1	13.7	44.8
1500	4238	A	41.6	19.3	25.1	13.4	81.0
		B	50.6	14.2	15.5	21.8	65.2
2000	5650	A	40.6	24.6	36.0	17.6	119
		B	54.3	16.4	19.8	32.0	87.2

CH_4

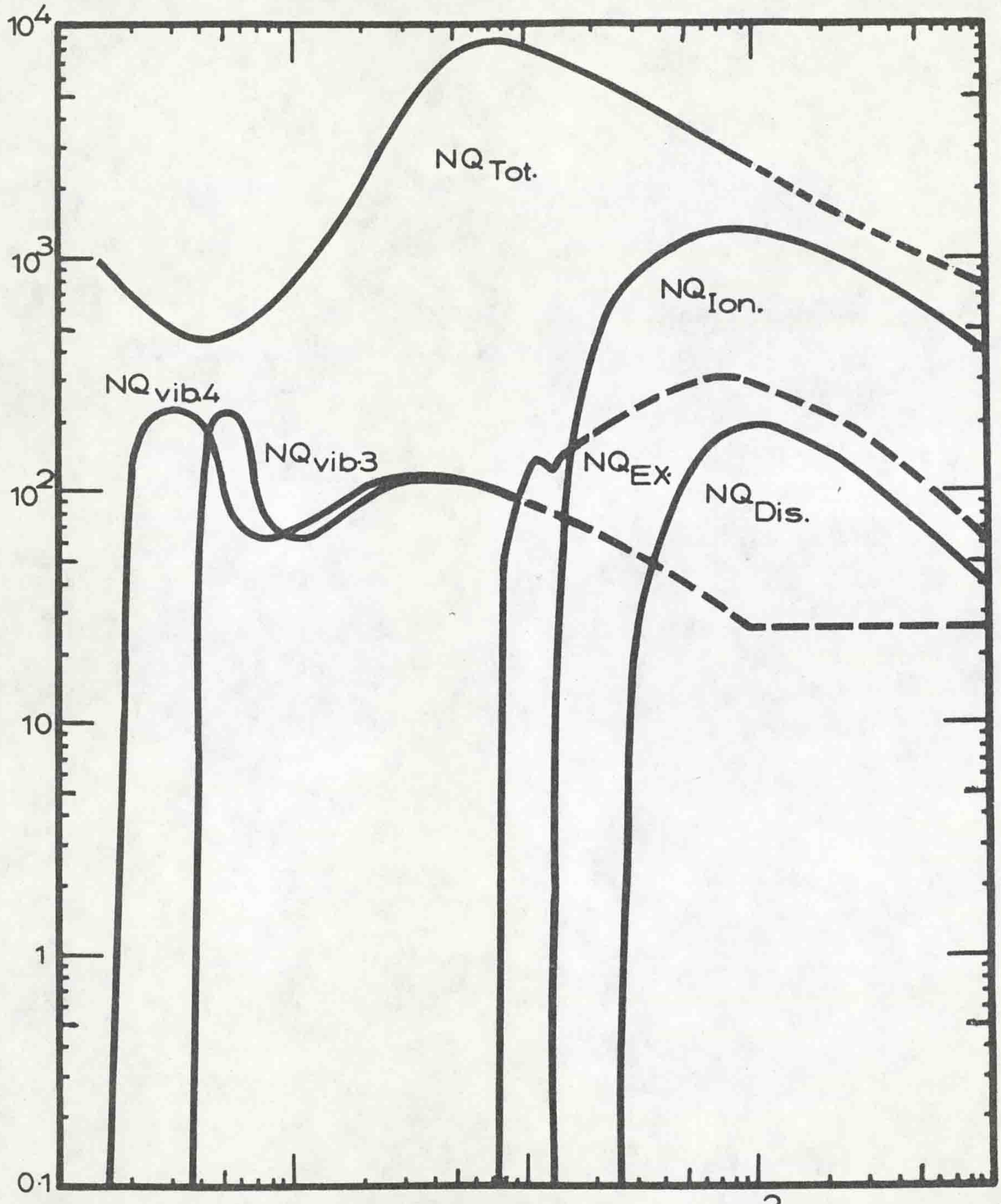

Fig. (4·7) Methane cross-sections NQ ($N = 3{\cdot}54 \times 10^{16}\ cm^{-3}$)

(- - - - - Estimated)

CH_4

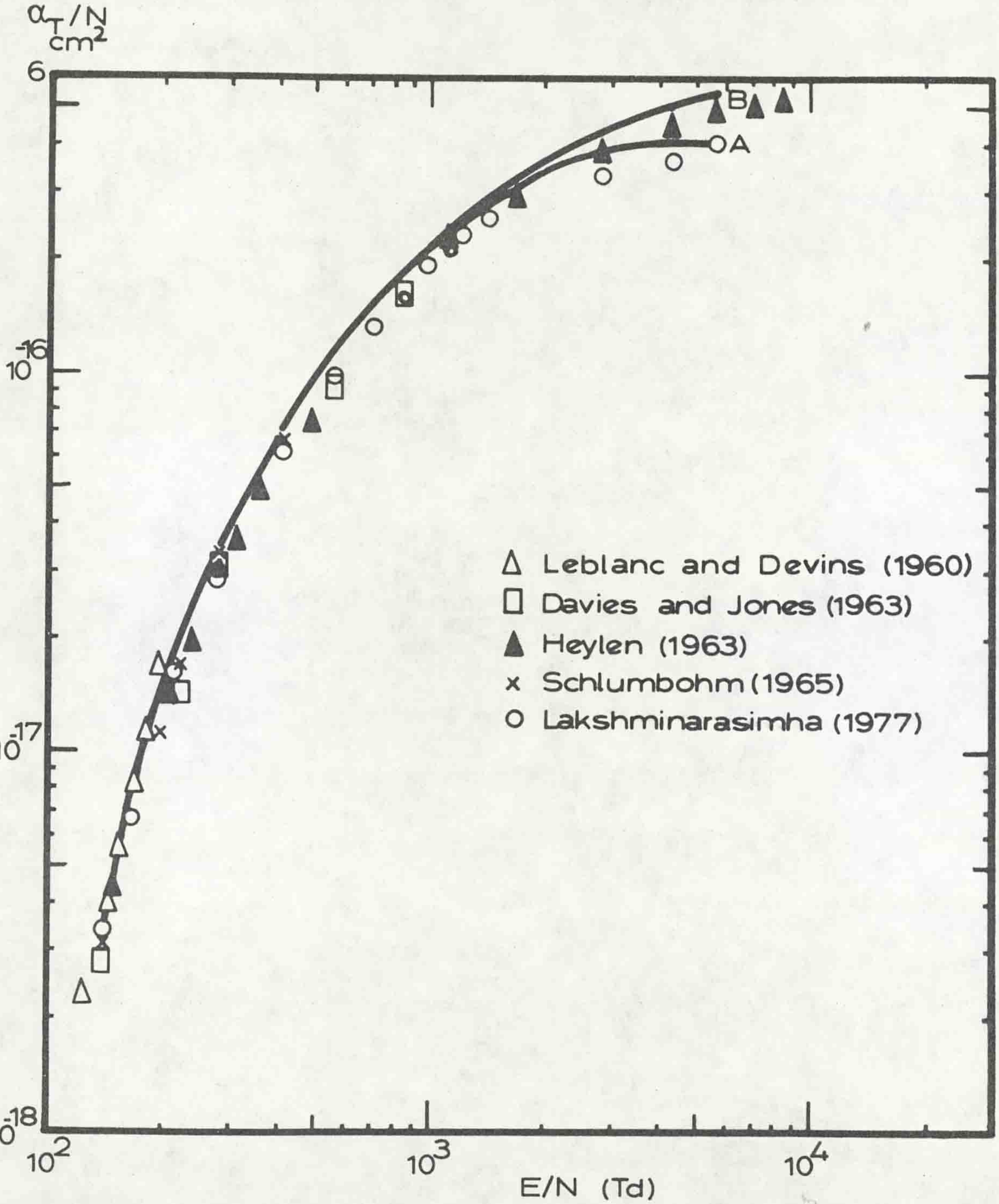

Fig.(4.8) Ionization Coefficient in Methane.

CH_4

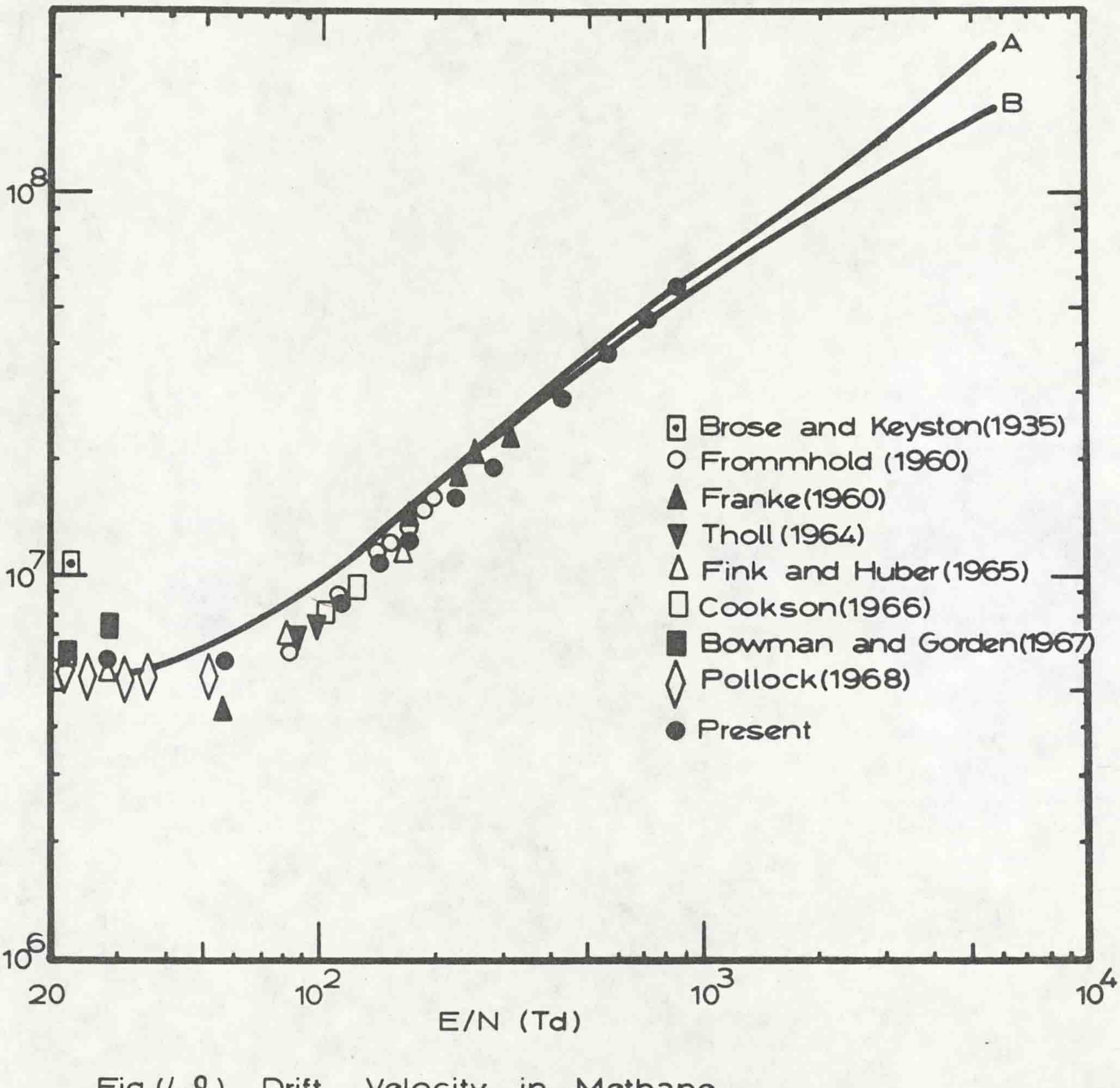

Fig. (4.9) Drift Velocity in Methane.

CH_4

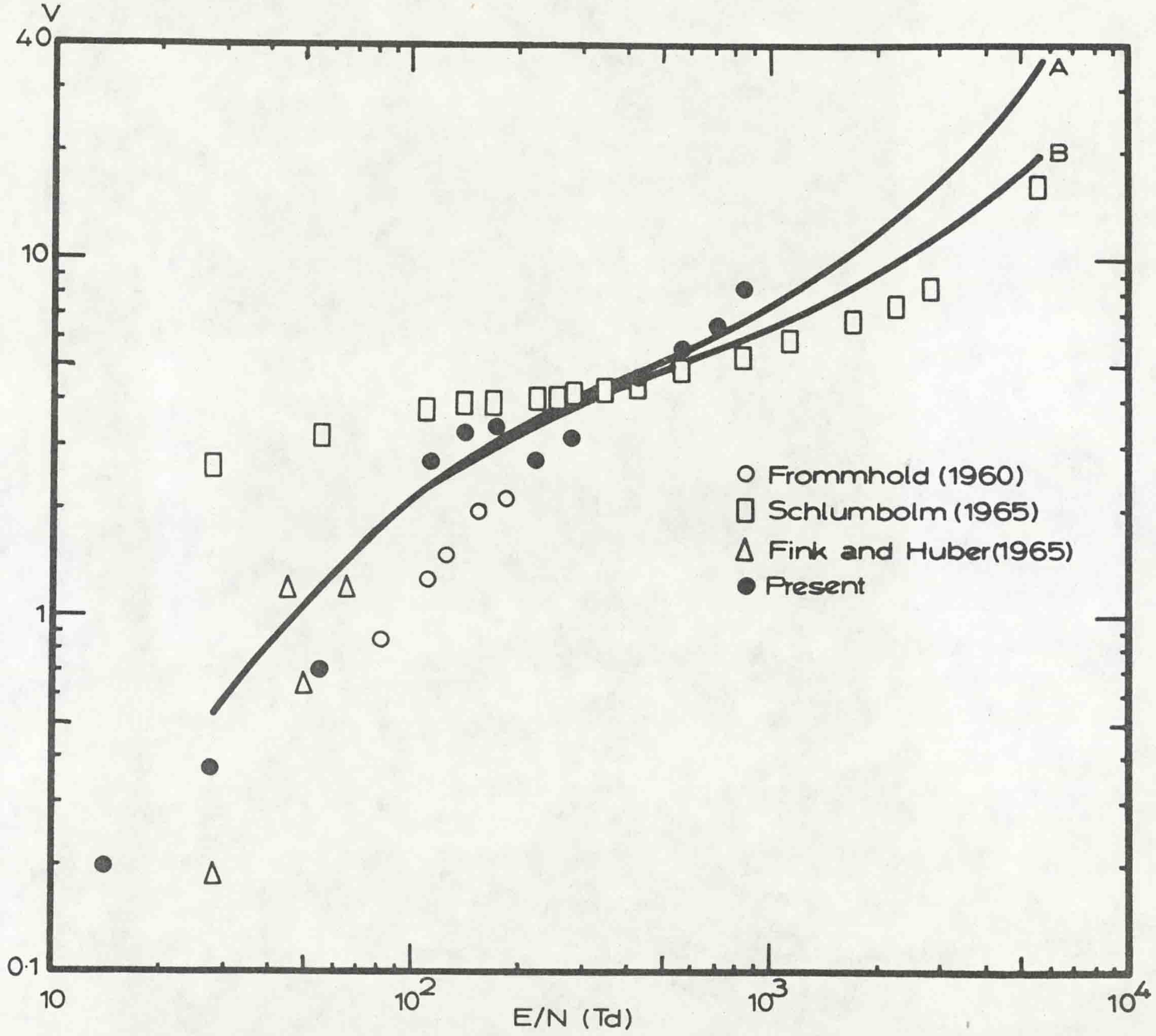

Fig.(4.10) Ratio of Longitudnal Diffusion Coefficient to Mobility in Methane.

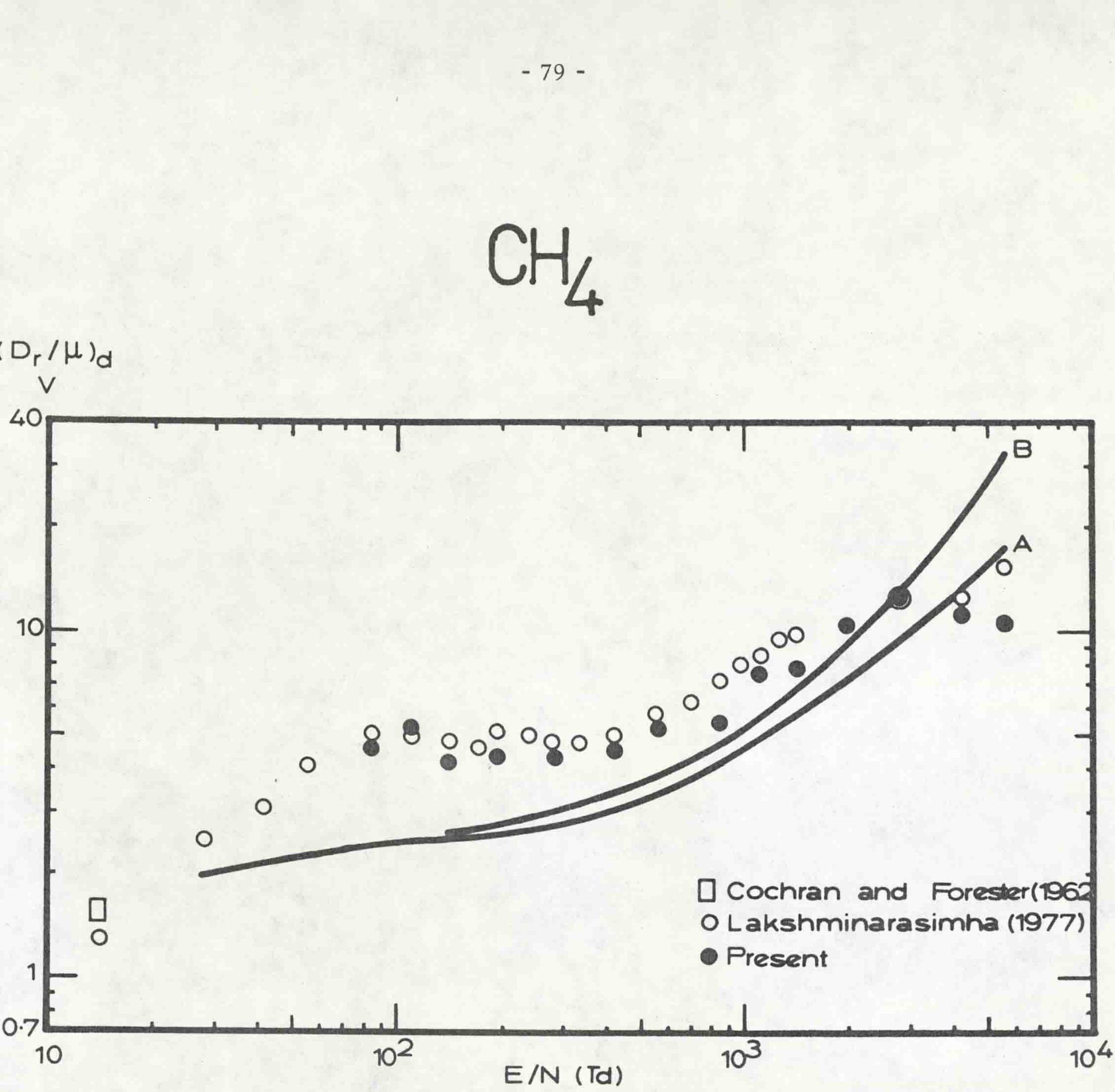

Fig(4.11) Ratio of Radial Diffusion Coefficient to Mobility in Methane.

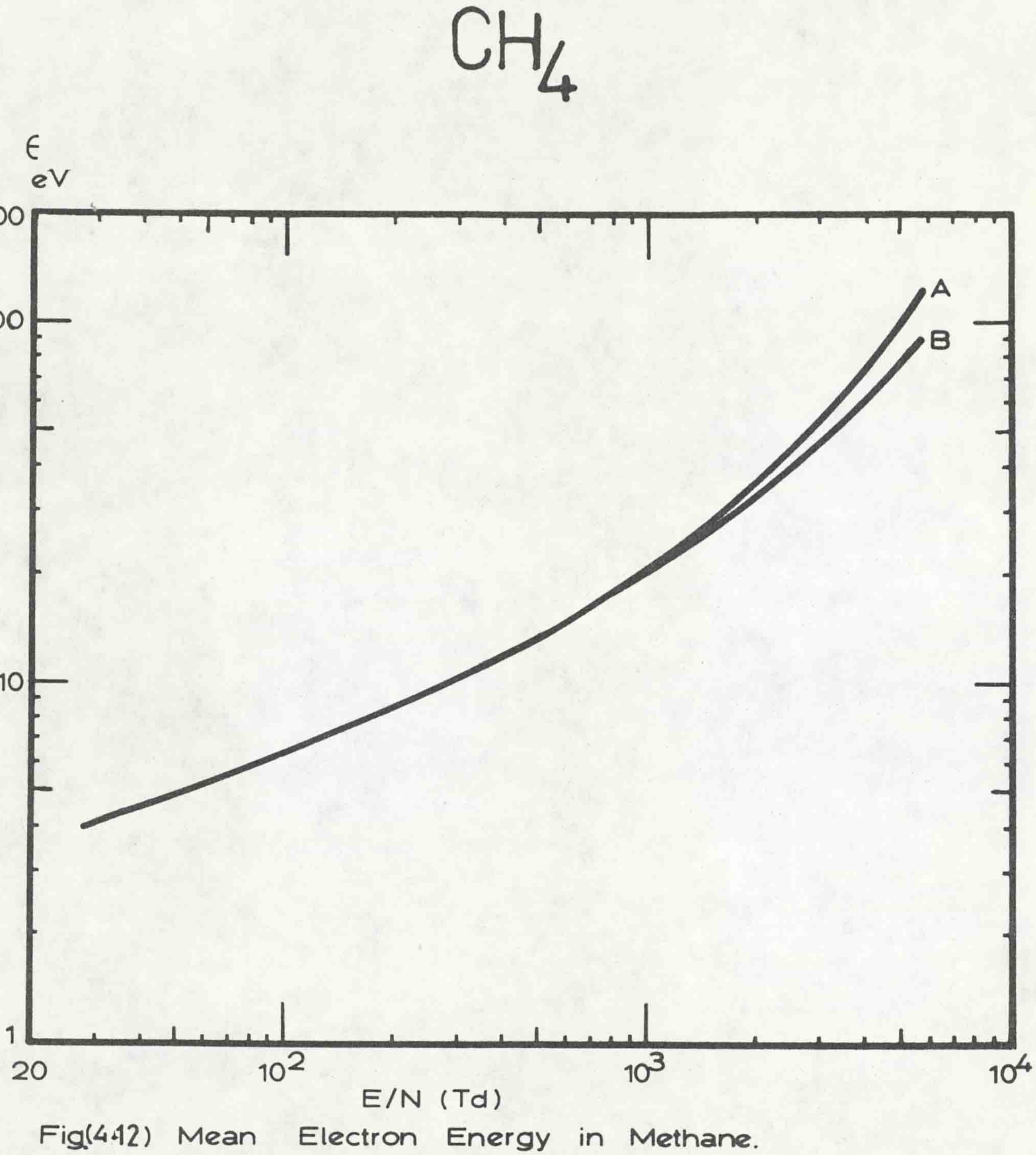

Fig(4.12) Mean Electron Energy in Methane.

CHAPTER FIVE

CHAPTER FIVE

THEORY OF THE BOLTZMANN EQUATION

5.1 INTRODUCTION OF THE BOLTZMANN EQUATION

Electron swarms drifting and diffusing in a uniform electric field can be described mathematically by considering the motion of the electrons in velocity and position space, a study of which produces the Boltzmann equation (Thomas, 1969). From this equation both the electron energy distribution equation and the transport equation may be determined and solutions of these equations give the swarm parameters. In earlier solutions, several approximations were made, in particular the distribution was assumed to be spherically symmetric in velocity space, and the effects of electron density gradients negligible. These solutions gave the diffusion coefficient parallel to the applied field (D_L) equal to the diffusion coefficient perpendicular to the applied field (D_r) the diffusion was isotropic.

However, Wagner, Davis and Hurst (1967) discovered experimentally that the electron swarm diffusion under the effect of an applied electric field is anisotropic. They found that D_L is different from D_r. Many workers (Lucas, 1970 ; Parker and Lowke, 1969) have successfully investigated this effect theoretically and have attributed it to the electron density gradients. Allowing for these effects has produced a position dependency of the energy distribution function in their solutions of the Boltzmann equation. However, D_L are not compared in this thesis and the advanced theory will not be reviewed.

5.2 THE BOLTZMANN EQUATION

In plane parallel geometry, consider a region bounded by two infinite planes, perpendicular to the direction of the electric field, distance x and x + dx from the cathode. Using the Lorentz approximation, the current density due to electrons in this region with energies between ε and $\varepsilon + d\varepsilon$ is given by $j(\varepsilon, x)\, d\varepsilon\, dx$ where :-

$$j(\varepsilon, x) = -\sqrt{\frac{2e}{m}}\,\frac{\varepsilon^{\frac{1}{2}}}{3NQ_m}\left\{ E\,\varepsilon^{\frac{1}{2}}\,\frac{\partial f}{\partial \varepsilon}(\varepsilon, x) + \varepsilon^{\frac{1}{2}}\,\frac{\partial f}{\partial x}(\varepsilon, x)\right\}. \qquad (5.1)$$

Q_m = the electron-atom momentum collision cross-section,

N = the gas number density,

ε = the energy of an electron in electron volts,

$\varepsilon^{\frac{1}{2}} f(\varepsilon, x)\, d\varepsilon$ = the number of electrons per unit volume with energies between ε and $\varepsilon + d\varepsilon$,

$f(\varepsilon, x)$ = the energy distribution function,

E = electric field,

m = electron mass,

e = electron charge,

The Boltzmann equation is the continuity equation which equates the rate of change of the electron density in the energy interval between zero and ε electron volts to the net flow of electrons into this volume :

$$\frac{\partial}{\partial t}\int_0^{\varepsilon} \varepsilon'^{\frac{1}{2}} f(\varepsilon', x)\, d\varepsilon' = R_c(\varepsilon) + R_E(\varepsilon) + R_x(\varepsilon)\ , \qquad (5.2)$$

where $R_c(\varepsilon)$ = the rate of change due to collisions

$$= \sqrt{\frac{2e}{m}}\ N\left[\frac{2m}{M}\ Q_m\ \varepsilon^2 f(\varepsilon, x) + \int_{\varepsilon}^{\varepsilon + \varepsilon_{ex}} \varepsilon'\, Q_{ex}(\varepsilon')\, f(\varepsilon', x)\, d\varepsilon'\right.$$

$$\left. + \left(\int_{\varepsilon}^{\frac{\varepsilon}{1-\Delta} + \varepsilon_i} + \int_{0}^{\frac{\varepsilon}{\Delta} + \varepsilon_i}\right) \varepsilon' Q_i(\varepsilon')\, f(\varepsilon', x)\, d\varepsilon'\right], \qquad (5.3)$$

with m = the mass of an electron,

M = the mass of a gas atom,

Q_{ex} = the electron excitation cross-section,

Q_i = the ionization cross-section.

Δ is the partition factor such that two electrons present after ionization have their energies partitioned in the ratio $\Delta : 1-\Delta$, also $R_E(\varepsilon)$ = the rate of change due to the electric field

$$= -E\,j(\varepsilon, x) \quad , \tag{5.4}$$

and $R_x(\varepsilon)$ = the rate of change due to the flow of electrons through the faces of the volume under consideration (i.e. the gradient term).

$$= -\frac{\partial}{\partial x} \int_0^{\varepsilon} j(\varepsilon', x)\, d\varepsilon' \quad . \tag{5.5}$$

The equation may be expressed as :-

$$\frac{\partial}{\partial t} \int_0^{\varepsilon} \varepsilon'^{\frac{1}{2}} f(\varepsilon', x)\, d\varepsilon' = \sqrt{\frac{2e}{m}}\, N \left[\frac{2m}{M} Q_m \varepsilon^2 f(\varepsilon, x) + \int_{\varepsilon}^{\varepsilon+\varepsilon_{ex}} \varepsilon' Q_{ex}(\varepsilon') f(\varepsilon', x)\, d\varepsilon' \right.$$
$$\left. + \left(\int_{\varepsilon}^{\frac{\varepsilon}{1-\Delta}+\varepsilon_i} + \int_0^{\frac{\varepsilon}{\Delta}+\varepsilon_i} \right) \varepsilon' Q_i(\varepsilon') f(\varepsilon', x)\, d\varepsilon' \right]$$
$$+ E \sqrt{\frac{2e}{m}} \frac{1}{3NQ_m} \left\{ \varepsilon E \frac{\partial f}{\partial \varepsilon}(\varepsilon, x) + \varepsilon \frac{\partial f}{\partial x}(\varepsilon, x) \right\}$$
$$+ \sqrt{\frac{2e}{m}} \frac{\partial}{\partial x} \int_0^{\varepsilon} \frac{1}{3NQ_m} \left\{ \varepsilon' E \frac{\partial f}{\partial \varepsilon'}(\varepsilon', x) + \varepsilon' \frac{\partial f}{\partial x}(\varepsilon', x) \right\} d\varepsilon' \quad . \tag{5.6}$$

5.3 THE TRANSPORT EQUATION

The transport equation may be derived by considering all electrons, i.e. let the energy ϵ tend to infinity in equation (5.6) :-

$$\frac{\partial}{\partial t} \int_0^\infty \epsilon^{\frac{1}{2}} f(\epsilon', x)\, d\epsilon' = \sqrt{\frac{2e}{m}}\, N \int_0^\infty \epsilon' Q_i f(\epsilon', x)\, d\epsilon'$$
$$+ \sqrt{\frac{2e}{m}} \frac{\partial}{\partial x} \left\{ \int_0^\infty \frac{1}{3NQ_m} \left[\epsilon' E \frac{\partial f}{\partial \epsilon}(\epsilon', x) + \epsilon \frac{\partial f}{\partial x}(\epsilon', x) \right] d\epsilon \right\} .$$

Now, defining n(x) :-

$$n(x) = \int_0^\infty \epsilon^{\frac{1}{2}} f(\epsilon, x)\, d\epsilon \qquad \text{gives}$$

$$\frac{\partial n(x)}{\partial t} = R_i n(x) - \frac{\partial}{\partial x} \left[v\, n(x) - \frac{\partial}{\partial x} \left\{ D\, n(x) \right\} \right] , \qquad (5.7)$$

where R_i = the rate of ionization,

v = the electron drift velocity,

D = the electron diffusion coefficient.

5.4 THE SOLUTION FOR A STEADY STATE TOWNSEND DISCHARGE

Assuming that $f(\epsilon, x)$ is separable, and for steady state conditions (i.e. n varies exponentially with distance, the energy distribution is constant) we may write :-

$$\left.\begin{aligned} f(\epsilon, x) &= n(x)\, F_o(\epsilon) \\ \frac{\partial n}{\partial x}(x) &= \alpha\, n(x) \end{aligned}\right\} . \qquad (5.8)$$